SEDIMENTARY CYCLICITY AND MICROPALEONTOLOGICAL INVESTIGATIONS IN THE UPPER TRIASSIC SHALLOW MARINE CARBONATE SUCCESSIONS (CENTRAL AND WESTERN TAURIDES, TURKEY)

A THESIS SUBMITTED TO
THE GRADUATE SCHOOL OF NATURAL AND APPLIED SCIENCES
OF
MIDDLE EAST TECHNICAL UNIVERSITY

BY

BURCU COŞKUN TUNABOYLU

IN PARTIAL FULFILLMENT OF THE REQUIREMENTS
FOR
THE DEGREE OF DOCTOR OF PHILOSOPHY
IN
GEOLOGICAL ENGINEERING

FEBRUARY 2008

Approval of the thesis:

SEDIMENTARY CYCLICITY AND MICROPALEONTOLOGICAL INVESTIGATIONS IN THE UPPER TRIASSIC SHALLOW MARINE CARBONATE SUCCESSIONS (CENTRAL AND WESTERN TAURIDES, TURKEY)

submitted by **BURCU COŞKUN TUNABOYLU** in partial fulfillment of the requirements for the degree of **Doctor of Philosophy in Geological Engineering Department, Middle East Technical University** by,

Prof. Dr. Canan Özgen ____________________
Dean, Graduate School of **Natural and Applied Sciences**

Prof. Dr. Vedat Doyuran ____________________
Head of Department, **Geological Engineering**

Prof. Dr. Demir Altıner ____________________
Supervisor, **Geological Engineering Dept., METU**

Examining Committee Members

Prof. Dr. M. Cemal Göncüoğlu ____________________
Geological Engineering Dept., METU

Prof. Dr. Demir Altıner ____________________
Geological Engineering Dept., METU

Prof. Dr. Asuman G. Türkmenoğlu ____________________
Geological Engineering Dept., METU

Assoc. Prof. Dr. Uğur Kağan Tekin ____________________
Geological Engineering Dept., Hacettepe University

Assist. Prof. Dr. İsmail Ömer Yılmaz ____________________
Geological Engineering Dept., METU

Date: (Thesis defense date)
04.02.2008

I hereby declare that all information in this document has been obtained and presented in accordance with academic rules and ethical conduct. I also declare that, as required by these rules and conduct, I have fully cited and referenced all material and results that are original to this work.

Name, Last Name: Burcu COŞKUN TUNABOYLU

Signature :

ABSTRACT

SEDIMENTARY CYCLICITY AND MICROPALEONTOLOGICAL INVESTIGATIONS IN THE UPPER TRIASSIC SHALLOW MARINE CARBONATE SUCCESSIONS (CENTRAL AND WESTERN TAURIDES, TURKEY)

COŞKUN TUNABOYLU, Burcu
Ph.D., Department of Geological Engineering
Supervisor: Prof. Dr. Demir ALTINER

February 2008, 182 pages

Shallowing-upward meter-scale cycles (parasequences) consisting of megalodont-bearing limestones or clay levels at the bottom and fenestral limestones, breccias, stromatolites or vadose pisoids at the top constitute the basic working units of the Upper Triassic successions in the Central and Western Taurides. These cycles are mainly represented by subtidal through supratidal carbonate facies and known as Lofer cycles in the literature. The presence of breccias, mud cracks, dissolution vugs and vadose pisoids indicates subaerially exposed conditions at the top of the cycles. Shallowing-upward meter-scale cycles are interpreted as 4^{th} and 5^{th} order cycles in this study.

Megalodont-bearing limestones of the subtidal zone are characterized by wackestones/packstones with abundant involutinids. However, involutinids are poorly represented in the intertidal-supratidal zone. To determine the relationship between cyclicity and foraminifers, the vertical variation of benthic foraminifer abundance has been analysed in the cycles. This analysis leads us to conclude that the foraminiferal abundance decreases from subtidal through supratidal zone. Furthermore, cluster analysis was performed in order to delineate the relation between the biofacies and foraminiferal associations. Micropaleontological analysis of the uppermost Triassic carbonates reveals the presence of restricted platform foraminiferal associations in the studied successions. Foraminiferal associations discovered in the samples belong to the Upper Norian (Sevatian)-Rhaetian *Triasina hantkeni* assemblage zone. Detailed examination of peritidal carbonates in the Central and Western Taurides against the studies, which claimed that the Dachstein-type platform carbonates are characterized by the transgressive models, should be explained by regressive models.

Key words: Upper Triassic, peritidal carbonates, Lofer cyclicity, benthic foraminifera, Central and Western Taurides.

ÖZ

ÜST TRİYAS SIĞ DENİZEL KARBONAT İSTİFLERİNDE
SEDİMANTER DEVİRSELLİK
VE MİKROPALEONTOLOJİK İNCELEMELER,
(ORTA VE BATI TOROSLAR, TÜRKİYE)

COŞKUN TUNABOYLU, Burcu
Doktora, Jeoloji Mühendisliği Bölümü
Tez Yöneticisi: Prof. Dr. Demir ALTINER

Şubat 2008, 182 sayfa

Genellikle tabanda megalodontlu kireçtaşı ve killi seviyelerden, tavanda ise fenestral yapılı kireçtaşı, breşler, stromatolitler ve vadoz pizolitlerden oluşan ve yukarı doğru sığlaşan metre ölçekli devirler (parasekanslar) Orta ve Batı Toroslardaki Üst Triyas istiflerinin temel birimlerini oluşturmaktadır. Devirler çoğunlukla gelgitaltı – gelgitüstü ortamında çökelen karbonat fasiyesleriyle temsil edilmekte olup literatürde Lofer devirleri olarak bilinmektedir. Breşlerin, çamur çatlaklarının, erime boşluklarının ve vadoz pizolitlerin bulunuşu devirlerin en üstünde su üstü olma koşullarının varlığını ve etkilerini göstermektedir. Yukarı doğru sığlaşan metre ölçeğindeki devirler bu çalışmada 4'ncü ve 5'nci derece devirler olarak tanımlanmıştır.

Gelgitaltı zona karşılık gelen megalodontlu kireçtaşları involutinid grubu foraminiferlerin bol ve yaygın olduğu vaketaşı-istiftaşı fasiyesleri ile temsil edilmektedir. Ancak, gelgitarası ve gelgitüstü zonlarda foraminiferlerin sayısı ve yayılımı azdır. Devirsellik ve foraminiferler arasındaki ilişkiyi belirlemek için, devirlerdeki bentik foraminiferlerin dikey yöndeki değişimi incelenmiş ve foraminiferlerin sedimanter devirselliğe olan tepkisi foraminifer bolluğunun gelgitaltından gelgitüstü zona doğru azaldığı şeklinde tespit edilmiştir. Ayrıca, biyofasiyes ve tür birlikteliklerini tasvir etmek için kümeleme analizi de gerçekleştirilmiştir. Gelgit zonu karbonatlarının mikropaleontolojik analizi,

incelenen istiflerde korunmuş platform foraminifer topluluklarının olduğunu göstermektedir. Foraminifer toplulukları Geç Noriyen-Resiyen yaş aralığına ait olup, *Triasina hantkeni* topluluk zonu bu karbonatlar içinde tanımlanmıştır. Dachstein-tip platform karbonatları transgresif modellerle açıklayan çalışmalara karşın, Orta ve Batı Toroslardaki gelgit çevresi karbonatlardaki ayrıntılı incelenmeler, bu karbonatların regresif modellerle açıklanması gerektiğini göstermiştir.

Anahtar kelimeler: Üst Triyas, gelgit çevresi karbonatları, Lofer devirselliği, bentik foraminifer, Orta ve Batı Toroslar.

To My Father

ACKNOWLEDGMENTS

I am greatly indebted to my supervisor Prof. Dr. Demir ALTINER for his valuable guidance advice, encouragement and constructive criticism during the preparation of this thesis.

I express my gratefulnes to Assist. Prof. Dr. İsmail Ömer Yılmaz for his valuable recommendations and detailed examination of the thesis.

I would like to thank Prof Dr. Bülent Coşkun for his help during the field studies, for his scientific support and encouragements during this study.

I am also indepted to Dr. Mustafa Şenel with sharing his regional experiences with us on the Taurides.

I would like to thank Ayşe Atakul regarding cluster analysis, Sezin Hasdiğen and Neslihan Temiz for their technical support and their encouragements.

I am also grateful to all my friends for their friendships and endless encouragements. Especially, I would like to thank Demet Özer, Ebru Öztürk and Elif Ülgen Hamzaoğlu for their encouragements.

Finally, I would like to express my grateful thanks to my parents for their support and encouragements during this study, and special thanks go to my husband for his patience and endless support.

TABLE OF CONTENTS

LIST OF TABLES

TABLES

LIST OF FIGURES

FIGURES

CHAPTER 1

1. INTRODUCTION

1.1. Purpose and Scope

Many researchers have been working on the Dachstein-type platform carbonates for understanding the general characteristics of the Lofer cycles and the factors controlling the development of the cyclic successions (e.g., Sander, 1936, Schwarzacher, 1948, 1954, Fischer, 1964, Goldhammer et al., 1990, Haas, 1982, 1991, 2004, Enos and Samankassou, 1998, 2002, Haas et al., 2007) in the Upper Triassic. Although there are so many studies on this issue, the cyclicity problems are still pending and comparitive studies are needed. In order to contribute to the correct interpretation of the Lofer cycles, the sequence stratigraphy of the Upper Triassic (Norian-Rhaetian) peritidal carbonates in the Central and Western Taurides, by means of paleontological and sedimentary facies data, constitutes the main purpose of this study. For this purpose, meter-scale stratigraphic sections have been measured in the Anamas-Akseki Autocthon, the Beydağları-Karacahisar Autochthon and the Lycian Nappes where the best preserved sections of the Dachstein-type platform carbonates crop out.

Shallow marine peritidal carbonates are mainly composed of shallowing-upward meter-scale cycles in the studied successions. Although field observations permit to establish the sedimentary cyclicity, microfacies analysis, use of sedimentary structures and the micropaleontology are used to evaluate the meter-scale cycles in the Upper Triassic successions. Based on detailed microfacies analyses and micropaleontological data, 4^{th}- and 5^{th}-order cycles are established as the building blocks of peritidal carbonates. Moreover, the Upper Triassic cyclicity in the peritidal carbonates of the Central and Western Taurides are compared with the Dachstein-type carbonates deposited along the shelf margins of the Neotethys Ocean (e.g., Fischer, 1964, Goldhammer et al., 1990, Haas, 2004, Haas et al., 2007).

Another purpose of this study is to examine and document the significance of the response of benthic foraminifers to the sedimentary cyclicity. Benthic foraminifers are excellent bioindicators to determine and understand the depositional environments. In the studied successions, involutinids are the main microssil group. They are used both for age and facies analyses in the detection of sedimentary cyclicity. Cluster analysis was also performed to delineate biofacies and species associations. Furthermore, taxonomic study is also presented for the Upper Triassic peritidal carbonates in this study.

1.2. Geographic Setting

This study has been carried out in three different regions in the Central and Western Taurides where Upper Triassic peritidal carbonates are largely exposed (Figure 1). Two localities studied are in the Central Taurides and located to the southeastern part of Eğridir Lake (Figure 1). The first locality is situated in the northeast of the Aksu village from where the study area near the Leylek Hill can be reached by a stabilized road. It is in the Isparta M26-a3 and M26-a4 quadrangles of 1:25000 scale (Figure 1). The second locality is in the southeastern part of Kuzca village along the Kasımlar-Kuzca road, in the Isparta M26-d4 quadrangle of 1:25000 scale (Figure 1). The third locality is in the Western Taurides, located in the southeast of the Bozburun Peninsula near Söğüt village (Figure 1). The study area can be reached by a mountain road from the İçmeler/Marmaris Town. It is in the Marmaris O20-d1 quadrangle of 1:25000 scale.

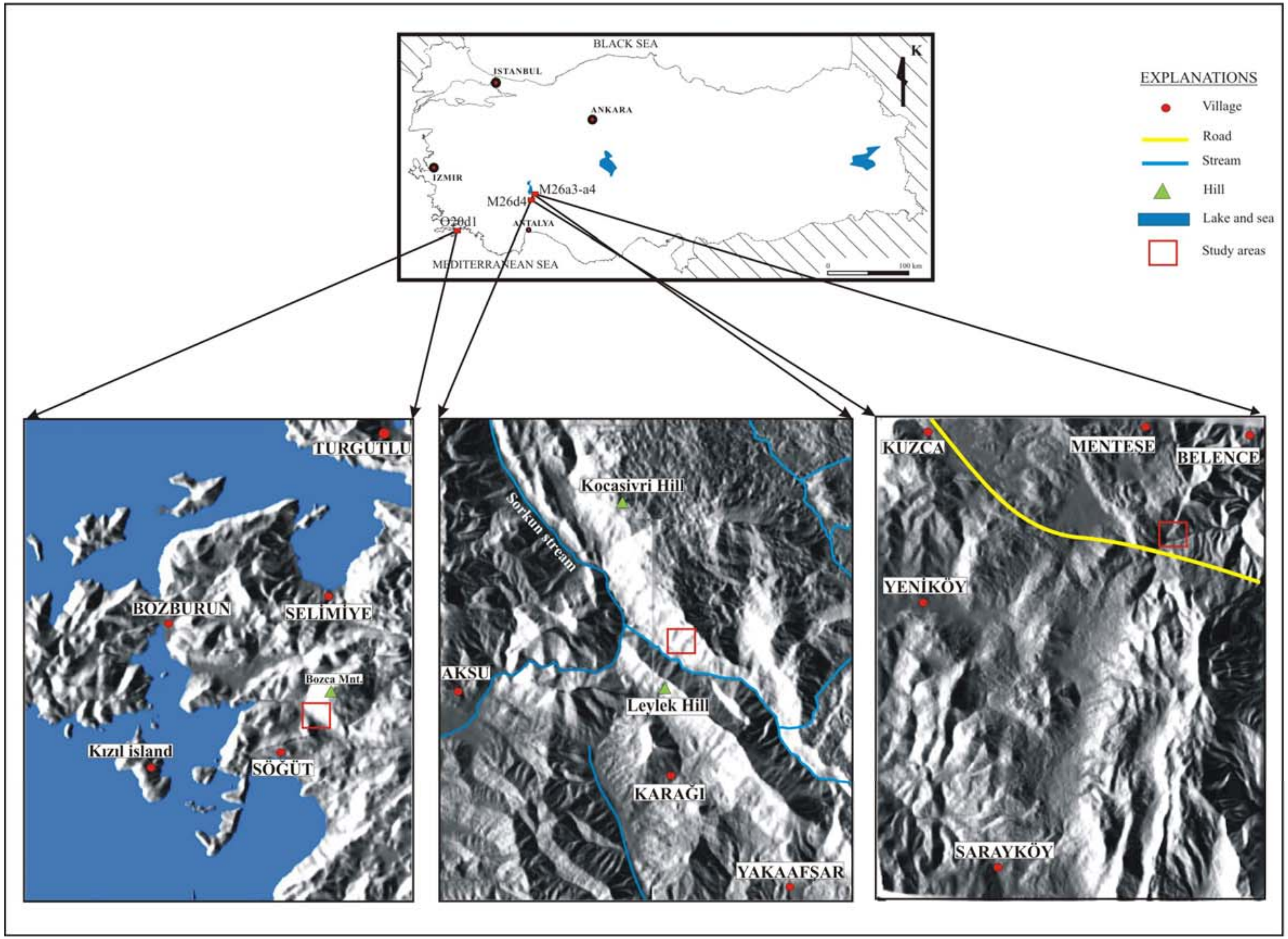

Figure 1. Geographic settings of the study areas and the locations of the measured sections.

1.3. METHODOLOGY

The sequence stratigraphic studies in the field require a detailed sampling and examination of the units at outcrops. Therefore, selection of sections for the detailed measurements and sampling were based on field studies in the southeastern part of the Eğridir Lake and southwestern part of the Marmaris Town. Green colored claystones, megalodont-bearing limestones, and stromatolites were selected as key levels for understanding the Upper Triassic cyclicity in these peritidal carbonates. As they are good indicators for understanding the depositional environment and the detection of the relative sea-level changes, they have been particularly used for constructing the cyclicity in these carbonates. Studying and sampling of the Leylek, Kuzca and Marmaris sections were carried out both in the field and in the laboratory. In the field, samples were collected from each layer and for thick subtidal beds, more samples were collected as much as possible from the basal, middle and the upper part in order to eliminate missed-beds. In the Leylek locality, 33 m and 44.13 m thick stratigraphic sections, in Kuzca locality, 1.52 m, 9.1 m, 19.86 m and 2.3 m thick stratigraphic sections, in Marmaris locality, 23.25 m and 36 m thick stratigraphic sections were measured. 7th, 13th, 14th and 18th parasequence of the Leylek-1 Section, 4th, 5th, 6th, 7th, 8th, 9th, 10th and 11th parasequence of the Leylek-2 Section were resampled in order to differentiate smaller-scale parasequences. For the purpose of whole study, 185 samples from the Leylek Hill area, 55 samples from the Kuzca locality and 88 samples from the Marmaris locality were collected. In order to determine the cyclicity in the Upper Triassic, fourth- and fifth-order sea level changes (parasequences) were investigated by detecting the major facies changes indicating rapid flooding. The field evaluations are supported by careful microfacies and micropaleontological analyses in the laboratory works. With all these observations and evaluations, a correlation have been proposed between measured sections in different localities in order to explain sea level changes in different regions of the Central and Western Taurides.

On the other hand, the response of benthic foraminifers to sedimentary cyclicity has been analysed in detail and treated under a separate chapter. The facts that they are excellent bioindicators, the relationship between the cyclicity and the response of foraminifers to this sedimetary cyclicity have been studied. Involutinid foraminifers which constitute the main microfossil group of these carbonates have been counted per sample. The variations in abundance have perfectly displayed the biotic response to sedimentary cyclicity. Moreover, the cluster analysis has been applied for the purpose of grouping benthic foraminiferal genera in samples and for distinguishing cycle bottom and top facies in the parasequences.

1.4. PREVIOUS WORKS

The Taurides which is one of the major tectonic units of Turkey, is located on the Alpine-Himalian Orogenic Belt in the eastern Mediterranean region (Şengör and Yılmaz, 1981). Several studies have been carried out to investigate the stratigraphy, sedimentology and tectonics of this mountain chain. It consists of allochthonous and autochthonous units with distinct stratigraphical, structural and metamorphic features. The earliest studies were carried out by Blumenthal (1944, 1947, 1951, 1956) about the geology of the Tauride Belt around Seydişehir-Beyşehir, the Aladağ unit around Beyşehir-Bozkır Towns, northern part of Alanya region, southwestern part of the Anamas Mountain, eastern part of Eğridir Lake and the area between the Aegean Sea and Antalya Gulf. Blumenthal's studies have served as guides to other researchers for later studies in the Tauride Belt. After Blumenthal, various geological studies have been performed for different purposes by many researchers on the Tauride Belt (e.g., Graciansky, 1968, Brunn et al., 1971, Özgül, 1976, 1984, 1997, Gutnic et al., 1979, Şenel et al., 1992, 1996, 1998, Özgül and Kozlu, 2002, Şenel, 2004). Some of them considered allochthonous units as "nappes" (e.g., Blumenthal, 1947, Brunn et al., 1971, Monod, 1977, Gutnic et al., 1979), while Özgül (1976, 1984) defined tectonostratigraphic units comprising both allochthonous and autochthonous units (Geyik Dağı, Aladağ, Bolkar Dağı, Bozkır, Antalya and Alanya units).

From west to the east, several researchers have been working on the Upper Triassic platform-type carbonates in many parts of the Taurides which constitute the main issue of this study.

In the Eastern Taurides, Blumenthal (1952) was the first who studied the morphology, stratigraphy and structural features of the Aladağ Mountains. He defined nappe systems comprising platform-type carbonates deposited between Upper Devonian and Lower Cretaceous. Among these nappes, Beyaz Aladağ Nappe was named by Blumenthal (1952) which consists of thick dolomitic limestone sequences. Although he described carbonate successions at the southern edge of the Aladağ Mountains, Metz (1939, 1956) was the one who firstly described megalodont-bearing Triassic sequences in this region. Özgül (1976) differentiated Bozkır, Aladağ and Geyik Dağı Units in the Aladağ region in which they contain Upper Triassic platform-type carbonates. Tekeli et al. (1984) also defined sequences consisting of limestones, dolomitic limestones and dolomites in the Beyaz Aladağ sequence in the Eastern Taurides. A typical feature of this sequence was defined as the abundance of megalodont in the lower levels and the gradual decrease towards the top of the sequence. Involutinids were seen as the main component grains in mudstone-wackestone facies. Furthermore, the micrite matrix was found to be pelloidal and intraclastic and fenestral fabrics, geopetal sediment were determined commonly in packstone-grainstone facies. Tekeli et al. (1984) emphasized that a thick cyclic sequence was formed by carbonate deposits in this region. Özgül and Turşucu (1984) studied in the northeastern end of the Tauride Belt and they found Upper Triassic neritic carbonates as the oldest member of the Munzur Limestone in the study area. *Auloconus permodiscoides*, *Glomospirella friedli*, *Aulotortus sinuosa sinuosa*, *Aulotortus gaschei* and some other foraminifers were determined in this region. Partial dolomitization was also encountered in these levels. Perinçek and Kozlu (1984) investigated the area between Adana-Kayseri and Malatya. In the southwestern part of the study area, the Andırın Limestone was represented by a limestone succession with a Middle-Late Triassic to Cenomanian age. The Triassic portion consists of megalodont-bearing limestone, containing intraformational conglomerates, pelloids, oolites and dolomitic limestones. Varol et al. (1986) firstly presented Middle-Upper Triassic in the autochthonous Geyik Dağı Unit of the Eastern Taurides (Sarız-Tufanbeyli region, Kayseri) which was thought to be composed of only Lower Triassic rocks before. They found dolomitic limestones alternating with massive dolomites, which contain *Aulotortus* gr. *sinuosus*, *Aulotortus* sp. etc. Özgül and Kozlu (2002) also studied the Geyik Dağı unit of the Eastern Taurides around the Kozan, Feke, Saimbeyli, Tufanbeyli, Develi and Pınarbaşı villages and described dolomites, neritic limestones and shales within this region. The succesion contains *Endoteba* sp., involutinids and duostiminids of Middle-Late Triassic age.

In the Western Taurides, the geological studies around the Marmaris-Bozburun regions comprising the study area was initially investigated by Philipson

(1915), Brunn et al. (1971), Bernouilli et al. (1974), Brinkmann (1975). They defined nappe systems in these regions. The area between the Aegean Sea and the Antalya Gulf was firstly named as "Lycian Taurides" by Blumenthal (1944). Graciansky (1968, 1972) studied the stratigraphy of the Lycian Taurides around the Teke peninsula and found Upper Triassic successions consisting of thick dolomitic series in the Köyceğiz and around the northeastern part of the Fethiye (Table 1). Later, Brunn et al. (1971) defined "Lycian Nappes" between the Menderes massif to the west and the Bey Dağları to the east. To the east, Domuzdağ unit was determined which consists entirely of Upper Triassic and Liassic carbonates with megalodontd and involutinids. Poisson (1977) also studied the Domuzdağ unit in the Lycian nappes in which the Upper Triassic carbonates consisting of platform-type carbonates with megalodonts (Figure 2). Bilgin et al. (1997) and Şenel and Bilgin (1997) investigated the Lycian nappes around the Marmaris and Bozburun regions. The Upper Triassic part of the nappe was represented by megalodont-bearing limestones and was named as Güverdağı Formation by Bilgin et al. (1997). Güverdağı Formation is composed of megalodont-bearing neritic carbonates which gradually passes upward into ammonitico-rosso facies (Table 1).

In particular, Upper Triassic platform-type carbonates are widely exposed between Eğridir and Beyşehir Lakes in the Central Taurides. At Anamas Dağ, the Upper Triassic carbonates start with the Kasımlar shales and the succession is succeeded by the Menteşe Dolomites and ends with a horizon containing large megalodonts (Brunn et al., 1971; Dumont et al., 1972; Gutnic et al., 1979) known as the Leylek Limestone (Table 1). The Leylek Limestone name was firstly introduced by Vegh-Neubrandt et al. (1976) for the megalodont-bearing limestones. It starts at the base with limestones containing *Involutina sinuosa sinuosa* and continues upward with dolomitized micrites with megalodonts which have the index foraminifer *Triasina hantkeni* (Monod, 1977). The uppermost part of this section consists of dolomites with megalodonts and stromatolites (Monod, 1977). The Rhaetian fossil assemblages within them were thought to correspond to Dachstein Kalk fossil assemblages (Gutnic et al., 1979). Monod (1977) observed megalodont-bearing limestones also in the Kırkkavak Formation at the northern part of Antalya Gulf, in the Oymapınar region, Kasımlar region, Dipoyraz Mountain, Barla Mountain and the southwestern part of the Anamas Mountain. Similar successions

Table 1. Principal units of the Upper Triassic formations in the Central and Western Taurides.

<table>
<tr><th></th><th></th><th colspan="6">Central Taurides</th><th colspan="4">Western Taurides</th></tr>
<tr><th></th><th></th><th>Brunn et al., 1971
Anamas Mnt.</th><th>Dumont et al., 1972
Anamas Mnt.</th><th>Gutnic et al. 1979
Anamas Mnt.</th><th>Özgül 1984
Anamas Mnt.</th><th>Şenel et al. 1996
Anamas Mnt.</th><th>This study
Central Taurides
Anamas Mnt.</th><th>Graciansky, 1972
Lycian Nappes</th><th>Poisson, 1977
Lycian Nappes
Domuzdağ</th><th>Bilgin et al. 1997
Lycian Nappes</th><th>This study
Western Taurides
Lycian Nappes</th></tr>
<tr><td rowspan="2">UPPER TRIASSIC</td><td>Rhaetian</td><td>megalodont limestone</td><td>megalodont limestone</td><td>Leylek Limestone</td><td>stromatolitic limestone</td><td>Leylek Limestone</td><td rowspan="2">Cyclic carbonates with megalodonts and stromatolites</td><td rowspan="2">limestone and dolomite</td><td rowspan="2">megalodont bearing carbonates</td><td>megalodont-bearing neritic carbonates</td><td rowspan="2">Cyclic carbonates with megalodonts and stromatolites</td></tr>
<tr><td>Norian</td><td>Menteşe Dolomite</td><td>Dolomitic Limestone</td><td>Menteşe Dolomite</td><td>dolomite</td><td>Menteşe Dolomite</td><td></td></tr>
</table>

were also recognized at Barla Dağ (Brunn et al., 1971; Dumont et al., 1972), eastern flank of Beydağları (Marcoux, 1979), near Sütçüler (Akbulut, 1980), Dipoyraz Dağ Massif (Dumont & Monod, 1976), in the Geyik Dağı Unit and Bozkır unit (Özgül, 1976, 1984), in the Tahtalı Dağ Unit of the Antalya Nappes (Marcoux, 1979; Şenel et al., 1996). In the northern part of Manavgat, Monod (1977) and Demirtaşlı (1987) defined a continous succession of Upper Triassic-Cenomanian. The Upper Triassic part of this succession is represented by Menteşe Dolomite (Upper Norian-Lower Rhaetian), Leylek Limestone (Rhaetian) and Üzümdere Formation(Upper Rhaetian-Lower Liassic) respectively (Şenel et al., 1996). Leylek Limestone was represented megalodont-bearing limestone with the Late Triassic foraminiferal association (Table 1).

Upper Triassic platform-type carbonates were also recognized in the world and the cyclicity within these carbonates have been studied since the 19th century by many researchers. Upper Triassic platform carbonate successions occur in the Northern Calcareous Alps (Fischer, 1964) and also in the Southern Alps (Bosselini and Hardie, 1988; Goldhammer et al., 1990), Julian Alps (Ogorelec and Buser, 1996), northern part of Pannonian Basin (Schwarzacher and Haas, 1986; Haas, 1991; Balog et al., 1997), Central and Inner Western Carpathians (Michalik, 1980, 1993) and Dinarides (Dimitrijevic and Dimitrijevic, 1991).

The cyclic depositional pattern of Alpine Upper Triassic carbonates was initially recognized by Sander (1936) in the Loferer Steinberge near Lofer and the Steinernes Meer, Salzburg and later investigated by his student Schwarzacher (1948). Sander (1936) first recognized meter-scale sedimetary cycles in the Dachstein Limestone. He termed this rhytmic facies as the Lofer facies because of its excellent exposure in the Loferer Steinberge near Lofer. Schwarzacher (1948, 1954), aggreing with Sander (1936), carried out further studies on these cycles and described superimposed cycles in the Transdunabian Central Range. Sander (1936) and Schwarzacher (1948, 1954) suggested that the ultimate control of cycles is due to changes in the earth's orbit, known as Milankovitch cycles. However, the ideal Lofer cycle was firstly defined by Fischer (1964) who published a fundamental study on the Lofer cyclothems (Figure 2). He suggested the loferites for a limestone or dolomite riddled by shrinkage pores. This study had a deep impact on the interpretation of cyclic carbonate sequences and was widely used as a referance example of meter-scale cycles produced by high-frequency sea-level oscillations. Fischer defined an upward-deepening facies trend and proposed orbital control of the cyclicity. He described the ideal Lofer cycle as a subtidal Member C with normal marine biota, an intertidal Member B and a supratidal Member A (Figure 2). Cyclothems in the mid-part of the formation show a basal diconformity. Underlying dessication and solution cavities are filled by an insoluble-rich, commonly red limestone, interpreted as a reworked soil. The supratidal member A may or may not have a terrestrial horizon on top. Above lies a thin unit of dolomitic limestone with algal mats, containing a variety of dessication structures; this was interpreted as intertidal. The main and last unit of the cyclothem is a massive limestone with varied biota, considered as subtidal. The cyclothems were attributed to a eustatic fluctuation of low amplitude and a period of between 20,000 and 100,000 years. It has been widely accepted that the cyclic succession of peritidal carbonates resulted from the effects of eustatic sea level changes and tectonics (Table 2).

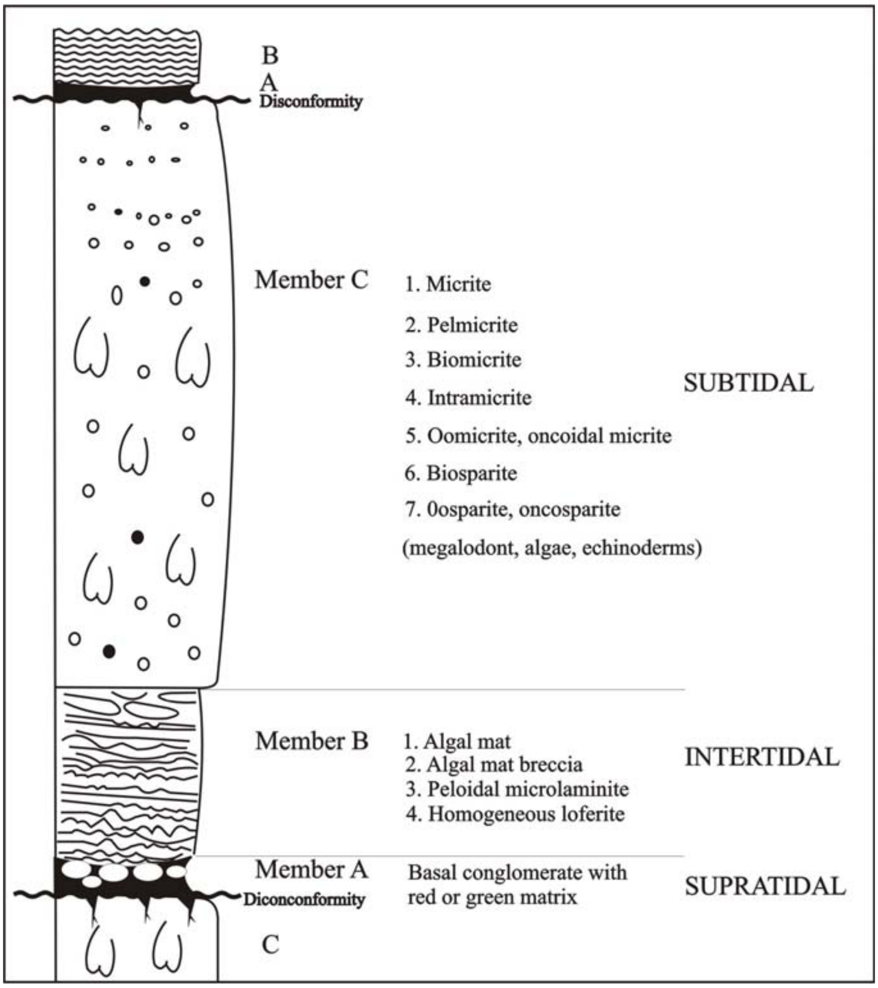

Figure 2. Fischer (1964)'s idealized Lofer cycle and their characteristic features.

Table 2. Evaluation of Lofer cycles since Fischer (1964), showing characteristic features of the cyclicities.

Researchers	Study Area	Types of Cyclicity	Subtidal Unit	Intertidal Unit	Supratidal Unit	Controlling Factors
Fischer, 1964	Austria, NCA	deepening	megalodont limestone	loferites with algal mats and abundant dessication features	argillaceous member with red or green matrix	tectonic&eustatic
Bosselini, 1967	Venetian Prealps	regressive transgressive intertidal subtidal	massive crystalline dolomites with megalodont,gastropod etc.	biogenic dolomites with stromatolites	intraformational breccia with reddish or greenish argillaceous material	subsidence&sea level variations
Haas, 1982	Hungary	transgressive transgressive-regressive	megalodont-bearing limestones	algal laminites, dolomitic limestones	argillaceous layer	Milankovitch-driven climatic changes
Bosselini and Hardie, 1988	Southern Alps	shallowing-upward	grainstone and packstone with megalodont, dolomites	laminites	laminites	-
Goldhammer et al., 1990	Southern Alps, NCA	shallowing-upward	wackestone to grainstone with megalodonts	dolomites, laminites, shrinkage pores	intraformational conglomerate	subsidence sea level changes Milankovitch-type orbital forcing autocyclicity
Satterley&Brandner, 1995	Austria, NCA	shallowing-upward	megalodont-bearing limestone	laminated loferite, homogeneous loferite	soil	autocyclic processes
Satterley, 1996	Austria	shallowing-upward	wackestone, packstone or grainstone	homogeneous dolomitic mudstone, algal laminated or fenestral dolomitic mudstone	soil conglomerate with a red or green fine-grained matrix	autocylic&tectonic processes
Ogorelec&Buser, 1986	Julian Alps (Slovenia)	deepening-upward	megalodont-bearing limestone	stromatolites, mudcracks, loferites breccias with residual clay		tectonic
Balog et al., 1997	Hungary, Transdunabian Range	transgressive/regressive	wackestone/packstone with megalodont	tidal-flat laminites	reworked paleosol (red or green)	Milankovitch-driven climatic changes and related sea level changes

Table 2. continuing

Researchers	Study Area	Types of Cyclicity	Subtidal Unit	Intertidal Unit	Supratidal Unit	Controlling Factors
Enos&Samankassou, 1998	Austria	-deepening -shallowing -deepening- shallowing	molluscan wackestone and packstone with diverse biota	fenestral porosity, stromatolitic lamination, partial dolomitization, intraclasts and dessication cracks		Autocyclicity
Sattler and Schlaf, 1999	Julian Alps (Slovenia)	deepening	peloid-wackestone and packstone, oncoid bindstone	dolomitic, bindstones with loferitic pores	caliche-pisoids and crusts	Climate
Haas and Demeny, 2002	Hungary, Transdunabian Range	deepening	megalodont-bearing limestone	laminites	greenish argillaceous, intraclastic carbonates	climate, eustatic oscillation
Preto and Hinnov, 2003	northern Italy	mostly regressive few symmetric	peloidal dolostones with megalodont	loferites	carbonate breccias	eustatic oscillation under Milankovitch control Allocyclicity
Novak, 2003	Slovenia	deepening	micritic limestone with megalodont	stromatolitic and other laminated carbonate rocks	intraformational breccia	-
Haas, 2004	Hungary, Transdunabian Range	transgressive transgressive/regressive	peloidal wackestone or packstone with shallow marine biota	microbial stromatolite	red or green argillaceous, intraclastic carbonate	Allocyclicity
Haas et al., 2007	Austria, Dachstein Plateau	-transgressive -transgressive-regressive	megalodont-bearing limestone	stromatolite, mudstone rich in fenestral pores (birdseyes)	red or green argillaceous carbonate layer	Allocyclicity
This study	Central and Western Taurides, southern Turkey	shallowing-upward	megalodont-bearing limestone	Dolomitic limestone, dismicrites with geopetal structures, black pebble, fenestral limestone, stromatolite, breccioid limestone and vadose pisoid		-

Fischer's (1964) deepening-upward interpretation has been opposed (Bosselini and Hardie, 1988; Preto and Hinnov, 2003 etc) and adopted (Bosselini, 1967; Fruth and Scherreiks, 1975, 1982; Ogorelec and Buser, 1996; Sattler and Schlaf, 1999; Haas and Demeny, 2002) by many researchers in the following years (Table 2). More recent studies have suggested that the Alpine Triassic cycles are shallowing-upward and that the laminites are in fact regressive (Table 2).

Later, Haas (1982, 1991) modified the basic pattern of the Lofer cycles, proposing a symmetric transgression-regression cycle and suggested Milankovitch driven climatic changes as the main controlling factors of the Lofer cyclicity (Table 2). Schwarzacher and Haas (1986), Balog et. al. (1997) and Cozzi et al. (2003) also suggested Milankovitch-driven climatic changes and related sea level changes as the main controlling factor of the Lofer cyclicity (Table 2).

In contrast to Fischer (1964), Goldhammer et al. (1990) and Satterley (1996) reinterpreted the ideal Lofer cycle as shallowing-upward (Table 2). Goldhammer et al. (1990) found that shallowing-upward cycles are commonly covered by soil caps. Soils occur on top of subtidal units (as in the subtidal facies of the Dolomia Principale) or on top of laminites (as in the peritidal facies of the Dolomia Principale). Goldhammer et al. (1990) interpreted facies A as soil, although Fischer (1964) described as "reworked residue of weathered material". They also suggested that Lofer facies deposition was controlled by short-term variations in subsidence rate and found little evidence of Milankovitch-type orbital forcing (Table 2). Satterley (1996) stressed that evidence for subaerial exposure is usually absent and explained the importance of autocyclic and tectonic processes in generating small and large-scale cycles in the Upper Triassic of the Northern and Southern Alps (Table 2). Enos and Samankassou (1998) measured a section at Steinernes Meer near Fischer's and Satterley's sections. They focused on Member A because of its crucial importance in the interpretation of the Lofer cycles (shoaling or deepening upward). However, they did not recognize the member A. They found only B and C members and concluded that the sequence is thus rhytmic rather than cyclic. Later, they searched the lateral continuity of the beds in Steinernes Meer (Enos and Samankassou, 2002) and showed that most of the beds disappeared or the thicknesses are varied laterally. They reinforced Satterley's conclusion that autocyclic processes (e.g., tides or storms) may have played a major role in the deposition of the Lofer cycles (Table 2).

In the last decades, two main models were accepted for explaining the Lofer cycles: allocyclicity (Fischer, 1964, 1975; Haas, 1982, 1991; Schwarzacher and Haas, 1986; Balog et al., 1997; Cozzi et al., 2003; Haas, 2004; Haas et al., 2007) and autocyclicity (Satterley and Brandner, 1995; Satterley, 1996; Enos and Samankassou, 1998, 2002). In the allocyclic model, it was accepted that the orbitally forced sea-level oscillation controlled the formation of the Lofer cycles (Haas, 2004). On the other hand, autocyclic model (Ginsburg, 1971) was explained by the progradation of tidal flats as a result of landward movement of the carbonate sediment from the subtidal carbonate factory.

In order to decide whether the allocyclic model or the autocyclic one is more appropriate for sedimentation of Dachstein-type platform carbonates, Haas (2004) studied cycle-bounding erosion surfaces and the related peritidal facies. He described peritidal-subtidal (lagoonal) cycles which were bounded by well-developed disconformity surfaces. He suggested that the cycle-bounding disconformities are subaerial erosional surfaces in the non-dolomitised Dachstein Limestones and subaerial exposure conditions were accompanied by significant erosion. Therefore, he explained cycle-bounding disconformities as an evidence of eustatic control of the cyclicity and justified the application of allocyclic models (Table 2). Later, Haas et al. (2007) also focused on the boundaries of the Lofer cycles to discuss the patterns and origin of the Lofer cycles. They defined the boundaries as erosional disconformities showing features of karstification. The reddish or greenish argillaceous carbonate member (facies A) cannot be interpreted as paleosol-derived material in contrast to Fischer (1964), Goldhammer et al. (1990) etc. Facies A was represented by tidal flat deposit consisting predominantly of subtidal carbonate mud redeposited by storms. An ABC facies succession was found at the base of many cycles, suggesting a transgressive trend, and a regressive trend at the upper part of some cycles. They suggested periodical sea-level drop followed by renewed transgression and confirmed the allocyclic model for the explanation of the origin of Lofer cycles (Table 2).

Although there are so many sequence stratigraphic studies in Turkey (Table 3) (e.g., Çiner, 1996, Çiner et al., 1996a, 1996b, 2002, Bassant et al., 2005, Şafak et al., 2005, Ilgar and Nemec, 2005), the sequence stratigraphic studies on carbonates have been carried out by Altıner's research group http://www.metu.edu.tr/~wwwssm/ since 1997 (Table 3). They have discussed the cyclicity and sequence stratigraphy of the peritidal carbonates in southern Turkey.

Table 3. List of the sequence stratigrahic studies in Turkey.

RESEARCHERS	STUDY AREA	TIME INTERVAL
Çiner et al., 1996a	Haymana Basin, Ankara	Middle Eocene
Yılmaz, 1997 (MSc)	Central Taurides	U. Jurassic-U. Cretaceous
Akçar, 1998 (MSc)	Western Taurides	L. Cretaceous
Bayazıtoğlu, 1998(MSc)	Central Taurides	Aptian-Albian
Gaziulusoy, 1999 (MSc)	Western Taurides	Aptian-Albian
Altıner et al., 1999	Western Taurides	Kimmeridgian-Cenomanian
Varol et al., 2000	Western Pontides	L.Cretaceous- L. Eocene
Yılmaz and Altıner, 2001	Western Taurides	Kimmeridgian-Cenomanian
Çiner et al., 2002	Sivas Basin	Lower to Middle Miocene
Pütürgeli, 2002 (MSc)	Central Taurides	Midian (U. Permian)
Şen, 2002 (MSc)	Central Taurides	M. Carboniferous
Ünal et al., 2003	Central Taurides	Permian-Triassic
Bassant et al., 2005	Mut Basin	Burdigalian
Şafak et al., 2005	Mut Basin	Mid-Cenozoic
Ilgar and Nemec, 2005	Ermenek Basin	Early Miocene
Peynircioğlu, 2005(MSc)	Central Taurides	Tournasian-Visean
Atakul, 2006(MSc)	Central Taurides	Mid-Carboniferous
Yılmaz&Altıner, 2006a	Pontides	Barremian-Aptian
Yılmaz&Altıner, 2006b	Central Taurides	Mid-Aptian
Yılmaz&Altıner, 2007	Western Pontides	L. Cretaceous
Yılmaz, 2008	Western Sakarya	L.-U. Cretaceous
This study	Central& Western Taurides	Upper Norian-Rhaetian

Researchers carried out bed-scale studies and described the shallowing-upward character of metre-scale cycles. In different ages and areas of the Central Taurides, they studied Paleozoic to Upper Cretaceous carbonates in several M.Sc theisis (Yılmaz, 1997; Akçar, 1998; Bayazıtoğlu, 1998; Gaziulusoy, 1999; Pütürgeli, 2002; Şen, 2002; Peynircioğlu, 2005; Atakul, 2006). The high resolution sequence stratigraphic study on carbonates in Turkey was firstly published by Altıner et al. (1999) in which the Upper Jurassic-Upper Cretaceous sequence stratigraphic correlation of the peritidal carbonates in the Western Taurides were presented. Following, Yılmaz and Altıner (2001) defined the use of sedimentary structures in the recognition of sequence boundaries in the Upper Jurassic–Upper Cretaceous peritidal carbonates of the Central Taurides. The cyclic sedimentation across the Permian-Triassic boundary in the Central Taurides (Ünal et al., 2003), cyclic stratigraphy of paleokarst structures in Aptian peritidal carbonate successions in southwest Turkey (Yılmaz&Altıner, 2006a), cyclostratigraphy and sequence boundaries of Barremian-Aptian inner platform successions in northwestern Turkey (Yılmaz&Altıner, 2006b) were also investigated in southern Turkey.

Although there are many sequence stratigraphic studies on carbonates in southern Turkey, Upper Triassic peritidal carbonates have not been studied yet. The Upper Triassic peritidal successions, which consist of Lofer-type cycles, have been firstly investigated in this study.

1.5. REGIONAL GEOLOGICAL SETTING

The Taurides which is one of the major tectonic units of Turkey is divided into three parts based on their geological and morphological characteristics (Figure 3) as Western Taurides, Central Taurides and Eastern Taurides (Özgül, 1984).

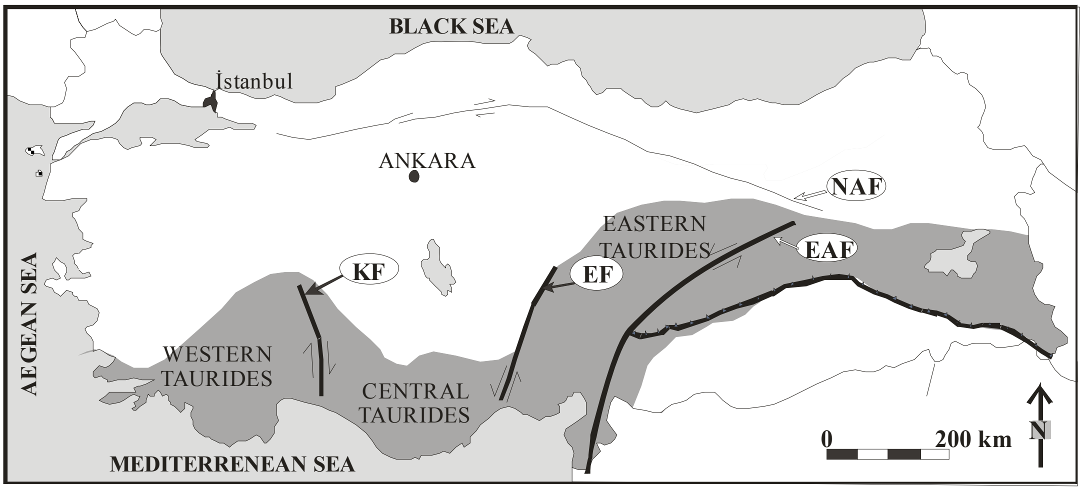

Figure 3. The broad geographical subdivision of the Tauride Belt (Özgül, 1984). (KF:Kırkkavak Fault, EF:Ecemiş Fault, EAF:East Anatolian Fault, NAF:North Anatolian Fault)

In the Western and Central Taurides, several units were distinguished based on their stratigraphic position, character of metamorphism, the rock units which they contain and their present structural position (Özgül, 1976). They were named as Bolkardağı Unit, Aladağ Unit, Geyikdağı Unit, Alanya Unit, Bozkır Unit and Antalya Unit. On the other hand, Brunn et al. (1971) defined allocthonous and autochthonous unitsappear with distinct stratigraphical, structural and metamorphic features (Özgül, 1976, 1984, 1997). These units are represented by autochthonous-paraautochthonous units (Anamas-Akseki Autochthon, Beydağları-Karacahisar Autochthon) and allochthonous units (Lycian Nappes, Antalya Nappes, Beyşehir-Hoyran-Hadim nappes, Alanya nappe) (Figure 4). Among these units, autochthonous units consist of platform-type deposits where as the nappes above them comprise oceanic crust, slope, basin, rift systems as well as parts of plaform-type deposits (Şenel et al., 1996).

In the Central Taurides, Beydağları-Karacahisar Autochthon, Anamas-Akseki Autochthon and Antalya Nappes are widely exposed (Figure 4).

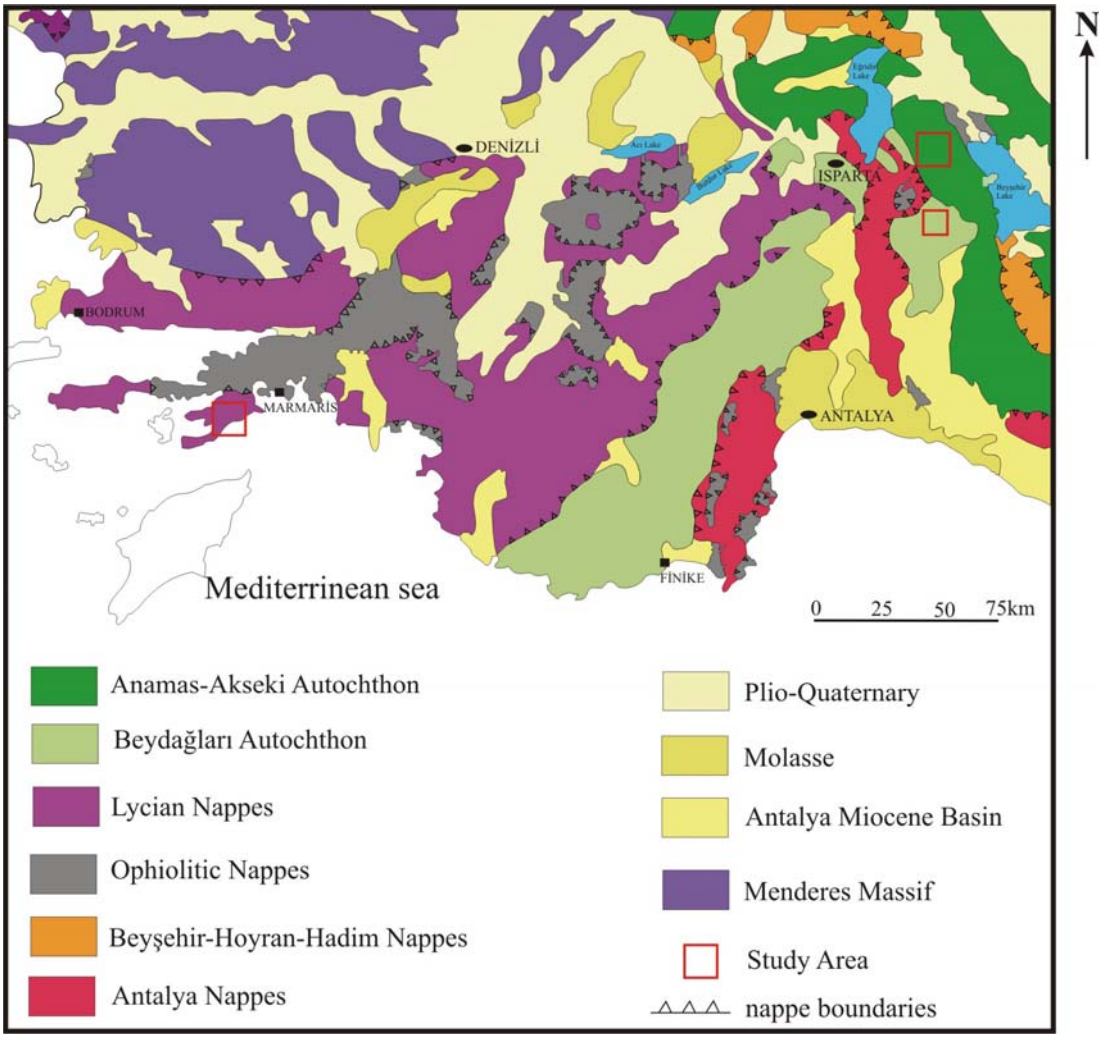

Figure 4. Geological map of the study area in the Central and Western Taurides (Şenel, 1997).

Antalya Nappes (Lefevre, 1967; Brunn et al. 1971) which is also known as the Antalya unit (Özgül, 1976), or “Antalya Complex” (Woodcock and Robertson, 1977) appear at the southern part of the Central Taurides (Figure 4). They were thrusted over the autochthonous units during the Lutetian time (Şenel et al., 1996) (Figure 5). They were subdivided into 3 units as the “Çataltepe Unit”, “Alakırçay

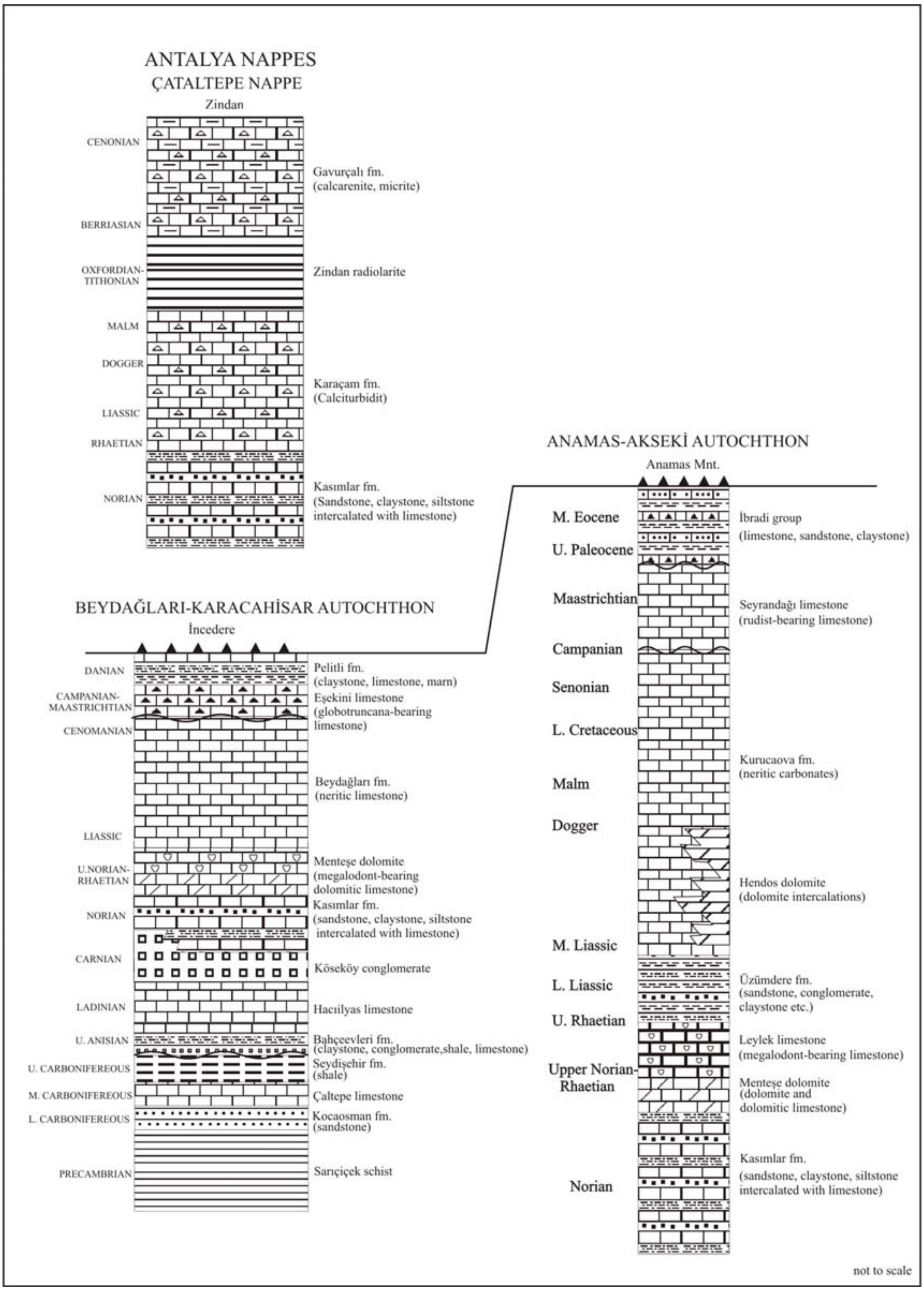

Figure 5 . Stratigraphic sections of the Anamas-Akseki Autochthon, Beydağları-Karacahisar Autochthon and the Antalya Nappes (simplified from Şenel et al., 1996).

Unit" and the "Tahtalıdağ Unit" by Brunn et al. (1971). Şenel et al. (1992) differentiated them as the "Çataltepe Nappe", "Alakırçay Nappe", "Tahtalıdağ Nappe and the "Tekirova Ophiolitic Nappe" based on their stratigraphical and lithological properties. Çataltepe Nappe is the lowermost unit of the Antalya Nappes and contains late Triassic shelf deposit and Jurassic-Cretaceous slope and basinal deposits (Şenel et al., 1996). 6 structural units were identified: Şeyhdere, Sofular, Zindan, Yaka, Yılanlı and Kocakulak unit. Among these units, Zindan unit, which can be recognized at the western part of the study area, contains Kasımlar Formation, Karaçam formation, Zindan radiolarites and Gavurçalı formation (Figure 5). Kasımlar formation is composed of plant-bearing sandstones, siltstones and claystones with intercalations of limestones. Karaçam formation consists of calcirudites and calcarenites. Zindan radiolarites contains cherts and the Gavurçalı Formation consists of calcarenites and micrites.

Beydağları-Karacahisar autochthon was named as the "Karacahisar unit" by Dumont and Kerey (1975) and "Geyik Dağı Unit" by Özgül (1976). It can be seen as tectonic windows (Şenel et al., 1996) under the Antalya Nappes. The succession is mainly represented by Precambrian-Cambrian, Carboniferous and Middle Triassic-Lower Paleocene units (Figure 5). It consists of Sarıçiçek shists, Kocaosman Formation, Seydişehir Formation, Bahçeevleri Formation, Hacıilyas Limestone, Köseköy Conglomerate, Kasımlar Formation, Menteşe Dolomite, Beydağları Formation, Eşekini Limestone and Pelitli Formation. The Upper Triassic units belong to the Kasımlar formation and Menteşe Dolomites. Kasımlar formation of Norian age is composed mainly of claystone, siltstone and sandstone with limestone intercalations (Figure 5). The Upper Norian-Rhaetian Menteşe Dolomite comprises basically dolomites and dolomitic limestones with megalodont and stromatolites. The overlying Jurassic-Cretaceous Beydağları formation contains thick neritic carbonates. The Campanian-Maastrichtian Eşekini Limestone includes cherty micrites and the Danian Pelitli Formation consist of claystone, clayey limestone, sandstone and conglomerates (Figure 5).

Anamas-Akseki Autochthon, one of the paraautochthonous units of the Central Taurides, is composed of platform-type carbonates with a Lower Paleozoic basement of Cambrian and Ordovician rocks and a transgressive Mesozoic-Lower Tertiary made up largely of carbonates (Özgül, 1984). This unit was also named as the "Anamas-Akseki Unit" by Dumont (1976) and the "Geyik Dağı Unit" by Özgül

(1976). The Mesozoic successions of this unit lies with an unconformity over the Lower Paleozoic basement. Although the Paleozoic basement rocks crop out in the Seydişehir (Monod, 1977) and Sultan Mountains (Haude, 1972), in the studied region at Anamas Dağ, the base of the study area is made up of Upper Triassic rocks (Figure 5). The succession includes Kasımlar formation, Menteşe Dolomites, Leylek Limestone, Üzümdere formation, Hendos Dolomite, Kurucaova formation, Seyrandağı Limestone and İbradi Group (Şenel et al., 1996). The megalodont-bearing limestones which were named as Menteşe Dolomite in the Beydağları-Karacahisar Autochthon were differentiated as Leylek Limestone in the Anamas-Akseki Autochthon. The Upper Norian-Rhaetian deposits of the Leylek Limestone is composed of cyclic carbonates with megalodont and stromatolites (Monod, 1977). Succeeding rocks consist of the Upper Rhaetian-Liassic Üzümdere formation which includes sandstone, claystone, conglomerate and limestone. The Kurucaova formation of Jurassic-Cretaceous age is composed of neritic limestone and laterally intercalated with Hendos Dolomite. Seyrandağı Limestone includes rudist-bearing limestone and unconformably overlying by İbradi Group, having limestone, sandstone, claystone etc (Şenel et al., 1996).

In the Western Taurides, Lycian Nappes and Marmaris Ophiolitic Nappes are widely exposed (Figure 4). Lycian Nappes are represented by Bodrum nappe, Gülbahar nappe and Marmaris ophiolitic nappes in the study area (Şenel, 1997) (Figure 6). Marmaris Ophiolitic Nappe forms the uppermost Lycian Nappe pile and consists of Kızılcadağ melange and olistostrome with Marmaris peridotites (Figure 6). Gülbahar Nappe is situated between the Marmaris Ophiolitic Nappes and the Bodrum Nappe and composed of Turunç and Ağla units (Figure 6). At last, Bodrum nappe is represented by Çökek and Bozburun units. Bozburun unit consists of the Middle-Upper Triassic Bayırköy formation, Upper Triassic-Liassic Güverdağı Formation and Upper Cenonian Karanasıflar Formation (Figure 6). The Carnian-Norian of Bayırköy Formation is composed of dolomite, claystone and siltstone. The overlying Upper Triassic-Liassic Güverdağı Formation includes megalodont-bearing algal limestones (Bilgin et al., 1997). It contains ammonotico-rosso facies in the upper levels. Unconformably succeeding Karanasıflar Formation of Late Cenonian age comprises mainly limestone and cherty breccia (Figure 6).

Within the broad geological frame, this study mainly focuses on the megalodont-bearing limestones, namely the Leylek Limestone, Menteşe Dolomite and the Güverdağı Formation within the Upper Norian-Rhaetian peritidal successions of the Anamas-Akseki Autochthon and the Beydağları-Karacahisar Autochthon in the Central Taurides and the Lycian Nappes in the Western Taurides, respectively.

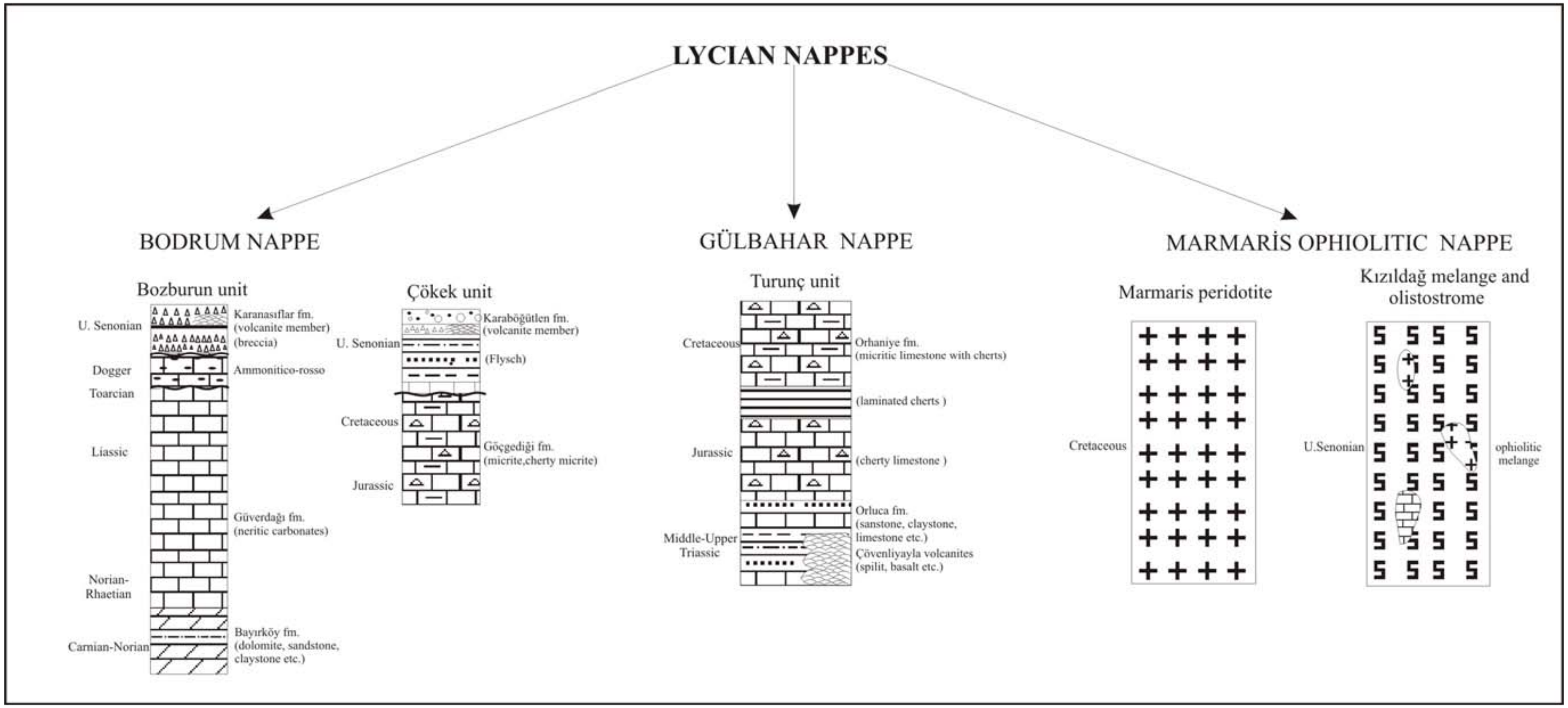

Figure 6. Some of the structural units of the Lycian Nappes in the Western Taurides (simplified from Şenel & Bilgin, 1997)

CHAPTER 2

2. STRATIGRAPHY

2.1 Lithostratigraphy

2.1.1 Stratigraphy in the Central Taurides

The study area in the Central Taurides consist of Upper Triassic-Eocene deposits of the Anamas-Akseki Autochthon and the Precambrian-Paleocene deposits of the Beydağları-Karacahisar Autocthon (Figure 7, 8). The Upper Triassic (Norian-Rhaetian) units are mainly represented by platform-type carbonates within these successions. In the Anamas-Akseki Autochthon, the succession starts with the Kasımlar formation which is composed of plant remain bearing sandstone, siltstone and claystone intercalated with limestone (Figure 9). The overlying Menteşe Dolomite of Upper Norian-Rhaetian age contains dolomite, dolomitic limestone and pass upward into the Leylek Limestone which consists of megalodont-bearing cyclic carbonates (Figure 9). Gradually succeeding unit Üzümdere formation of latest Rhaetian-Liassic age includes sandstone, claystone and limestone (Figure 9). The succession continues with Kurucaova formation with neritic carbonates, Seyrandağı Limestone with rudist-bearing limestone and the İbradi Group with limestone, sandstone and claystone (Figure 9). Among these formations, Seyrandağı Limestone and the İbradi Group are exposed outside of the study area (Şenel et al., 1996).

In the Beydağları-Karacahisar Autochthon, although the succession starts with Sarıçiçek Shists (Precambrian), Kocaosman Formation (Lower Carbonifereous), Çaltepe Limestone (Middle Carboniferous), Seydişehir Formation (Upper Carboniferous-Ordovician), Bahçeevleri Formation (Upper Anisian), Hacıilyas Limestone (Ladinian) and Köseköy conglomerates (Carnian) (Şenel et al., 1996), they are not exposed in the study area and they are not explained in this chapter (Figure10).

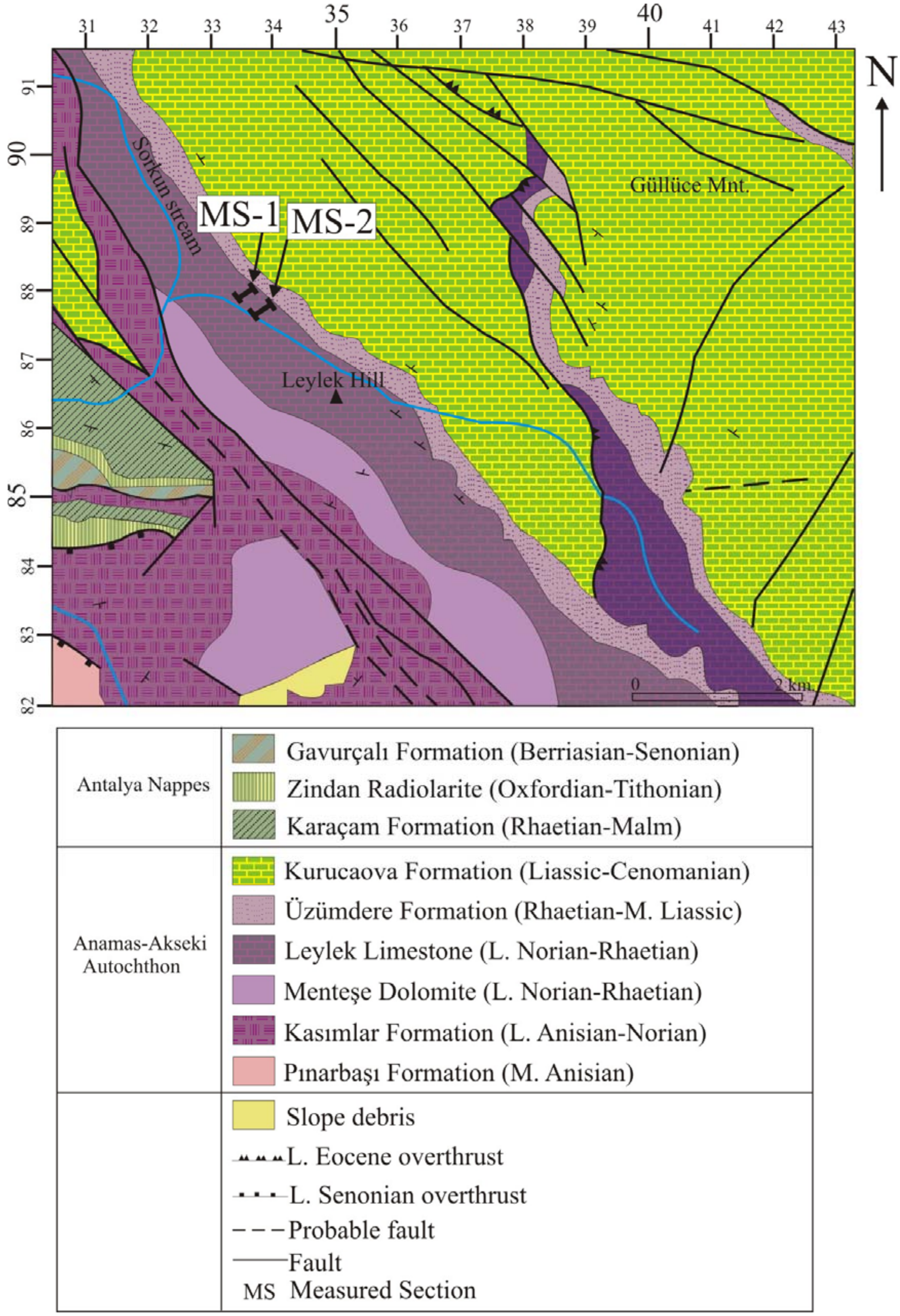

Figure 7. Geological map of the study area in the Anamas-Akseki Autochthon (Şenel, 1997).

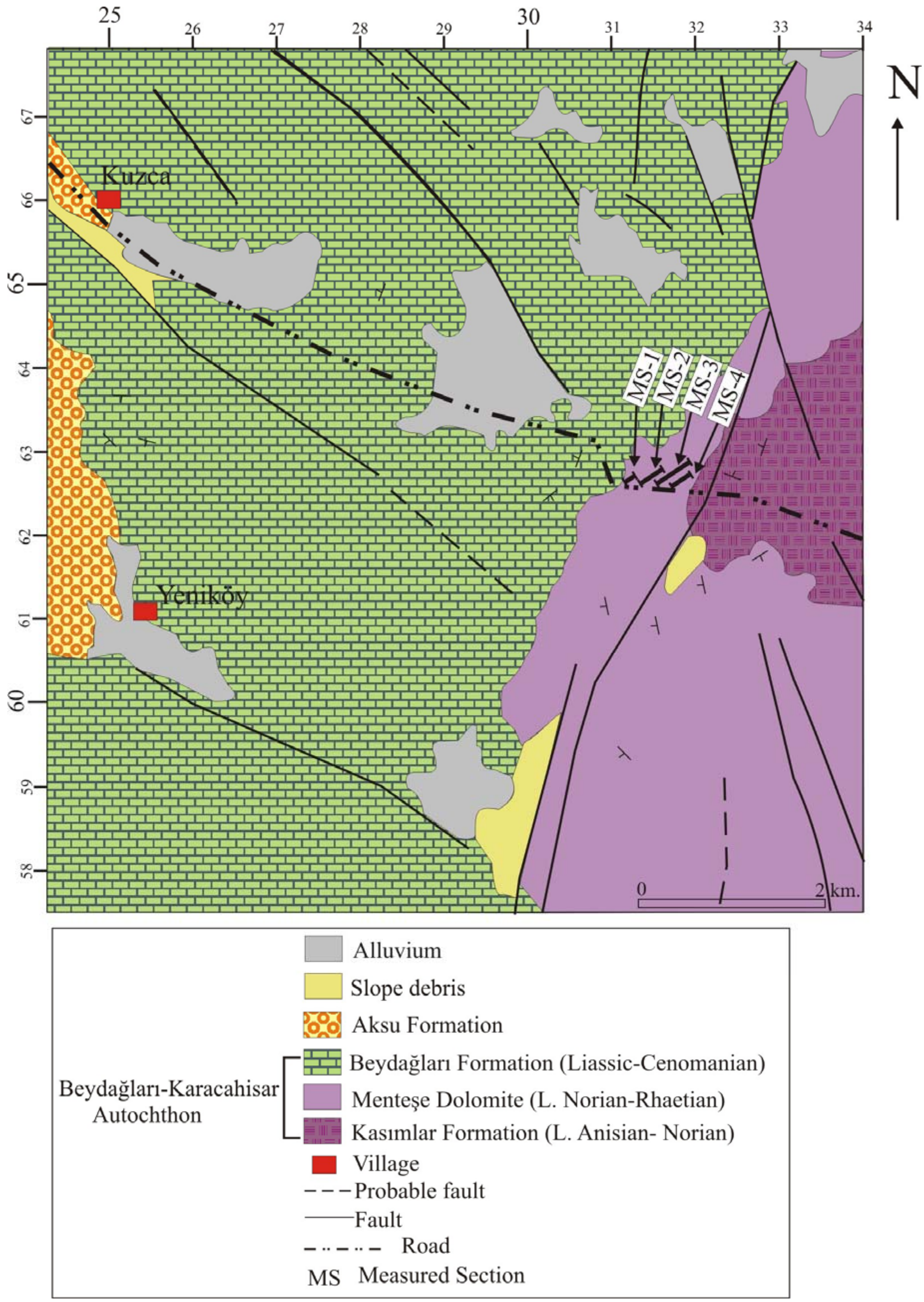

Figure 8. Geological map of the study area in the Beydağları-Karacahisar Autocthon (Şenel, 1997).

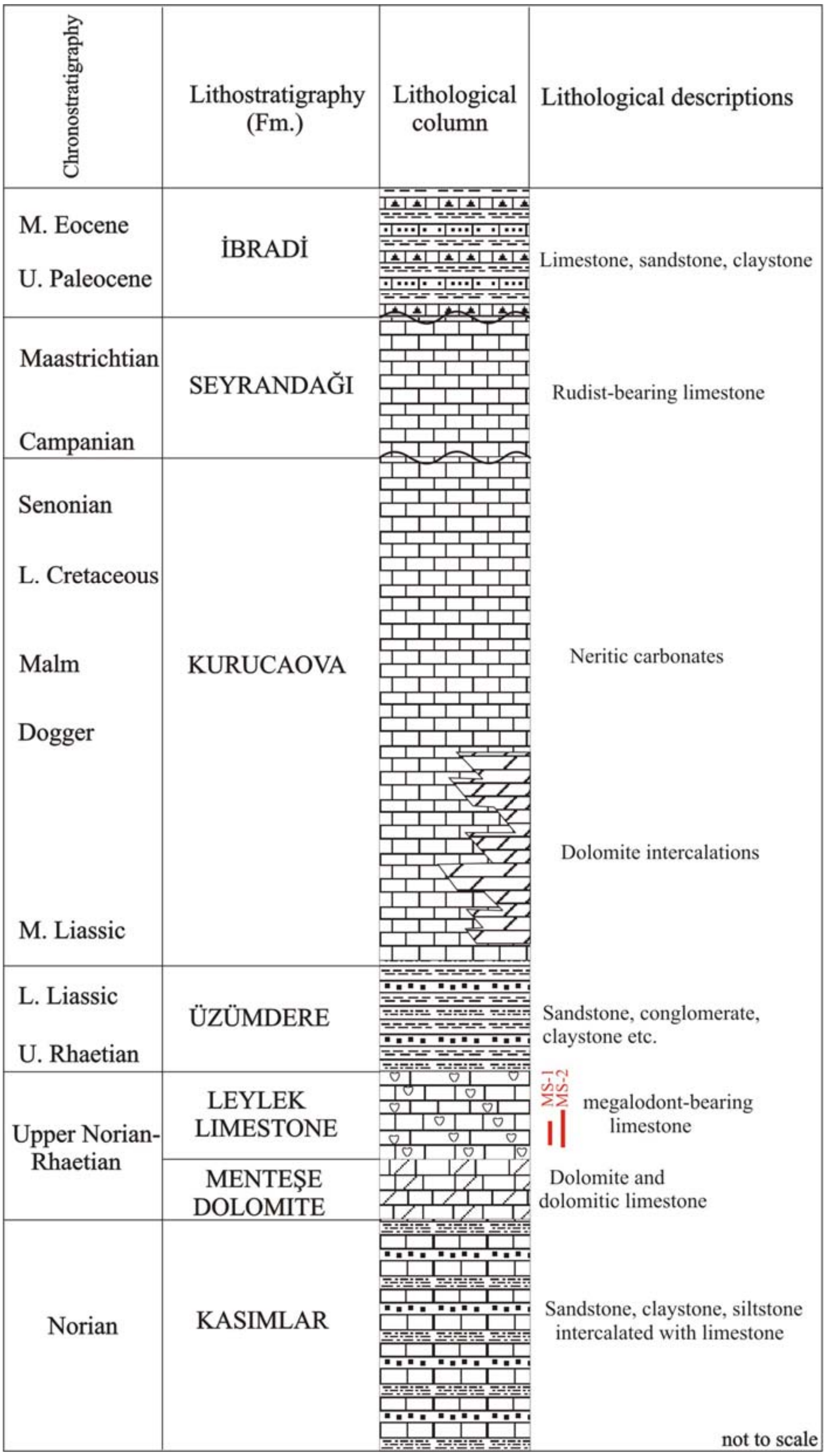

Figure 9. Generalized stratigraphic columnar section of the Anamas Mountain in the Central Taurides (Şenel et al., 1996), showing the locations of the measured sections (MS).

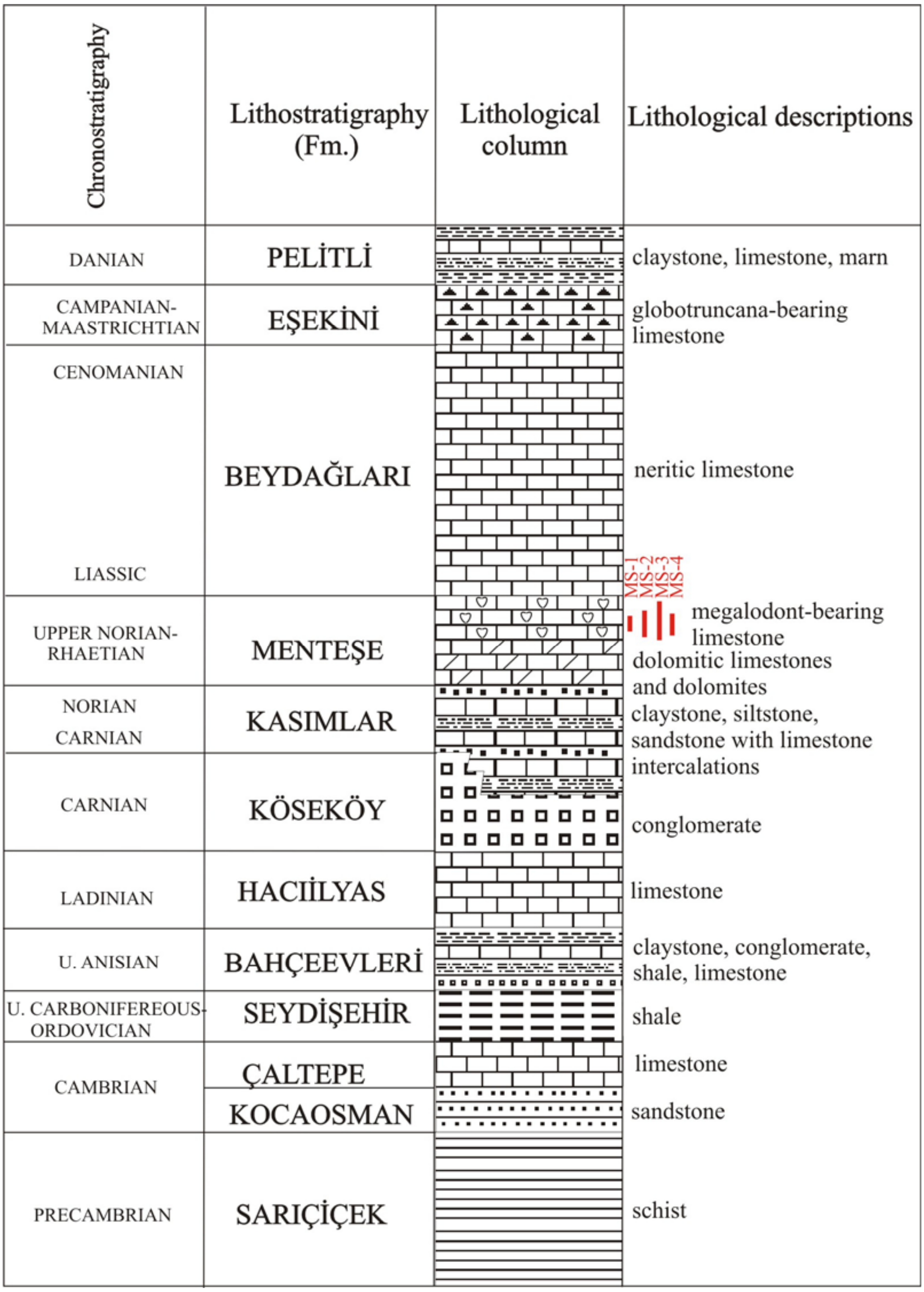

Figure 10. Generalized stratigraphic columnar section of the Beydağları-Karacahisar Autocthon in the Central Taurides (Şenel et al., 1996), showing the locations of the measured sections (MS).

The overlying Kasımlar formation is the same unit defined in the Anamas-Akseki Autochthon (Şenel et al., 1996). Menteşe Dolomite conformably overlies the Kasımlar formation which is mainly composed of dolomites, dolomitic limestones and megalodont-bearing limestone (Figure 10). The succession continues with the Beydağları formation of Jurassic-Cretaceous age, comprising thick carbonates (Figure 10). Succeeding units are the Eşekini Limestone of Campanian-Maastrichtian age which includes *Globotruncana*-bearing limestone and Pelitli Formation of Danian age with claystone, clayey limestone, sandstone and conglomerate (Figure 10). They are also exposed outside of the study area.

Among these formations, one of our study area is in the Upper Norian-Rhaetian carbonates of the Leylek Limestone of the Anamas-Akseki Autochthon (Figure 9) and the other is in the Upper Norian-Rhaetian carbonates of the Menteşe Dolomite of the Beydağları-Karacahisar Autochthon (Figure 10). Within this generalized stratigraphic framework, the studied successions were measured in megalodont-bearing carbonates in order to document the Lofer cyclicity in the Upper Triassic (Upper Norian-Rhaetian).

2.1.1.1 Kasımlar Formation

Kasımlar formation was named by Dumont & Kerey (1975). The type section is located in the Yakaafşar village in the Anamas Mountain. The thickness was measured as 1200-1500 m. In the type section, the formation was represented by plant remain bearing sandstones, siltstones and claystones with intercalations of limestones (Figuer 9, 10). Towards the top of the formation, limestones sometimes contain reefoidal blocks (Gutnic et al., 1979). Kasımlar formation overlies the Köseköy Conglomerates (Carnian) in the Beydağları-Karacahisar Autochthon (Figure 10), but it constitutes the basement rocks in the Anamas Mountain (Figure 9) (Şenel et al., 1996). The formation is conformably overlain by the Menteşe Dolomites (Gutnic et al., 1979) both in the Anamas-Akseki Autochthon and the Beydağları-Karacahisar Autochthon (Figure 9, 10). In the Anamas Mountain, Kasımlar formation contains mainly the *Halobia*, *Heterestridium* etc. (Gutnic et al., 1979) and also include plant remains within the sandstones. Based on the paleontological data, Kasımlar formation is Late Anisian-Norian in age. This formation was deposited in a shelf to slope environment (Şenel, 1997).

2.1.1.2 Menteşe Dolomite

Menteşe Dolomite was described by Dumont and Kerey (1975). The type section is situated in the southern part of the Kınık Tepe near Yakaafşar village (Şenel et al., 1992). Although the Menteşe Dolomites were defined as comprising the megalodont-bearing limestones in the Beydağları-Karacahisar Autochthon (Figure 10), the uppermost levels were named as Leylek Limestone in the Anamas Mountain (Şenel et al., 1996) (Figure 9). The thickness of this formation varies between 300-550 m. It consists of dolomites in the lower levels and megalodont-bearing limestones and dolomitic limestones in the upper levels (Monod, 1977). This formation conformably overlies the Kasımlar formation and is overlain by the Beydağları formation in the Beydağları-Karacahisar Autochthon (Figure 10) and also overlain by the Leylek Limestone in the Anamas-Akseki Autochthon (Figure 9). Based on the foraminiferal fauna (*Triasina hantkeni*, Involutinidae etc.), Menteşe Dolomite is Late Norian-Rhaetian in age. It was deposited in a shallow marine depositional settings (Şenel, 1997).

Within this formation, 4 meter-scale section were measured. The measured sections are composed of big megalodont-bearing limestones (Figure 11) and also stromatolites, fenestral limestones and levels with vadose pisoids. Megalodont-bearing limestone is commonly thick and consists of bioclastic wackestone and packstone with foraminifer, gastropoda, echinoid etc. A red colored vadose pisoidic level is also recognized in one of the measured section which may correspond to an important sea level fall in the Upper Norian-Rhaetian (Figure 12). Furthermore, Lofer-type cyclicity is determined in the Menteşe Dolomite. The microfossils, involutinids in particular, are abundant in the megalodont-bearing levels. According to the determined fauna (*Triasina hantkeni*, *Auloconus permodiscoides*, *Aulotortus* gr. *sinuosus* etc.), the measured portion of the Menteşe Dolomite is Late Norian-Rhaetian in age and based on the microfacies analysis which will be desribed in the next chapter, this formation was deposited in a shallow marine, peritidal environment.

Figure 11. Outcrop view of megalodont-bearing limestones (m) in the Menteşe Dolomite (Kuzca-3 Section, Sample No. K-41).

Figure 12. Field photograph of the vadose pisoids in the Menteşe Dolomite, indicating a sea level fall in the Late Norian-Rhaetian (Kuzca-4 Section, Sample No. K-45R, K-45S).

2.1.1.3 Leylek Limestone

The megalodont-bearing limestones were named as the Leylek Limestone (Vegh-Neubrandt et al., 1976) in the Anamas Mountain. Later, it was described by Gutnic et al. (1979) in the southern part of the Anamas Mountain. The type section was described in the Leylek Hill and the thickness was measured 250 m. It is characterized by megalodont-bearing limestones. The succession starts with the dolomite and dolomitic limestone alternation at the base and ends with fossilifereous, megalodont-bearing limestones, dolomitic limestones and clayey limestones (Şenel et al., 1996). It contains stromatolites, loferites, megalodonts and corresponds to the Dachsteinkalk succesions (Gutnic et al., 1979). Leylek Limestone conformably overlies the Menteşe Dolomite (Dumont and Kerey, 1975) and is conformably overlain by the Üzümdere formation (Figure 9). Based on the foraminiferal fauna (*Triasina hantkeni*, Involutinidae), Leylek Limestone is Late Norian-Rhaetian in age. It was deposited in a shallow marine environment (Şenel et al., 1996).

Within the Leylek Limestone, 2 meter-scale sections and some other more detailed sections were measured. The succession consists of the alternation of the carbonates and the claystones. Carbonates are thick and composed of mainly big megalodont-bearing limestones and also contain stromatolites, fenestral limestones, dolomitic limestones and breccias (Figure 13, 14). The megalodont-bearing limestones are commonly pelloidal bioclastic wackestone-packstone in character and have abundant involutinids. On the other hand, the clay levels are very thin and green in color. They are commonly overlying the stromatolites and are overlain by megalodont-bearing limestones. The studied successions in the Leylek Limestone also show Lofer-type cyclicity as in the Menteşe Dolomite. The megalodont-bearing levels contain abundant microfossils, involutinids in particular. Based on the foraminiferal fauna determined in this study (*Triasina hantkeni*, *Auloconus permodiscoides* etc.), the Leylek Limestone is found to be Late Norian-Rhaetian in age and based on the microfacies analysis which will be desribed in the next chapter, this formation was deposited in a shallow marine, peritidal environment.

Figure 13. Outcrop view of the stromatolite (s) in the Leylek Limestone which overlies the fenestral limestone (f) (Leylek-1 Section, Sample No. B-45, B-46).

Figure 14. Outcrop view of the fenestral limestone (f), breccioid limestone (b) which are overlain by subtidal facies (s) in the Menteşe Dolomite (Kuzca-1 Section, Sample No. K-4, K-5 and K-6).

2.1.1.4 Üzümdere Formation

This formation was investigated by Ziegler (1938) in the northwestern part of the Akseki town. The type section is located in the Sorkun Plateau (Gutnic et al., 1979) and the thickness was measured as 370 m (Şenel et al., 1992). Üzümdere formation consists of sandstone, conglomerate, claystone and limestone (Şenel, 1997). The limestones, interlayered with sandstone, mudstone and sandy limestones consist of wackestone-packstone, floatstone and grainstone with foraminifer, gastropod, megalodont, crinoid and dascylad algal fragments and carbonate mudstone with fenestral structure. The coal bearing detritics are made up of red to green mudstones and claystones with sandstone interlayers. Upper levels of the formation is composed of grainstones and wackestones with gastropoda, algae, echinoid and foraminifer (Şenel, 1997). This formation conformably overlies the Leylek Limestone and is overlain by the Kurucaova formation (Figure 9). Triassic-Liassic transition layers which include the Rhaetian and middle Liassic foraminiferal-algal assemblage appear within this formation (Işıntek et al., 2005). The Rhaetian foraminiferal fauna consists of *Endoteba* sp., *Endotebanella* sp., *Gandinella* sp., *Aulotortus friedli*, *Aulotortus* gr. *sinuosus*, *Triasina hantkeni* and some other associated foraminifers. The middle Liassic fossil assemblage consists of *Earlandia* sp., *Mayncina termieri*, *Pseudocyclammina liassica*, *Siphovalvulina* sp. etc. (Işıntek et al., 2005). Based on the fossil content, Üzümdere formation is Rhaetian-Middle Liassic in age. It was deposited in a shallow water to beach marine environment and more or less connected with terrigenous systems (Işıntek et al., 2005).

2.1.1.5 Kurucaova Formation

Kurucaova formation was described by Şenel et al. (1992). The thickness was measured as 1700 m. It consists of neritic limestones and laterally intercalated with Hendos Dolomite which is mainly composed of dolomites. It caps the Üzümdere formation conformably (Şenel et al., 1992) and unconformably overlain by Seyrandağı Formation (Figure 9). According to the fossil content, *Paleodasycladus mediterraneus*, *Pseudocyclammina liassica*, *Haurania* sp., *Orbitopsella* sp., *Mesoendothyra croatica*, *Salpingoporella annulata*, *Cuneolina pavonia*, *Debarina* *hahounerensis* etc., the age of the Kurucaova formation is middle Liassic-Cenomanian (Şenel et al., 1996). It was deposited in a shallow marine depositional settings (Şenel, 1997).

2.1.2 Stratigraphy in the Western Taurides

The study area is located on Lycian Nappes which is widely exposed in the Western Taurides (Figure 15). The studied successions consist of Upper Triassic-Eocene deposits of the Lycian Nappes (Şenel and Bilgin, 1997) in which the Upper Triassic units are represented by neritic carbonates (Figure 16). The succesion starts with Bayırköy Formation of Middle-Late Triassic age which contains dolomite, claystone and siltstone (Figure 16). The overlying Güverdağı Formation of Late Triassic-Liassic age includes neritic limestones and contain megalodont-bearing carbonates in the lower levels (Figure 16). The upper levels consist of ammonit-bearing limestones (ammonotico-rosso facies) which is Toarcian-Dogger in age (Figure 16). The succesion ends with Late Senonian Karanasıflar Formation, consisting of breccias (Şenel and Bilgin, 1997).

2.1.2.1 Bayırköy Formation

Bayırköy Formation was described by Bilgin et al. (1997). The thickness is 120 m (Şenel ve Bilgin, 1997) and the type section is located in the southern part of the Bayırköy village. The formation consists of dolomites, dolomitic limestones, siltstones, claystones, clayey limestones and recrystalized limestones (Şenel ve Bilgin, 1997). In the upper levels dolomite and dolomitic limestone increase (Figure16). Occasionally limestones contain lamellibranch and radiolarians. The basement rocks are constituted by Bayırköy Formation in the study area and it is conformably overlain by Güverdağı Formation. Based on the fossil content (*Aulotortus* gr. *sinuosus*, *Glomospira* sp., *Macroporella* sp. etc.) and the age is Carnian-Norian (Bilgin et al., 1997). Bayırköy Formation was deposited in a shelf-slope environment (Şenel & Bilgin, 1997).

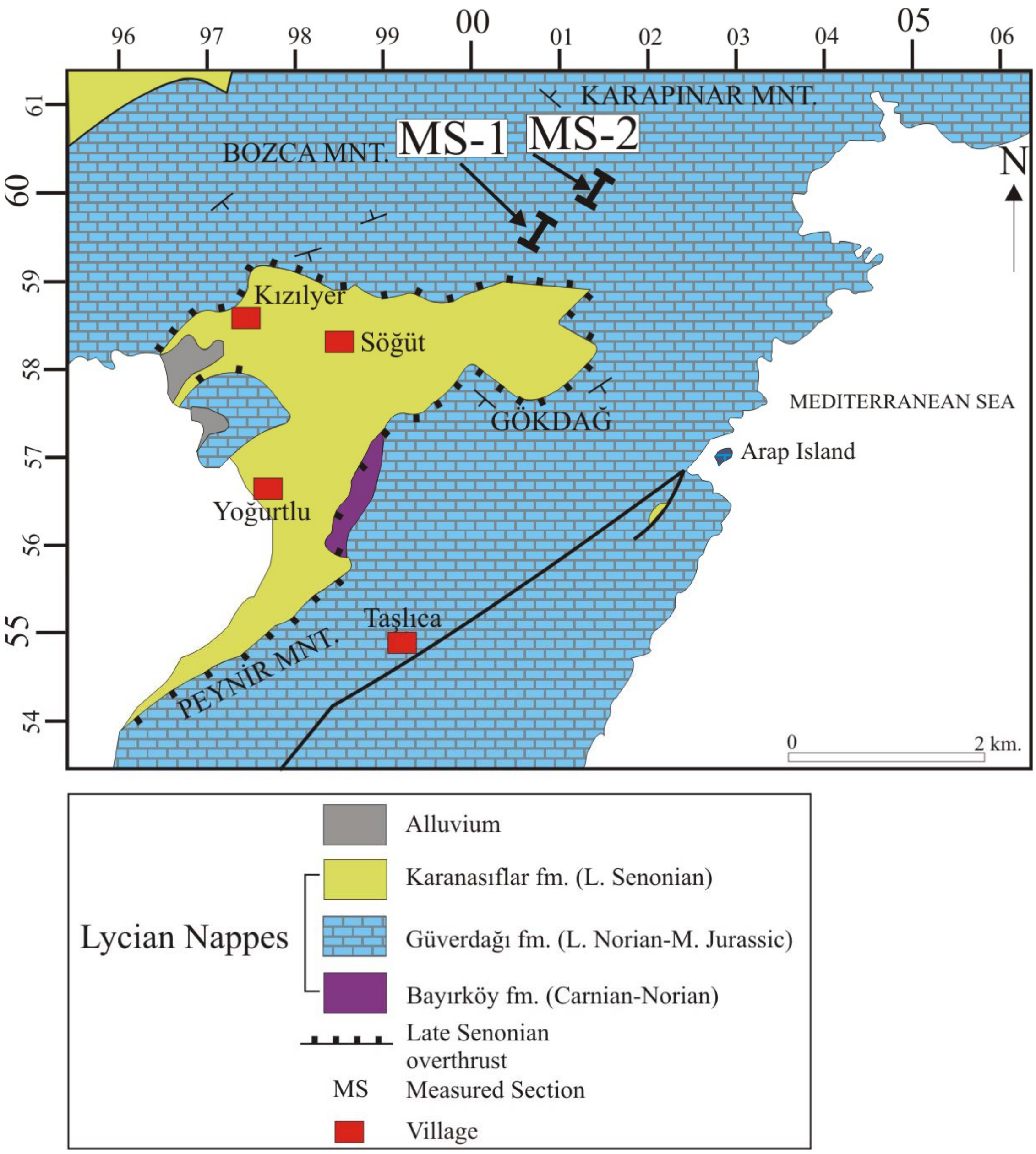

Figure 15. Geological map of the study area in the Lycian nappes (Şenel & Bilgin, 1997).

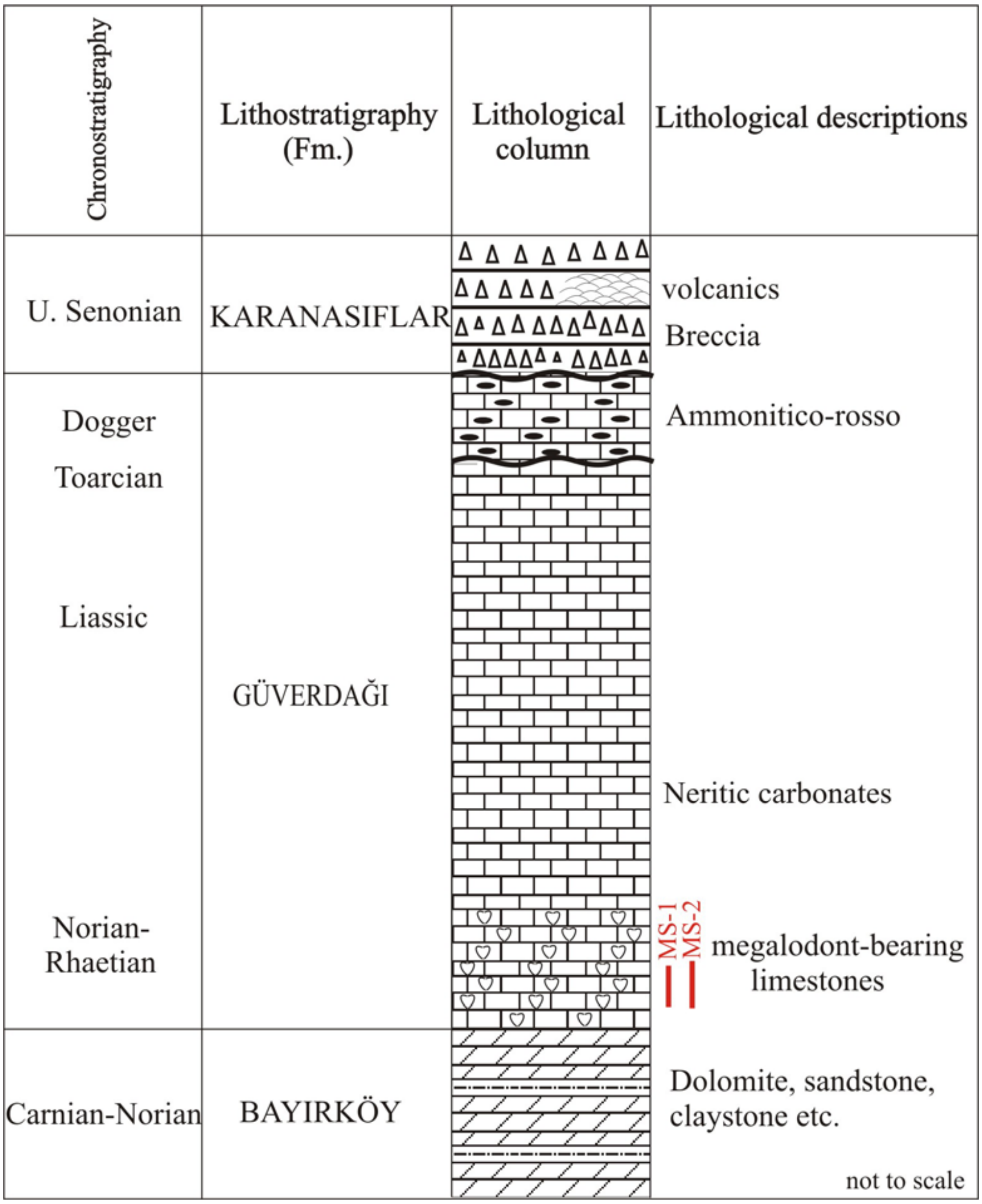

Figure 16. Generalized stratigraphic columnar section of the study area in the Western Taurides (Bilgin et al., 1997), showing the location of the measured sections (MS).

2.1.2.2 Güverdağı Formation

Güverdağı Formation was defined by Bilgin et al. (1997). The thickness was measured 800 m. The type section can be barely seen around the Güverdağı, because of the massif and fractured appeareance of this formation Bilgin et al. (1997). The succession starts with neritic carbonates and ends with ammonit-bearing limestone (Figure 16). The Upper Norian-Rhaetian part of the formation consists of megalodont-bearing limestones (Figure 17), dolomitic limestones, fenestral limestones, breccias and stromatolites. The studied successions display the Lofer cyclicity. Güverdağı Formation conformably overlies the Bayırköy Formation and is unconformably overlain by the Karanasıflar Formation (Figure 16). Especially, the megalodont-bearing limestones contain abundant involutinids (*Triasina hantkeni*, *Aulotortus* gr. *sinuosus* etc.) and the age is found to be Upper Norian-Rhaetian in these portions. Towards the upper parts, on the basis of the foraminiferal fauna *Involutina liassica*, *Planiinvolutina* sp. etc., the age is found to be Liassic. Güverdağı Formation was deposited in a shallow marine depositional settings (Bilgin et al., 1997).

Within the megalodont-bearing limestone of the Güverdağı Formation, 2 meter-scale sections were measured. The successions mainly consist of dolomitic limestone, stromatolite (Figure 18), fenestral limestone and breccia. The limestones are composed of wackestone and packstone lithofacies with big megalodonts (Figure 17), foraminifers etc. They also show Lofer-type cyclicity as in the Menteşe Dolomite and the Leylek Limestone. According to the determined foraminiferal fauna, the measured portion of the Güverdağı Formation is Late Norian-Rhaetian in age and based on the microfacies analysis, it was deposited in a shallow marine, peritidal environment.

Figure 17. The megalodont-bearing limestone in the Güverdağı Formation (Sample No. M-95).

Figure 18. The stromatolitic level (s) in the Güverdağı Formation which overlies the megalodont-bearing limestone (m) (Sample No. M-88, M-89).

2.1.2.3 Karanasıflar Formation

This formation was named by Şenel et al. (1989) at the north of Fethiye. The thickness was measured 700m. The type section is located in the Osmaniye. It is composed of breccia which contains limestone and chert fragments (Şenel and Bilgin, 1997). At the bottom of the formation, red colored *Globotruncana*-bearing micrites are present. Volcanics are also recognized within the breccia levels. Karanasıflar Formation unconformably overlies the Güverdağı Formation (Figure 16) and passes into the Karaböğürtlen formation in the lateral direction (Şenel and Bilgin, 1997) which is exposed outside of the study area. Karanasıflar Formation is unfossilifereous but Late Senonian age is accepted (Şenel et al., 1994).

2.2. Biostratigraphy

The big megalodont-bearing carbonates of the Central and Western Taurides are mainly represented by Late Norian-Rhaetian foraminiferal assemblage consisting of *Triasina hantkeni* Majzon, 1955, together with *Aulotortus communis* (Kristan, 1957), *Aulotortus* gr. *sinuosus* Weynschenk, 1956, *Aulotortus tenuis* (Kristan, 1957), *Aulotortus tumidus* (Kristan-Tollmann, 1964), *Aulotortus friedli* (Kristan-Tollmann, 1962), *Aulotortus gaschei* (Koehn-Zaninetti et Brönnimann, 1968), *Aulotortus praegaschei* (Koehn-Zaninetti, 1968), *Aulotortus impressus* (Kristan-Tollmann, 1964), *Aulotortus sinuosus pragsoides* (Oberhauser, 1964), *Aulotortus sinuosus oberhauseri* (Salaj in Salaj, Biely & Bistricky, 1967), *Auloconus permodiscoides* (Oberhauser, 1964). In addition, nodosarids, trochamminids and ammodiscids are also present in the studied successions. The involutinids are commonly strongly recrystalized. This association is dominated by *Aulotortus*. *Triasina hantkeni* is less common and the *Auloconus* is very rare. The age indicated by the foraminiferal association is Late Norian-Rhaetian which are mainly found in the megalodont-bearing limestones consisting of wackestones to packstones with abundant involutinids. This microfacies is defined usually within a micritic matrix and peloids, rare intraclasts also occur within them. The biogenic compounds are mainly foraminifers, together with rare gastropods and algae. The foraminiferal association defined in the studied successions is similar with the foraminiferal associations determined in the lagoonal depositional settings (e.g., Martini et al., 1997; 2004;

Işıntek, 2002). The rich association of involutinids characterizes the megalodont-bearing wackestone-packstone facies which indicates a low enegy environmental conditions, protected from open marine and reefal influences. In addition, the depositional environment corresponds to the restricted-platform interior (FZ 8) zone of the Standard Facies Zones of Flügel (2004) within a rimmed carbonate platform. High number of shallow marine biota within a micritic, pelloidal wackestone-packstone facies, lime mudstone facies are the common lithofacies types showing restricted-platform interior conditions.

2.2.1. *Triasina hantkeni* assemblage zone

In the measured sections one biozone has been established based on the benthic foraminifer *Triasina hantkeni* Majzon. This biozone encompasses the Late Norian-Rhaetian interval and characterized by the *Triasina hantkeni* assemblage zone (Table 4). *Triasina hantkeni* assemblage zone is characterized by the first appereance of *Triasina hantkeni* Majzon and the last appereance of Late Triassic foraminifers in the studied successions (*Aulotortus communis* (Kristan, 1957), *Aulotortus* gr. *sinuosus* Weynschenk, 1956, *Aulotortus tenuis* (Kristan, 1957), *Aulotortus tumidus* (Kristan-Tollmann, 1964), *Aulotortus friedli* (Kristan-Tollmann, 1962), *Aulotortus gaschei* (Koehn-Zaninetti et Brönnimann, 1968), *Aulotortus praegaschei* (Koehn-Zaninetti, 1968), *Aulotortus impressus* (Kristan-Tollmann, 1964), *Aulotortus sinuosus pragsoides* (Oberhauser, 1964), *Aulotortus sinuosus oberhauseri* (Salaj in Salaj, Biely & Bistricky, 1967), *Auloconus permodiscoides* (Oberhauser, 1964)). This zone is determined in the Leylek-1, Leylek-2, Kuzca-2, Kuzca-3, Marmaris-1 and Marmaris-2 sections (Table 5, 6, 7, 8, 9, 10). The distribution of the foraminifers along the sections is irregular (Table 5-14) and especially in some sections, the lower parts of the sections are on debate. For this reason, assemblage zone is used for the Late Norian-Rhaetian biozone definition and the lower part of the sections is attributed to undifferentiated Norian in the measured sections (Table 5, 6, 7, 8, 9, 10). *Triasina hantkeni* Majzon biozone was firstly described from the western Carpathians as a range zone in the Rhaetian (Salaj, 1969) (Table 4). Following, Zaninetti (1976) defined *Triasina hantkeni* Majzon in the Late Norian-Rhaetian of Europe, Tunisia and Turkey. Al-Shaibani et al. (1982) also found *Triasina hantkeni* Majzon in the Late Norian-Rhaetian along the whole Tethys

(Table 4). Kiessling and Flügel (2000) investigated the Late Triassic Limestones from the North Palawan Block (Philippines). The age was indicated as Rhaetian based on the occurrence of *Triasina hantkeni* Majzon in wacke- and packstones with abundant involutinid foraminifera and some calcareous algae. These facies types correspond to platform carbonates known from other parts of Southeast Asia (Eastern Sulawesi and Banda Basin; Malay Peninsula and Malay Basin). On the basis of the stratigraphic index foraminifer *Triasina hantkeni* Majzon, which occurs at different levels of the Upper Triassic succession of Seram and Eastern Sulawesi (Indonesia), Martini et al. (1997, 2004) determined *Triasina hantkeni* biozone in the Late Norian (Sevatian)-Rhaetian (Table 4). Işıntek (2002) determined *Triasina hantkeni* biozone as the marker of the Rhaetian stage in the Karaburun peninsula (Işıntek, 2002) in western Turkey (Table 4). Becaletto et al. (2005) found *Triasina hantkeni* Majzon in the Late Norian to Rhaetian age of the Çetmi accretionary melange, cropping out in the Biga Peninsula of northwest Turkey (Table 4). Ekmekçi et al. (2006) also determined *Triasina hantkeni* assemblage zone in the Eastern Taurides (Table 4). Okay & Altıner (2007) described similar sequences with *Triasina hantkeni* biozone in the Late Norian (Sevatian) to Rhaetian of the Urbut sequence of the Bornova Flysch Zone (Table 4). Michalik et al. (2007) determined *Glomospirella friedli-Triasina hantkeni* assemblage zone in the Zliechov Basin, Western Carpathians (Table 4). They were correlated this zone with both the *Choristoceras haueri* and *Ch. marshi* ammonoid zones (Rhaetian) and also with the *Misikella posthernsteini* conodont zone.

Within this biostratigraphic framework, *Triasina hantkeni* assemblage zone is found in the Upper Norian (Sevatian)-Rhaetian stage of the Leylek Limestone, Menteşe Dolomite and the Güverdağı Formation.

Table 4. Correlation of Late Triassic foraminiferal zones in different studies.

Stage	Substage	Salaj, 1969 Western Carpathians	Al Shaibani et al., 1982 Tethyan Realm	Işıntek, 2002 Karaburun Peninsula	Martini et al., 2004 Indonesia	Becaletto et al., 2005 NW Anatolia	Ekmekçi et al., 2006 Eastern Taurides	Michalik et al., 2007 Western Carpathians	Okay&Altıner, 2007 Bornova Flysch Zone	This study Central&Western Taurides
LATE TRIASSIC	RHAETIAN	*Triasina hantkeni* range zone	*Triasina hantkeni* range zone	*Triasina hantkeni* zone	*Triasina hantkeni* zone	*Triasina hantkeni* zone	*Triasina hantkeni* assemblage zone	*Glomospirella friedli-Triasina hantkeni* assemblage zone	*Triasina hantkeni* zone	*Triasina hantkeni* assemblage zone
	NORIAN									

Table 5. Foraminiferal distribution chart of Leylek-1 Section.

Stage / Substage	Zone	Sample No.	*Triasina hantkeni*	*Aulotortus communis*	*Aulotortus tenuis*	*Aulotortus impressus*	*Aulotortus tumidus*	*Aulotortus gaschei*	*Aulotortus* gr. *sinuosus*	*Auloconus permodiscoides*	*Aulotortus* spp.	*Auloconus* sp.	Nodosariidae
UPPER NORIAN (SEVATIAN) - RHAETIAN	*TRIASINA HANTKENI* ASSEMBLAGE ZONE	B-51	■								■	■	
		B-50											
		B-49											
		B-48									■	■	■
		B-47									■		
		B-46											
		B-45											
		B-44											
		B-43											
		B-42									■		
		B-41											
		B-40	■	■			■	■	■		■		
		B-39											
		B-38											
		B-37											
		B-36											
		B-35									■		
		B-34									■		
		B-33									■		
		B-32											
		B-31											
		B-30											
		B-29									■		
		B-28											
		B-27			■				■		■		
		B-26											
		B-25											
		B-24											
		B-23									■	■	
		B-22											
		B-21											
		B-20								■	■	■	
		B-19											
		B-18	■										
UNDIFFERENTIATED NORIAN		B-17											
		B-16											
		B-15											
		B-14									■		■
		B-13											
		B-12											
		B-11									■		
		B-10				■					■		
		B-9									■		
		B-8									■		
		B-7											
		B-6											
		B-5											
		B-4											
		B-3											
		B-2											
		B-1											

Table 6. Foraminiferal distribution chart of Leylek-2 Section.

Stage / Substage	Zone	Sample No.	*Triasina hantkeni*	*Aulotortus communis*	*Aulotortus impressus*	*Aulotortus tumidus*	*Aulotortus gaschei*	*Aulotortus praegaschei*	*Aulotortus* gr. *sinuosus*	*Auloconus permodiscoides*	*Aulotortus* spp.	Auloconus sp.	Nodosariidae
UPPER NORIAN (SEVATIAN) - RHAETIAN	*TRIASINA HANTKENI* ASSEMBLAGE ZONE	C-50									■		
		C-49									■		
		C-48			■		■			■	■	■	
		C-47											
		C-46											
		C-45	■					■	■		■		
		C-44									■		■
		C-43											
		C-42									■		
		C-41	■						■		■	■	
		C-40								■	■	■	
		C-39											
		C-38											
		C-37											
		C-36		■					■		■	■	■
		C-35											
		C-34											
		C-33											
		C-32											
		C-31									■		
		C-30											
		C-29											
		C-28											
		C-27	■			■					■		
		C-26											
		C-25									■		■
		C-24									■		
		C-23											
		C-22											
		C-21							■		■		
		C-20	■										
Un. Nor.		C-19									■		
		C-18											

Table 7. Foraminiferal distribution chart of Kuzca-2 Section.

Stage / Substage	Zone	Sample No.	*Triasina hantkeni*	*Aulotortus communis*	*Aulotortus tumidus*	*Aulotortus friedli*	*Aulotortus* gr. *sinuosus*	*Auloconus permodiscoides*	*Aulotortus* spp.	Auloconus sp.	Nodosariidae	Trochamminidae
UPPER NORIAN(SEVATIAN)-RHAETIAN	*Triasina hantkeni* assemblage zone	K-31	■						■			
		K-30	■	■		■	■					
		K-29	■		■							
		K-28							■			
		K-27										
		K-26	■		■				■	■		
Undiff. Norian		K-25										
		K-24						■	■	■		
		K-23									■	
		K-22										
		K-21							■			■

Table 8 . Foraminiferal distribution chart of Kuzca-3 Section.

Stage / Substage	Zone	Sample No.	*Triasina hantkeni*	*Aulotortus* gr. *sinuosus*	*Aulotortus* spp.	Auloconus sp.	Trochamminidae	*Aulotortus communis*
UPPER NORIAN(SEVATIAN)-RHAETIAN	*Triasina hantkeni* assemblage zone	K-44			■			
		K-43						
		K-42			■			
		K-41				■		
		K-40			■	■		
		K-39						
		K-38						
		K-37					■	
		K-36						
		K-35	■		■			
Un. Nor.		K-34		■	■	■		
		K-33			■			
		K-32		■	■			■

Table 9. Foraminiferal distribution chart of Marmaris-1 Section.

Stage / Substage	Zone	Sample No.	*Triasina hantkeni*	*Aulotortus tenuis*	*Aulotortus impressus*	*Aulotortus friedli*	*Aulotortus* gr. *sinuosus*	*Aulotortus* spp.	Aulocomus sp.
UPPER NORIAN (SEVATIAN) - RHAETIAN	*TRIASINA HANTKENI* ASSEMBLAGE ZONE	M-96						■	
		M-95						■	
		M-94	■						
		M-93							
		M-92							
		M-91							
		M-90						■	
		M-89							
		M-88		■	■			■	
		M-87							
		M-86							
		M-85				■		■	
		M-84	■						
		M-83	■					■	
		M-82	■					■	
		M-81							
		M-80							
		M-79							
		M-78							
		M-77							
		M-76							
		M-75	■					■	
		M-74						■	
		M-73	■					■	
Undifferentiated Norian		M-72					■	■	■
		M-71							
		M-70						■	
		M-69							
		M-68							
		M-67							
		M-66					■		
		M-65						■	■

Table 10. Foraminiferal distribution chart of Marmaris-2

Stage / Substage	Zone	Sample No.	*Triasina hantkeni*	*Aulotortus communis*	*Aulotortus tenuis*	*Aulotortus impressus*	*Aulotortus tumidus*	*Aulotortus friedli*	*Aulotortus* gr. *sinuosus*	*Aulotortus sinuosus pragsoides*	*Aulotortus sinuosus oberhauseri*	*Auloconus permodiscoides*	*Aulotortus* spp.	*Auloconus* sp.	*Glomospira* sp.	*Glomospirella* sp.	Nodosariidae	Trochamminidae
UPPER NORIAN (SEVATIAN) - RHAETIAN	*TRIASINA HANTKENI* ASSEMBLAGE ZONE	M-152												■				
		M-151																
		M-150							■				■					
		M-149																
		M-148																
		M-147																
		M-146											■					
		M-145											■					
		M-144											■					
		M-143											■	■			■	
		M-142											■					
		M-141											■					
		M-140	■										■	■				
		M-139											■					
		M-138											■					
		M-137																
		M-136																
		M-135																
		M-134																
		M-133																
		M-132											■					
		M-131																
		M-130											■					
		M-129											■					
		M-128											■					
		M-127											■					
		M-126																
		M-125																
		M-124											■					
		M-123							■				■					
		M-122																
		M-121																
		M-120											■					
		M-119											■				■	
		M-118											■					
		M-117																
		M-116																
		M-115																
		M-114		■					■			■	■	■			■	
		M-113																
		M-112											■		■			
		M-111											■					
		M-110											■					
		M-109																
		M-108																
		M-107											■					
		M-106			■													
		M-105	■	■		■	■		■	■	■		■			■		
Undifferentiated Norian		M-104											■					
		M-103											■					
		M-102											■					
		M-101																
		M-100						■					■					■
		M-99											■					
		M-98											■					
		M-97											■					

Table 11. Foraminiferal distribution chart of 7th, 13th and 14th parasequences of Leylek-1 Section.

Sample No.	*Triasina hantkeni*	*Aulotortus impressus*	*Auloconus permodiscoides*	*Aulotortus* spp.	*Auloconus* sp.	Nodosariidae	Trochamminidae
B-20K							
B-20J							
B-20I							
B-20H				■			
B-20G				■	■		
B-20F				■	■		
B-20E	■		■	■	■		■
B-20D	■		■	■		■	
B-20C				■			
B-20B				■	■		
B-20A		■		■			

Sample No.	*Triasina hantkeni*	*Aulotortus* gr. *sinuosus*	*Auloconus permodiscoides*	*Aulotortus* spp.	Auloconus sp.	Nodosariidae	Trochamminidae
B-33N		■					■
B-33M			■	■		■	
B-33L							
B-33K							
B-33J							
B-33I							
B-33H	■			■			
B-33G				■			
B-33F							
B-33E		■		■			
B-33D				■			
B-33C				■			
B-33B				■			
B-33A				■			

Table 12. Foraminiferal distribution chart of 18th parasequence of Leylek-1 Section.

Sample No.	*Triasina hantkeni*	*Aulotortus tumidus*	*Auloconus permodiscoides*	*Aulotortus* spp.	Auloconus sp.	Nodosariidae
B-47N	■			■		
B-47M						
B-47L				■		■
B-47K				■		
B-47J						
B-47I						
B-47H				■	■	
B-47G				■		
B-47F	■	■	■	■	■	■
B-47E				■		
B-47D				■		
B-47C						
B-47B				■		
B-47A				■		

Table 13. Foraminiferal distribution chart of 4th, 5th & 6th, 7th, 8th, 9th & 10th parasequences of Leylek-2 Section.

Sample No.	*Aulotortus communis*	*Aulotortus tenuis*	*Aulotortus impressus*	*Aulotortus gaschei*	*Aulotortus* gr. *sinuosus*	*Aulotortus sinuosus pragsoides*	*Aulotortus* spp.	*Auloconus* sp.	Nodosariidae
C-25Z3									
C-25Z2									
C-25Z1							■		
C-25Z									
C-25Y									
C-25V									
C-25U							■		■
C-25T									
C-25S									
C-25R							■		
C-25P									
C-25O	■						■	■	
C-25N							■		
C-25M									
C-25L									
C-25K									
C-25J									
C-25I									
C-25H							■		
C-25G									
C-25F									
C-25E									
C-25D								■	
C-25C							■	■	
C-25B						■	■		
C-25A		■	■	■	■		■		

Sample No.	*Triasina hantkeni*	*Aulotortus communis*	*Aulotortus tenuis*	*Aulotortus* spp.	*Auloconus* sp.	Trochamminidae	Nodosariidae
C-33Z4							
C-33Z3				■	■		
C-33Z2							
C-33Z1				■	■		
C-33Z				■			
C-33Y				■			
C-33V				■	■		
C-33U				■			
C-33T							
C-33S				■	■		
C-33R				■	■		■
C-33P				■		■	
C-33O				■	■		■
C-33N							
C-33M		■		■	■		
C-33L				■	■		
C-33K	■			■	■		
C-33J	■			■	■	■	
C-33I							
C-33H				■			
C-33G			■	■	■		
C-33F				■			
C-33E							
C-33D				■			
C-33C				■			

Table 14 . Foraminiferal distribution chart of Kuzca-1 Section.

Stage / Substage	NORIAN - RHAETIAN											
Sample No.	K-1	K-2	K-3	K-4	K-5	K-6	K-7	K-8	K-9	K-10	K-11	K-12
Aulotortus communis	■											
Aulotortus gr. *sinuosus*								■				
Aulotortus spp.	■	■	■	■	■	■	■				■	

CHAPTER 3

3. SEQUENCE STRATIGRAPHY

The concept of sequence was modified from Sloss (1963) who considered sequences as an unconformity bounded rock-stratigraphic units of higher rank. He recognized that such sequences have chronostratigraphic significance. In comparison to Sloss's sequences, a seismic stratigraphic interpretation procedure utilizing discontinuities for subdividing sedimentary rocks was evolved in the 1970's by Vail et al. (1977a). This performed a great reform in stratigraphy. Seismic stratigraphy is a geologic approach to the stratigraphic interpretation of seismic data (Vail and Mitchum, 1977). From the geometry of seismic reflections, geologic time correlations, definition of depositional units, thickness of the units, paleobathymetry, burial history and geologic history interpretations can be made. In these years, geologic concepts were described based on the depositional sequences. Depositional sequence is defined as a stratigraphic unit composed of a relatively conformable succession of genetically related strata and bounded by unconformities or their correlative conformities (Mitchum et al., 1977). The relationship between relative sea-level change and depositional stratal patterns were established. Global cycle charts were also constructed (Vail et al., 1977b). Finally all these progresses led to to the concept of sequence stratigraphy with the combination of outcrop and well log data.

Sequence Stratigraphy is the study of rock relationships within a chronostratigraphic framework of repetitive, genetically related strata bounded by surfaces of erosion, non-deposition or their correlative conformities (Van Wagoner et al., 1988). It represents the sea level changes in accordance with transgressions and regressions. This method is important for making basin analysis, paleogeographic reconstructions, geologic history interpretations, resource evaluations of sedimentary basins, global stratigraphic correlations. The fundamental unit of sequence stratigraphy is the sequence, which is bounded by unconformities and their correlative conformities (Van Wagoner et al., 1988). A sequence can be subdivided into systems tracts which was defined by the stacking patterns of parasequence sets and parasequences bounded by marine-flooding surfaces (Van Wagoner et al., 1988). Parasequence concept was firstly defined by Van Wagoner et al. (1988). In the same year, Posamentier et al. (1988) published the eustatic controls on clastic deposition. However, Sarg (1988) applied the sequence stratigraphic model to carbonate platforms. He showed that the controlling factors of the carbonates was more complicated than the siliciclastics and the rates of relative changes in sea level controlled the depositional stratal patterns, facies distribution and productivity of carbonate platforms. He defined the facies characteristics of the facies belts from the coastal area to the basin as supratidal-intertidal flats, shallow-marine shelf, platform or bank margin, foreslope and basin facies. He described tidal-flat facies as small-scale shoaling-upward subtidal to supratidal cycles or parasequences. In the following years, Mitchum et al. (1991) described high-frequency cycles in siliciclastics which occured most commonly with fourth-order cyclicity and some with fifth-order cyclicity. High-frequency cyclicity of fourth-order and higher had been also recognized in carbonate rocks (Fischer, 1964, 1991; Strasser, 1988; Goldhammer et al., 1990 etc.). Moreover, Goldhammer et al. (1990) suggested that high-frequency cycles were controlled by short-term variations in subsidence rate and found evidence of Milankovitch-type orbital forcing within the cycles.

In our sequence stratigraphic study, we define cyclicity within the Upper Triassic peritidal carbonates. The studied successions have been examined in the sense of sequence stratigraphy principles. Facies changes and the response of benthic foraminifers to the sedimentary cyclicity will be discussed in the following sections.

3.1. Meter-scale shallowing-upward cycles (Parasequences)

The fundamental building blocks of sequences and systems tracts are parasequences and parasequence sets (Mitchum et al., 1991). A parasequence, as defined by Van Wagoner (1985), is a relatively conformable succession of genetically related beds or bedsets (within a parasequence set) bounded by marine flooding surfaces or their correlative surfaces. Parasequences are often systematically organized into parasequence sets within larger scale successions. Stacking patterns of the parasequence sets are used in conjuction with bounding surfaces and their position within a sequence to define systems tracts (Van Wagoner et al., 1988). Parasequences which are the smallest fundamental unit of systems tracts can be delineated by lithofacies, their bounding surfaces or the contacts between each system. They are best developed in shallow marine sediments and they are shallowing-upward sedimentary cycles.

Systems tracts are genetically associated stratigraphic units that were deposited during specific phases of the relative sea-level cycle (Posamentier, et al, 1988). These units are represented in the rock record as three-dimensional facies assemblages. They are defined on the basis of bounding surfaces, position within a sequence, and parasequence stacking pattern. Systems tracts are also characterized by geometry and facies associations (Van Wagoner et al., 1988). The transgressive systems tract is characterized by one or more retrogradational parasequence sets. The highstand systems tract is characterized by one or more aggradational parasequence sets (Van Wagoner et al., 1988).

In this study, shallowing-upward meter-scale cycles are recorded in the Central and Western Taurides. They are termed as 4^{th}- and 5^{th}-order cycles which constitute the basic working units of the Upper Triassic successions. Furthermore, systems tracts are defined on the basis of the cycle types within the successions. Although different types of cycles are observed within the measured sections, cycles are mainly characterized by the vertical succession of 3 facies.

3.1.1. FACIES A

Facies A is a thin, green color claystone which is found only in the first locality near Leylek Hill in the Central Taurides (Figure 19). The alternation of claystone and carbonate units are easily recognizable in the field. Facies A is situated at the bottom of the cycles which is overlain by several microfacies types. On the other hand, some cycles are devoid of Facies A. In order to understand whether the claystone is situated at the bottom or top of a cycle (parasequence), clay and whole rock analysis were carried out in the clay analysis laboratory of the General Directorate of the Mineral Research and Exploration (MTA). 4 claystone samples were subjected to clay analysis and whole rock analysis were made on 15 samples (Figure 20, 21). The clay analysis was made on the B-2, B-12, B-24 and B-36 samples of the Leylek-1 Section (Figure 20). According to the acquired data, the main clay mineral found is illite in the claystones (Figure 20). Chlorite and few kaolinite are also recognized. Illite is the most common marine clay mineral which may be subjected to multiple redeposition (Flügel, 2004). The illite abundance increases in hydrodynamically active environments. Facies A is represented by the high abundance of illite if compared with the abundance of kaolinite and chlorite (Figure 20). Thus, it is interpreted as the lithology formed at the bottom of the cycles. According to the whole rock analysis of the claystones, dolomite is found to be the main mineral (Figure 20). On the other hand, calcite, feldispar, mica and quartz are also recognized. In order to decide the position of the claystones in the cycles (parasequences), the above and below levels of the claystones were also analyzed. The megolodont-bearing limestones, breccioid limestones, fenestral limestones, dismicrites and stromatolites which overlie and underlie the claystones were selected for analysis in the Leylek-1 and Leylek-2 Sections (Figure 21). The whole rock analysis of the B-33I, B-33J, B-33K, B-33L, C-25P, C-25R, C-33I and C-33J were done (Figure 21). In these analyses, dolomite is the main mineral, except in few samples (B-33J, C-33J). The other minerals are calcite, clay, feldispar and mica. However in the B-33J and C-33J, the main mineral found is calcite. Based on the whole rock analysis, it is difficult to build up a relationship between the claystones and the carbonates since the whole rock mineralogy of the claystones and carbonates do not exhibit a consistent relation. Therefore, we prefer to place claystone levels at the bottom of the cycles because of the high abundances of the illite and dolomite in the claystones. Therefore, the claystone levels have been considered at the bottom of cycles which correspond to a shallow subtidal environment.

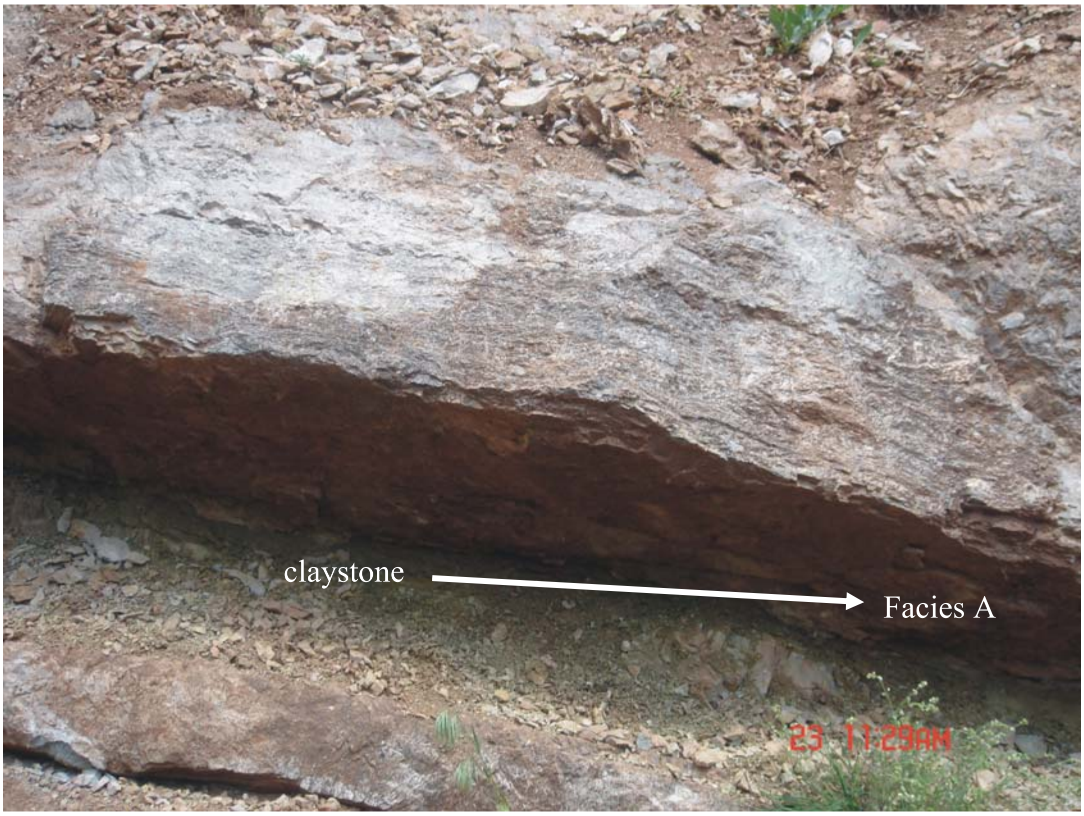

Figure 19. Outcrop view of claystone (Facies A), which is overlain by fenestral limestones (Facies C), Leylek Hill locality, Central Taurides.

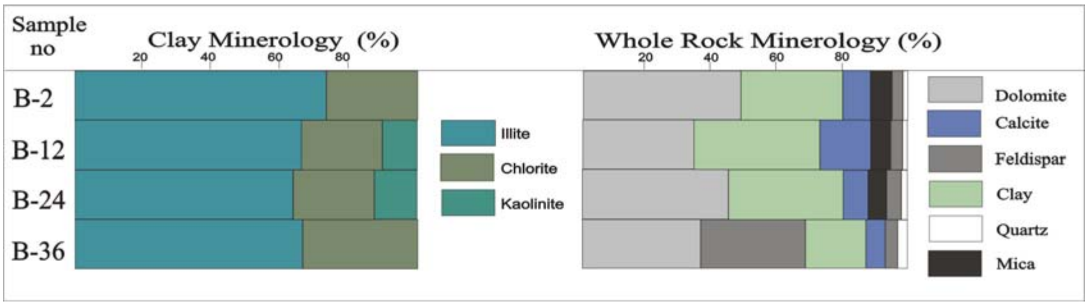

Figure 20. The clay and whole rock mineralogy of clay samples (B-2, B-12, B-24, B-36) in which the illite and dolomite is abundant.

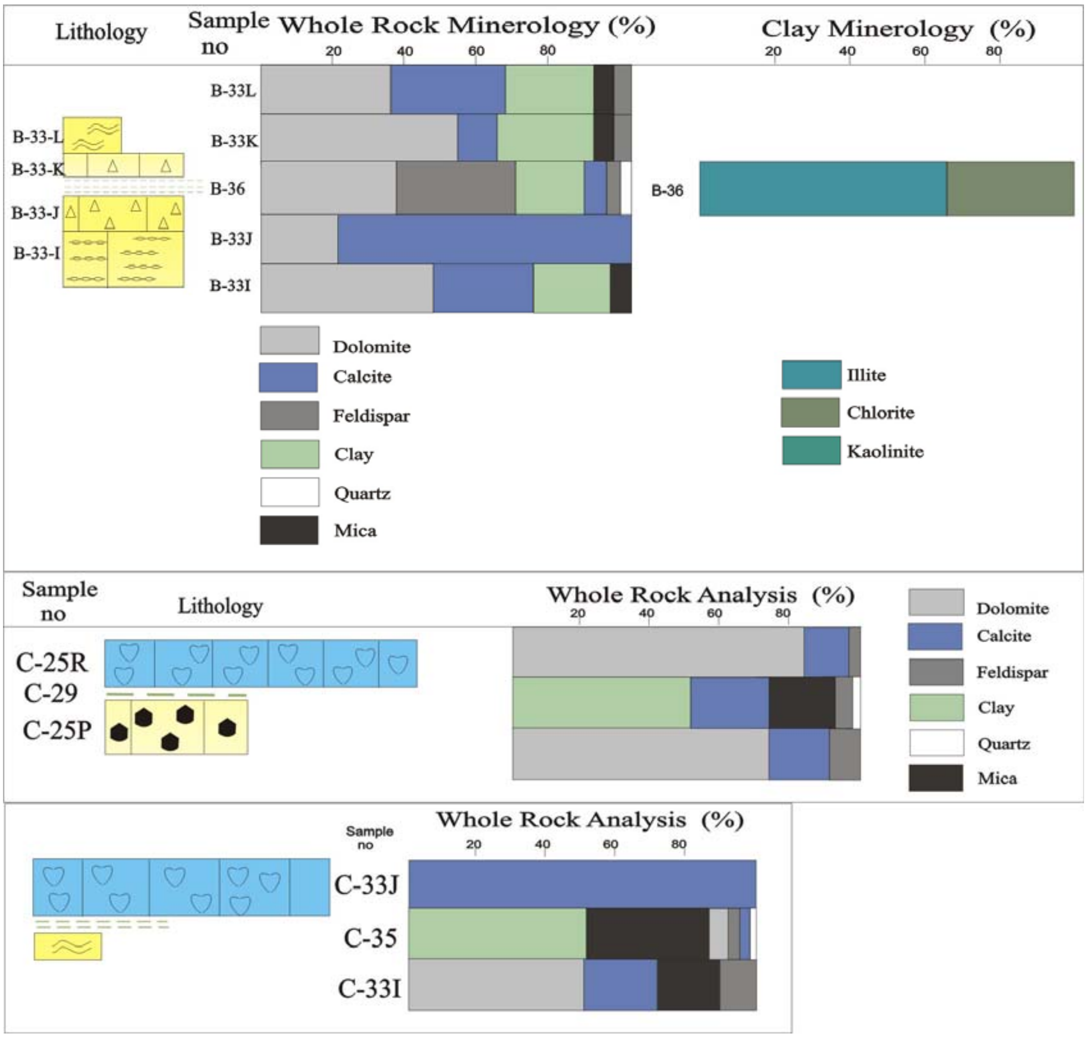

Figure 21. The clay and whole rock analysis of carbonate and claystone samples.

3.1.2. FACIES B

Facies B consists mainly of thickly bedded, light grey megalodont-bearing limestones (Figure 22) and also lesser amount of foraminiferal limestones. Megalodont-bearing limestones consist of wackestones to packstones with abundant involutinid group foraminifers (Figure 23 A-C). The involutinids are commonly recrystalized (Figure 23 A). Other common fossil groups are bivalves (Figure 23D), gastropods and algae. Pellets are also common within the facies B (Figure 23B). The matrix is generally composed of micrite.

This facies mainly occur at the bottom of the cycles. This micritic, megalodont-bearing lithofacies occur in a low energy, lagoonal settings. The megalodonts live on shallow muddy substrates in a lagoonal low-energy environments (Flügel, 2004). The depositional environment corresponds to the restricted-platform interior (FZ 8) zone of the Standard Facies Zones of Flügel (2004) (Figure 24). High number of shallow marine biota within a micritic, pelloidal wackestone-packstone facies show restricted-platform interior conditions.

This facies corresponds to the “megalodont limestone” (member C) of Fischer (1964), and to subfacies C differentiated by Goldhammer et al. (1990). Fischer described this facies as a subtidal massive limestone member comprising wackestones and grainstones with submarine hardgrounds. He found the megalodonts in life position together with gastropods and dasyclad algae. Goldhammer et al. (1990) defined subfacies C as the limestone consisting of wackestones to grainstones including abundant megalodonts. Both of them interpreted this facies as a subtidal deposit. In this study, Facies C is also regarded as a subtidal deposit.

Figure 22. Outcrop view of megalodont-bearing limestones (m) of subtidal facies, which is underlain by stromatolites (s) (Marmaris-1 Section, Sample No. M-91, M-92).

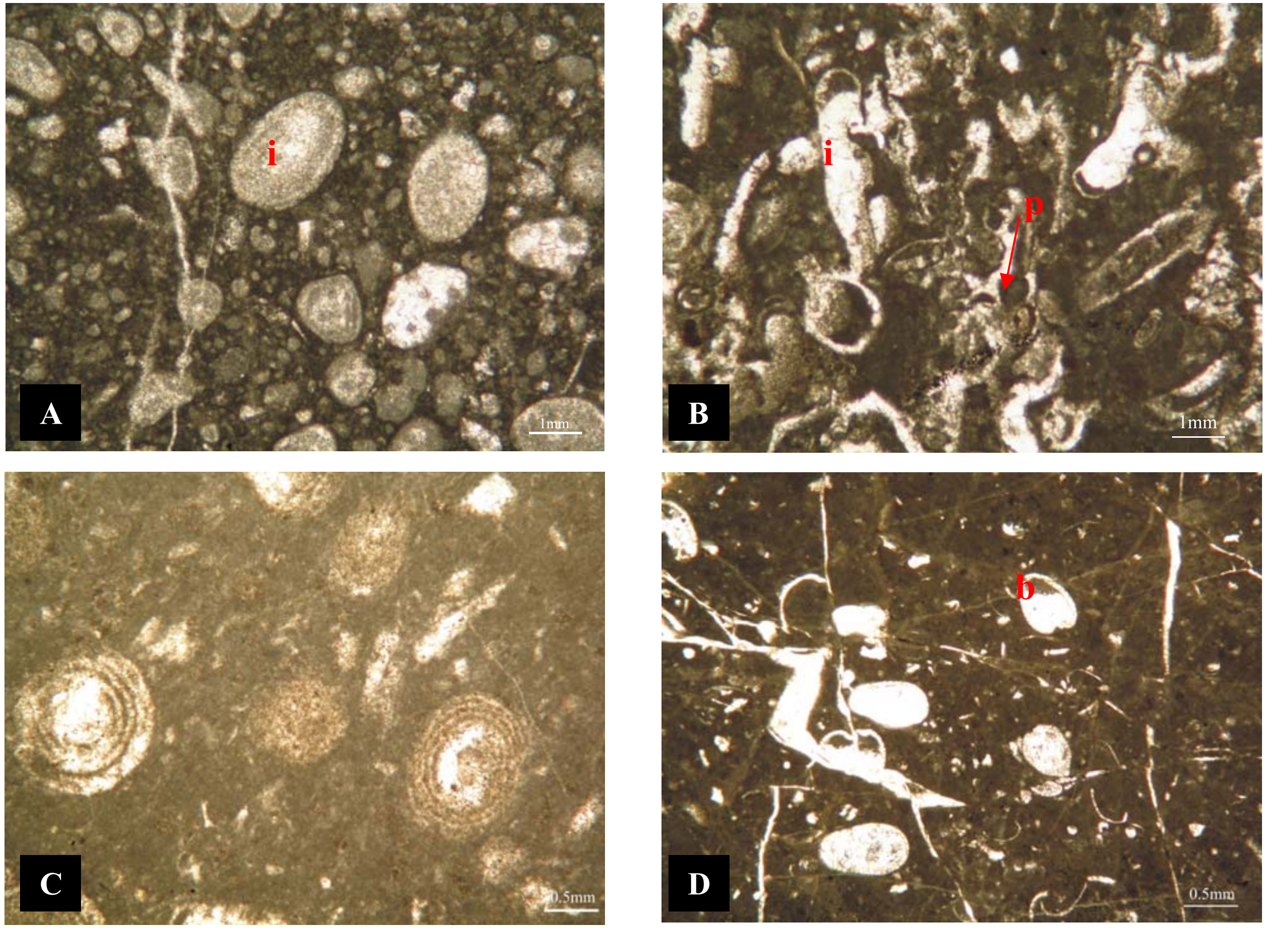

Figure 23. Photomicrographs of Facies B **A.** Bioclastic packstone facies, including recrystalized involutinid foraminifers (i: involutinid) (sample C-25). **B.** Bioclastic packstone (i: involutinid, p: pellet), (sample C-25A) **C.** Bioclastic wackestone with abundant *Triasina hantkeni* Majzon (sample B-20G) **D.** Bivalve wackestone (b: bivalve), (sample C-27).

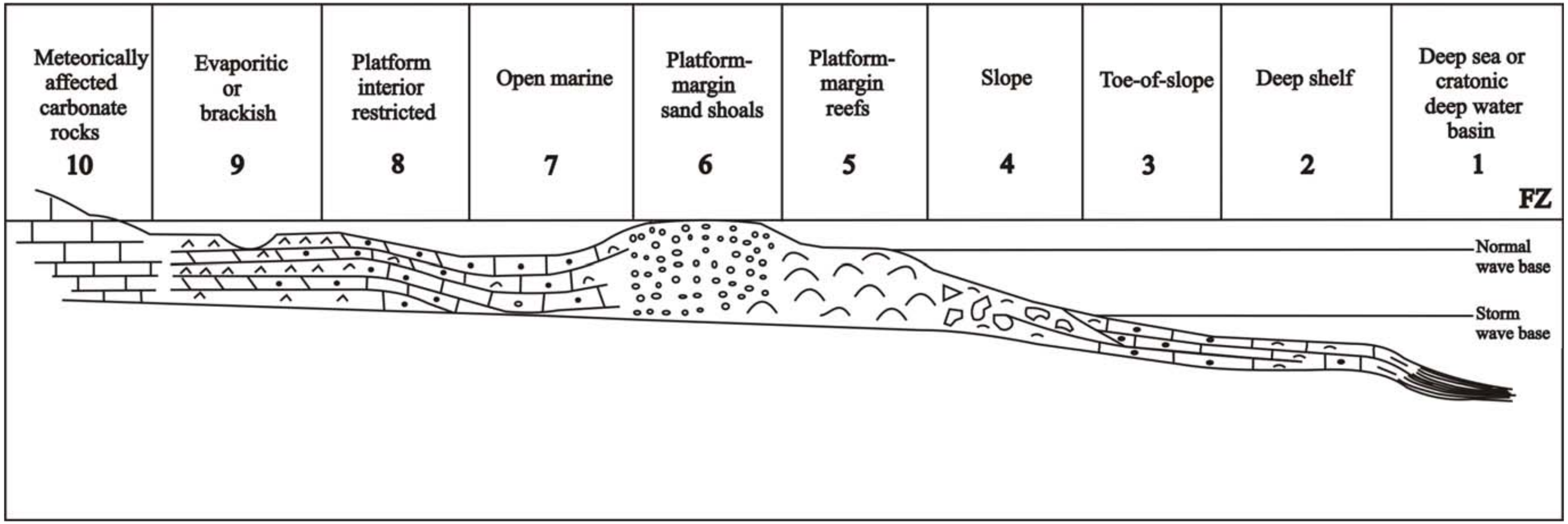

Figure 24. The Standard Microfacies Zones of the modified Wilson model (Flügel, 2004) in which the depositional environment corresponds to the rimmed platform interior (FZ 8).

3.1.2. FACIES C

Facies C is characterized by dolomitic limestones (Figure 25), dismicrites with geopetal structures (Figure 26A), black pebbles (Figure 26B), breccias (Figure 27), laminated mudstone (Figure 28A), stromatolites (Figure 28B-C-D), fenestral limestones (Figure 29A-B) and vadose pisoids (Figure 29C-D). This type of facies is poorly fossiliferous to unfossilifereous and occur at the top of the cycles.

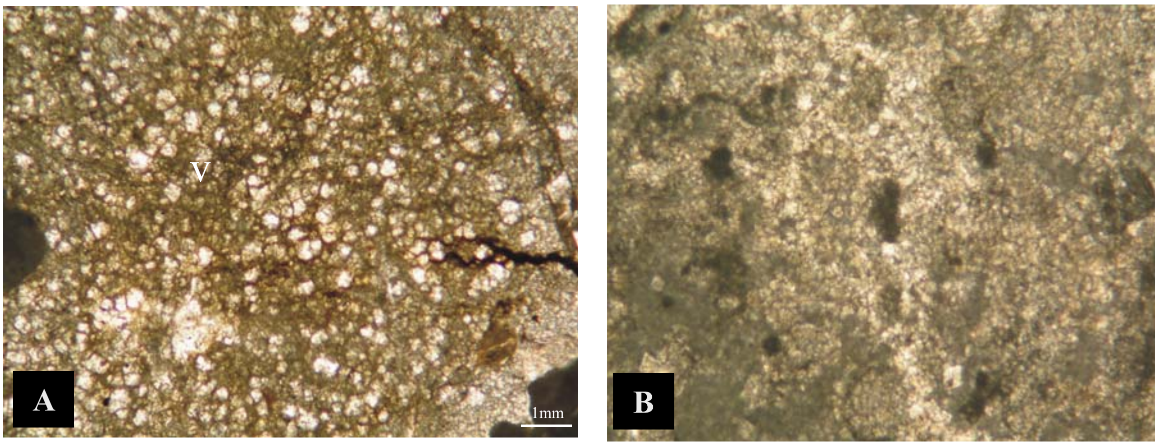

Figure 25. Photomicrograph of dolomitic limestones (sample B-5).

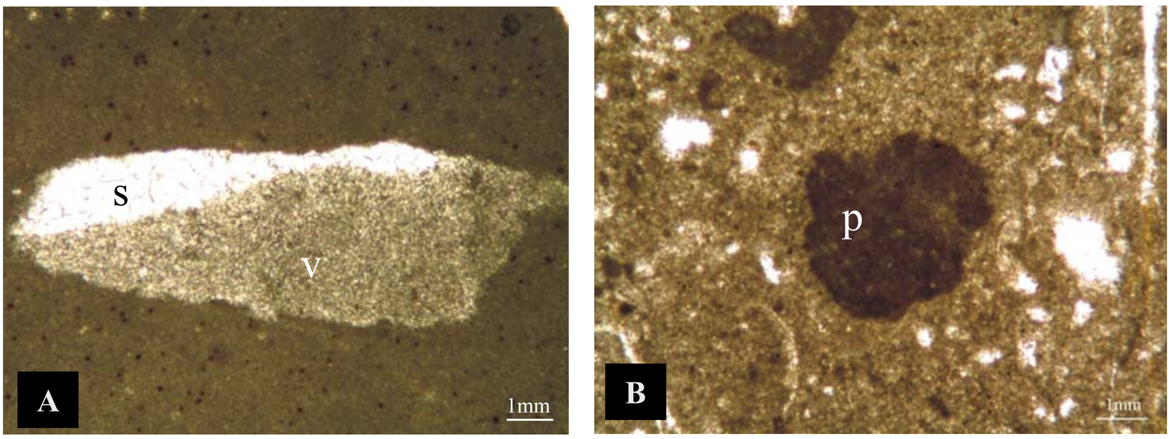

Figure 26. Photomicrographs of **A.** dismicrite with geopetal vadose silt (v, vadose silt; s, sparry calcite) which is found towards the top of parasequences (sample B-25). **B.** Black pebble (p) within a breccia level (sample B-9).

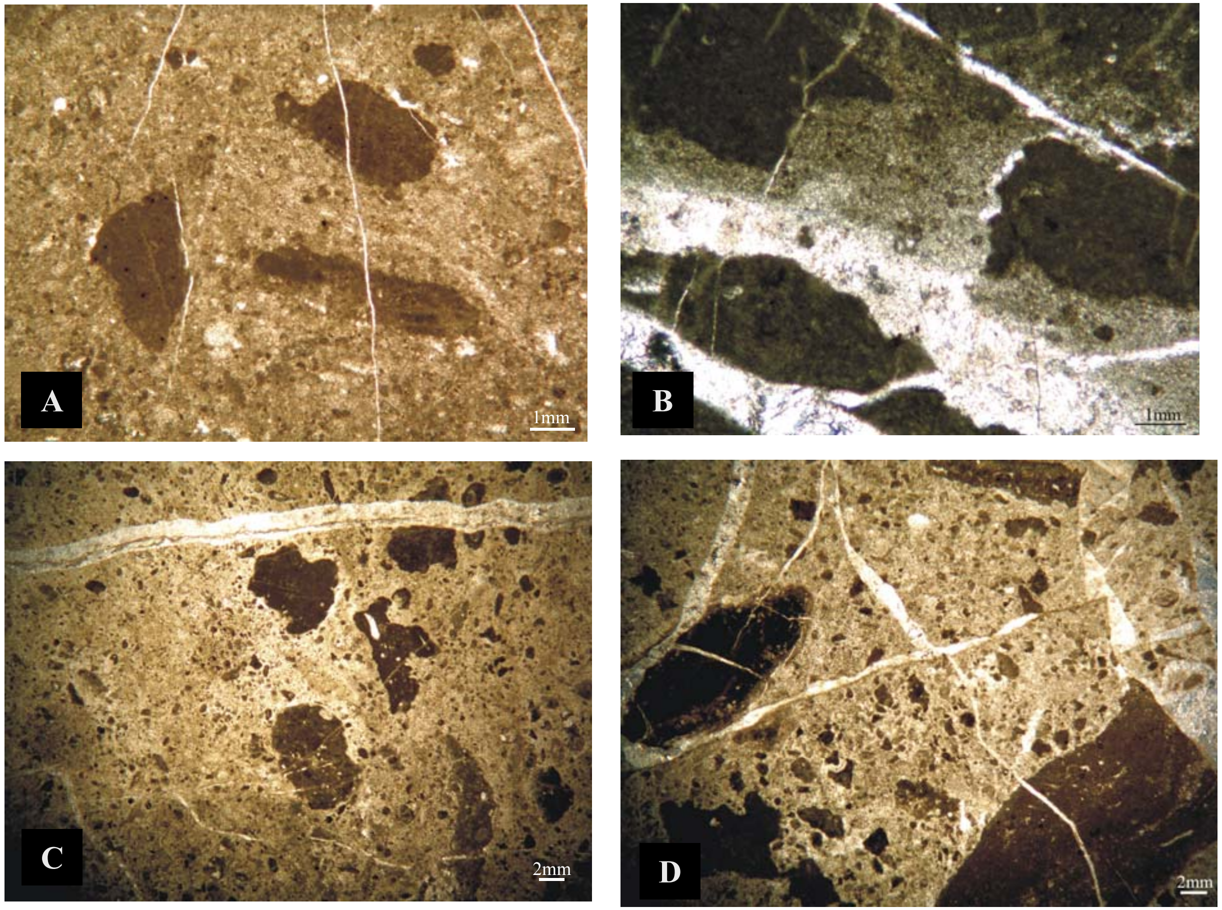

Figure 27. Photomicrographs of breccias indicating a subaerial exposure (Flügel, 2004), supratidal facies, Facies C, (sample B-20-H, B-10, B-33G, B-47C).

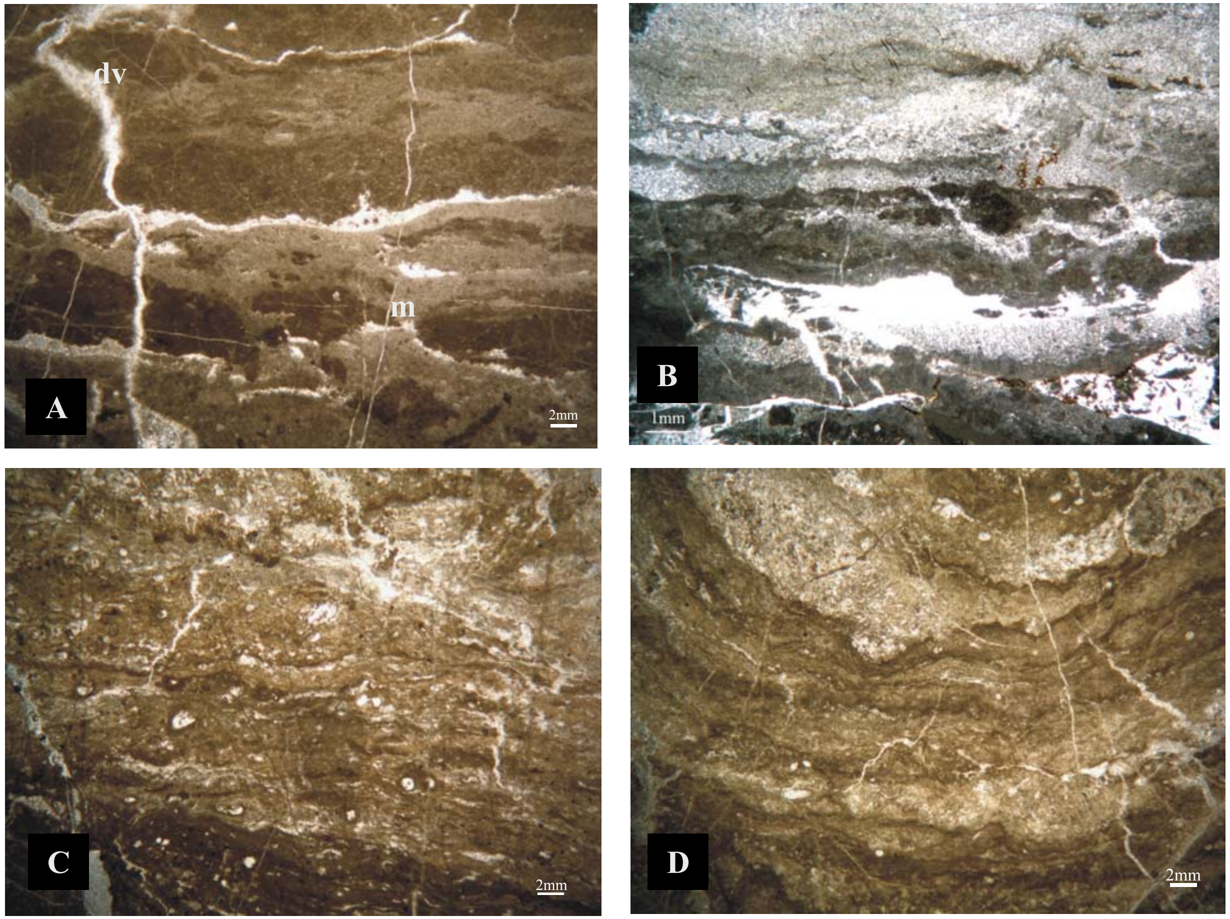

Figure 28. Photomicrographs of **A.** laminated mudstone including dark clasts, dissolution vugs (dv), mud cracks (m) (sample B-10) **B-C-D.** Laminated stromatolite bindstone (sample C-33N, B-38, B-33N).

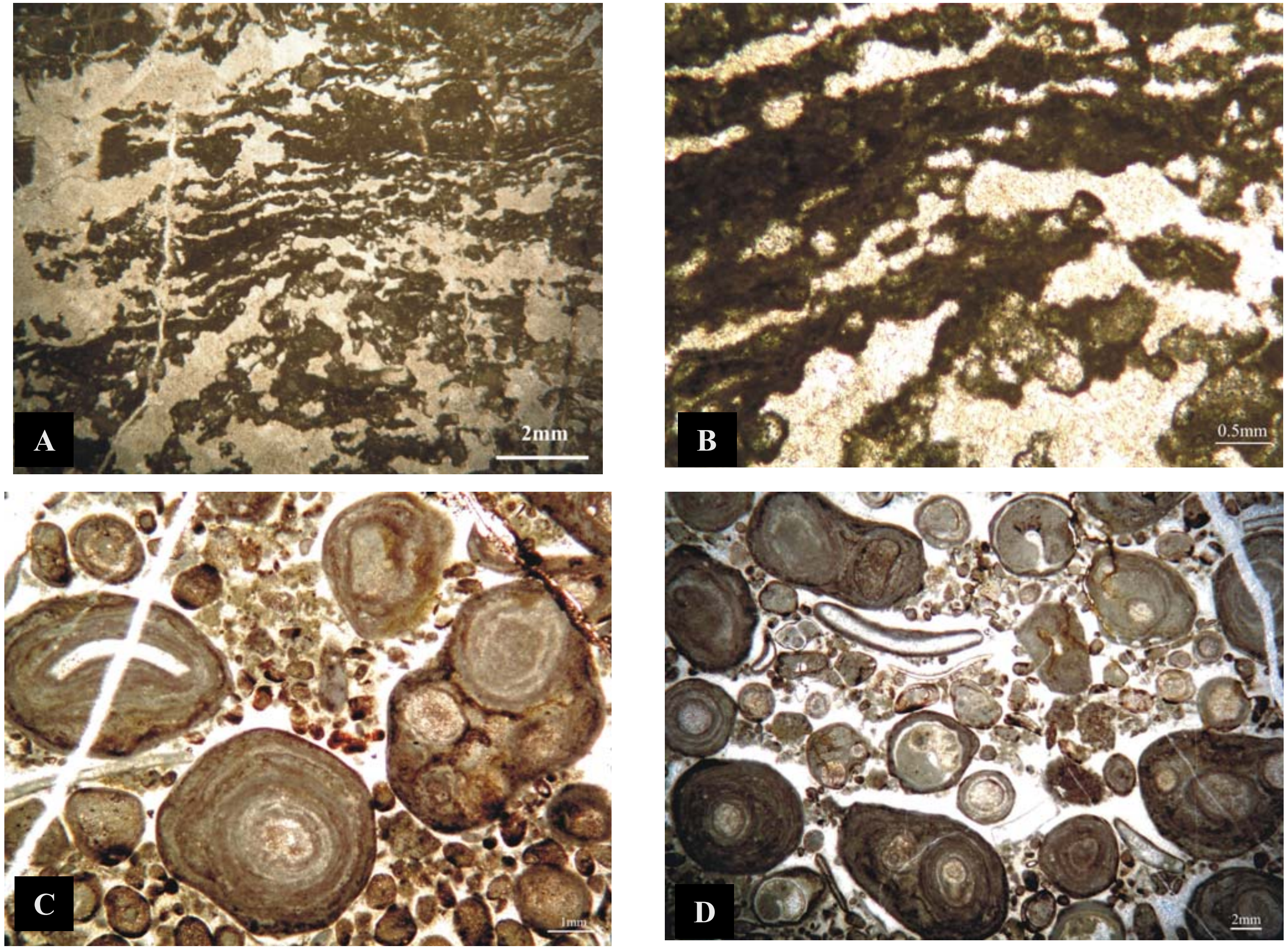

Figure 29. Photomicrographs of **A-B.** Laminoid-fenestral fabrics including blocky-calcite crystals, Facies C, upper intertidal and supratidal environments (sample B-47M), **C-D.** Vadose pisoids (Facies C), indicating supratidal environment (sample K-45O, K-45P).

The breccia levels consist of angular, subangular and rarely rounded micrite clasts and they are intraformational (Figure 27). Clasts and matrix are genetically related. The clasts are mainly composed of lime mudstone facies. Their sizes range from mm to cm scale. Some pebbles (Figure 26 B) consisting of black-colored limestone clasts (Shinn and Lidz, 1988) are a valuable tool for identifying partial or complete subaerial exposure of limestones (Strasser and Davaud, 1983). Black pebbles are also good markers of sea-level lowstand phases connected with subaerial exposure (Flügel, 2004). Records of the lowstand conditions may be reworked in the subaerial exposure structures (Yılmaz and Altıner, 2006a). Evidence of black pebbles in limestones show subaerial exposure, changes in sea-level fluctuations, breaks in marine sedimentation etc. (Flügel, 2004). The matrix is composed of vadose silt or micrite. Subaerial exposure structures such as dissolution vugs, mud cracks are also commonly recognized in these levels. This texture was interpreted as the 'intraformational conglomerate' by Fischer (1964) and regarded as an indication of supratidal reworking. Goldhammer et al. (1990) also differentiated this facies as intraformational conglomerate. In this study, this facies is interpreted as intraformational breccia which have been deposited in a supratidal environment (Ginsburg et al., 1977; Yılmaz & Altıner, 2006a).

Laminated stromatolite bindstones are the characteristic facies type of the cycle (parasequence) tops (Figure 28B-C-D). The sample shows finely wrinkled laminae arranged in dense and closely-spaced growth patterns. The irregularly-shaped white calcite-filled structures indicate burrowing and disintegration of the microbial mats by grazing organisms (Flügel, 2004). This facies is very common in the intertidal-supratidal zone. It is regarded as the member B of the 'Lofer cycle' (Fischer, 1964) and considered as the cycle bottom. In this study, laminated stromatolitic bindstones exist at the top of the cycles and regarded as intertidal-supratidal deposits (Flügel, 2004).

Fenestral fabrics are common in the facies C and observed towards the top of parasequences (Figure 29A-B). They are composed of voids and some of these fabrics resemble windows and called "fenestral fabrics" (Tebbutt et al., 1965). Fenestral pores can also be interpreted as shrinkage and/or gas bubble pores (Shinn, 1983b). Peritidal cycles are commonly capped by fenestrate structures containing laminoid types (Figure 29A-B) (Shinn 1983a, b). The voids are partially or completely filled with blocky-calcite crystals. Commonly the laminoid-type fenestrae are recognized in the parasequences (Groover and Read, 1978). They are developing in laminated sediments, particularly in microbial carbonates (Flügel, 2004). Laminoid-fenestral fabrics occur preferentially in shallow near-coast supratidal and upper intertidal environments (Flügel, 2004). This facies corresponds to the "algal mat loferite"described by Fischer (1964) and to subfacies B1 (shrinkage pores) differentiated by Goldhammer et al. (1990). The laminoid fenestrae are characteristic of the upper intertidal and supratidal zones. The distribution of the laminoid fenestrae is closely related to microbial mats (Flügel, 2004). Fenestral fabrics are regarded as upper intertidal and supratidal deposits in this study.

In the Kuzca locality of the Central Taurides, vadose pisoids are determined which are the common constituents of supratidal vadose caps of peritidal cycles (Figure 29 C-D). They are commonly cemented by meteoric cements. They are formed by accretionary growth on a shelf crest within shoaling upward sequences in a protected hypersaline environment (Flügel, 2004). The grains are linked by outer laminae, pendent and meniscus cement. Nuclei are commonly composed of peloids. Vadoids originate in a vadose fresh water and in vadose-marine environments (e.g., supratidal areas). They are formed by early diagenetic meteoric carbonate precipitation, during subaerial exposure (Flügel, 2004). They are formed under meteoric-vadose and marine-vadose conditions. Vadose pisoids which is a subaerial exposure cap in the studied section must be the result of relative sea level oscillation and may correspond to an important sea level fall in the Upper Norian-Rhaetian time interval.

Based on the detailed facies analysis, mainly 3 facies have been recognized in the studied successions. These are 1. A thin, green color claystone facies A, 2. a subtidal facies B with shallow marine biota, 3. an intertidal-supratidal facies C in which the subtidal units pass upward into intertidal and supratidal units. They are deposited in a restricted, lagoonal environment. Cycle bottoms are constituted by facies A and B, whereas cycle tops are formed by facies C. A typical cycle boundary occurs between facies C and facies A or facies B. The flooding is marked by facies A and facies B in the cycles. This represents abrupt shifts from subtidal deposits to intertidal-supratidal deposits. Although there are few cyclicity differences between the localities, the main facies trend is from subtidal to supratidal.

3.2. Types of shallowing-upward cycles (parasequences)

Based on the facies analysis, 5 main types of cycles and 33 sub-type cycles are determined within the studied successions. They are meter-scale cycles which are generally represented by subtidal to supratidal facies. Most cycles are incomplete; many are missing the clay unit; some are missing the subtidal unit or the intertidal parts. The symbols used in the sections are shown in Table 15.

Table 15. Symbols used in sections.

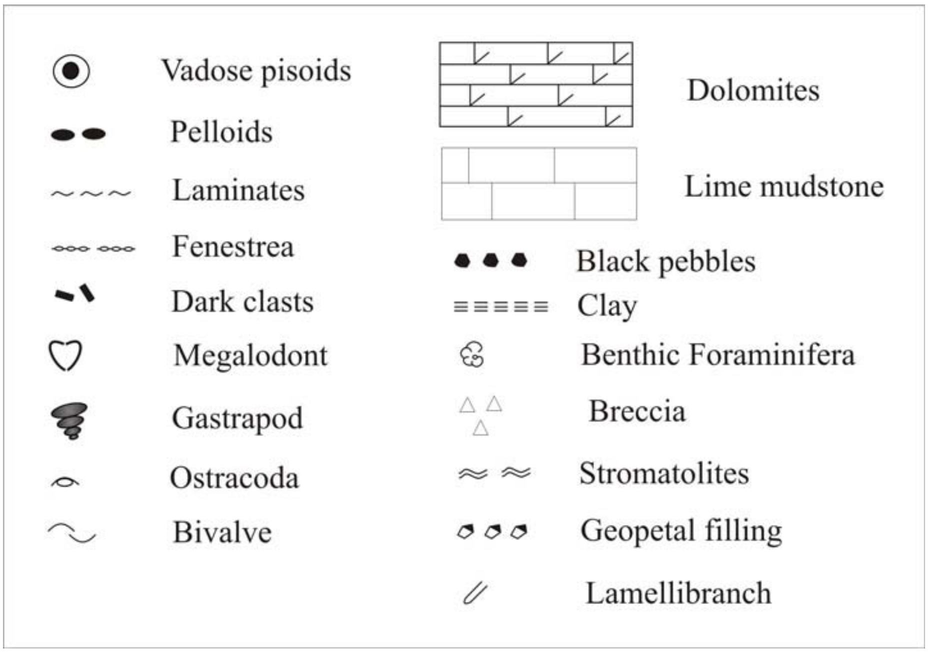

3.2.1. A-type cycles

A-type cycles are characterized by the existence of thin claystones at the base. The cycles start with the claystone and followed by several microfacies types. These types of cycles can only be seen in the first locality near Leylek Hill in the Central Taurides. Based on the internal variations, 12 sub-types were determined. A1 sub-type is overlain by dismicrites with black pebble. A2 sub-type is overlain by dolomitic pelloidal wackestone, fenestral limestones and stromatolites respectively. A3 sub-type is capped by fenestral limestones and stromatolites. A4 sub-type is overlain by dismicrites with geopetal structures and breccioid limestone. A5 sub-type is only capped by breccioid limestone. A6 sub-type is overlain by dismicrites with geopetal structures, fenestral limestones and capped by stromatolites. A7 is overlain by dolomitic limestone containig breccias and capped by fenestral limestones. A1 to A7 sub-type cycles are commonly inter- to supratidal in character owing to the absence of megalodont-bearing limestones and bioclastic wackestone-packstone facies above the clay levels. However, A8 to A12 sub-type consists of megalodont-bearing limestones at the bottom of the cycles. A8 is capped only by megalodont-bearing limestone. A9 sub-type is overlain by megalodont-bearing limestone, dismicrites with black pebbles and capped by fenestral limestone. A10 sub-type is overlain by megalodont-bearing limestone and breccioid limestone. A11 is overlain by megalodont-bearing limestone and capped by dismicrites with geopetal structures. A12 is capped by foraminiferal wackestone and capped by stromatolites. A8 to A12 sub-type cycles are more subtidal in character.

A TYPE CYCLES

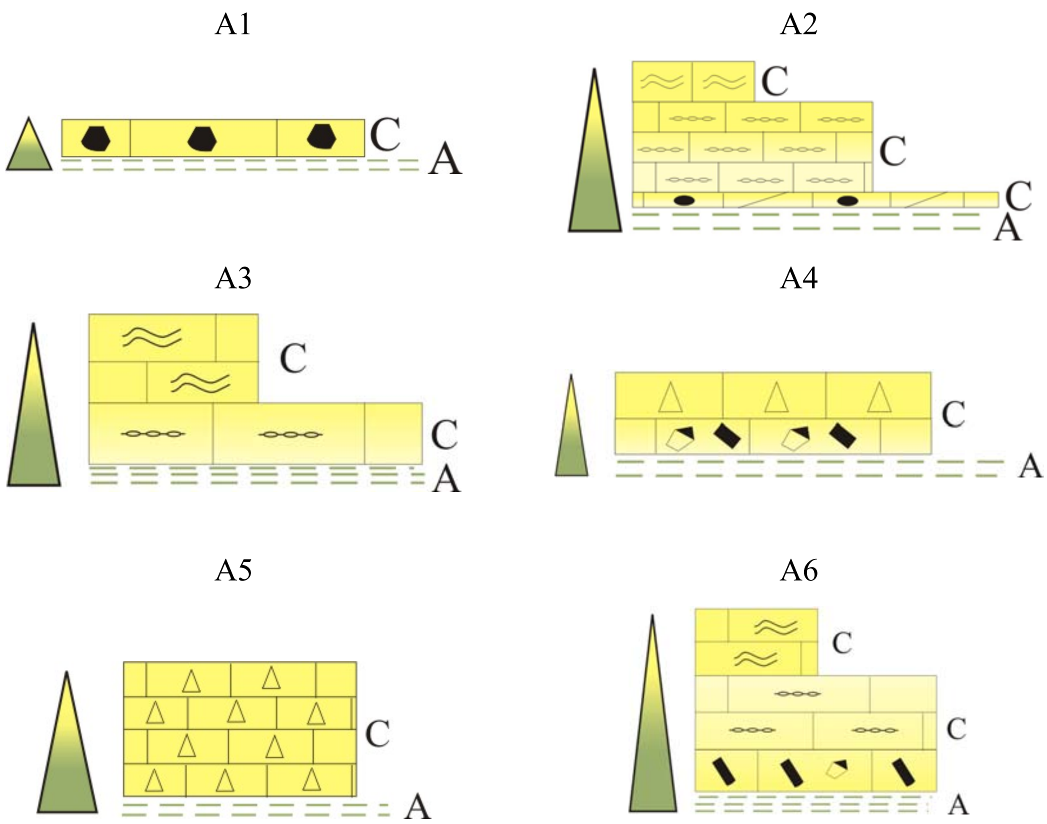

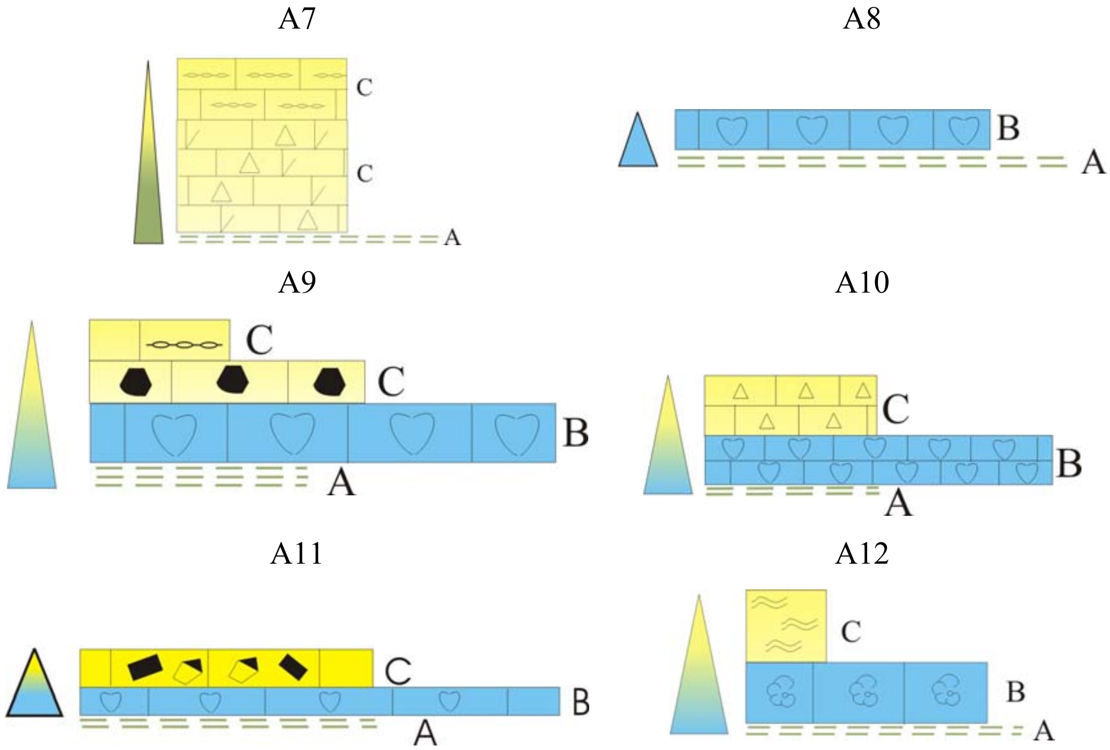

3.2.2. B type cycles

B type cycles are represented by megalodont-bearing limestones at the base of the cycles. They are commonly subtidal in character at the base but inter- to supratidal character towards the top of the cycles. The base of the cycles are constituted by bioclastic wackestone to grainstone facies and is succeeded upwards with several microfacies types. According to the variations, 10 sub-types are identified. All sub-types have megalodont-bearing limestones at the base and continues as follows: B1 sub-type is capped by fenestral limestones. B2 sub-type is overlain by breccioid limestone and stromatolite. B3 sub-type is capped by dismicrites with geopetal structures including also limestone clasts. B4 sub-type is capped only by stromatolites and B5 is overlain by dismicrites with geopetal structures and dismicrites including black pebbles respectively. B6 sub-type is overlain by unfossilifereous lime mudstone and capped by fenestral limestones. B7 sub-type is capped by dismicrites including black pebbles. B8 sub-type have is overlain by fenestral limestones and breccioid limestone respectively. B9 sub-type is composed of only megalodont-bearing limestones and B10 sub-type is capped by pelloidal-bioclastic packstones-grainstones.

B TYPE CYCLES

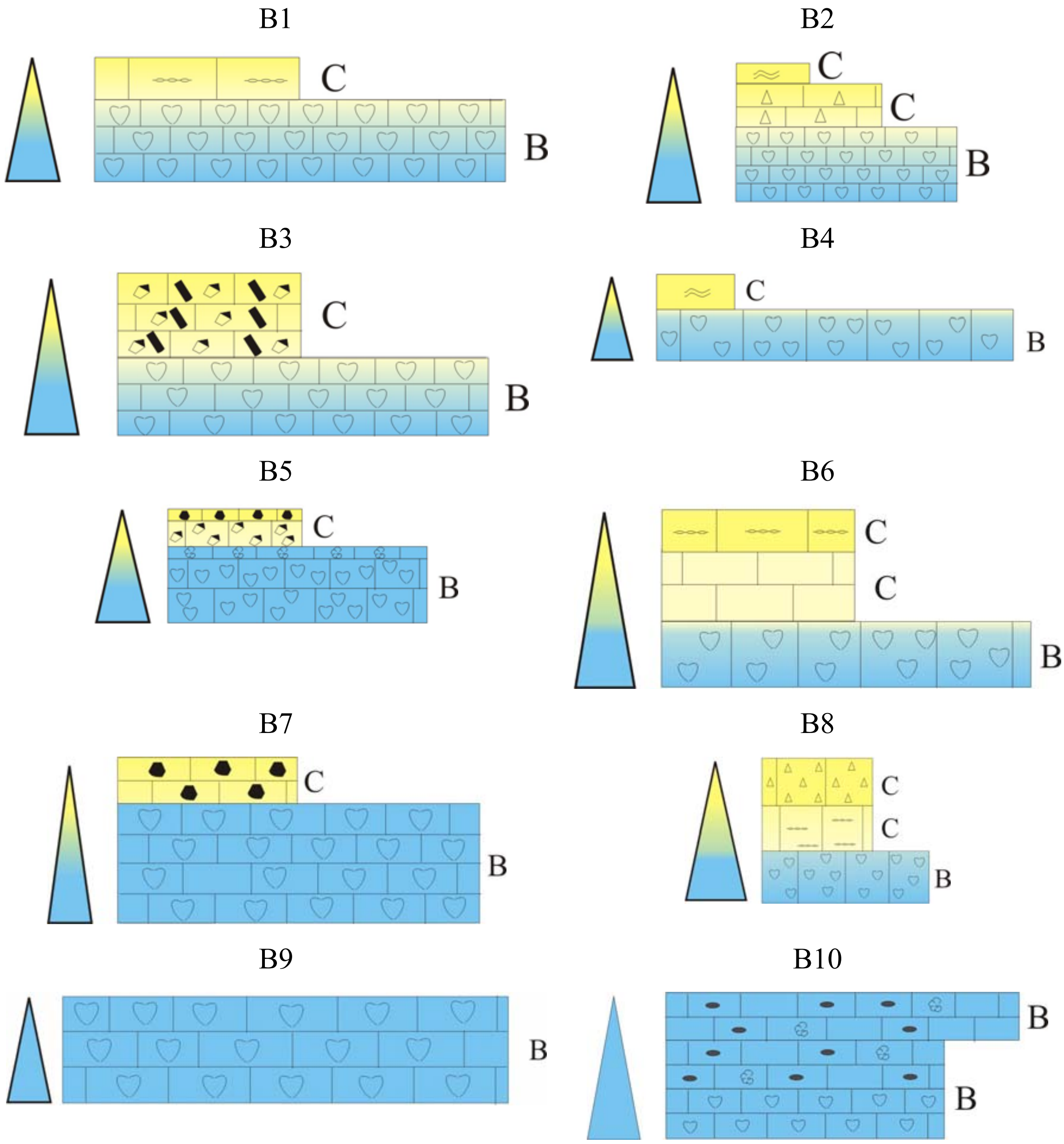

3.2.3. C type cycles

C type cycles are characterized by foraminiferal wackestone to grainstone lithofacies at the base and several microfacies types at the top of the cycles. This type of cycles resemble B type cycles but lack of megalodonts in the subtidal part. 8 sub-types are recognized. C1 sub-type starts with foraminiferal wackestone at the base and continues with breccioid limestone and stromatolites. C2 sub-type starts with foraminiferal wackestone, megalodont-bearing limestone and foraminiferal packstone respectively and capped by dismicrites with geopetal structures and fenestral limestones. C3 sub-type is capped only by stromatolites. C4 sub-type is overlain by fenestral limestones and stromatolites. C5 sub-type is followed by dismicrites with geopetal structures, fenestral limestones and stromatolites. C6 sub-type is only capped by fenestral limestones. C7 sub-type is overlain by megaldont-bearing limestones. C8 sub-type is different from other sub-type cycles. It starts with foraminiferal packstone and pass upward into ostracodal wacke- and packstones and capped by vadose pisoids.

C TYPE CYCLES

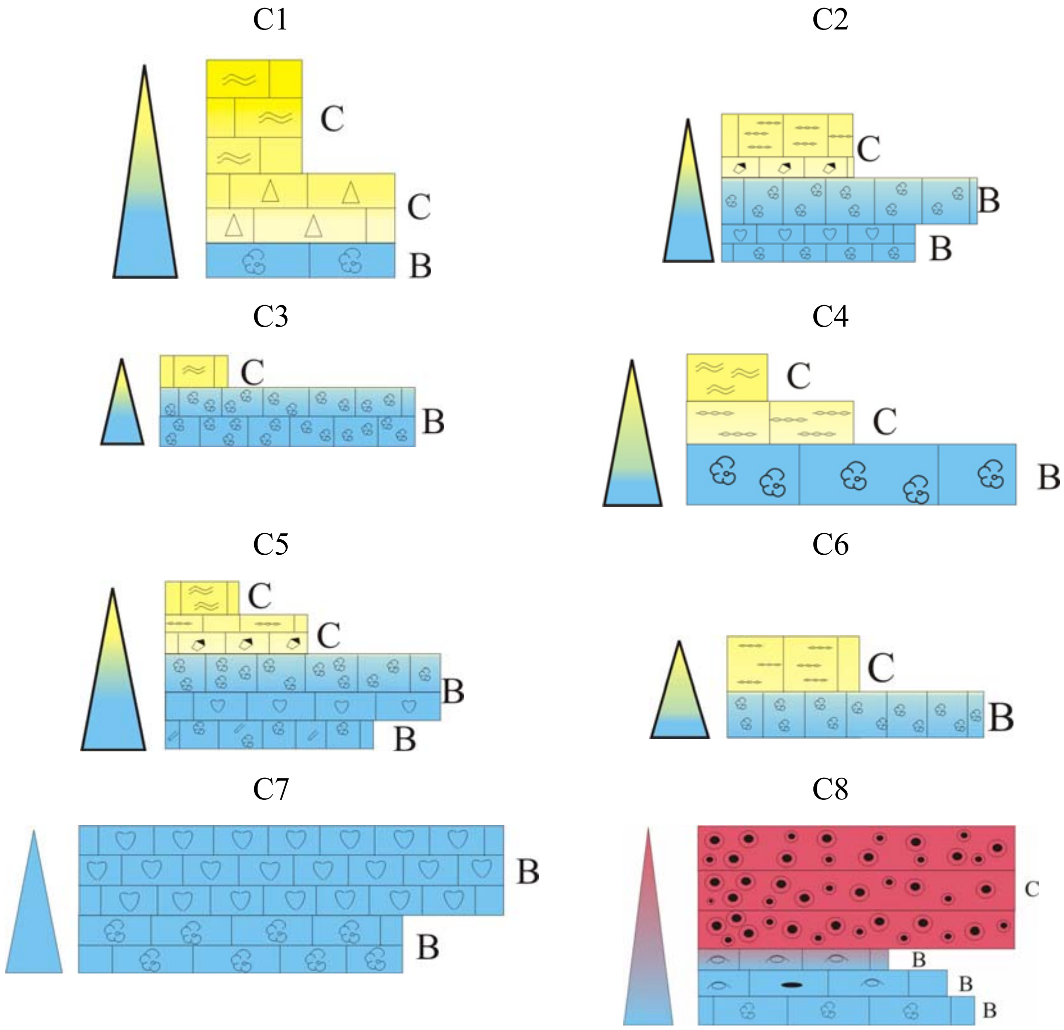

3.2.4. D type cycles

D type cycles are characterized by dolomitic limestones at the base of the cycles. These type of cycles are rarely seen in the studied succesions, only in the Marmaris sections. 2 sub-types are determined. D1 sub-type consists of dolomitic limestone at the base and fenestral limestones at the top. D2 sub-type is overlain by breccioid limestone, fenestral limestones and capped by stromatolites. D type cycles are commonly inter- to supratidal in character.

D1

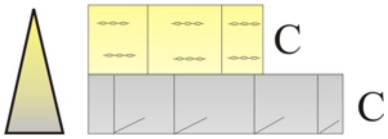

D2

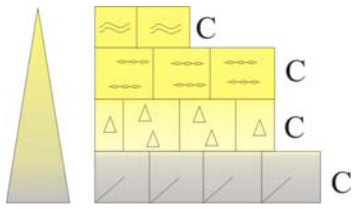

3.2.5. E type cycles

This type of cycle starts with ostracoda bearing wackestone and is capped by breccia. This cycle is seen only in one level.

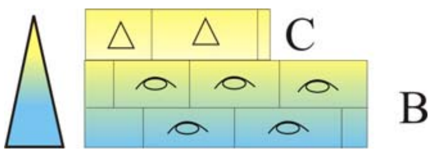

Among these cycle types, A and D type cycles are mostly inter- to supratidal in character, however B, C and E type cycles are subtidal to supratidal in character. The main feature of some of the B,C and E type cycles is the occurrence of subtidal deposits at the base of the cycles. On the other hand, A and D type cycles are mostly composed of inter- to supratidal deposits except for few sub-types (A8, A9, A10, A11, A12). In the measured sections, types of cycles are used to identify systems tracts and to construct the depositional model for the Lofer cycles in the Upper Triassic carbonates.

In this study, 8 sections were measured in order to examine shallowing-upward meter-scale cycles in the Upper Triassic carbonates of the Central and Western Taurides (Figure 30, 31, 32, 33, 34, 35, 36, 37). Furthermore, 12 parasequences were examined in detail to define smaller-scale parasequences within the successions (Figure 38, 40, 42, 44, 45, 46). All of the sections show Lofer-type cyclicity which was firstly described by Fischer (1964) in the Northern Calcareous Alps. Although there are some facies similarities with the Fischer's study, the cyclicity trend is commonly different in the Central and Western Taurides. Shallowing-upward meter-scale cycles constitute the basic working units of the studied successions, whereas Fischer defined deepening-upward cycles. Cycles are composed of subtidal through supratidal facies, however Fischer described supratidal through subtidal units. On the other hand, the occurrence of megalodont-bearing limestones, fenestral structures, stromatolites and some other facies types are similar with the Fischer's facies interpretations.

Leylek-1 and Leylek-2 sections are composed of carbonates alternating with thin, green claystone levels. Leylek-1 Section has a thickness of 33 m and contains 18 parasequences (Figure 30) whereas Leylek-2 Section measures 44.13 m and has 12 parasequences (Figure 31). The cycles are termed as 4^{th}-order cycles. In Leylek-1 Section A, B and C type cycles are recognized. Although A-type cycles (A1, A2, A3, A4, A5, A6 and A11) are common in Leylek-1 Section, thickness of B-type cycles (B2, B3 and B9) increase towards the top of the section. The lower levels of the Leylek-1 Section which are commonly composed of inter- to supratidal facies indicate regressive trend in these levels. Towards the upper levels, the thickness of the megalodont-bearing limestones increase and the cycles show transgressive character. The lower levels of the Leylek-1 Section in which the A-type cycles are common are interpreted as transgressive systems tract deposits, while the upper parts consisting commonly of B type cycles are interpreted as highstand systems tracts deposits.

With respect to Leylek-1 section, Leylek-2 Section consists of more subtidal units. A, B and E type cycles appear in this section. A-type cycles are composed of A7, A8, A9, A10 sub-type cycles which indicate subtidal condtions, except A7 sub-type cycle. B7, B9 sub-type cycles are also observed throughout the section. Similar with the upper levels of the Leylek-1 Section, Leylek-2 Section which has a thick megalodont-bearing limestones is interpreted as highstand systems tracts deposits.

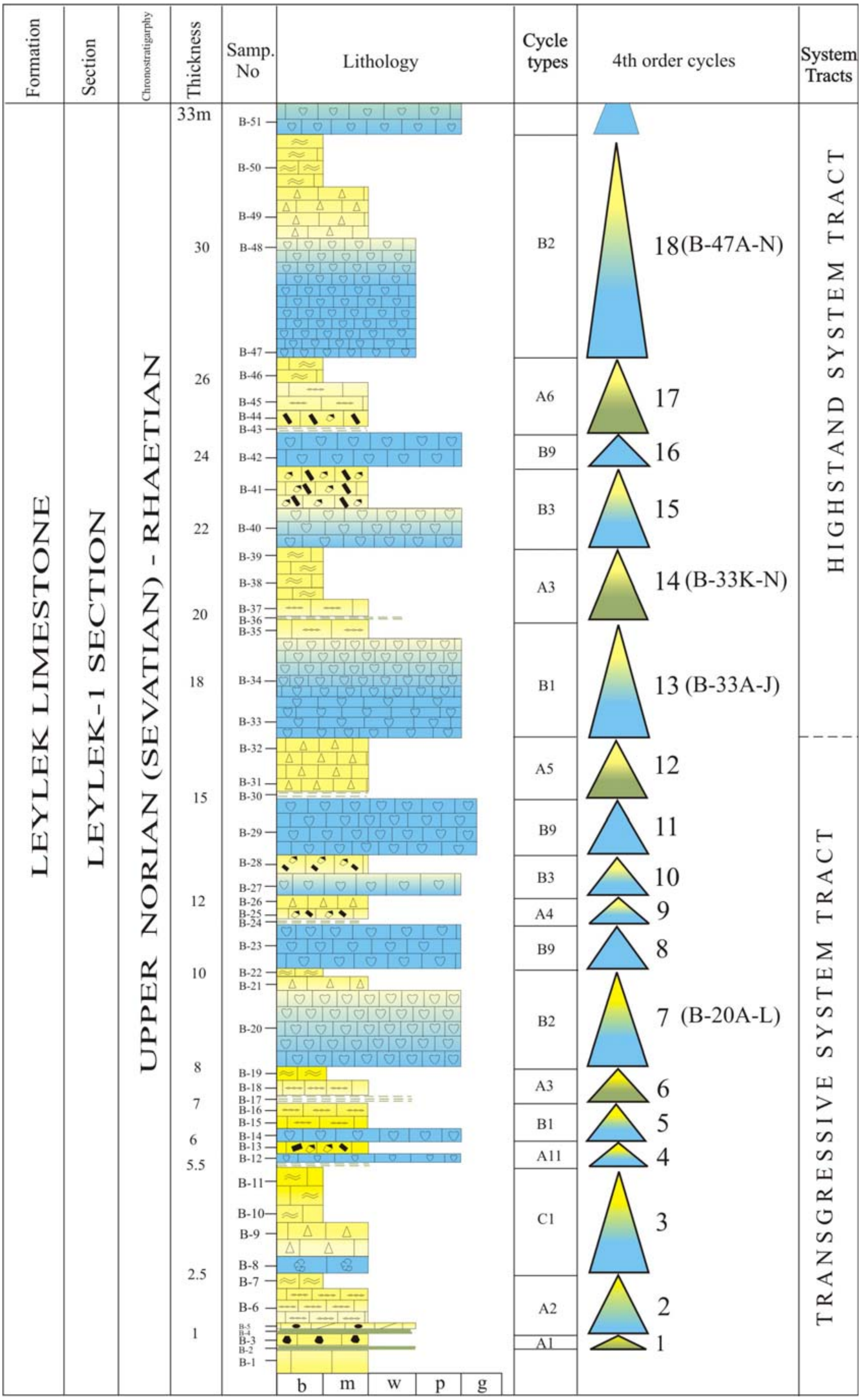

Figure 30. Leylek-1 Section, showing meter-scale cycles.

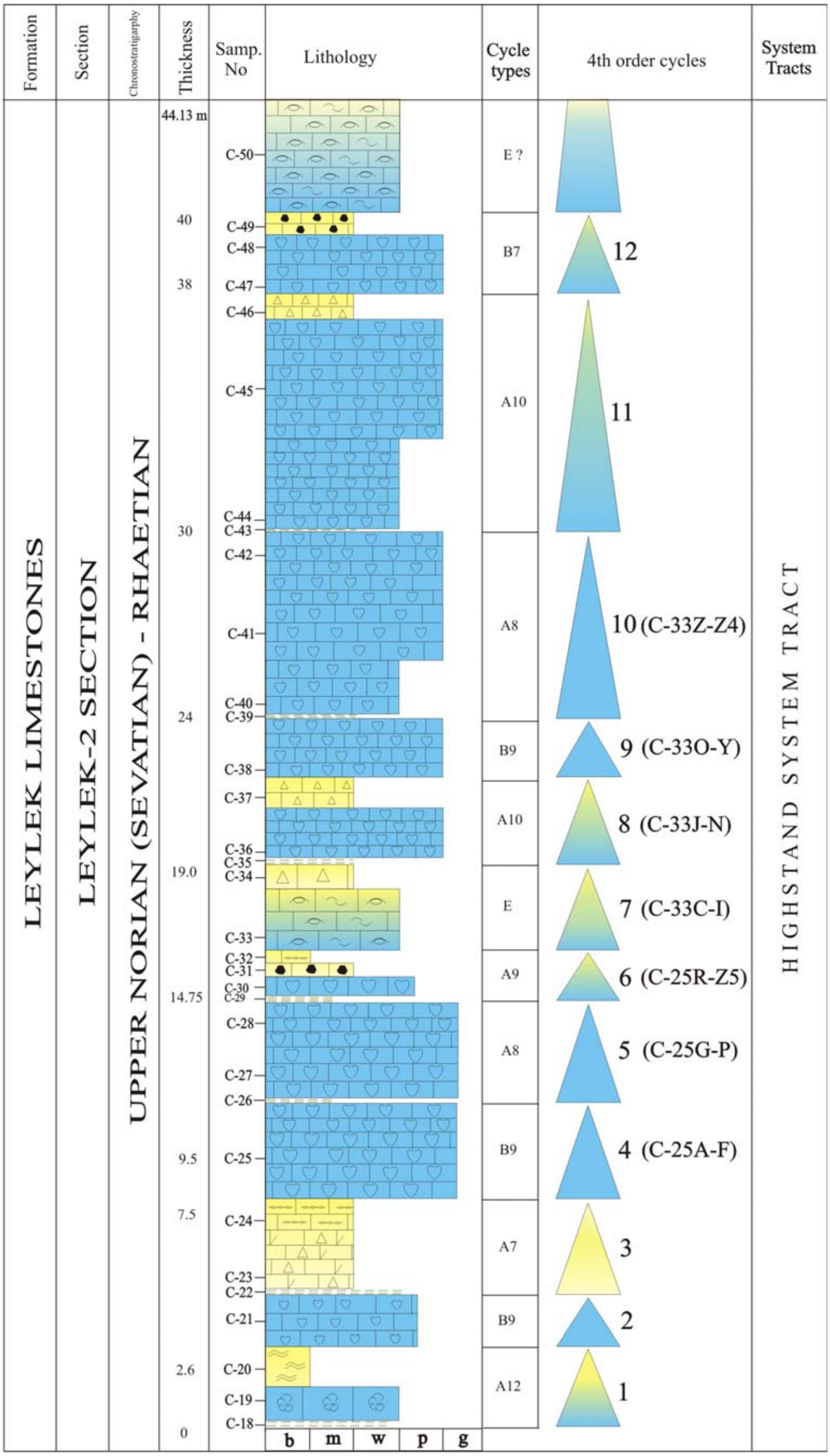

Figure 31. Leylek-2 Section, consisting of 12 parasequences.

In the second locality near Kuzca village, 4 meter-scale sections were measured. The cyclicity of the studied successions shows some differences from the successions near Leylek Hill. The main difference is the lack of claystone levels at the bottom of the cycles. The measured sections are entirely composed of carbonates.

Kuzca-1 Section is a 1.52m thick section (Figure 32). 12 samples were collected and one parasequence was detected. The cycle starts with megalodont-bearing wackestones and followed by fenestral limestones and breccioid limestones. The upper parts of the Kuzca-1 Section is wholly composed of subtidal deposits. Foraminiferal wackestones and packstones, megalodont-bearing packstones are the common facies types in the upper levels of the section. In Kuzca-1 Section, B8 subtype cycle is determined. Kuzca-2 Section is interpreted as forming by highstand systems tracts deposits in which the subtidal deposits are common.

Kuzca-2 Section measures 9.1 m and 11 samples were collected (Figure 33). 2 parasequences were determined. The first parsequence starts with foraminiferal wackestones and followed by megalodont-bearing packstones. The second parasequence consists of foraminiferal wackestones at the bottom and foraminiferal packstones-grainstones through the top. The upper parts of the Kuzca-2 Section consists of foraminiferal packstones and forms the cycle tops. Both of the first and second cycle are in subtidal character. C type cycles (C7) are observed within the section. Kuzca-2 Section which has thick subtidal units is interpreted as forming by highstand systems tracts deposits.

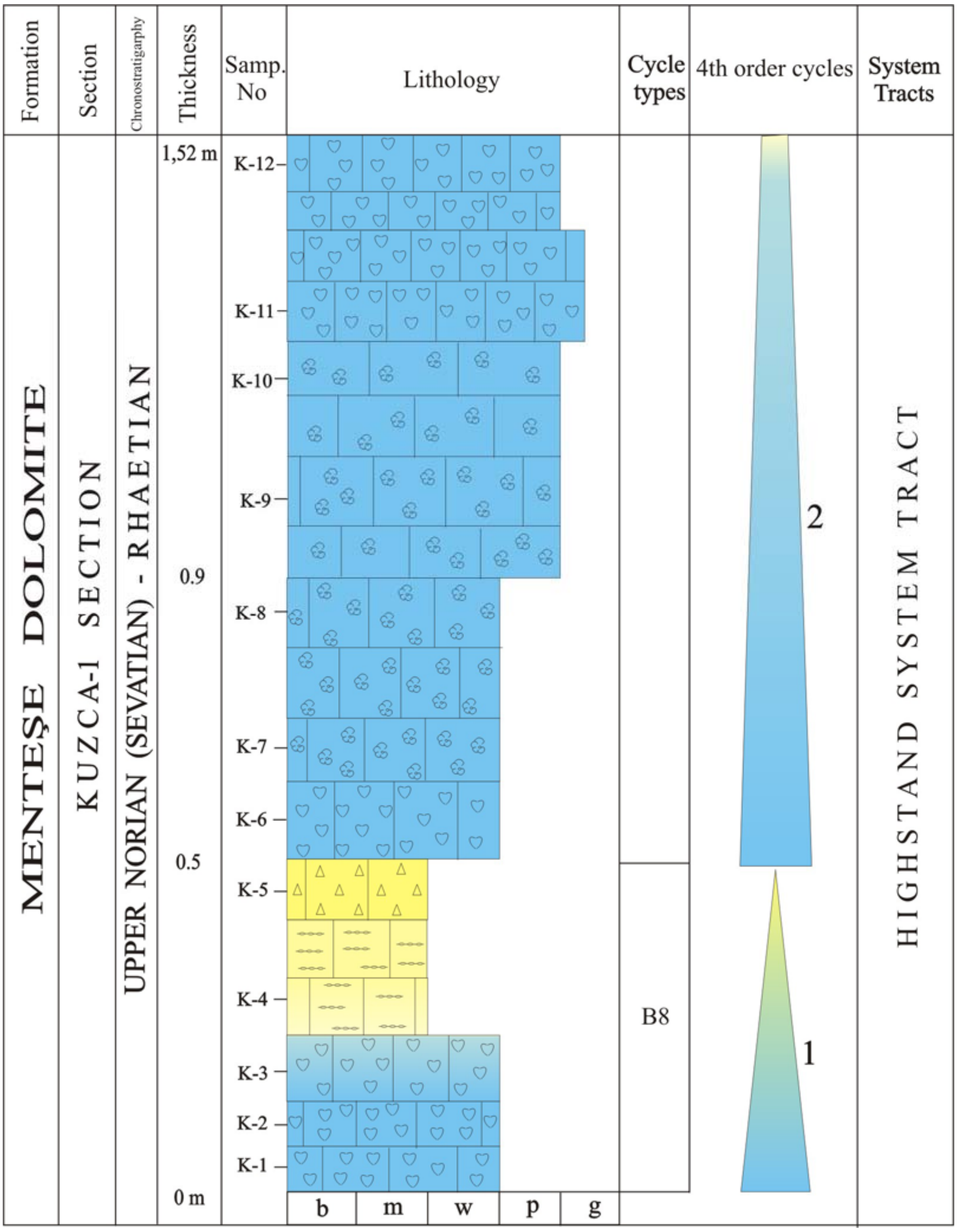

Figure 32. Kuzca-1 Section, showing shallowing-upward parasequence starting with subtidal facies and capped by fenestral limestones and breccioid limestones.

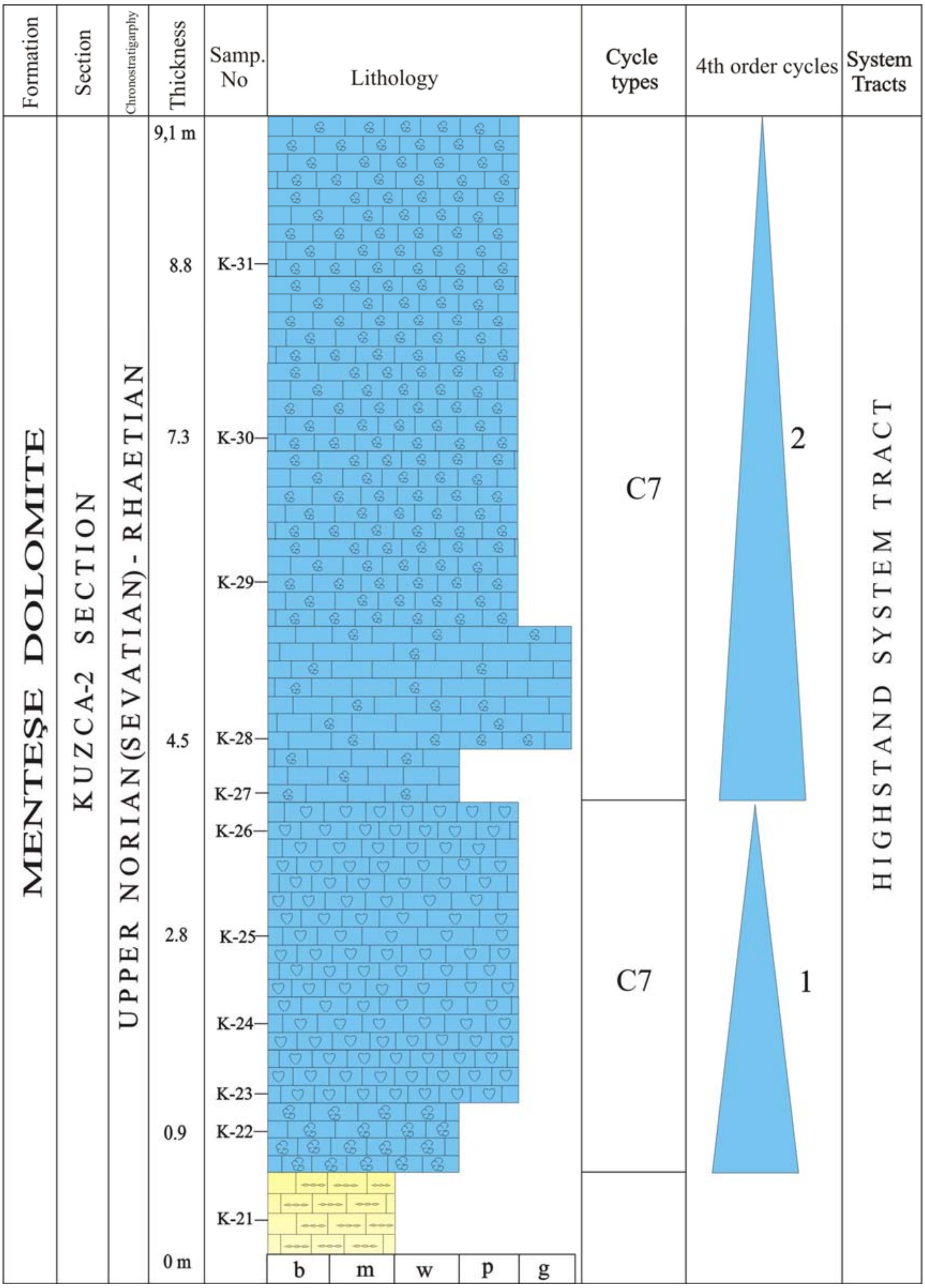

Figure 33. Kuzca-2 Section, showing shallowing-upward parasequences of commonly subtidal character.

Kuzca-3 Section has a thickness of 19.86 m and 13 samples were collected (Figure 34). It contains 2 parasequences. Subtidal deposits are also dominant in this section. The first parasequence starts with foraminiferal wackestones and continues upward with megalodont-bearing packstones and foraminiferal wackestones. The parasequence ends with fenestral limestones which indicates the first parasequence top. The second parasequence starts with recrystalized limestones. Although the position of this level within the cycle is not clear, it is included into the third parasequence as the basal facies. Recrystalized limestones are capped by megalodont-bearing packstones and followed by peloidal, foraminiferal packstones and grainstones. The upper parts of the section consists of foraminiferal packstones. B and C type cycles are recognized (B10, C2 and C6). These type of cycles indicate subtidal conditions, therefore Kuzca-3 Section is interpreted as forming by highstand systems tracts deposits as such in the Kuzca-1 and Kuzca-2 sections.

Kuzca-4 Section has a thickness of 2.3 m and characterized by 19 samples (Figure 35). Section starts with bioclastic packstone-grainstone facies and continues upward with ostracod-bearing packstone-wackestone lithofacies, and capped by red colored vadose pisoids. The red colored vadose pisoidic level has a 1.2 m thickness. 14 samples were taken from the vadose pisoidic zone. Few gastropoda fragments are found within them. This special level has been observed only in this section. The cycle starting with bioclastic packstone-grainstone facies ends with a subaerial exposure cap, probably indicating an important sea level fall in the Upper Triassic time. It could be the result of a prominent relative sea level fall. This level is overlain by dolomitic limestones which could be the base of a new cycle. C8 sub-type cycle is observed in the section.

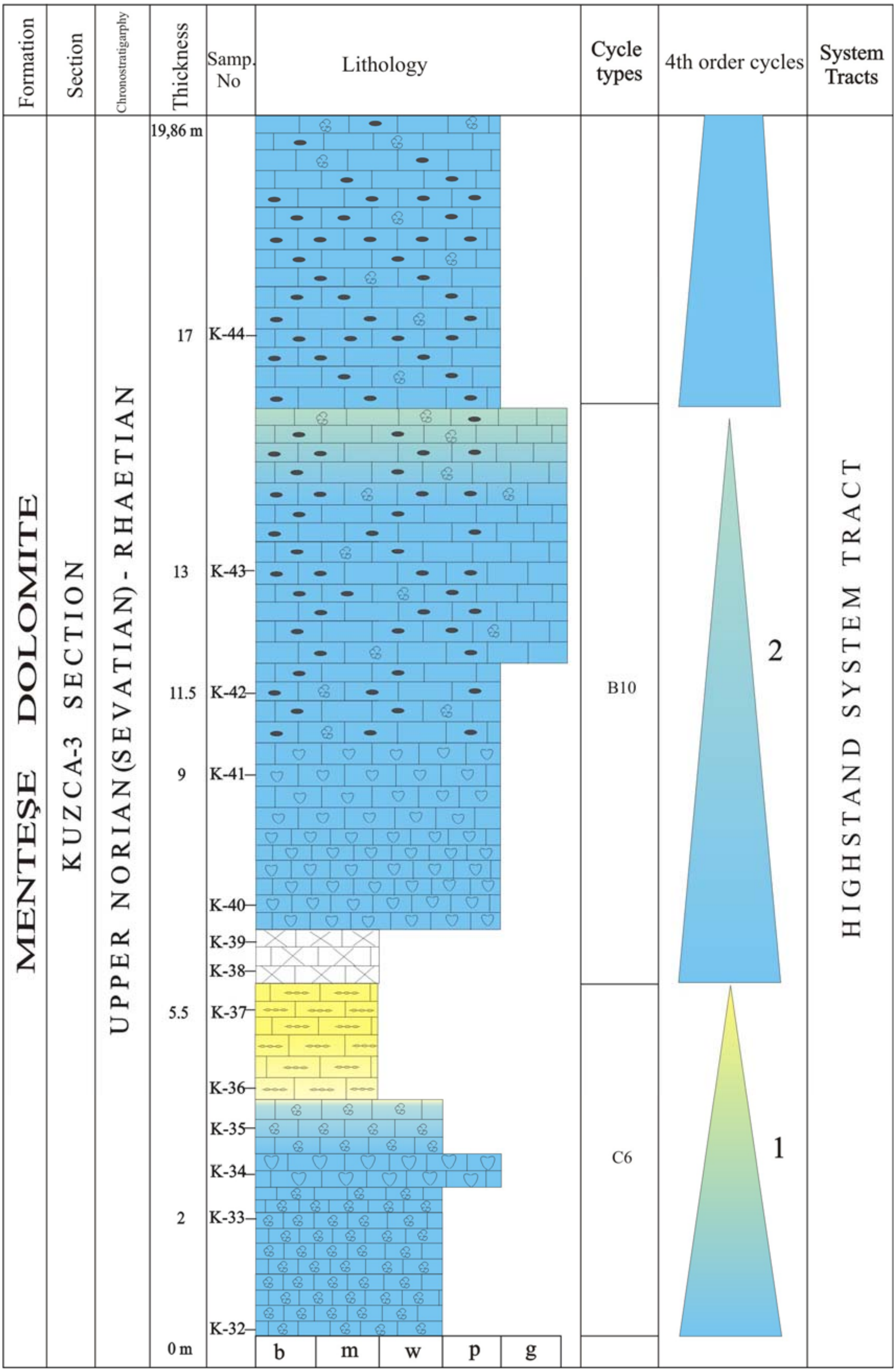

Figure 34. Kuzca-3 Section, showing shallowing-upward parasequences which are commonly in subtidal character.

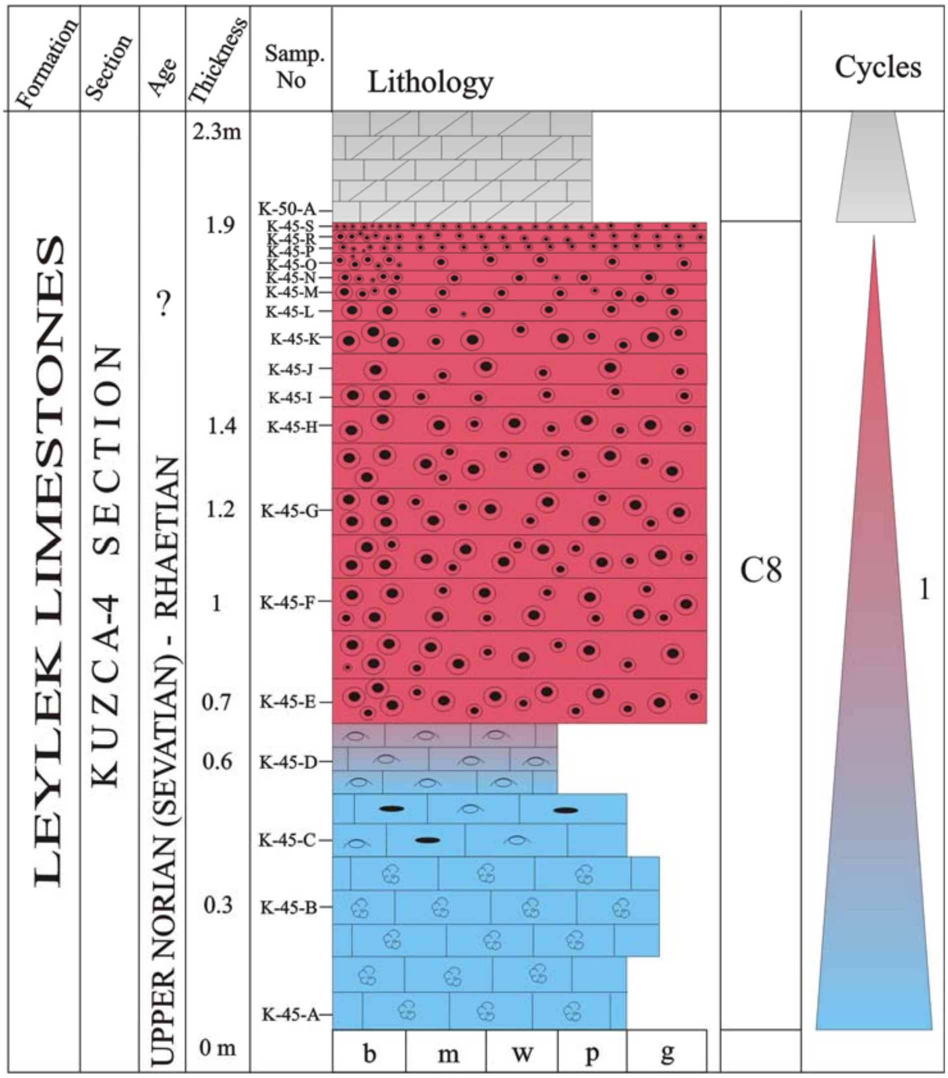

Figure 35. Kuzca-4 Section, showing shallowing-upward parasequences. Red color vadose pisoids are located at the top of the parasequence which indicate subaerial exposure conditions.

In the Western Taurides, two meter-scale sections were measured (Figure 36, 37). Marmaris-1 has a thickness of 23.25 m and Marmaris-2 measures 36 m. 4^{th} order meter-scale cycles are determined within the studied successions. Marmaris-1 Section consists of 9 parasequences (Figure 36) and they are termed as B, C and D type cycles (B4, B9, C7 and D1 sub-types). Inter- to supratidal deposits consisting of fenestral limestones, stromatolites are common in the lower levels of the Marmaris-1 section. However in the uppermost levels, megalodont-bearing limestones are much

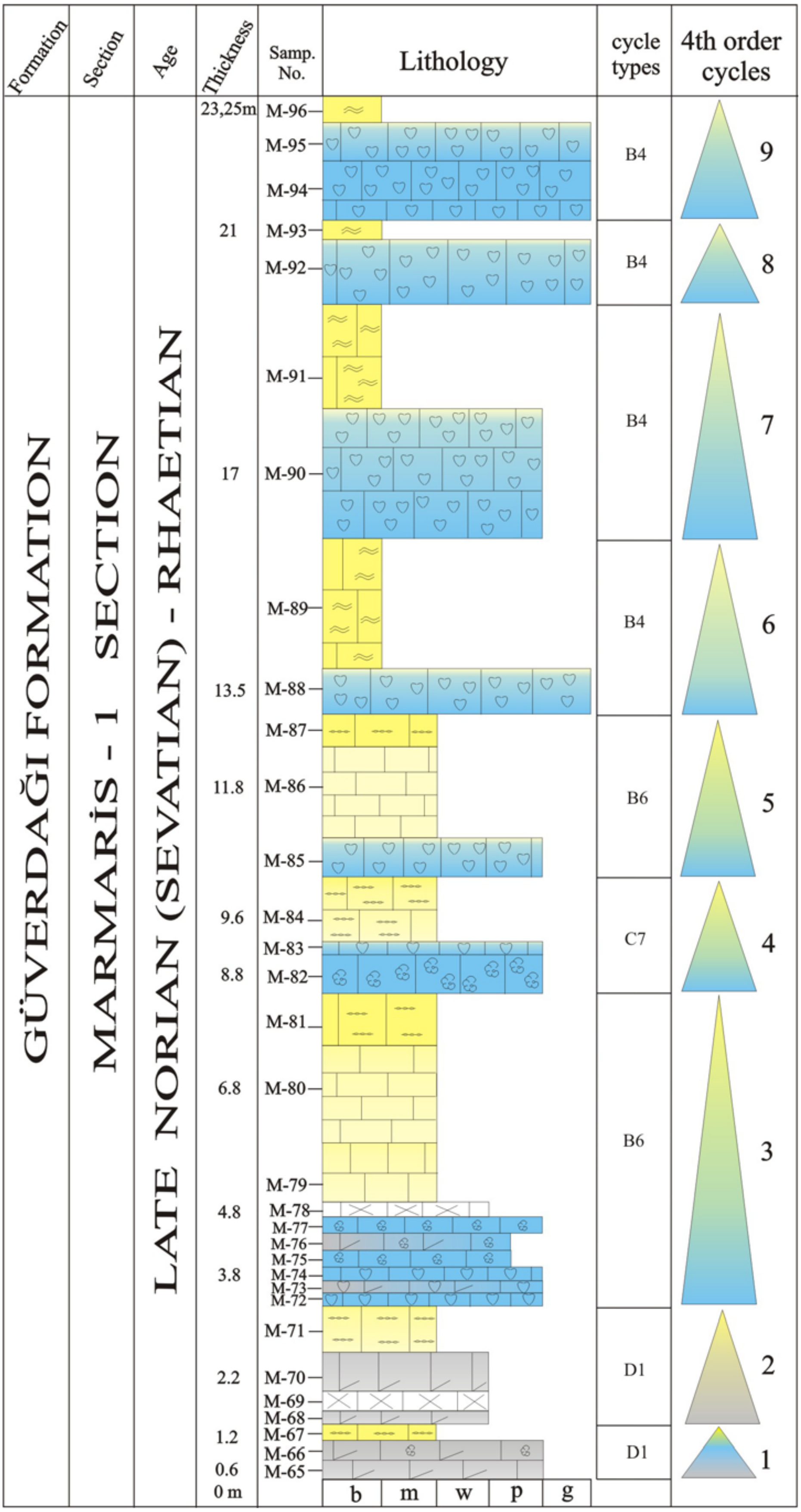

Figure 36. Marmaris-1 Section, showing 4^{th}-order cycles (parasequences).

more thicker than the inter- to supratidal deposits. Consequently, the lower levels of the Marmaris-1 Section in which the D1, B4, B9 and C7 sub-type cycles are found is interpreted as transgressive systems tract deposits. However, towards the top of the section highstand systems tract deposits are common which are commonly characterized by thick megalodont-bearing limestones.

Marmaris-2 Section is composed of 11 parasequences (Figure 37). B and C type cycles are determined in the section (B1, B4, B5, C6, C7 and C8 sub-types). As a whole, subtidal deposits which is represented by megalodont-bearing limestones and bioclastic packstones are common in the section. They are thick and capped by generally thin inter-to supratidal deposits such as stromatolites, breccioid limestones, fenestral limestones etc. On account of having more and thick subtidal units, Marmaris-2 Section is interpreted as forming by highstand systems tract deposits.

There is a close relationship between the measured sections in the Central and Western Taurides (Figure 38). Correlation of the cycle types and sytems tracts defined in the sections indicate some similarities and differences between the sections. Leylek-1 and Marmaris-1 Section are similar with having transgressive systems tract deposits in the lower levels and highstand systems tract deposits in the upper levels. On the other hand, Leylek-2 and Marmaris-2 Sections commonly consists of highstand systems tracts. As a comment, Leylek-2, Kuzca-1, Kuzca-2, Kuzca-3 and Marmaris-2 Sections could correspond to the upper levels of the Leylek-1 and Marmaris-1 sections.

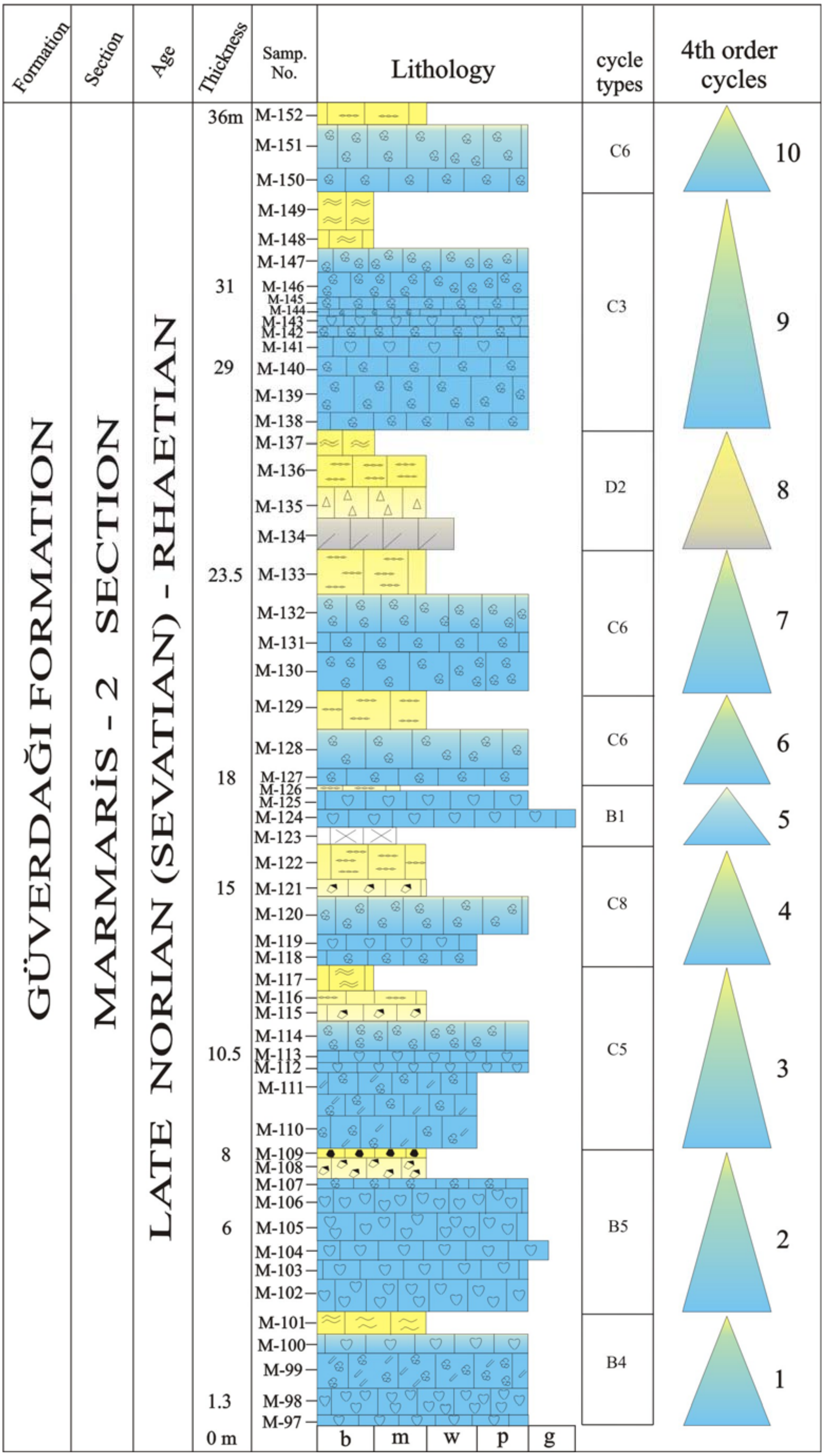

Figure 37. Marmaris-2 Section, showing 4th-order cycles (parasequences).

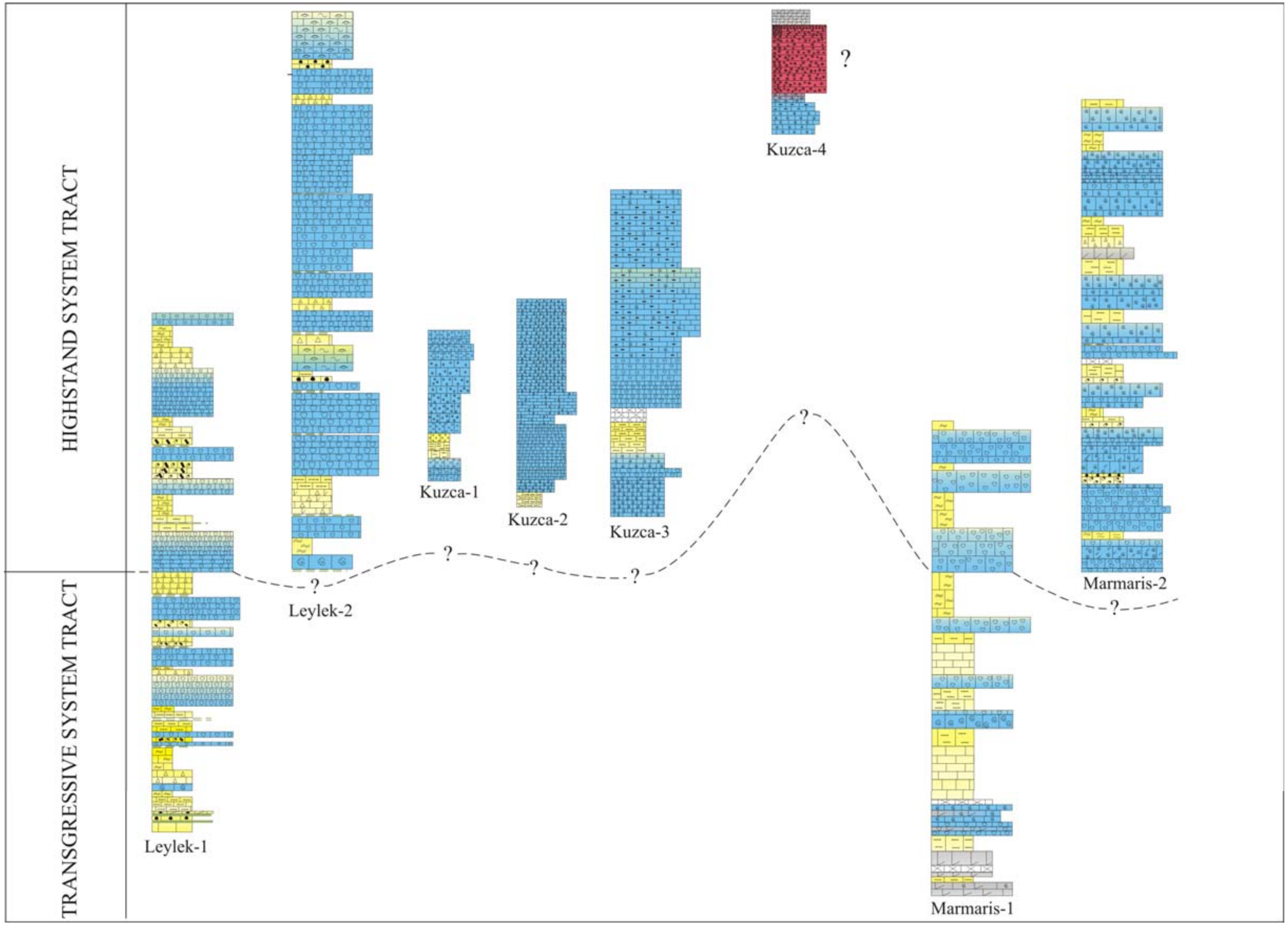

Figure 38. Correlation of the measured sections based on the systems tract that they characterize.

In order to evaluate each facies change within the beds, the parasequences were resampled in the field. 7th, 13th, 14th and 18th parasequence of the Leylek-1 Section; 4th, 5th, 6th, 7th, 8th, 9th, 10th and 11th parasequence of the Leylek-2 Section were examined in detail.

7th parasequence of Leylek-1 Section is a 2.6m thick parasequence and starts with megalodont-bearing limestones, followed by breccioid limestones and stromatolites (Figure 39, 40). After resampling, two smaller-scale parasequences (5th order cycles) are identified within the 7th parasequence. 12 samples were collected. The megalodont-bearing limestones which is at the bottom is overlying by breccioid limestones. Above, megalodont-bearing limestones reappear and pass upward into dismicrites with black pebbles, fenestral limestones, laminated structures and finally capped by stromatolites. The lower levels of the 7th parasequence show subtidal conditions, whereas the upper parts are commonly in intertidal/supratidal character.

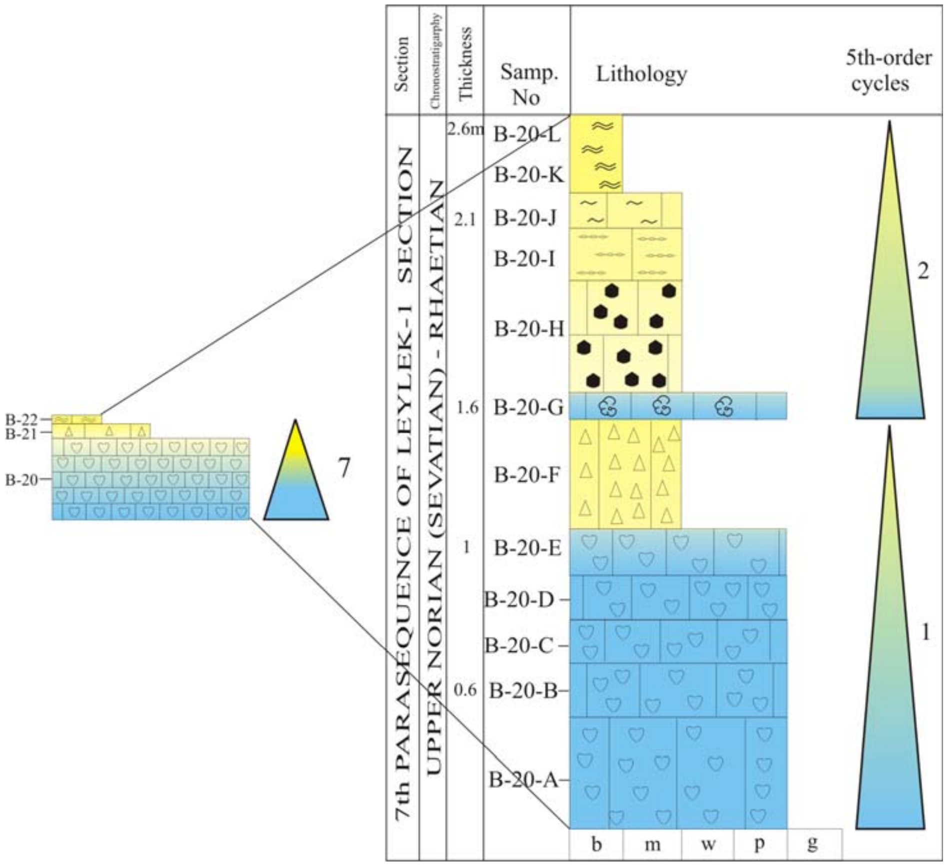

Figure 39. The 7th parasequence of the Leylek-1 Section, showing shallowing-upward parasequences of 5th order.

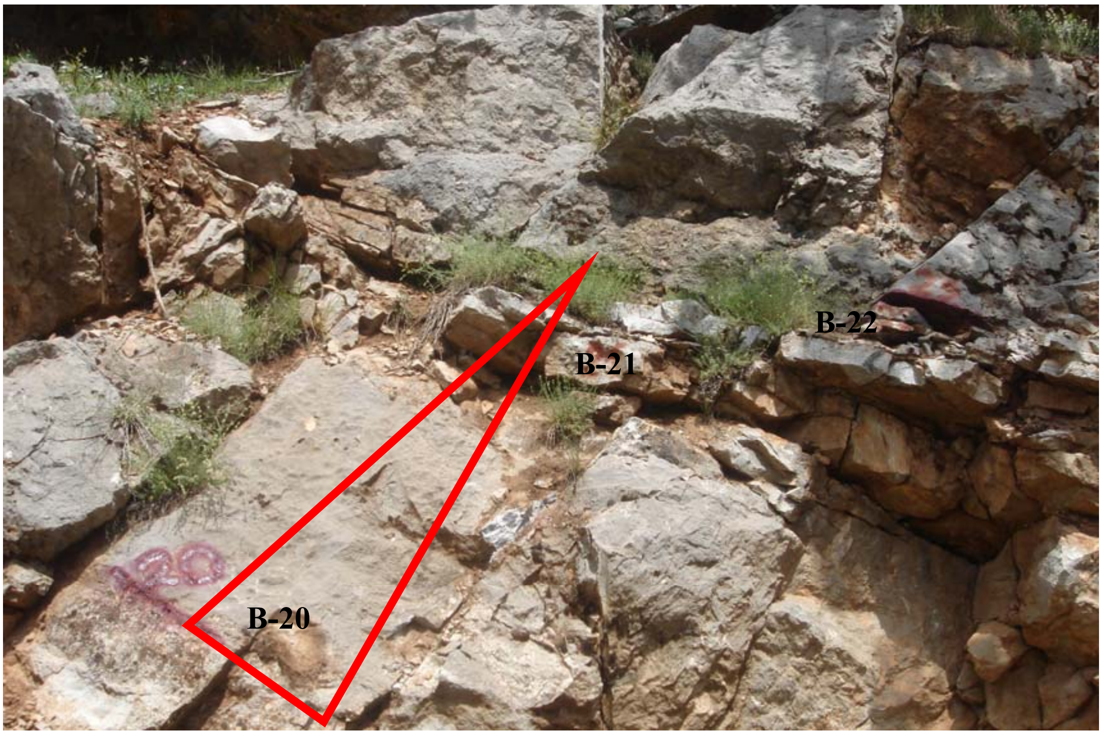

Figure 40. Outcrop view of 7^{th} parasequence of Leylek-1 Section.

13^{th} parasequence of Leylek-1 Section measures 3.70 m and contains megalodont-bearing limestone at the bottom and the fenestral limestones at the top (Figure 41, 42). During detailed sampling, 10 samples were taken within this parasequence and divided into 3 sub-parasequence (5^{th}-order cycles). As usual, the lower parts are composed of megalodont-bearing limestones and upper parts are in intertidal/supratidal character. The upper 2 sub-parasequences are completely formed by intertidal/supratidal facies.

14^{th} parasequence of Leylek- 1 Section has a thickness of 0.8 m and contain a thin claystone level at the bottom and fenestral limestones, stromatolites at the top (Figure 41). 4 samples were collected within the 14^{th} parasequence and differentiated into two sub-parasequence (5^{th}-order cycles) starting with thin claystone, followed by breccioid limestones and stromatolites. Above, foraminiferal and peloidal packstone lithofacies is overlain by stromatolites that forms the second sub-parasequence (5^{th}-order) of the 14^{th} parasequence.

18^{th} parasequence of Leylek-1 Section has a thickness of 5.8 m and consists of megalodont-bearing limestones, breccioid limestones and stromatolites respectively. 14 samples were collected and 3 sub-parasequences are identified

(Figure 43, 44). The first sub-parasequence consists of megalodont-bearing limestones, unfossiliferous lime mudstone and capped by breccioid limestones. In the second sub-parasequence, the subtidal part is thicker than in the first sub-parasequence, but the upper levels are precisely the same. The third sub-parasequence has a foraminiferal packstone lithofacies at the bottom and fenestral limestones and stromatolites at the top.

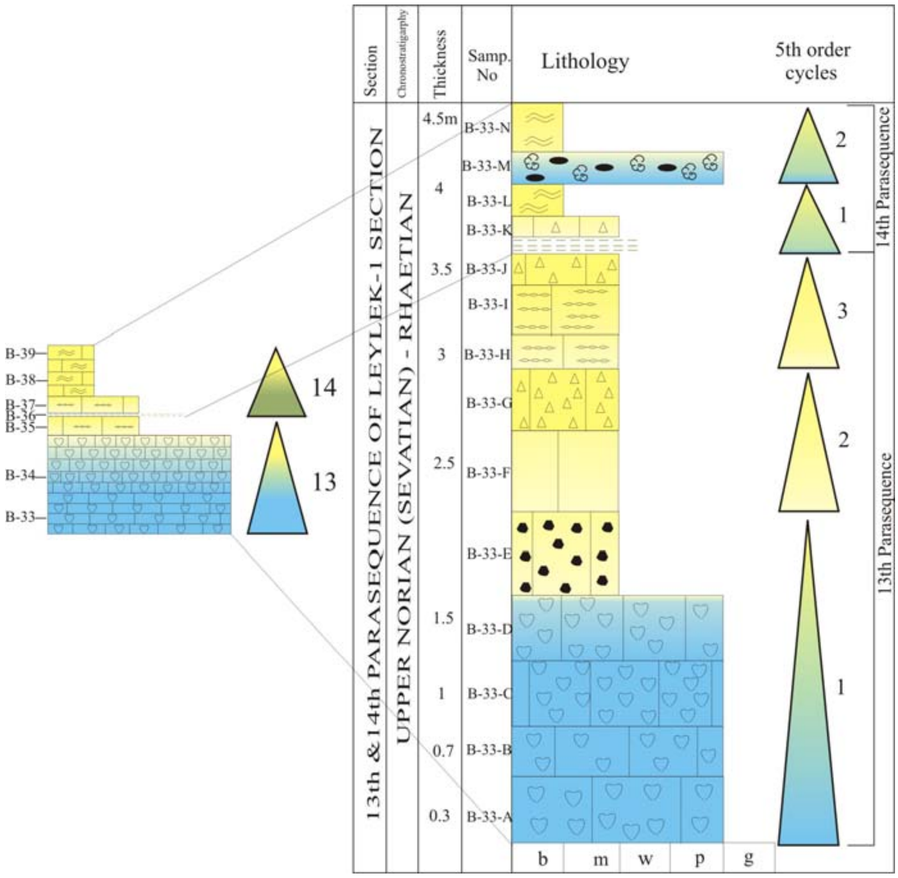

Figure 41. The 13^{th} & 14^{th} parasequences of the Leylek-1 Section, showing shallowing-upward parasequences of 5^{th}-order, starting with megalodont-bearing limestones which are followed by fenestral limestones, breccias and stromatolites.

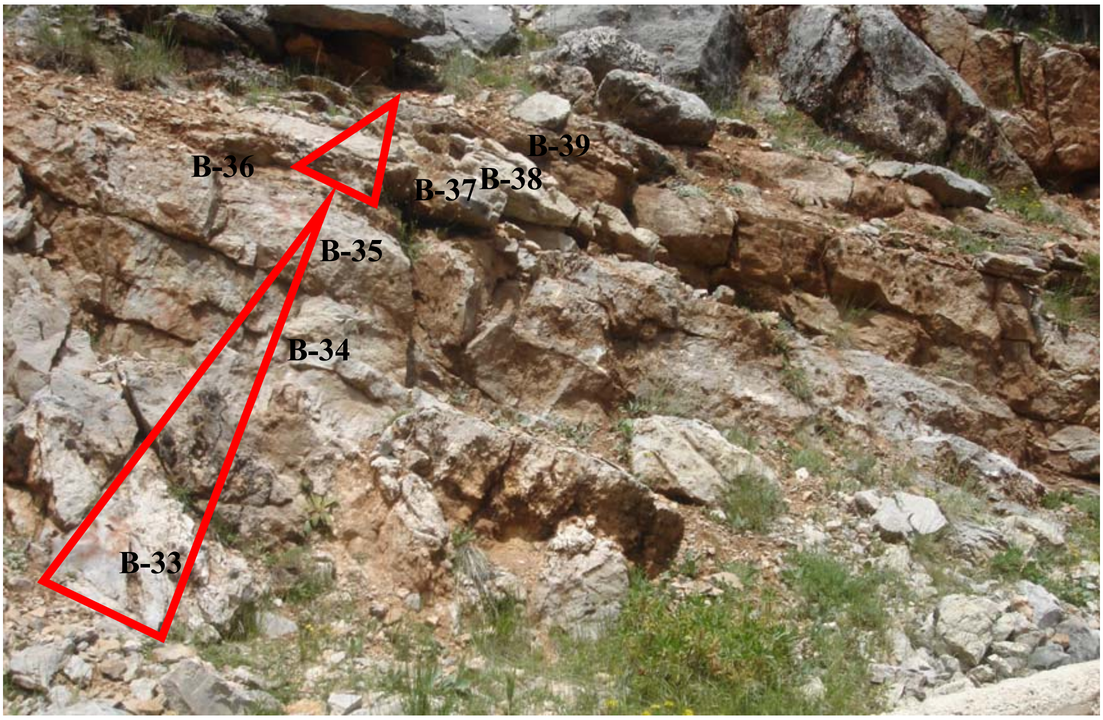

Figure 42. Outcrop view of 13th & 14th parasequences of Leylek-1 Section.

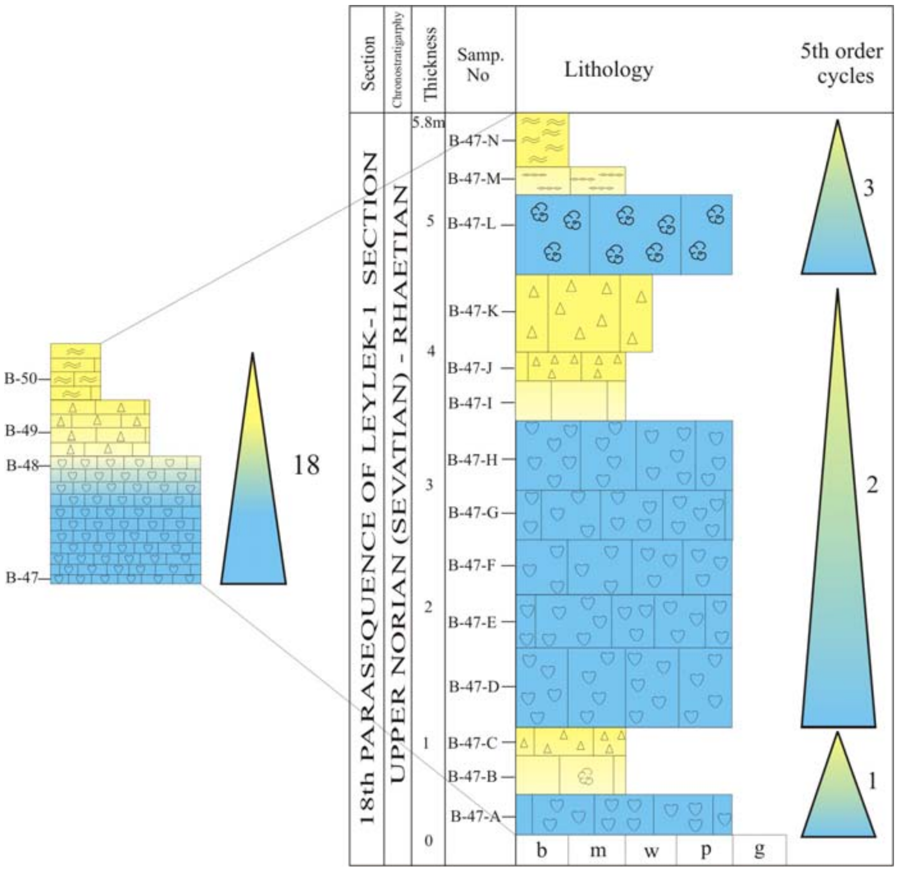

Figure 43. The 18th parasequence of the Leylek-1 Section, showing 3 shallowing-upward parasequences of 5th-order.

Figure 44. Outcrop view of 18th parasequence of Leylek-1 Section.

4th parasequence of the Leylek-2 Section is 3.1m. It contains 3 sub-parasequences (Figure 45). The first parasequence starts with megalodont-bearing limestones and ends with dismicrites with geopetal structures. The second parasequence consists entirely of foraminiferal and peloidal packstone-grainstone facies, indicating a subtidal zone. The third parasequence is a clay-based parasequence, containing dismicrites with geopetal structures and black pebbles indicating subaerially exposed conditions.

5th parasequence of Leylek-2 Section has a thickness of 3.7 m and consists of 3 sub-parasequence. 11 samples were collected (Figure 45). The first and second sub-parasequences are clay-based and commonly have intertidal/supratidal deposits in the upper levels of the cycles. Thin clay unit is overlain by unfossiliferous lime mudstone and stromatolites respectively. Above, dolomitic limestones are followed by breccioid limestones, forming the second sub-parasequence of the 5th parasequence. The third sub-parasequence is commonly in subtidal character. In this parasequence, megalodont-bearing limestones are overlain by black pebbles which indicate subtidal through subaerially exposed condtions.

6^{th} parasequence of Leylek-2 Section has a thickness of 3.2 m. 13 samples were collected. 4 sub-parasequences were identified (Figure 45). Initial 3 sub-parasequence starts with megalodont-bearing limestone beds and continue with breccia, fenestral limestones and stromatolites, respectively. Last parasequence is commonly in intertidal-supratidal in character. Dolomitic limestone is capped by fenestral limestones and stromatolites.

The 7^{th}, 8^{th}, 9^{th} and 10^{th} parasequence of Leylek-2 Section are almost in subtidal character rather than intertidal/supratidal (Figure 46). 7^{th} parasequence has a thickness of 5.3m and contains 3 sub-parasequences. The succession starts with foraminiferal wackestone and ends with an ostracoda wackestone which forms the first sub-parasequence. The second contains a clay unit at the base and is overlain by stromatolites. The third sub-parasequence is commonly subtidal, including megalodont-bearing limestones at the base and black pebbles and stromatolites at the top (Figure 46).

8^{th} parasequence differs from 7^{th} parasequence with the claystone level which forms the base of this parasequence. It is a 4.2 m thick parasequence. Claystone is followed by thick megalodont-bearing limestones and breccioid limestones (Figure 46).

9^{th} parasequence of Leylek-2 Section is a 6.4 m thick parasequence and contains also claystone at the base. As such in the 8^{th} parasequence, subtidal deposits are common. A thin dismicrite level containing black pebbles forms the top of this parasequence (Figure 46).

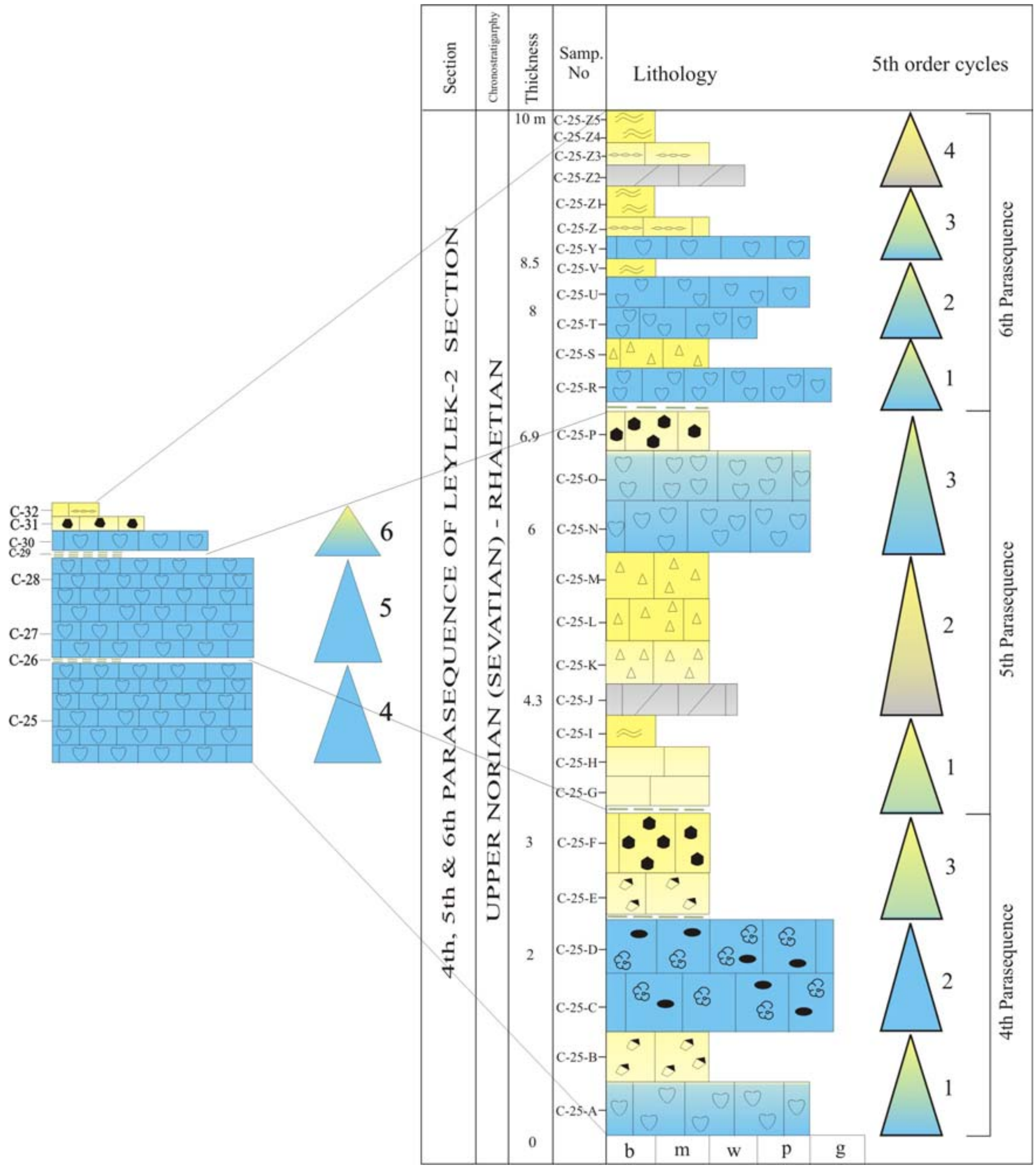

Figure 45. 5th-order cycles (parasequences) within the 4th, 5th and 6th parasequences of Leylek-2 Section, showing shallowing-upward character.

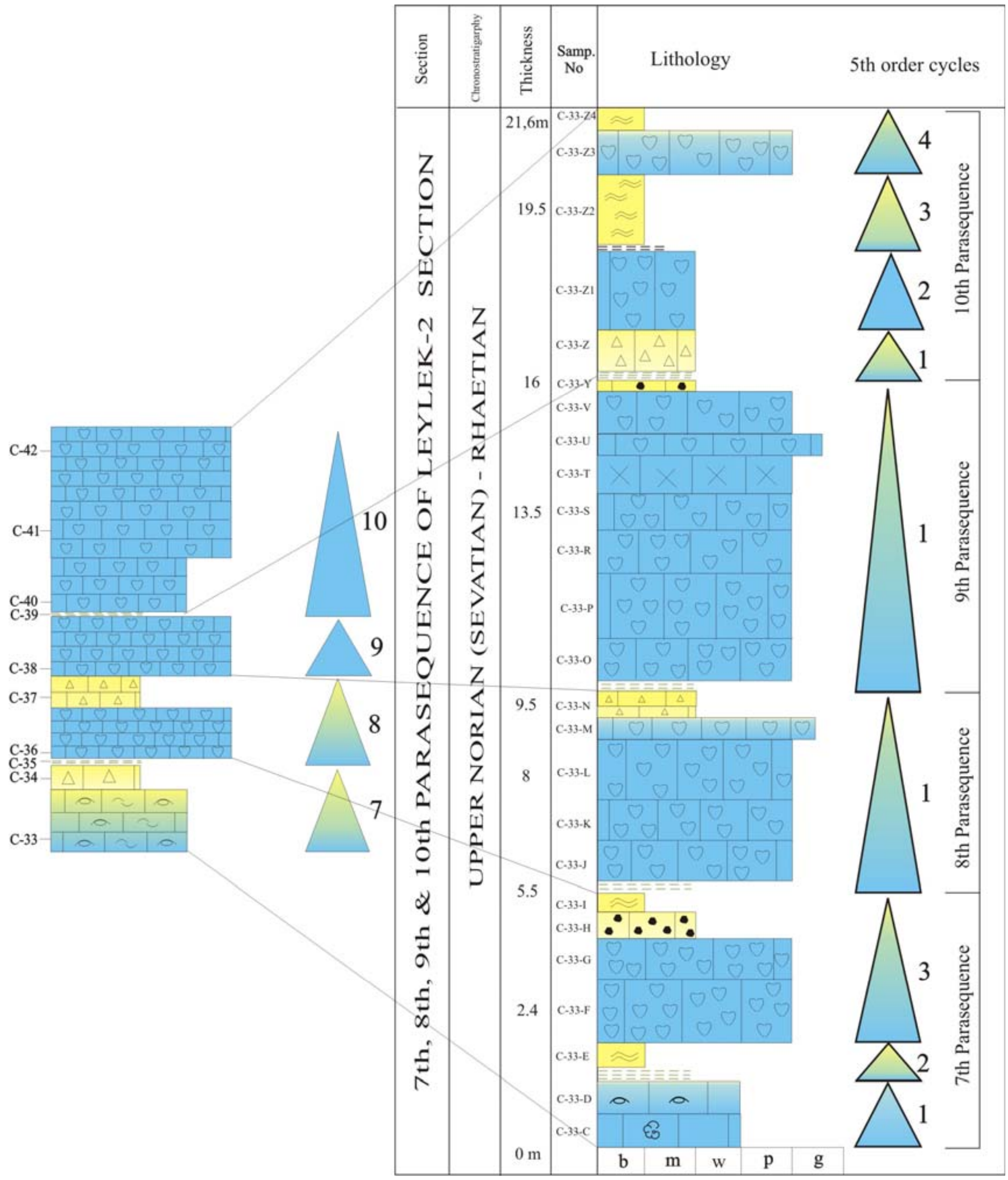

Figure 46. 5th-order cycles (parasequences) within the 7th, 8th 9th and 10th parasequences of the Leylek-2 Section, characterized by prominent subtidal facies.

10th parasequence has a thickness of 5.7m, contains 4 subfacies (Figure 46). The base is represented by a thin claystone and overlain by breccias which forms the first sub-parasequence. The second sub-parasequence is entirely characterized by megalodont-bearing limestones. The thin claystone overlies the megalodont-bearing limestones, indicating a flooding at the bottom of the third sub-parasequence. Claystone is capped by stromatolites which constitute the upper part of the third sub-parasequence. The fourth sub-parasequence consists of megalodont-bearing limestone which is overlying by stromatolites (Figure 46).

11th parasequence of the Leylek-2 Section is a 2.8 m thick parasequence and contains 3 sub-parasequences (Figure 47). 8 samples were collected. The sub-parasequences are generally in subtidal character like in the 7th, 8th and 9th parasequence of the Leylek-2 Section. The first sub-parasequence starts with a thick megalodont-bearing limestone, continues upward with a foraminiferal wackestone level including ostracoda and black pebbles forming the cycle top. The bases of the second and third sub-parasequences are formed by claystone which is overlain by lime mudstones with rare fossils and black pebbles. The top of the third sub-parasequence contains breccioid limestones and stromatolites (Figure 47).

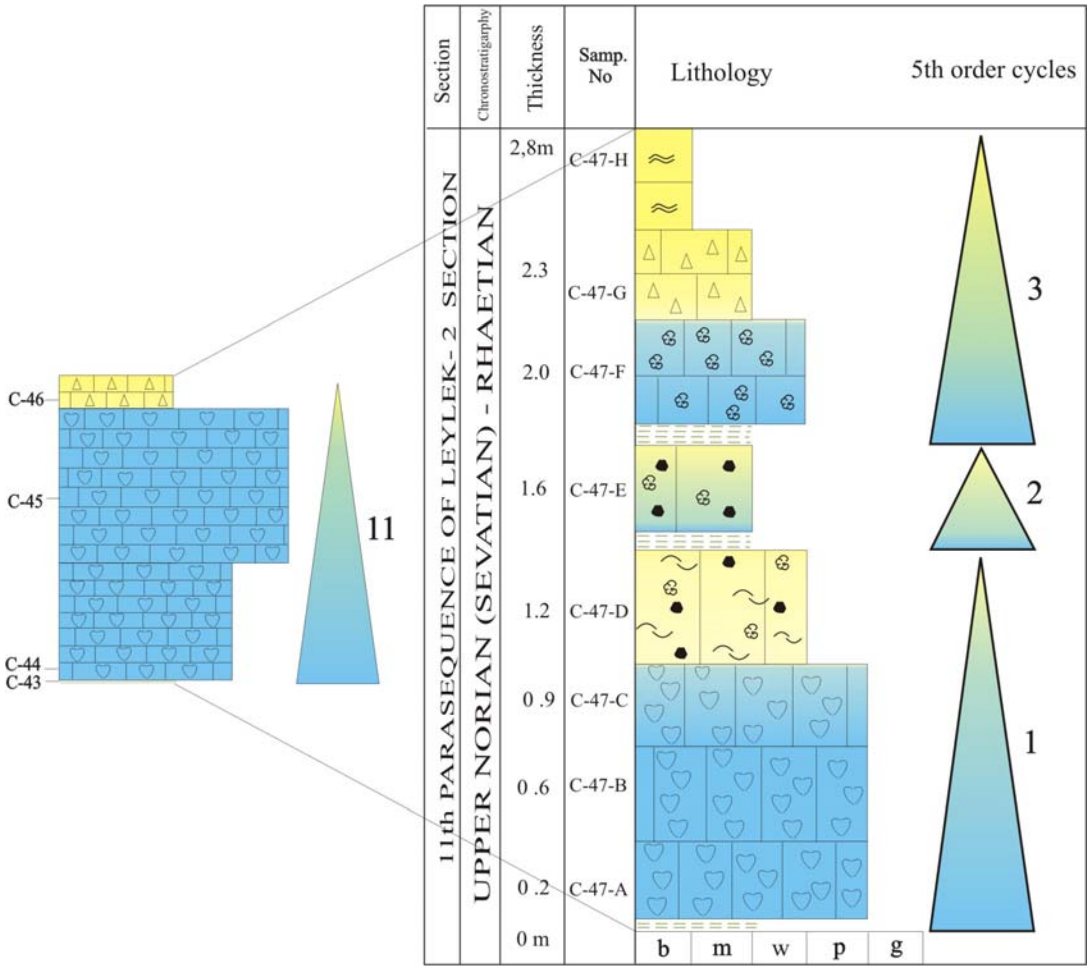

Figure 47. 5th-order cycles (parasequences) recognized in the 11th parasequence of Leylek-2 Section, showing shallowing-upward character.

Based on the cycle types (4th-order cycles in particular) and the successive occurrence of parasequences along the measured sections, a depositional model has been constructed for the Upper Triassic Lofer-type carbonates in the Central and Western Taurides (Figure 48). Our studies have provided additional informations about the nature of the cycles in the studied successions. The cycles are characterized by the vertical succession of the 3 main facies and they were deposited in a shallow marine environment. The cycles are generally composed of thickly bedded shallow subtidal facies or thin claystone levels at the bottom and capped by inter to supratidal facies (Figure 48). The transgressive and regressive portions of the cycles can be easily traced within the determined cycle types. Megalodont-bearing limestones, foraminiferal limestones and claystones reflect transgressive portions whereas dismicrites with black pebbles and clasts, fenestral limestones and stromatolites indicate regressive portions within the cycles. The studied successions also provided clear evidence of subaerial exposure at the top of the cycles. In this case, breccias and vadose pisoids were deposited. In contrast, Fischer (1964); Haas et al. (2007) stressed the evidence of subaerial exposure at the base of the cycles. In this model, stromatolites are also observed at the top of the subaerially exposed surfaces. This indicates that after the environment was subaerially exposed, accomodation space was rapidly being filled with stromatolites.

Cycles (parasequences) are bounded by marine flooding surfaces which are corresponding to the claystones, megalodont-bearing limestones and foraminiferal limestones at the bottom of the cycles. However, the subtidal deposits were proposed to form the cycle tops in the transgressive Lofer cycle models (Fischer, 1964; Haas, 1991 et). This trangressive Lofer cycle models do not fit with our findings for the Upper Triassic carbonates in the Central and Western Taurides. We interpret the Lofer cycle by a regressive model in which the subtidal deposits pass upward into inter to supratidal deposits. Moreover, the presence of siliciclastic input (clays) in the studied successions can be related to the topography, geometry of the Tauride platform during Late Triassic. They could be reworked into the depositional basin from elsewhere in the Taurides. In the proposed model, Lofer cycles are produced by small-scale sea-level changes and show upward-shallowing character.

Although the cycles are characterized by subtidal through supratidal facies, there are also some other types which are incomplete. In some cycles, transgressive portions at the bottom of the cycles are devoid of megalodont-bearing limestones or foraminiferal limestones (Figure 48). In these cycles, trangressive portions of the cycles are represented directly by thin claystones. Such cycles are commonly composed of inter to supratidal deposits and exhibit more regressive character rather than transgressive character. However, most of the cycles are commonly subtidal in character in which the megalodont-bearing limestones and foraminiferal limestones are thick and deposited at the bottom of the cycles. They were capped by thin-bedded inter to supratidal deposits. The typical Lofer cycles are composed of thickly bedded subtidal limestones and thin-bedded inter to supratidal limestones in this study, similar to those described by Fischer (1964, 1991), Goldhammer et al. (1990), Balog et al. (1997), Haas (2004) etc in the Tethyan Realm. However, there are some cyclicity differences with these studies concerning Lofer cycles. These differences will be discussed in the next section.

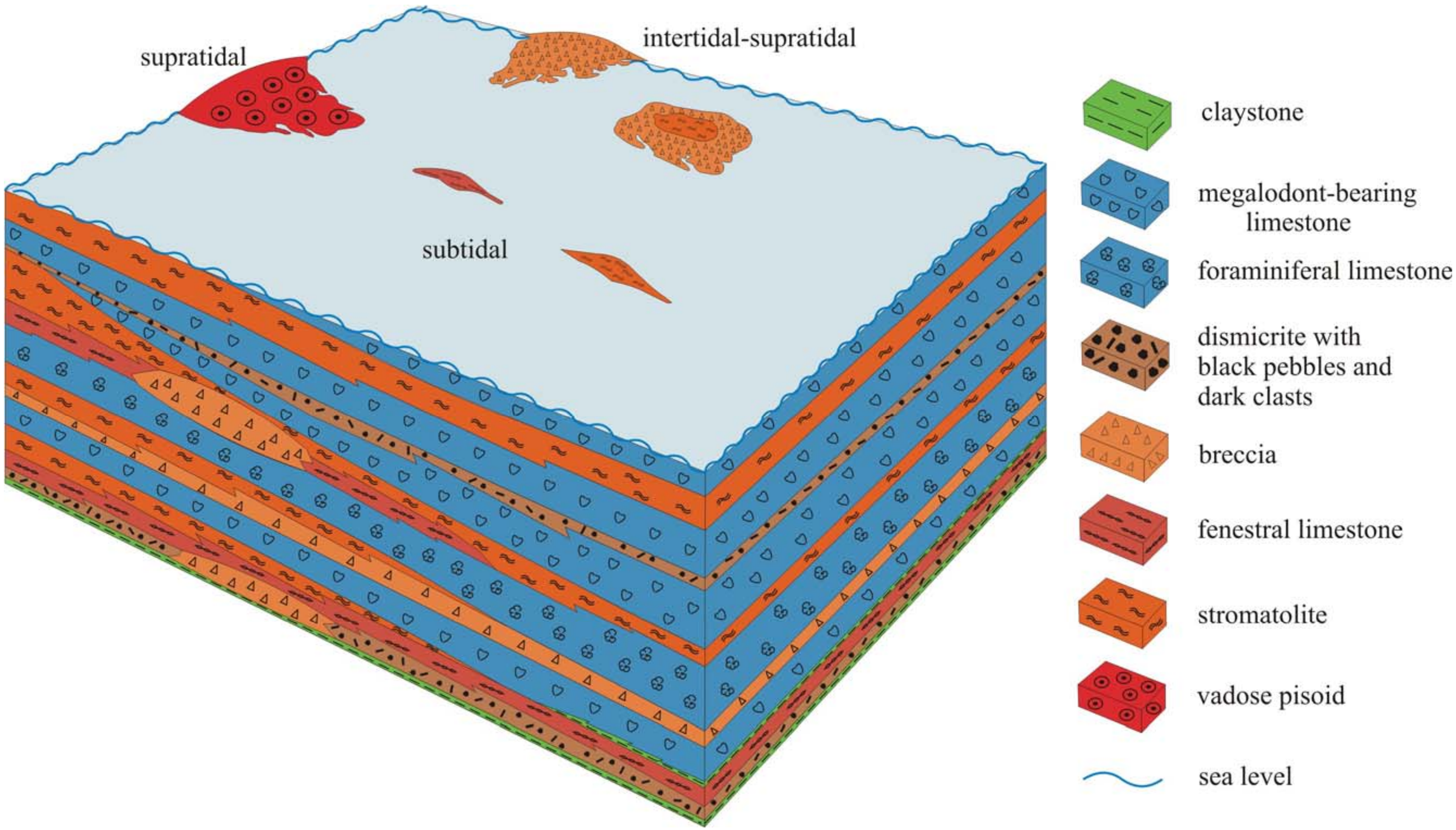

Figure 48. Depositional model of the Lofer-type cyclicity in the Central and Western Taurides, illustrating the stacking patterns of some of the parasequences in the studied successions.

3.3. Review of Upper Triassic cyclicity models and criticism of the previously suggested models

Sander (1936) was the first who recognized cyclothems in the Dachstein Formation. He determined thin units of dolomitic limestones, showing partly a milimeter-lamination, alternating with massive limestone units in the Loferer Steinberge near Lofer. He defined this rhytmic facies as Lofer facies, because of its excellent exposure in the Loferer Steinberge near Lofer. He discussed the complex fabrics of the laminated rocks, cycles and their origin.

Although Sander (1936) and his student Schwarzacher defined the Lofer cyclothems, the ideal Lofer cyclothem was firstly proposed by Fischer (1964) in the Northern Calcareous Alps (Austria). He recognized that the Lofer cyclothem typically consists of a disconformity at the base, a supratidal basal argillaceous member (red or green), an intertidal member containing algal mats and other sediments showing shrinkage features attributed to dessication and a subtidal massive limestone member with a varied biota (Figure 46). He defined a deepening-upward cyclicity and proposed tectonic and eustacy as the main controlling factors of the cyclicity.

Goldhammer et al. (1990) measured a 192 m thick section, consisting of 61 disconformity-bounded cycles. They recognized four subfacies within the Steinernes Meer section. Subfacies C consist of wackestones to grainstones with submarine hardgrounds and a rich fauna including abundant megalodonts. Subfacies B2 is composed of dolomitic, burrowed, peloidal wackestones and packstones with a restricted fauna of thin-shelled gastropods and ostracods. Subfacies B1 contains dolomitic laminite commonly containing prism and sheet cracks, crinkled laminae and shrinkage pores. Subfacies A includes intraformational conglomerate commonly containing clasts of the other subfacies in a green, brown or red argillaceous matrix. They interpreted subfacies A as soil, although Fischer (1964) defined as “reworked residue of weathered material”. In contrast to Fischer, they found regressive cycles. They also suggested that Lofer facies deposition was controlled by short-term variations in subsidence rate, leading to chaotic stratigraphic distribution of cycle thickness and diagenetic features and found little evidence of Milankovitch-type orbital forcing. After Fischer (1964), Haas (1982, 1991), Balog et al. (1997), Preto and Hinnov (2003) also suggested Milankovitch-type climatic changes and related sea level changes as the main controlling factors of the Lofer cyclicity.

Satterley (1996) proposed shallowing-upward Lofer cycles at Steinernes Meer. He emphasized that the Lofer cycles are formed by autocyclic processes.

Enos and Samankassou (1998) also measured a section at Steinernes Meer near Fischer's, Goldhammer et al.'s and Satterley's sections. Although they focused on the member A in their studies, they found only the alternation of B and C members. They did not find the Member A in their sections. Later, Enos and Samankassou (2002) searched the lateral continuity of the beds in Steinernes Meer and concluded that the autocyclic processes may have played a major role in the deposition of the Lofer cycles.

Haas et al. (2007) studied the successions of the Dachstein Limestone in the Dachstein Plateau (Austria). They recognized meter-scale cycles consisting of facies types, which were defined by Fischer (1964) as typical members of the Lofer cycles (A, B, C facies). Their interpretations are much closer to Fischer's opinion, although not precisely the same. Facies C consists of subtidal platform carbonates. Facies B has two basic types: stromatolites and mudstone rich in fenestral pores (birdseyes). Facies A contains thin red or green argillaceous carbonate layer and also consists of ostracode mudstone with a great number of thin-shelled ostracodes and rare foraminifers. In contrast to Fischer (1964), Goldhammer et al. (1990) and Satterley (1996), they didn't find in situ soil formation in facies A. However, they found abundant black pebbles in some layers that are considered as diagnostic for tidal flat deposits (Shinn, 1983). They interpreted the facies A as a transgressive tidal flat deposit. They showed that the cycles are bounded by uneven disconformity surfaces. According to their observations, the disconformities are generally covered by facies A and usually overlain by facies B, followed by facies C. Karstic features at the disconformity and below it and the evidence of subaerial exposure at the base of the cycles suggested periodical sea-level drop followed by renewed transgression and confirmed the allocyclic model for the explanation of the origin of the Lofer cycles.

Our present studies in southern Turkey show similarities and differences with the previous studies about the Lofer cycles. In contrast to Fischer (1964) and Haas (1991, 2004), we observed meter-scale shallowing-upward cycles in the Upper Triassic successions of the Central and Western Taurides (Figure 49). It is clearly visible that the subtidal facies is followed by intertidal and supratidal facies.

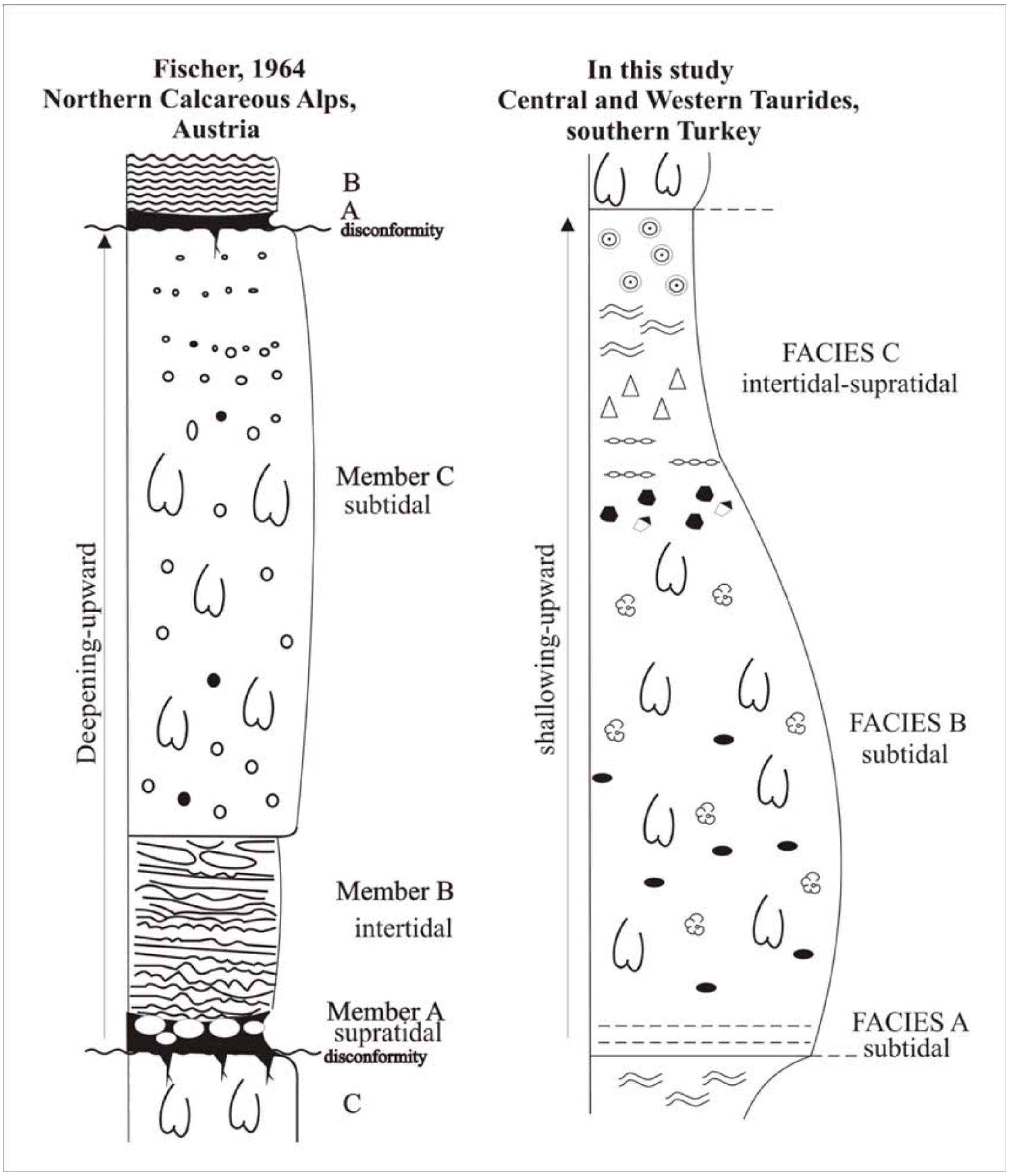

Figure 49. Differences between the Fischer (1964)'s idealized cycle and the Lofer cycle in this study.

Cycles are typically consisting of 3 types of facies. Clay- based cycles start with a thin, green colored claystone (facies A), overlain by bioclastic wackestone-packstone with abundant megalodonts (facies B) and followed by dolomitic limestones, lime mudstone with geopetal structures, laminated mudstone, fenestral limestones, breccioid limestones, stromatolites and vadose pisoids (facies C). The cycles with lack of claystone at the base consists of B and C facies. Clay unit has been only reported from the Leylek Limestone in the Central Taurides. Overlying megalodont-bearing limestones are characteristic of a subtidal zone and consist of bioclastic wackestones-packstones. Occasionally, bivalve and ostracoda wackestone, mudstone-wackestone with rare biota were also recognized. Facies B corresponds to the "megalodont limestone" (member C) of Fischer (1964) and to subfacies C differentiated by Goldhammer et al. (1990). Fischer described this facies as a subtidal massive limestone member with a varied biota and considered this facies as constituting the cycle tops. Goldhammer et al. (1990) defined this facies as limestones consisting of wackestones to grainstones with submarine hardgrounds and abundant megalodonts and interpreted as cycle bottom facies. In this study, facies B is interpreted as the subtidal facies and corresponds to the bottom of the cycles as in Goldhammer et al. (1990). The subtidal facies is overlain by intertidal-supratidal facies C. Megalodont-bearing limestones are generally followed by fenestral limestones which corresponds to the "algal mat loferite" described by Fischer (1964) and to subfacies B1 (shrinkage pores) differentiated by Goldhammer et al. (1990). Fenestral limestones are interpreted as upper intertidal-supratidal deposits (Flügel, 2004) in this study. Cycles are capped by breccias which indicate subaerial exposure conditions. This texture was interpreted as the 'intraformational conglomerate' by Fischer (1964) and regarded as an indication of supratidal reworking. Goldhammer et al. (1990) also differentiated this facies as intraformational conglomerate. We interpret this facies as breccioid limestone of intraformational character.

The limestone clasts are commonly angular or subangular rather than rounded and composed of micrites. Fischer (1964) and Goldhammer et al. (1990) considered that this facies is at the bottom of the cycles. But in this study, it is recognized at the top of the cycles. Some blackened pebbles were also encountered within these carbonates. These pebbles are indicative of subaerial exposure of limestones (Strasser and Davaud, 1983). Stromatolitic bindstones were also found at the top of the cycles. They commonly cover the breccia levels. This indicates that after the environment was subaerially exposed, accomodation space was rapidly being filled with stromatolites. This facies is regarded as member B of the 'Lofer cycle by Fischer (1964) and considered as the cycle bottom. In this study, this facies is considered as forming the cycle tops and regarded as upper intertidal-supratidal deposits (Flügel, 2004). Moreover, we did not find in-situ soil formation (Fischer's member A) in the studied successions.

Although there are so many studies on the Lofer cycles, the problem about the general characteristics of the Lofer cycles and the factors controlling the development of the cyclic successions are still continuing. We recorded meter-scale shallowing-upward cycles in southern Turkey and they are termed as 4^{th} and 5^{th} order cycles. In previous studies, high-frequency small-scale cycles are commonly attributed to sea level fluctuations in the Milankovitch band (Read and Goldhammer, 1988; Strasser, 1994 etc) and the existence of high frequencey 4^{th}-order sea level fluctuations are explained by changes in the Earth's orbital parameters (Strasser, 1988; Goldhammer et al., 1990). Future works must concentrate on the origin of the Lofer cycles whether they are allocyclic or autocyclic because the problem about the origin is still pending.

CHAPTER 4

4. RESPONSE OF FORAMINIFERS TO CYCLICITY

The sequence stratigraphic study, carried out in the Upper Triassic peritidal carbonates of the Central and Western Taurides, has allowed to recognise lithofacies and their associations. In this frame, the vertical variation of benthic foraminifer abundance has been analysed in the cycles. The benthic foraminifers are excellent bioindicators and, through their assemblages it is possible to determine and understand the environment and its process. The distribution patterns of benthic foraminifers are closely associated with the environmental conditions they inhabited. They have proved to be extremely useful in recognizing facies zones. In recent years, the response of foraminifers to cyclicity have become a popular subject in environmental geology (e.g., Weber et al., 2001, Xu et al., 2005, Amodio, 2006, Michalik et al., 2007). In the sedimentary record, shallow-water carbonates are one of the most sensitive to climatic variations as well as high-frequency sea-level oscillations. Those type of sediments which were deposited in platform interior settings, are cyclic in nature and show characteristic shallowing-upward trend.

The purpose of this chapter is to characterize the response of foraminifers to sedimentary cyclicity in shallow marine Upper Triassic cyclic carbonates. The main foraminifera group found in the studied successions is involutinids. In order to find out the response of involutinid group foraminifers to cyclicity, the number of involutinids were counted in some of the samples (Table 16). In this sense, the 7th, 13th, 18th parasequence of the Leylek-1 Section (Figure 50, 51, 52) and the 5th, 7th, 8th parasequence of the Leylek-2 Section (Figure 53, 54) were analysed. In the 7th parasequence of the Leylek-1 Section, two smaller-scale sub-parasequences have been identified (Figure 50). At the bottom of the 1st sub-parasequence, a thick megalodont-bearing limestones are overlain by breccioid limestones. The number of involutinids show variations in the megalodontid part of the parasequence due to the dolomitization and recrytallization processes. In the B-20E sample, involutinids

Table 16. The number of involitinid groups of foraminifers in each sample.

Sample no.	Number of Involutins	Sample no.	Number of Involutins	Sample no.	Number of Involutins	Sample no.	Number of Involutins
B-20A	9	B-33A	10	B-47A	352	C-33F	15
B-20B	40	B-33B	33	B-47B	26	C-33G	6
B-20C	40	B-33C	29	B-47C	0	C-33H	3
B-20D	72	B-33D	67	B-47D	75	C-33I	0
B-20E	193	B-33E	35	B-47E	65	C-33J	173
B-20F	23	B-33F	0	B-47F	63	C-33K	77
B-20G	40	B-33G	20	B-47G	18	C-33L	42
B-20H	6	B-33H	9	B-47H	35	C-33M	43
B-20I	0	B-33I	0	B-47I	0	C-33N	0
B-20J	1	B-33J	0	B-47J	0	C-25J	0
B-20K	0			B-4K	1	C-25K	0
B-20L	0			B-47L	24	C-25L	0
				B-47M	0	C-25M	0
				B-47N	8	C-25N	213
						C-25O	283
						C-25P	0

reaches the maximum number. After, it decreases in the B-20F sample corresponding to top of the 1st sub-parasequence (Figure 50). The 2nd sub-parasequence within the 7th parasequence consist of foraminiferal packstone at the base and dismicrites with black pebbles, fenestral limestones and stromatolites at the top (Figure 50). This parasequence clearly show the response of involutinids to the cyclicity. At the bottom, the number of involutinids is high, however at the top, the number decreases and finally gets zero (Figure 50). In the 13th parasequence of the Leylek-1 Section, the similar cases have been also recognized. It consists of 3 smaller-scale sub-parasequences (Figure 51). The 1st sub-parasequence has a thick subtidal part with respect to the intertidal-supratidal portion. The involutinids show variations in the subtidal part. It reaches the maximum number in the B-33D sample. At the top of the sub-parasequence, dismicrites with black pebbles contain fairly a good number of involutinids. This parasequence indicates that the number of involutinids do not always decrease or get zero at the top of the cycles (Figure 51). Also the 2nd sub-parasequence shows the similar conditions with the 1st sub-parasequence. Dismicrite which is corresponding to the bottom of the 2nd sub-parasequence is unfossiliferous, however, the breccioid limestones include nearly 20 involutinids (Figure 51). The 3rd

sub-parasequence consists of fenestral limestones at the bottom and breccioid limestones at the top (Figure 51). In this example, the number of involutinids decreases from cycle bottoms through cycle tops.

The 18th parasequence of the Leylek-1 Section has been also analysed to find the involutinid responses in the cycles. It consists of 3 sub-parasequence (Figure 52). These sub-parasequences fit the general opinion about the responses of involutinids to cyclicities. The megalodont-bearing limestones and foraminiferal packstones at the botttom of the cycles have high number of involutinids, on the other hand the cycle tops are unfossilifereous or contain few involutinids (Figure 52). The similar involutinid countings were also realized on the 5th, and 7th, 8th parasequences of the Leylek-2 Section. The 5th parasequence of the Leylek-2 Section consists of 2 sub-parasequences (Figure 53). The 1st sub-parasequence starts with dolomitic limestones and followed by breccioid limestones. Owing to the dolomitization process, the dolomitic limestone is unfossiliferous and also the breccioid limestones do not contain involutinids. The 2nd sub-parasequence consist of thick megalodont-bearing limestones at the bottom and dismicrites with black pebbles at the top. The number of involutinids is high in the subtidal part, however zero at the cycle top (Figure 53). The number of involutinids were also counted in the 7th and 8th parasequence of the Leylek-2 Section (Figure 54). The responses of involutinids to the cyclicity is quite clear. The 7th parasequence is constituted by megalodont-bearing limestones at the bottom and dismicrite with black pebbles and stromatolites at the top. The 8th parasequence also contain megalodont-bearing limestones at the bottom and breccioid limestones at the top. In both of the parasequences, the number of involutinids decreases towards the top of the parasequence and gets zero at the top (Figure 54).

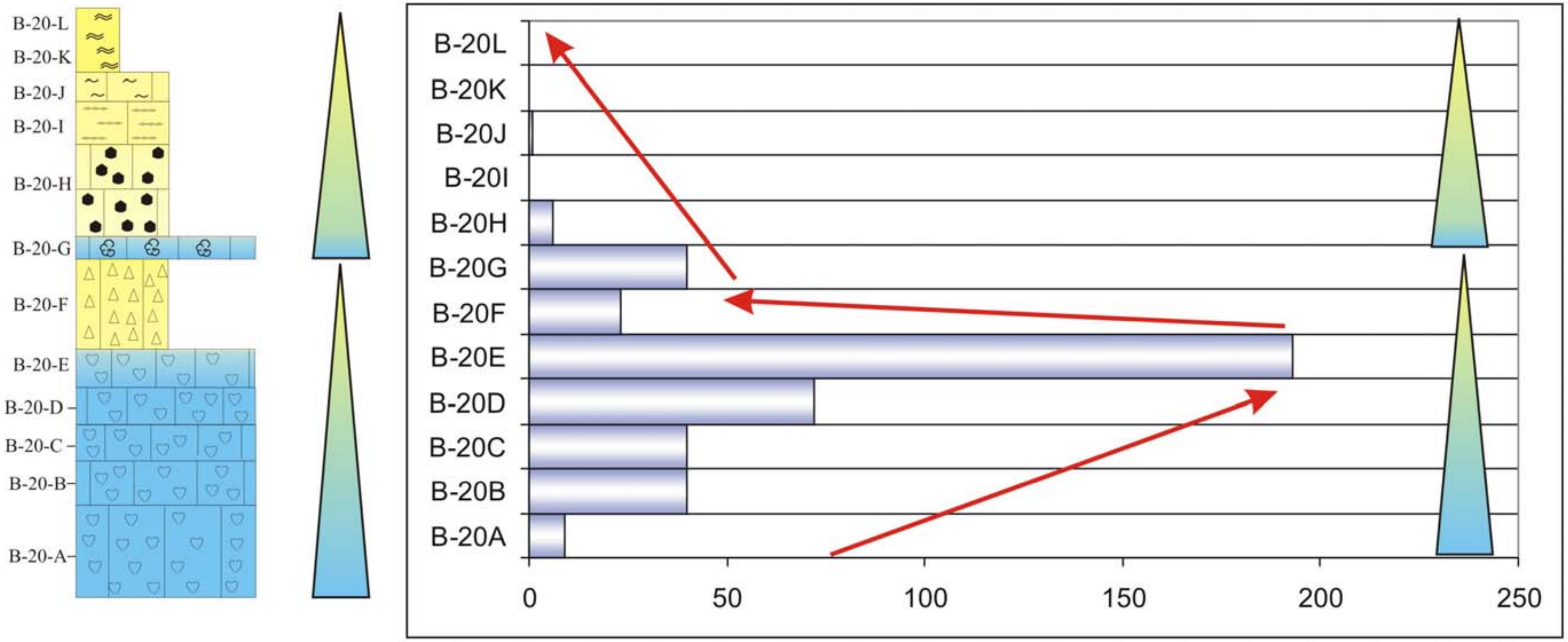

Figure 50. The abundance of foraminifers in the 7th parasequence of the Leylek-1 Section in order to find out the response of involutinids to cyclicity.

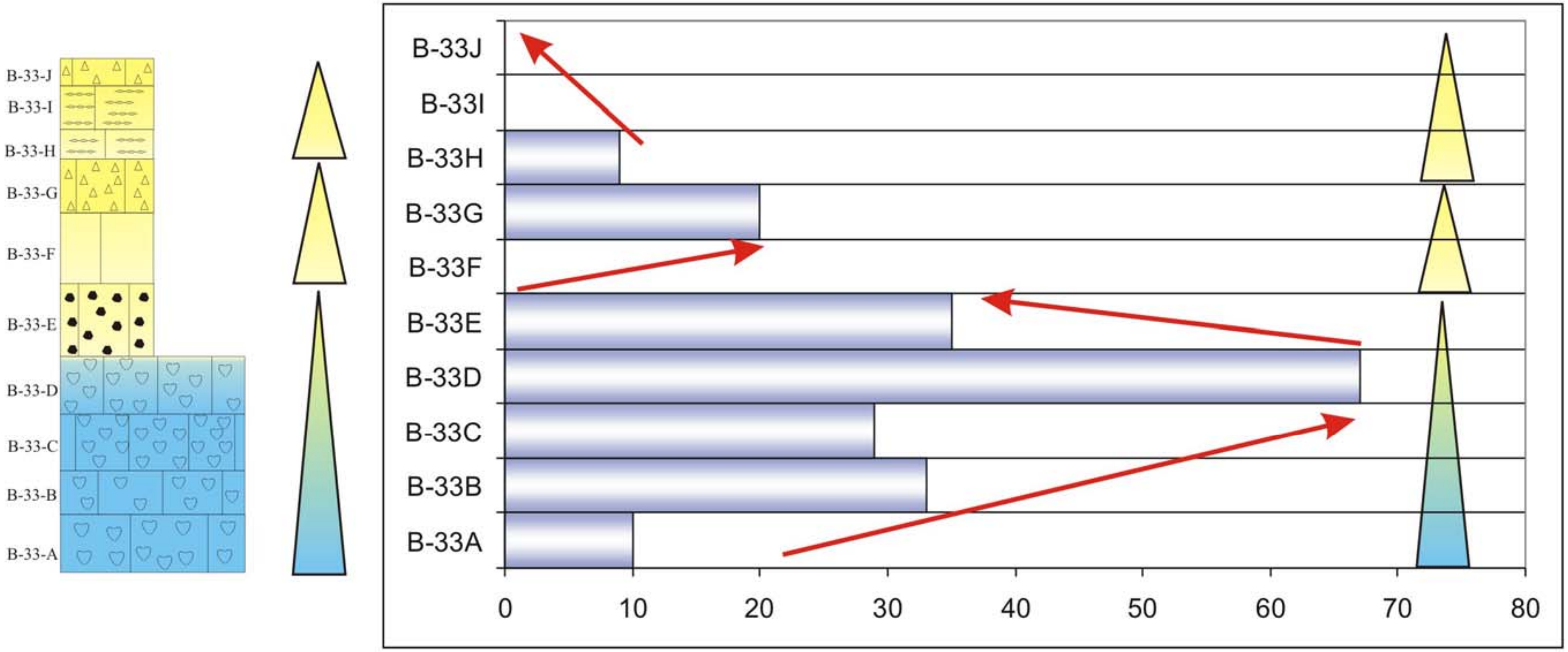

Figure 51. The abundance of foraminifers in the 13th parasequence of the Leylek-1 Section in order to find out the response of involutinids to cyclicity.

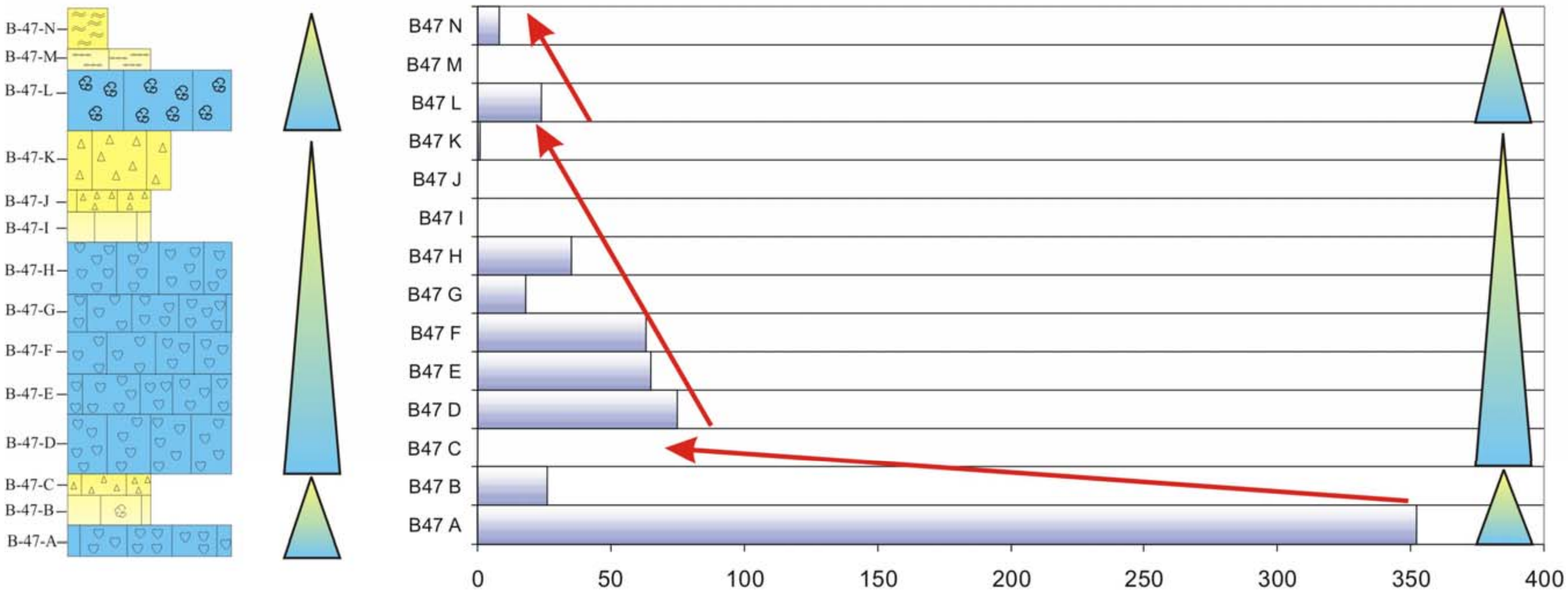

Figure 52. The abundance of foraminifers in the 18th parasequence of the Leylek-1 Section in order to find out the response of involutinids to cyclicity.

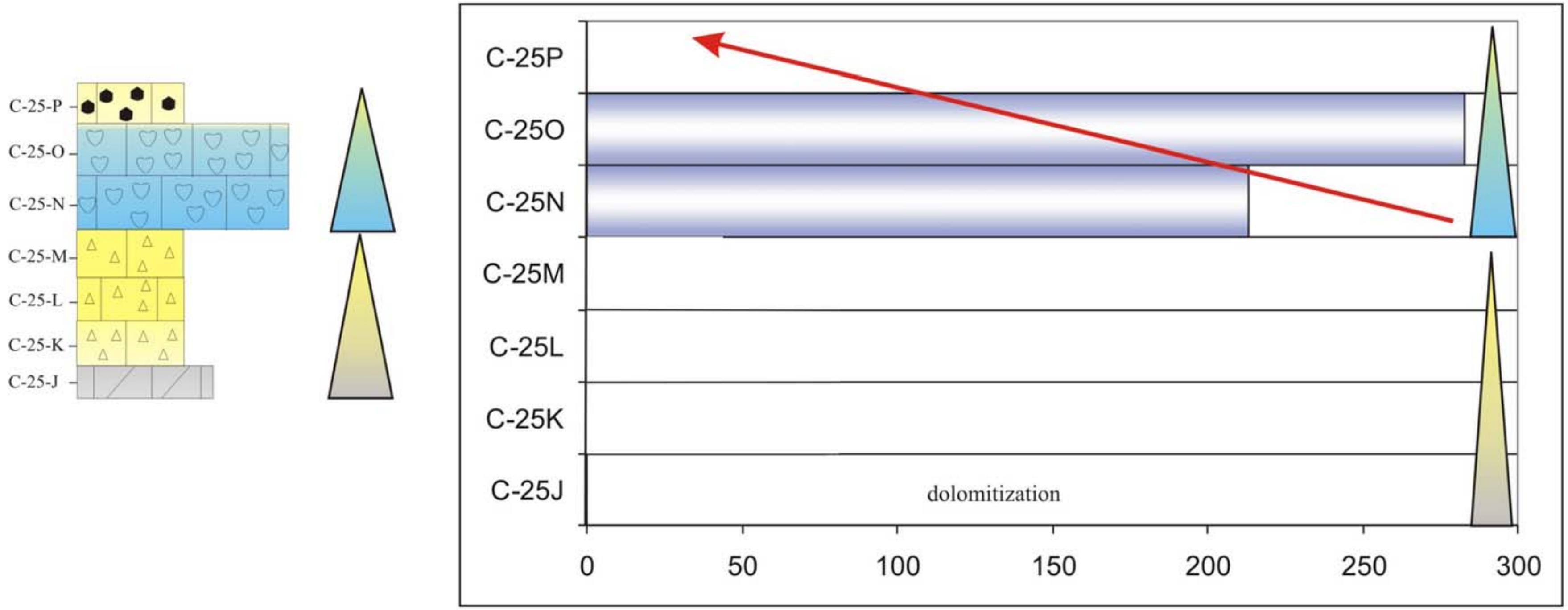

Figure 53. The abundance of foraminifers in the 5th parasequence of the Leylek-2 Section in order to find out the response of involutinids to cyclicity.

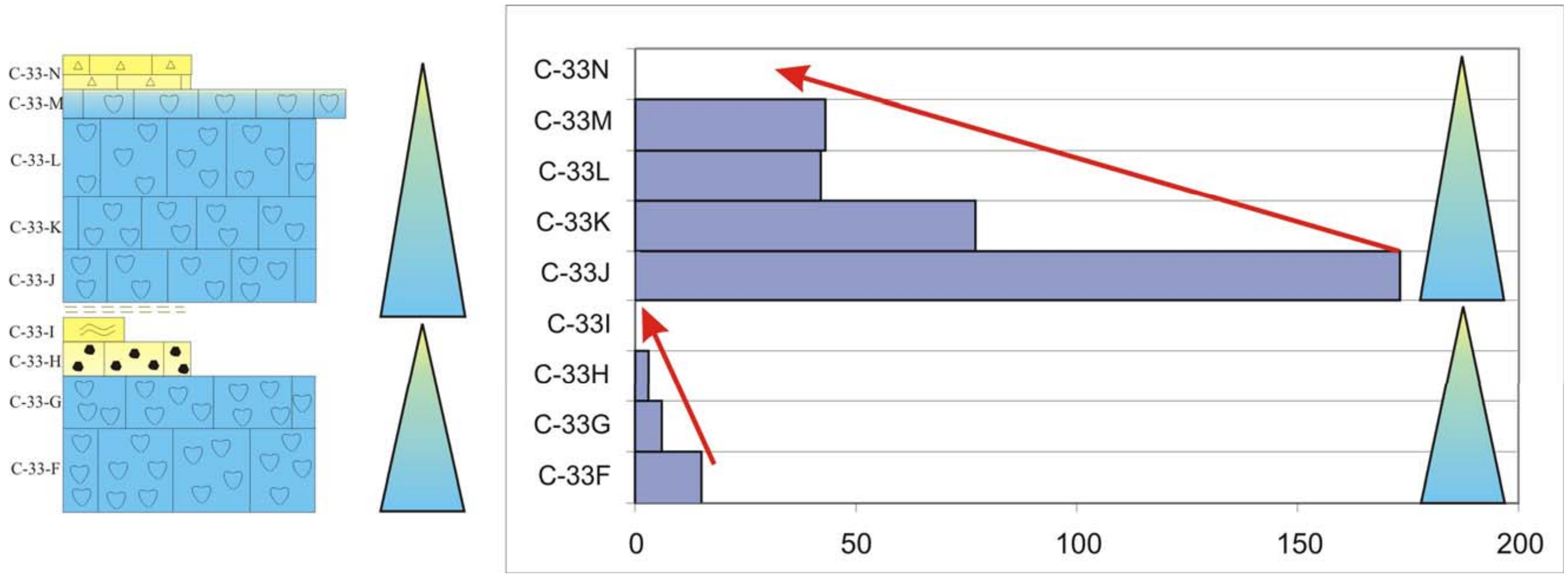

Figure 54. The abundance of foraminifers in the 7th & 8th parasequences of the Leylek-2 Section in order to find out the response of involutinids to cyclicity.

Within the studied successions, the abundance of foraminifers display a good response to the determined cyclicity. In general, the abundance of involutinids decreases from cycle bottoms through cycle tops, but a few exceptions are present. The base of the cycles are formed by megalodont-bearing limestones and foraminiferal limestones and the top of the cycles are composed of fenestral limestones, stromatolites, breccias etc. Although, the megalodont-bearing limestones contain high abundance of involutinids at the bottom of the cycles, they sometimes show variations in itself due to the dolomitization and recrystallization processes. On the other hand, the abundance of involutinids is commonly less at the top of the cycles. Although, the cycle tops almost have less abundance of involutinids relative to cycle bottoms, there are few exceptions that reflect the opposite of this evidence. As a consequence, the involutinid group foraminifers seem to be good indicators in identifying the Upper Norian-Rhaetian shallowing-upward cycles as an independent tool in stratigraphy. On the whole, foraminiferal abundance decreases from subtidal through supratidal environments, but the number of involutinids are not to be zero at all time.

Cluster analysis is a class of statistical techniques to identify groups and subgroups in a multivariate data set and is firstly used by Tryon (1939). Since 1970's, this method has been widely used in geology (e.g., Davis, 1973, Hesp and Rigby, 1973, Obial and James, 1973, Levinson, 1974, Howarth and Sinding-Larsen, 1983, Mitchell and Carr, 1998, Parker and Arnold, 1999, Weber et al., 2001, Sheps, 2004, Davis et al., 2006, Bernal et al., 2006, Covelli et al., 2006, Zhang et al., 2006, Hofrichter and Winkler, 2006, Segura et al., 2007, Fermani et al., 2007, Buffen et al., 2007, Sarkar et al., 2007, Hussain, 2007). The purpose of cluster analysis is to discover a system of organizing observations, into groups where members of the groups share properties in common. It is cognitively easier for people to predict properties of objects based on group membership, all of whom share similar properties. It is generally cognitively difficult to deal with individuals and predict behavior or properties based on observations of other behaviors or properties. It is typical method for data exploration and visualization. It sorts through the raw data and groups them into clusters. A cluster is a group of relatively homogeneous cases or observations. Objects in a cluster are similar to each other. They are also dissimilar to objects outside the cluster, particularly objects in other clusters. Measures of similarity between objects (Q-mode cluster analysis) or descriptors (R-mode cluster analysis) is the first step of this process. Variable-per-variable relations are shown by R-mode cluster analysis, sample-per-sample relations by Q-mode cluster analysis (Flügel, 2004). Variables are often standardized in order to neglect the strong effects of magnitude. The degree of similarity between variables or pairs of samples is expressed by various similarity coefficients. The interpretation of the groups are made by using dendrograms. A dendrogram is the most commonly used method of summarizing the hierarchical clustering results. Cluster analysis dendrograms are useful in grouping samples with similar component distributions and also used for facies differentiation only in the context of evaluating qualitative microfacies criteria.

A common approach to do a cluster analysis is to first create a table of relative similarities or differences between all objects and second to use this information to combine the objects into groups. The table of relative similarities is called a proximities matrix. The method of combining objects into groups is called a clustering algorithm. The idea is to combine objects that are similar to one another into separate groups. Cluster analysis starts with a data matrix, where objects are rows and observations are columns. From this beginning, a table is constructed where objects are both rows and columns and the numbers in the table are measures of similarity or differences between the two observations. The difference between a proximities matrix in cluster analysis and a correlation matrix is that a correlation matrix contains similarities between variables while the proximities matrix contains similarities between observations. The researcher has dual problems at this point. The first is a decision about what variables to collect and include in the analysis. Selection of irrelevant measures will not aid in classification. The second problem is how to combine multiple measures into a single number, the similarity between the two observations. This is the point where univariate and multivariate cluster analysis separate. Univariate cluster analysis groups are based on a single measure, while multivariate cluster analysis is based on multiple measures (Stockburger, 1996).

In this study, the foraminiferal diversity changes along the cycles were determined and in order to describe the most pronounced changes in the benthic foraminifera assemblage, a cluster analysis was performed (Figure 55, 56). Cluster analysis is recently the most commonly used multivariate statistical technique in the foraminiferal literature (e.g., Mitchell and Carr, 1998, Weber et al., 2001, Sheps, 2004, Segura et al., 2007, Fermani et al., 2007, Buffen et al., 2007). It is especially powerful in delineating biofacies and species associations. The aim is to order or arrange samples or variables in relation to environmental parameters. In the first analysis, Q-mode cluster analysis was performed within the 7th, 13th and 14th parasequences of the Leylek-1 Section (Figure 55). A total of 26 samples have been selected. The percentage of the pelloids and the number of *Aulotortus* genus within the samples were determined (see Appendix B). 2 main clusters have been obtained from Q-mode cluster analysis. Cluster I consists of the samples B-20H, B-20I, B-20J, B-20K, B-20L, B-33F, B-33G, B-33I, B-33J, B-33K, B-33L which correspond to the top of the cycles. They are represented by fenestral limestone, breccia, stromatolite, dismicrite including black pebbles. The percentage of the pelloids and the number of *Aulotortus* is less in these samples. On the other hand, Cluster II consists of the samples B-20A, B-33A, B-20F, B-33M, B-20G, B-20B, B-20C, B-33B, B-33C, B-20D, B-33D, B-20E, B-33E, B-33H, B-33N which correspond to the bottom of the cycles. They are mainly composed of megalodont-bearing limestones and foraminiferal limestones. They contain high percentage of pelloids and *Aulotortus* species, thus grouped in a different cluster. The samples which are grouped in the Cluster I are intertidal-supratidal deposits and corresponds to the top of the parasequences. The samples grouped in the Cluster II correspond to the subtidal deposits and constitute the bottom of the cycles. However, there are some exceptions in Cluster II that characterizes the cycle top facies (B-20F, B-33E, B-33H and B-33N). Although, they do not contain pelloids, they contain less involutinids. Therefore, these samples are also grouped in Cluster II. But in general, the percentage of the pelloids and the number of *Aulotortus* species are high at the bottom of the parasequences and less at the top of the parasequences. Therefore the cycle top and bottom samples are grouped in different clusters.

The second analysis concerns the R-mode cluster analysis and a total of 79 samples have been analysed (see Appendix B). 5 main taxa have been used witihin the analysis named as *Aulotortus*, *Auloconus*, nodosarids, trochamminids and *Triasina hantkeni* (Figure 56). Because of the rareness of the most of foraminifer groups recorded in this study, species having greatest relative abundance within any sample has been only used in the cluster analysis. In this manner, 2 main clusters have been obtained from R-mode cluster analysis (Figure 56). Cluster I consists of *Aulotortus* and Cluster II consists of *Auloconus*, *Triasina hantkeni*, nodosarids and trochamminids. These groups of foraminifers are grouped in different clusters due to the depositional settings they inhabited. *Aulotortus* is commonly found in the packstone lithofacies, however the others prefer much more muddy wackestone lithofacies, low energy depositional settings.

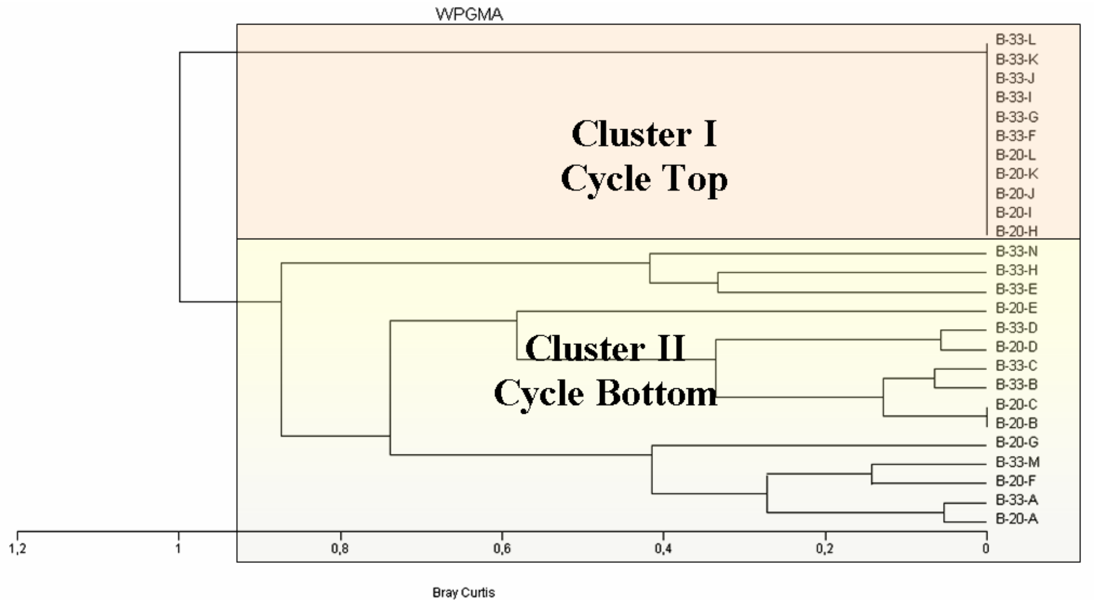

Figure 55. Q-mode cluster analysis, showing the cycle bottom and cycle top facies.

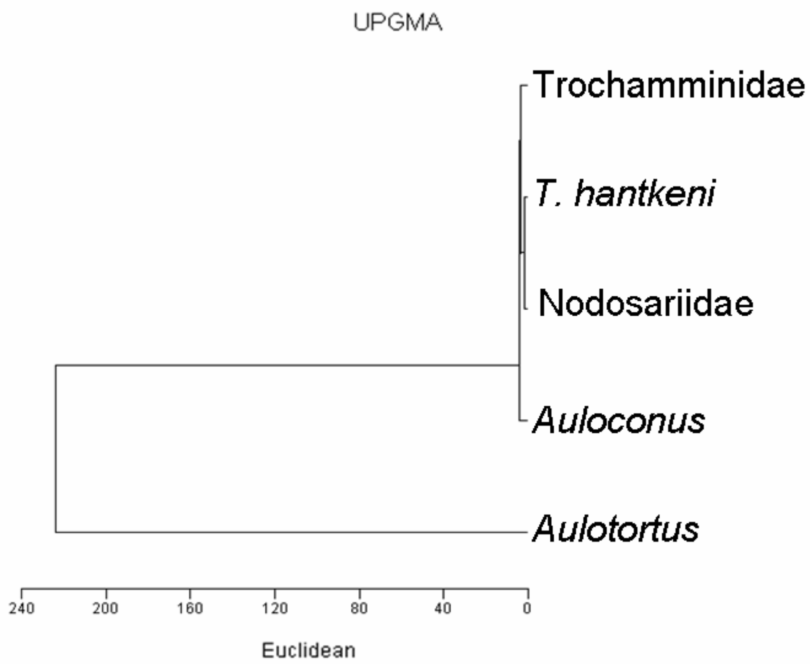

Figure 56. Dendrogram resulting from R-mode cluster analysis.

CHAPTER 5

5. SYSTEMATIC PALEONTOLOGY

TAXONOMY

FORAMINIFERIDA EICHWALD, 1830

INVOLUTININA HOHENEGGER & PILLER, 1977

INVOLUTINIDAE BUTSCHLI, 1880

TRIASININAE LOEBLICH AND TAPPAN, 1986

Genus: *Triasina* MAJZON, 1954

Type species: *Triasina hantkeni* MAJZON, 1954

Pl. 1, fig. 1-7

1954 *Triasina hantkeni* Majzon, pl.1, fig. 1-2, pl.2, figs. 4-5, pl.3, fig. 6.

1971 *Triasina hantkeni*- Zaninetti et Brönniman, p. 74, pl. 10, fig. 3-6.

1976 *Triasina hantkeni*- Zaninetti, p. 239, pl. 15, fig. 2-3.

1980 *Triasina hantkeni*- Yan, p. 1172, pl. 73, fig. 10, 11.

1982 *Triasina hantkeni*- Turati e Radrizzoni, p. 624, tav. 50, fig. 1.

1982 *Triasina hantkeni*- Al-Shaibani et al., p. 139, pl. 1, fig. 3.

1983 *Triasina hantkeni*- Al-Shaibani et al., p. 309, pl. 1, fig. 1-3, 5, 6.

1984 *Triasina hantkeni*- Al-Shaibani et al., p. 309, pl. 1, fig. 1

1985 *Triasina hantkeni*- Ciarapica et Zaninetti, p. 129, pl. V, fig. 2.

1986 *Triasina hantkeni*- Zaninetti et al., p. 267, pl. 2, fig. 11,12.

1987 *Triasina hantkeni*- Ciarapica et al., p. 387, pl. XX, fig. 1-6.

1988 *Triasina hantkeni*- Peybernes et al., p. 147, pl.1, fig. 12.

1990 *Triasina hantkeni*- De Castro, pl. 4, fig. 1-9; pl. 5, fig. 1-9; pl. 6, fig. 1-3.

1990 *Triasina hantkeni*- Jadoul et al., p. 392, pl. 40, fig. 1, 3.

1997 *Triasina hantkeni*- Martini et al., p. 90, pl. 1, fig. 8.

2002 *Triasina hantkeni*- Işıntek, p. 163, pl. 43, figs. 2, 4-8.

2003 *Triasina hantkeni*- Beccaletto, pl. 2D.

2004 *Triasina hantkeni*- Martini et al., p. 90, pl. 4, figs. 2-4.

2005 *Triasina hantkeni*- Mancinelli et al., pl.1, fig. l, m.

2005 *Triasina hantkeni*- Jadoul et al., fig. 4/G

2007 *Triasina hantkeni*- Okay & Altıner, p. 12, pl. 1, fig. 1-3.

Description :

Test is spherical to subspherical in shape and bilocular. Coiling is planispiral and involute, consisting of a proloculus and a second tubular chamber. Proloculus has not been recognized in the present specimens. The chamber cavity contains many short and robust pillars. Number of coils seven to eight; generally the initial whorls cannot be seen because of intense recrystallization in the interior part of the test. In the latest half coil of one of the specimen, seventeen pillars are counted. In the perfectly axial sections, the umblical region is nearly concave. Wall recrystalized. Aperture not observed.

Dimensions:

Diameter : 1.15mm-1.8mm

Width : 1.02mm-1.8mm

Height of the cavity : 0.08mm

Material :

Found in the Leylek Limestone, Menteşe Dolomite and the Güverdağı Formation. Sample no. B-40, B-51, B-47F, B-47N, C-41, C-45, C-25A, C-33J, C-33R, C-47C, K-26, K-29, K-30, K-31, K-35, K-51, K-57, K-45A, M-88.

Remarks :

The main difference of *Triasina hantkeni* from *Aulotortus* species is its larger size (Figure 57). *Triasina hantkeni* in our specimens is similar with the forms described from the Dachstein limestone (Majzon, 1954), but the sizes are greater than the types described. *Triasina hantkeni* differs from the *Triasina oberhauseri* in having a spherical to subspherical shape and more developed pillars in its test.

Stratigraphic distribution :

The stratigraphic distribution of *Triasina hantkeni* is Late Norian (Sevatian)-Rhaetian (Al-Shaibani et al., 1982; Martini et al., 1997, 2004; Okay & Altıner, 2007). Based on the stratigraphic distribution of *Triasina hantkeni*, a late Norian to Rhaetian age is also proposed to the studied successions in the Leylek Limestone Menteşe Dolomite and Güverdağı Formation.

Geographic distribution :

Triasina hantkeni is widespread along the whole Triassic Tethys. In the western Tethys, the taxon has been recorded in the Morocco Rif (Raoult, 1962) and France Western Alps (Zaninetti et al., 1986; Dumont & Zaninetti, 1985). In the easternmost Tethys, it has been recorded in the Ceram Island (Al-Shaibani et al., 1984) and in the Philippines (Fontaine et al., 1979). In the Central-Southern Apennines, *Triasina hantkeni* is found within the Upper Triassic platform carbonates (Mancinelli et al., 2005). It is also found in Malezia, central China, Himalians and Indonesia (Al-Shaibani et al., 1982). In Turkey, *Triasina hantkeni* has been recorded in the Taurides by Zaninetti (1976) for the first time. The latest occurrence has been recorded by Okay & Altıner (2007) from the Bornova flysch zone. In this study, *Triasina hantkeni* has been found in the central and Western Taurides.

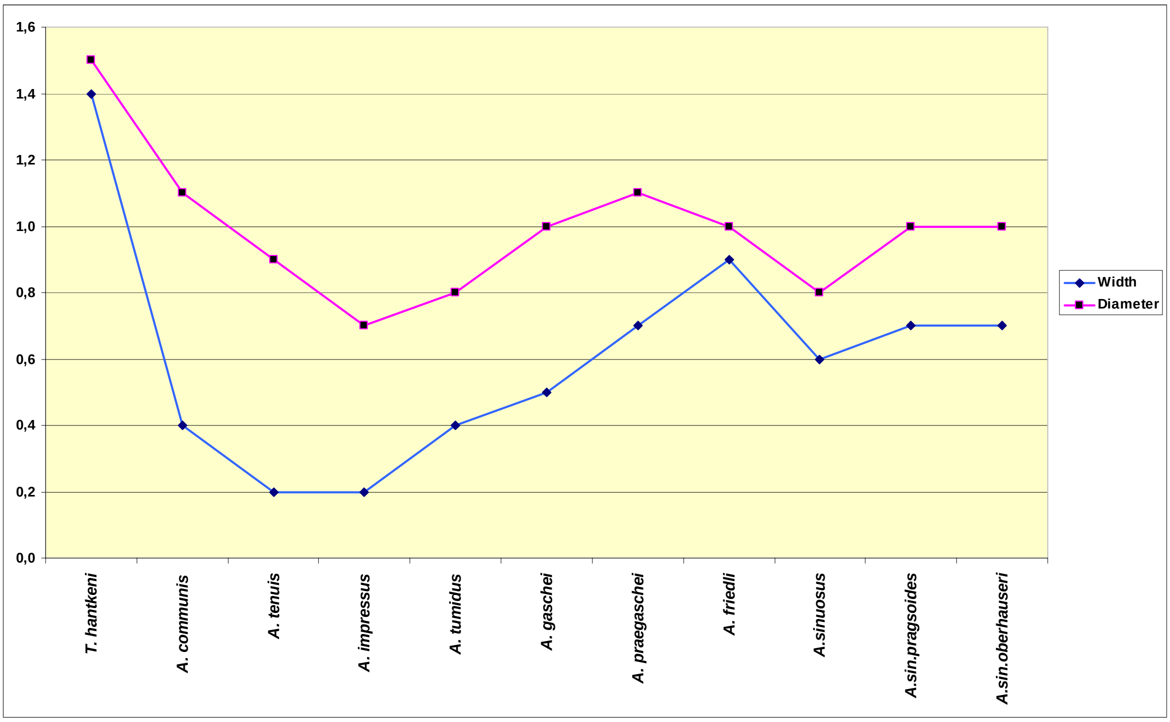

Figure 57. The diameter and width values (mm.) of the involutinid group foraminifers.

AULOTORTINAE ZANINETTI, 1984

Genus : *Aulotortus* WEYNSCHENK, 1956

Aulotortus communis (KRISTAN, 1957)

Pl. 1, fig. 8-11

1957 *Angulodiscus communis* Kristan, pl. 23, fig. 1-7.

1970 *Involutina communis*- Brönnimann et al., p.36, pl. 2, fig. 1-2.

1971 *Involutina* cf. *communis*- Zaninetti et Brönnimann, p. 74, pl. 10, fig. 4.

1972 *Involutina communis*- Zaninetti et al., p. 250, pl. 1, fig. 1-3.

1974 *Involutina communis*- Zaninetti et Brönnimann, p. 423, pl. 3, fig. 13-15, 16?

1976 *Involutina communis*- Zaninetti, p. 227, pl. 9, fig.1

1978 *Involutina communis*- Zaninetti et al., p. 893, pl. 89, fig. 2, 5, 6.

1980 *Involutina communis*- Altıner et Zaninetti, p. 755, pl. 86, fig. 18-20.

1983 *Aulotortus communis*- Al-Shaibani et al., p. 309, pl. 1, fig. 9, 10, 14.

1987 *Aulotortus communis*- Ciarapica et al., p. 357, pl. V, fig. 1-4; p. 361, pl VII, fig. 2, 3, 5, 6; p. 377, pl XV, fig. 1-9; p. 381, pl. XVII, fig. 2?, 10.

1988 *Aulotortus communis*- Peybernes et al., p. 147, pl. VII, fig. 4, 5.

1989 *Aulotortus communis*- Martini et al., p. 21, pl. 2, fig. 6.

1990 *Aulotortus communis*- Jadoul et al., p. 390, pl. 38, fig. 1a.

2002 *Aulotortus communis*- Işıntek, p. 157, pl. 40, figs. 1-9.

Description :

Test is lenticular to elipsoidal in shape and bilocular. Proloculus has not been recognized in the studied specimens. Bilocular second chamber is planispirally coiled and involute. Initial whorls may slightly oscillate, last whorls are regularly planispiral. In axial sections, symmetrical profile can be clearly seen. Height of the tubular chamber which appears crescent in shape increases gradually during the ontogenesis. Due to recrystallization, in a few specimens, only the last whorl can be seen. Umbilical region is filled with sparry calcite. Wall and umbilical lamellae are recrystalized.

Dimensions:

Diameter : 0.7mm-1.5mm

Width : 0.3mm-0.5mm

Material :

Found in the Leylek Limestone, Menteşe Dolomite and the Güverdağı Formation. Sample no. B-40, C-25O, C-33M, K-1, K-23, K-32, M-105, M-106, M-112, M-132.

Remarks :

Aulotortus communis differs from *Aulotortus* gr. *sinuosus* in having nearly planispiral coiling and symmetrical profile in axial sections. It has also lenticular shape rather than spherical shape as in *Aulotortus* gr. s*inuosus* and also have wider diameter than *Aulotortus* gr. s*inuosus* (Figure 54).

Stratigraphic and Geographic distribution :

Aulotortus communis has been reported from the Upper Triassic in the Lycian Nappes (Brönnimann et al., 1970). In the Eastern Taurides (Pınarbaşı region), it was determined in the Norian (Altıner and Zaninetti, 1980). Zaninetti (1972) recognized *Aulotortus communis* in the Rhaetian of Iran and in the Late Norian-Rhaetian interval (Zaninetti, 1976). Işıntek (2005) described this form in the Rhaetian of Karaburun Peninsula. Our specimens are recovered from the Upper Norian-Rhaetian carbonates of the central and Western Taurides in southern Turkey.

Aulotortus tumidus (KRISTAN-TOLLMANN, 1964)

Pl. 2, fig. 1-4

1964 *Angulodiscus tumidus* Kristan-Tollmann, abb. 3, fig. 1-6.
1972 *Involutina tumida*- Zaninetti et al., p. 251, pl. 1, fig. 5.
1976 *Involutina tumida*- Zaninetti, p. 227, pl. 9 fig. 8-10.
1980 *Involutina tumida*- Altıner et Zaninetti, p. 755, pl. 86, fig. 21.
1983 *Aulotortus tumidus*- Al-Shaibani et al., p. 309, pl. 1, fig. 11, 12.
1987 *Aulotortus tumidus*- Ciarapica et al., p. 357, pl. V, fig. 10.
1989 *Aulotortus tumidus*- Martini et al., p. 19, pl. 8, fig. 4.
1998 *Aulotortus tumidus*- Donato & Alberto, p. 138, pl. 5, fig.2.
2002 *Aulotortus tumidus*- Işıntek, p. 158, pl. 43, figs. 2, 4-8.
2005 *Aulotortus tumidus*- Mancinelli et al., pl. 1, fig. c, r.
2006 *Aulotortus tumidus*- Kobayashi et al., p. 323, fig. 7, 1-8.

Description :

Test is lenticular in shape. Coiling is planispiral and involute except the last one or two whorls which are evolute. Umbilical region is nearly convex and commonly recrystalized. The inner whorls cannot be recognized because of recrystalization. Wall is recrystalized.

Dimensions:

Diameter : 0.5mm-1.1mm

Width : 0.2mm-0.4mm

Material :

Found in the Leylek Limestone, Menteşe Dolomite and the Güverdağı Formation. Sample no. B-47F, K-26, K-29, M-105.

Remarks :

Aulotortus tumidus differs from *Aulotortus impressa* by having evolute coiling in the last one or two whorls and being convex umbilical region. The main difference of *Aulotortus tumidus* from *Aulotortus sinuosus* is the more flattened shape in axial sections and the 2/3 evolute whorls of the last stage of the enrollment. In the studied samples, the early whorls of the enrollment are not visible.

Stratigraphic distribution:

The stratigraphic range of *Aulotortus tumidus* is Late Triassic (Zaninetti, 1976). In Turkey, it was found in the Norian (Altıner & Zaninetti). Our specimens were recovered from Late Norian-Rhaetian.

Aulotortus gaschei (KOEHN-ZANINETTI et BRONNIMANN, 1968)

Pl. 2, fig. 5-7

1968 *Angulodiscus* ? *gaschei* Koehn-Zaninetti et Brönnimann, p. 81, pl. 1, fig. A-F, p. 82, pl. 2, Fig. A-F.

1971 *Involutina gaschei*- Zaninetti et Brönnimann, p. 75, pl. 10, fig. 1.

1974 *Involutina gaschei*- Brönnimann et al., p. 41, pl. 4, fig. 13-14, p. 43, pl. 5, fig. 2, 4, 6.

1975 *Involutina gaschei*- Zaninetti et Thiebault, p. 236, pl. 2, fig. 5, 7-12.

1975 *Involutina gaschei*- Dager, pl. 1, fig. 8-9.

1975 *Involutina gaschei*- Zaninetti et Thiebault, p. 236, pl. 2, fig. 5, 6, 7-12.

1976 *Involutina gaschei*- Zaninetti, p. 227, pl. 9, fig. 13-15.

1980 *Involutina gaschei*- Altıner et Zaninetti, p. 755, pl. 86, fig. 12-15.

1982 *Aulotortus gaschei*- Tuzcu et al., p. 133, pl. 1, fig. 3.

1983 *Aulotortus gaschei*- Al-Shaibani et al., p. 309, pl. 1, fig. 17-22.

2007 *Aulotortus gaschei*- Okay & Altıner, p. 12, fig. 13-15.

Description :

Test is lenticular to subspherical in shape. Coiling is regularly planispiral in the initial stages and strongly oscillating in the last two or three stages. Proloculus cannot be recognized because of the recrystalization. Dimensions of the tubular chamber increase gradually and the sections of the tubular chamber are nearly crescent in shape. Wall is recrystalized.

Dimensions:

Diameter : 0.6mm-1.3mm

Width : 0.4mm-0.5mm

Material :

Found in the Leylek Limestone. Sample no. B-40, C-25A.

Remarks :

Aulotortus gaschei was assumed to be the synonym of *Aulotortus friedli* (Hohenneger and Piller, 1975). *Aulotortus gaschei* shows a regular planispiral coiling in the internal part of its test but *Aulotortus friedli* is devoid of initial regular coilings. Our specimen is similar with the forms described in Alps, Austria (Koehn-Zaninetti et Brönnimann, 1968).

Stratigraphic distribution :

The stratigraphic distribution of *Aulotortus gaschei* is Norian-Rhaetian (Zaninetti, 1976). It was found in the Carnian-Norian interval of the Eastern Taurides (Altıner et Zaninetti, 1980). Okay & Altıner (2007) found *Aulotortus gaschei* in the Late Norian-Rhaetian interval. In this study, *Aulotortus gaschei* was also found in the Late Norian-Rhaetian.

Aulotortus impressus (KRISTAN-TOLLMANN, 1964)

Pl. 2, fig. 8-10

1964 *Angulodiscus impressa* Kristan-Tollmann, Abb. 2, fig. 11-13.

1970 *Involutina impressa*- Brönnimann et al., p. 24, fig.11.

1975 *Involutina impressus*- Dager, pl. 1, fig. 1-2.

1975 *Involutina impressa*- Zaninetti et Brönnimann, p. 272, pl. 33, fig. 6.

1976 *Involutina impressa*- Zaninetti, p. 227, pl. 9, fig. 11, 12.

1984 *Aulotortus* ex. gr. *impressus*- Ciarapica et Zaninetti, p. 121, pl. I, fig. 8.

1987 *Aulotortus impressus*- Ciarapica et al., p. 355, pl. IV, fig. 2.

2002 *Aulotortus* ? *impressus*- Işıntek, p. 159, pl. 41, fig. 5, 6.

2005 *Aulotortus impressus*- Mancinelli et al., pl.1, fig. e.

2007 *Aulotortus impressus*- Okay & Altıner, p. 12, fig. 16.

Description :

Test is discoidal. Coiling is planispiral and only the last one or two whorls are visible in the specimens. Dimesions of the tubular chamber increase gradually and the chamber cavity is crescent-shaped in axial sections. Umbilical region is slightly concave and recrystalized and the wall is also recrystalized.

Dimensions:

Diameter : 0.6mm-0.8mm

Width : 0.1mm-0.2mm

Material :

Found in the Leylek Limestone and the Güverdağı Formation. Sample no. B-20A, B-47N, C-48, C-25A, M-88, M-106.

Remarks :

Aulotortus impressus differs from *Aulotortus tenius* in having slightly compressed umbilical region rather than flat. *Aulotortus impressus* has a planispiral and involute coiling, on the other hand *Aulotortus tumidus* has an evolute last whorl.

Stratigraphic distribution :

Aulotortus impressus was found in the Late Triassic (Zaninetti, 1976). Okay & Altıner (2007) recorded *Aulotortus impressus* from the Late Norian (Sevatian)-Rhaetian of the Bornova flysch zone. Our specimens were recovered from the Late Norian-Rhaetian of the central and Western Taurides.

Aulotortus* gr. *sinuosus WEYNSCHENK, 1956

Pl. 3, fig. 1-9

1956 *Aulotortus sinuosus* Weynschenk, p. 27, pl. 6, fig. 1-3.

1968 *Involutina sinuosa sinuosa*- Koehn-Zaninetti, (not illustrated)

1975 *Involutina* gr. *sinuosus*- Zaninetti et Thiebault, p. 236, pl. 2, fig. 4.

1975 *Involutina sinuosa*- Zaninetti et Brönnimann, p. 273, pl. 33, fig. 4, 5, 10.

1976 *Aulotortus gaschei*- Zaninetti, p. 227, pl.9, fig.13-15.

1982 *Aulotortus sinuosus sinuosus*- Tuzcu et al., p. 133, pl. 1, fig. 1, 4, 5.

1983 *Aulotortus* ex. gr. *sinuosus*- Al-Shaibani et al., p. 309, pl. 1, fig. 23.

1984 *Aulotortus* ex. gr. *sinuosus*- Ciarapica et Zaninetti, p. 121, pl. I, fig.1, 2; p. 129, pl. V, fig. 1, 3.

1987 *Aulotortus* ex. gr. *sinuosus*- Ciarapica et al., p. 355, pl. IV, fig. 1; p. 357, pl V, fig. 5, 6, 8, 9; p. 381, pl. XVII, fig. 1, 3-9; p. 383, pl XVIII, fig. 5, 6, 9.

1990 *Aulotortus communis*- Jadoul et al., p. 390, pl. 38, fig. 4.

1990 *Aulotortus sinuosus*- De Castro, pl. 1, fig. 1-15; pl. 2, fig. 1-15; pl. 3, fig. 1-13; pl. 6, fig. 4-10.

1997 *Aulotortus* ex. gr. *sinuosus*- Martini et al., p. 166, pl. 1, fig. 2, 3, 7.

1998 *Aulotortus* gr. *sinuosus*- Donato & Alberto, p. 138, pl. 5, fig. 3, 6, 7.

2002 *Aulotortus* gr. *sinuosus*- Işıntek, p. 155, pl. 39, figs. 1-7.

2003 *Aulotortus* gr. *sinuosus*- Beccaletto, pl. 2B, 2C.

2004 *Aulotortus* ex. gr. *sinuosus*- Martini et al., p. 90, pl. 4, figs. 6, 7.

2006 *Aulotortus sinuosus*- Kobayashi et al., p. 323, fig. 7, 9-36.

2007 *Aulotortus* ex. gr. *sinuosus*- Okay & Altıner, p. 12, fig. 4-5.

Description :

Test is lenticular to subspherical in shape. Coiling is involute and the whorls are oscillating. Generally the oscillating last 1-3 whorls can be observed. Initial coilings cannot be recognized because of the intense recrystalization. Dimensions of the chambers increase during ontogenesis and are crescent in shape in axial sections. Wall recrystalized.

Dimensions:

Diameter : 0.5mm-1mm

Width : 0.4mm-0.7mm

Material :

Found in the Leylek Limestone, Menteşe Dolomite and the Güverdağı Formation. Sample no. B-29, B-34, B-40, B-51, C-21, C-37, C-25A, C-47A, K-8, K-30, K-32, K-34, M-72, M-105, M-107, M-112, M-124, M-127, M-150.

Remarks :

Aulotortus sinuosus differs from *Aulotortus sinuosus pragsoides* in having early and irregularly oscillating planispiral coiling.

Stratigraphic distribution :

The stratigraphic distribution of *Aulotortus sinuosus* is from middle Anisian to Rhaetian (Zaninetti, 1976). The species has been recognized since the Late

Ladinian but it seems to reach its widest diffusion in the Norian and Rhaetian stages (De Castro, 1990). It was found in the Anisian-Rhaetian of the Italy (di Bari & Baracca, 1998). *Aulotortus sinuosus* was found in the Late Norian (Sevatian)-Rhaetian of Seram (Martini et al., 2004) and in the Carnian of the northern Thailand (Kobayashi et al., 2006). Okay & Altıner found *Aulotortus* gr. *sinuosus* in the Late Norian (Sevatian)- Rhaetian of the Bornova flysch zone in western Turkey. In this study, it was recorded in the Late Norian-Rhaetian of the central and Western Taurides in southern Turkey.

Geographic distribution :

Aulotortus sinuosus was reported from southeast France (Dumont & Zaninetti, 1985), Switzerland, the Dolomites, Austrian Alpes, the Carpathian, the Dinarids and the Hellenids. It was also found in İran, in the Caucasus, in Pakistan, in Indonesia (Al-Shaibani et al., 1983). In Italy, *Aulotortus sinuosus* was found in the Northern Apennines associated with *Triasina hantkeni*, at La Spezia (Ciarapica & Zaninetti, 1984) and at Monte Cetona (Ciarapica & Zaninetti, 1985); in the Centra Apennines, at Gran Sasso (Chiocchini & Mancinelli, 1978) and in the Aurunci Mountains (Chiocchini & Mancinelli, 1977); in the Southern Apennines, in the Picentini Mountains; in Sicily, in the Monti di Palermo Mountains (Abate et al., 1984).

Aulotortus sinuosus pragsoides (OBERHAUSER, 1964)

Pl. 4, fig. 10-11

1964 *Permodiscus pragsoides* Oberhauser, pl. 1, fig. 10, 12-14, 16, 17; pl. 2, fig. 2, 3, 16, 23; pl. 4, fig. 8, 9.

1969 *Involutina sinuosa pragsoides*- Koehn-Zaninetti, fig. 25.

1973 *Involutina sinuosa pragsoides*- Brönnimann et al., p. 325, p. 19, fig.1-18; p. 327, pl. 20, fig. 1-7, 9, 10, 13

1974 *Involutina sinuosa pragsoides*- Brönnimann et al., p. 39, pl. 3, fig. 1-7, 9, 12, 14, 15, 17?, 18; p. 41, pl. 4, fig. 5, 16, 19.

1975 *Involutina sinuosa pragsoides*- Zaninetti et Thiebault, p. 236, pl. 2, fig. 1-3.

1975 *Involutina sinuosus pragsoides*- Dager, pl. 2, fig. 1-2.

1976 *Involutina sinuosa pragsoides*- Zaninetti, p. 233, pl. 12, fig. 1-3.

1980 *Involutina sinuosa pragsoides*- Altıner et Zaninetti, p. 755, pl. 86, fig. 6-11; p. 757, pl. 87, fig. 1.

2002 *Aulotortus sinuosus pragsoides*- Işıntek, p. 156, pl. 38, figs. 1-7

Description :

Test is lenticular to subspherical in shape. Coiling is planispiral, involute and slightly oscillating only in the last 2-3 whorls. The height of the tubular chamber which is crescent in shape in axial sections increases in each whorl. Umbilical region is convex and commonly recrystalized. Proloculus is not distinct. Wall and umbilical lamillae are recrystalized.

Dimensions:

Diameter : 0.9mm-1mm

Width : 0.5mm-0.7mm

Material :

Found in the Leylek Limestone and the Güverdağı Formation. Sample no. C-25B, M-105.

Remarks :

Aulotortus sinuosus pragsoides differs from *Aulotortus* gr. *sinuosus* in having planispiral coiling oscillating only in the last whorls.

Stratigraphic distribution :

The stratigraphic distribution of *Aulotortus sinuosus pragsoides* is Late Anisian-Rhaetian (Zaninetti, 1976). It was found in the Late Ladinian-Norian interval in the Eastern Taurides (Altıner et Zaninetti, 1980), in the Late Anisian of Yugoslavia (Brönnimann et al., 1973). *Aulotortus sinuosus pragsoides* was recovered from Late Norian- Rhaetian in the central and Western Taurides.

Aulotortus sinuosus oberhauseri (SALAJ in SALAJ, BIELY& BISTRICKY 1967)

Pl. 4, fig. 9

1967 *Rakusia oberhauseri*-Salaj, pl. 5, fig.3; pl. 8, fig. 4.

1976 *Involutina sinuosa oberhauseri*- Zaninetti, p. 239, pl. 15, fig. 9, 10.

1980 *Involutina sinuosa oberhauseri*- Altıner et Zaninetti, p. 757, pl. 87, fig. 4?, 7, 9.

Description :

Test lenticular. Coiling is planispiral, evolute in the early 4-5 stages and planispiral, involute in the last 3-4 stages. Prolocolous and earlier whorls are recrystalized. Umbilical region is convex and recystalized. Wall recrystalized.

Dimensions:

Diameter : 1mm

Width : 0.7mm

Material :

Found in the Güverdağı Formation. Sample no. M-105.

Remarks :

Aulotortus sinuosus oberhauseri differs from other *Aulotortus* species by having planispiral, evolute initial whorls and involute last whorls .

Stratigraphic distribution :

The stratigraphic distribution of *Aulotortus sinuosus oberhauseri* is Late Ladinian-Norian (Zaninetti, 1976). It was also found in the Norian of the Eastern Taurides (Altıner et Zaninetti, 1980). Our specimens were recovered from the Late Norian- Rhaetian of the central and Western Taurides in southern Turkey.

Aulotortus tenuis (KRISTAN, 1957)

Pl. 4, fig. 1-5

1957 *Angulodiscus tenuis* Kristan, pl. 22, fig. 18.

1972 *Involutina tenuis*- Zaninetti et al., p. 251, pl. 1, fig. 4.

1975 *Involutina* aff. *tenuis*- Zaninetti et Thiebault, p. 236, pl. 1, fig. 8-9.

1976 *Involutina tenuis*- Zaninetti, p. 227, pl. 9, fig. 2-4.

1980 *Involutina tenuis*- Yan, p. 1172, pl. 73, fig. 8.

1984 *Aulotortus* ex. gr. t*enuis*- Ciarapica & Zaninetti, p. 121, pl. 1, fig. 9.

1987 *Aulotortus tenuis*- Ciarapica et al., p. 355, pl. IV, figs. 6?, 10?; p. 379, pl XVI, fig. 1-4, 5?, 6, 7, 8?, 11; p. 383, pl. XVIII, fig. 13.

1990 *Aulotortus communis*- Jadoul et al., p. 391, pl. 38, fig. 7.

1997 *Aulotortus* aff. *tenuis*- Martini et al., p. 168, pl. 1, fig. 11.

2002 *Aulotortus tenuis*- Işıntek, p. 160, pl. 41, figs. 4, 7-10.

2005 *Aulotortus tenuis*- Mancinelli et al., pl.1, fig. b, n.

Description :

Test is discoidal. Coiling is planispiral, only the last one or two whorls are visible in the specimens. Coiling sometimes oscillates in the last stages of coiling. Umbilical region is flat and recrystalized. Proloculus is not distinct. Wall is recrystalized.

Dimensions:

Diameter : 0.7mm-1.8mm

Width : 0.2mm-0.4mm

Material :

Found in the Leylek Limestone and the Güverdağı Formation. Sample no. C-48, C-25A, C-25R, M-106.

Remarks :

Aulotortus tenuis differs from *Aulotortus impressa* in having a highly flattened test in the umbilical region and *Aulotortus tumidus* in having planispiral and involute coiling.

Stratigraphic distribution :

The stratigraphic distribution of *Aulotortus tenuis* is Late Triassic (Zaninetti, 1976). Our specimens were recorded from the Upper Norian-Rhaetian limestones.

Aulotortus praegaschei (KOEHN-ZANINETTI, 1968)

Pl. 4, fig. 6

1968 *Involutina gaschei praegaschei* Koehn-Zaninetti, fig. 39.

1976 *Involutina gaschei praegaschei*- Zaninetti, p. 237, pl. 14, fig. 17, 18, 22; p. 239, pl. 15, fig. 17-21.

1984 *Aulotortus praegaschei*- Ciarapica et Zaninetti, p. 121, pl. I, fig. 5-7.

1993 *Aulotortus praegaschei*- Frechengues et al., p. 117, pl. 2, figs. 2-4.

1994 *Aulotortus* ex. gr. *praegaschei*- Kamoun et al., p.379, pl. 2, fig. 5-7.

1997 *Aulotortus* ex. gr. *praegaschei*- Kamoun et al., p. 706, fig.3; 16, 21, 22.

2002 *Aulotortus praegaschei*- Işıntek, p. 153, pl. 36, figs. 3, 5, 7, 8, 10, 11.

Description :

Test is ovoid in shape and glomospirally coiled. Five whorls are recognized. Dimensions of the tubular chamber increases gradually in growth direction and crescent in shape. Proloculus is not distinct. Wall recrystalized.

Dimensions:

Diameter : 1.1mm

Width : 0.7mm

Material :

Found in the Leylek Limestone. Sample no. C-45.

Remarks :

Aulotortus praegaschei differs from *Aulotortus friedli* by the absence of oscillating planispiral coiled stage.

Stratigraphic distribution :

The stratigraphic distribution of *Aulotortus praegaschei* is Ladinian-Carnian (Zaninetti, 1976). In this study it was found in the Late Norian-Rhaetian interval.

Aulotortus friedli (KRISTAN-TOLLMANN, 1962)

Pl. 4, fig. 7-8

1962 *Glomospirella friedli* Kristan-Tollmann, pl. 1, fig. 1-9, 12-17.

1978 *Aulotortus friedli* Piller, pl. 8, fig. 1-8; pl. 9, fig. 1-6, 11-14; pl. 10, fig. 1-3, 4-6.

1985 *Aulotortus friedli*- Ciarapica et Zaninetti, p. 121, pl. 1, fig. 1-9; p. 123, pl. 2, fig. 1-8; p. 125, pl. 3, fig. 1-9.

1987 *Aulotortus friedli*- Ciarapica et al., p. 349, pl. I, fig. 17; p. 359, pl VI, fig. 1-13.

1988 *Aulotortus friedli*- Peybernes et al., p. 158, pl. VII, fig. 1?, 2, 3, 7?.

1990 *Aulotortus friedli*- Karakitsios et al., p.144, pl. II, fig. 14.

1990 *Aulotortus communis*- Jadoul et al., p. 390, pl. 38, fig. 2-3.

1997 *Aulotortus friedli*- Martini et al., p. 166, pl. 1, fig. 15, 17.

2002 *Aulotortus friedli*- Isıntek, p. 154, pl. 37, fig. 1-9.

2005 *Aulotortus friedli*- Mancinelli et al., pl. 1, fig. c, r.

2004 *Aulotortus friedli*- Martini et al., p. 90, pl. 4, figs 8.

2007 *Aulotortus friedli*- Okay & Altıner, p. 12, fig. 6-7, 8?.

Description :

Test is subspherical. Coiling is glomospiral in the early stages and followed by one or two slightly oscillated planispiral stages. Umbilical region is recrystalized, therefore initial coilings can be difficultly seen in the specimens. Proloculus is not distinct. Wall recrystalized.

Dimensions:

Diameter : 0.5mm-1.4mm

Width : 0.5mm-1.2mm

Material :

Found in the Leylek Limestone and the Güverdağı Formation. Sample no. C-33G, C-45, M-85, M-100.

Remarks :

Aulotortus friedli differs from *Aulotortus gaschei* in having oscillated planispiral last stages.

Stratigraphic distribution :

The stratigraphic distribution of *Aulotortus friedli* is Norian-Rhaetian (Zaninetti, 1976). Martini et al. (2004) found *Aulotortus friedli* in the Late Norian-Rhaetian of Seram (Indonesia). Okay & Altıner finally found *Aulotortus friedli* in the Late Norian (Sevatian)-Rhaetian of Bornova flysch zone. Our specimens were also recorded from Late Norian-Rhaetian limestone in southern Turkey.

Genus : *Auloconus* PILLER, 1978

Type species: *Auloconus permodiscoides* (OBERHAUSER, 1964)

Pl. 5, fig. 1-4;

1964 *Trocholina permodiscoides* Oberhauser, pl. 2, fig. 13-15, 18, 20, 22; pl. 3, fig.1.

1975 *Trocholina permodiscoides*- Zaninetti et Thiebault, p. 236, pl. 1, fig. 10, 11, 13-15, p. 236, pl. 2, fig. 13-15.

1997 *Auloconus permodiscoides*- Martini et al., p. 166, pl. 1, fig. 13, 19, 20.

2002 *Auloconus permodiscoides*- Işıntek, p. 150, pl. 33, fig. 1-3, 5, 7, 8.

2003 *Auloconus permodiscoides*- Beccaletto, pl. 2A, 2B, 2D.

2005 *Auloconus permodiscoides*- Mancinelli et al., pl. 1, fig. a.

2005 *Auloconus permodiscoides*- Jadoul et al., fig. 4/A

2007 *Auloconus permodiscoides*- Okay & Altıner, p. 12, fig. 17.

Description :

Test is conical in shape. Proloculus cannot be seen. Coiling is trochospiral and the umbilical region is commonly recrystalized. Only the final 2 or 3 crescent or semi-circular shaped chambers can be recognized in the specimens. Wall recrystalized.

Dimensions:

Diameter : 0.5mm-0.9mm

Width : 0.6mm-1.1mm

Material :

Found in the Leylek Limestone and Menteşe Dolomite. Sample no. B-47F, K-24

Stratigraphic distribution :

Auloconus permodiscoides was determined in the Norian-Rhaetian interval (Zaninetti, 1976) and finally in the Late Norian (Sevatian)-Rhaetian of the Bornova flysch zone (Okay & Altıner, 2007). *Auloconus permodiscoides* was also recorded from the Late Norian-Rhaetian interval in the central and Western Taurides.

AMMODISCACEA REUSS, 1862

AMMODISCIDAE REUSS, 1862

AMMOVERTELLININAE SAIDOVA, 1981

Genus: *Glomospira* RZEHAK, 1885

***Glomospira* sp.**

Pl. 5, fig. 8-9

Description :

Test is globular in shape. Proloculus and early whorls are slightly visible. Tubular undivided deuteroloculus is streptospirally coiled. In axial section, four whorls can be seen and in equatorial sections only the three whorls are visible. Wall is thin and made up of dark-coloured microgranular calcareous material. Aperture at the end of the tube but slightly visible.

Remarks:

Glomospira sp. is devoid of planispirally coiled last stages.

Stratigraphic distribution :

Glomospira sp. is found in the Late Norian-Rhaetian.

Genus: *Glomospirella* PLUMMER, 1945

***Glomospirella* sp.**

Pl. 7, fig. 5-8

Description :

Test discoidal. Proloculus followed by streptospirally enrolled undivided tubular second chamber, tubular chamber later becomes planispirally coiled in the last two or three whorls. Proloculus is not distinct. Wall finely agglutinated. Aperture at the open end of the tube.

Stratigraphic distribution :

Glomospirella sp. is found in the Late Norian-Rhaetian in this study.

ROTALIINA DELAGE & HEROUARD, 1896

NODOSARIICEA EHRENBERG, 1838

NODOSARIIDAE EHRENBERG, 1838

NODOSARIINAE EHRENBERG, 1838

Nodosarid foraminifer A

Pl. 7, fig. 9-10

Description :

Test rectilinear, consisting of uniserially arranged 3 or 4 chambers. Sizes of the chambers gradually increase in growth direction. Proloculus is not distinct. Wall is made up of light-colored hyalin calcite.

Remarks:

Nodosarid foraminifer A differs from nodosarid foraminifer B, C and D in having low height test and less chambers.

Stratigraphic distribution :

This form is found in the Norian-Rhaetian in this study.

Nodosarid foraminifer B

Pl. 8, fig. 1-3

Description :

Test elongated, consisting of uniserially arranged 8-9 chambers. Sizes of the chambers slightly increase in growth direction. Proloculus is not distinct. Wall is made up of light-colored hyalin calcite.

Remarks:

Nodosarid foraminifer B differs from nodosarid foraminifer A and C in having more chambers and high test.

Stratigraphic distribution :

This form is found in the Late Norian-Rhaetian in this study.

Nodosarid foraminifer C

Pl. 8, fig. 4

Description :

Test rectilinear, consisting of uniserially arranged 4 or 5 chambers. Sizes of the chambers gradually increase in growth direction. Chambers are distinctly globular. Wall is made up of light-colored hyalin calcite.

Remarks:

Nodosarid foraminifer C differs from nodosarid foraminifer A, B and D in having globular chambers.

Stratigraphic distribution :

This form is found in the Late Norian-Rhaetian in this study.

TEXTULARIINA DELAGE & HEROUARD, 1896

LITUOLACEA DE BLAINVILLE, 1827

TROCHAMMINIDAE SCHWAGER, 1877

TROCHAMMININAE SCHWAGER, 1877

Trochamminid foraminifer A

Pl. 8, fig. 7

Description :

Test is conical in shape. It consists of low globular shaped chambers and they are trochospirally coiled. Number of whorls are 3. Sizes of the chambers rapidly increase in growth direction. Umbilical cavity is present. Wall is dark-colored and microgranular.

Remarks:

Trochamminid foraminifer A differs from nodosarid foraminifer B and C in having low conical shape.

Stratigraphic distribution :

This form is found in the Late Norian-Rhaetian in this study.

Trochamminid foraminifer B

Pl. 8, fig. 8-9

Description :

Test is high conical in shape. Proloculus is distinct and globular in shape. It consists of 2 trochospirally coiled whorls. The size of the whorls rapidly increase in growth direction. Wall is finely agglutinated.

Stratigraphic distribution :

This form is found in the Late Norian-Rhaetian in this study.

Trochamminid foraminifer C

Pl. 8, fig. 8-9

Description :

Test is high conical in shape. Proloculus is distinct and nearly globular in shape. It consists of 4-5 trochospirally coiled whorls. The size of the whorls gradually increase in growth direction. Wall is made up of dark-coloured microgranular calcareous material

Stratigraphic distribution :

This form is found in the Late Norian-Rhaetian in this study.

CHAPTER 6

6. CONCLUSIONS

The studied carbonate successions in the Central and Western Taurides were deposited in a shallow marine environment during the Late Triassic. Sedimentary cyclicity and micropaleontological investigations which were carried out in three different localities of the Central and Western Taurides indicate different cyclicity characteristics and Upper Triassic foraminiferal assemlages within these carbonates. The micropaleontological analysis emphasizes the presence of a lagoonal foraminiferal association, dominated by the involutinids. They are characteristic of the wackestone to packstone facies with megalodonts. In this study, Upper Triassic was delineated by a biostratigraphical study based on the benthic foraminifers. Involutinids, nodosarids, trochamminids and the ammodiscidids are the main foraminifer groups that have been identified and illustrated. Based on the foraminiferal taxa, *Triasina hantkeni* assemblage zone is determined within the studied successions (Leylek-1, Leylek-2, Kuzca-1, Kuzca-2, Kuzca-3, Marmaris-1 and Marmaris-2 sections) and a Late Norian-Rhaetian age is attributed to these carbonates.

The studied successions are composed of Upper Triassic Lofer-type cyclic shallow marine carbonates. 8 meter-scale stratigraphic sections were measured within these carbonates and furthermore, 12 parasequences were examined in detail in order to understand the general characteristics of the Lofer cycles and the factors controlling the development of the cyclic successions. Based on the microfacies and paleontological analysis, the cyclicity trend in the Upper Triassic carbonates is found to be shallowing-upward. In the studied sections mainly an ABC facies succession was determined. The thin, green colored claystone defined as the facies A is interpreted as the lithology formed at the cycle bottoms and is characterized by the abundance of illite. Facies A represents the shallow subtidal environment based on the high abundance of illite if compared with the abundance of kaolinite and chlorite. The megalodont-bearing limestone facies (facies B) is regarded as the subtidal deposit represented by wackestones to packstones with abundant involutinid group foraminifers. The intertidal-supratidal facies (facies C) is represented by dolomitic limestones, fenestral limestones, dismicrites with geopetal fillings, black pebbles, breccias, stromatolites and vadose pisoids. Based on the microfacies data, 5 main types of cycles (A, B, C, D and E) and 34 sub-type cycles are determined. Cycles are generally represented by subtidal to supratidal deposits. However, most Lofer cycles are incomplete; many are missing clay units; some are missing the intertidal units or subtidal parts.

Sections measured in the Central and Western Taurides show differences in cyclicity and lithofacies. In the Leylek-1 and Leylek-2 sections, cycles are formed by the alternation of claystones and carbonates. In this region, two basic cycle types have been identified based on the presence or absence of the claystone at the bottom of the cycles. The cycles start with claystone at the base, is followed by megalodont-bearing limestones, dismicrites with geopetal fillings, black pebbles, fenestral limestones, breccias and stromatolites. However, Kuzca and Marmaris sections are entirely composed of carbonates. Shallowing-upward cycles are termed as 4^{th}-order cycles in the studied successions. They are bounded by marine-flooding surfaces at the bottom. 5^{th}-order higher frequency smaller-scale cycles are also recorded within the 4^{th}-order cycles. One 4^{th}-order cycle can contain 2-4 5^{th}-order cycles. It is suggested that most Lofer cycles were deposited under control of 5^{th}-order eustatic-sea-level oscillations (Strasser, 1994). In the Leylek-1 and Marmaris-1 sections, cycles are dominated by intertidal-supratidal facies in the lower levels and subtidal facies in the upper levels. However, in Leylek-2, Marmaris-2, Kuzca-1, Kuzca-2 and Kuzca-3 sections subtidal facies are dominant. The megalodont-bearing limestone dominated cycles with thick limestone beds corresponds to highstand systems tracts and stromatolite, fenestral limestone etc. dominated cycles corresponds to transgressive systems tracts. In addition, a red colored vadose pisoidic level was encountered in the Kuzca-4 section which is the common constituents of supratidal vadose caps of the peritidal cycles. The cycle with a subaerial exposure cap must be the result of relative sea level oscillation and may correspond to an important sea level fall in the Upper Norian-Rhaetian time interval.

Although the cyclicity of the Upper Triassic carbonates have been investigated by microfacies analysis, micropaleontological investigations are also important for controlling the cyclicity mechanisms within these carbonates. In order to understand the responses of foraminifers to carbonate cyclicity, involutinid group foraminifers which constitute the main microfossil group in the studied successions were counted throughout the cycles. This has indicated that the number of involutinid foraminifers increases at the bottom of the cycles, however decreases at the top of the cycles. In addition, cluster analysis was also performed in order to arrange samples and variables in relation to environmental parameters. Q-mode cluster analysis has been applied to 26 samples. 2 main clusters have been obtained. Cluster I consists of fenestral limestone, breccia, stromatolite, dismicrite with black pebble which were deposited at the top of the cycles. Cluster II consists of megalodont-bearing limestone and foraminiferal pelloidal packstone facies, depositing at the bottom of the cycles. R-mode cluster analysis has been performed to 79 samples and 5 taxa have been used (*Aulotortus*, *Auloconus*, *Triasina hantkeni* Majzon, nodosarids and trochamminids). 2 clusters have been obtained. Cluster I is formed by *Aulotortus* and Cluster II consists of *Auloconus*, *Triasina hantkeni* Majzon, nodosarids and trochamminids. These groups of foraminifers are grouped into different clusters due to the depositional settings they inhabited. *Aulotortus* exist in a higher energy conditions, however the others prefer much more muddy, low energy depositional settings.

Based on the cycle types and the successive occurrences of parasequences along the measured sections, a depositional model has been constructed for the Upper Triassic Lofer-type carbonates in the Central and Western Taurides. The depositional model proposed in this study is a generalized summary of the stacking patterns of parasequences. The cycles are commonly composed of thickly bedded shallow subtidal facies or thin claystone levels at the bottom and capped by inter to supratidal facies. Parasequences are bounded by marine flooding surfaces which are corresponding to the claystones, megalodont-bearing limestones and foraminiferal limestones and indicate the transgressive portion of the cycles. On the other hand, stromatolites, fenestral limestones, dismicrites with geopetal fillings and black pebbles are the indicative of the regressive portion of the cycles. The studied successions also provided clear evidence of subaerial exposure at the top of the cycles which is determined by breccias. However, stromatolites are prograded on top of the subaerially exposed surfaces and rapidly filled the accomodation space. Although Fischer (1964); Haas (1991, 2004), Haas et al. (2007) etc. proposed transgressive models for the Lofer cycles, we interpret the Lofer cycles by a regressive model in which the subtidal deposits pass upward into inter to supratidal deposits. The transgressive Lofer cycle model was largely based on the Dachstein Lofer Section (Fischer, 1964), which contains several soil at the bottom of the cycles and overlain by laminites. These findings do not seem to be conformable with our findings in the Central and Western Taurides. We did not find soils (Fischer's member A) in our studied successions. We observed thick megalodont-bearing limestones at the bottom of the cycles which are overlain by several inter to supratidal deposits. Consequently, Lofer cycles are in fact regressive and show shallowing-upward character.

In addition, the sequence stratigraphic works play an important role in oil exploration studies. In particular, the high-frequency sequences is important for controlling reservoir, source and seal rock distribution (Mitchum et al., 1991). Within this study, 4^{th}- and 5^{th}-order sequences will be used in future works for finding the petroleum potential of this region. In general, the successions which are common in thick megalodont-bearing limestones indicate highstand systems tract deposits while the stromatolites, fenestral limestones, breccias etc. dominant facies corresponds to the transgressive systems tract deposits. Finding the maximum flooding surface and lowstand systems tract deposits in the field will help us to find out the reservoir and the source rock within the studied region.

Further studies on the Upper Triassic Lofer cyclicity must be concentrated on the isotope analysis (δ13C & δ18O) in order to understand the relationship between the cycles and the climatic changes. Thus, the geochemical data will be supporting the paleontological and sedimentological data.

REFERENCES

Abate, B., Ciarapica, G. and Zaninetti, L. 1984. Triasina oberhauseri Koehn-Zaninetti et Brönniman, 1968, dans le Trias Superior Recifal (Facies "Back Reef") de la Plate-Forme Panormide, Sicile. Revue de Paleobiologie, 3, 19-25.

Akbulut, A. 1980. The geology of the Western Taurides in the area of Çandır (Sütçüler, Isparta), south the Eğridir Lake. Bulletin of the Geological Society of Turkey, 23/1, 1-10.

Akçar, N., 1998. Meter-scale cyclic deposits in the Lower Cretaceous peritidal Carbonates of the Üzümlü Area (Western Taurides, Turkey). M. S. Thesis, Middle East Technical University, Ankara, Turkey, 109 p. (unpublished).

Al-Shaibani, S., Altıner, D., Brönnimann, P., Carter, D.J. and Zaninetti, L. 1982. *Triasina hantkeni* Majzon, 1954 (Foraminifere) dans le Trias superieur de la Tethys (Europe et Asie). Arch. Sc. Geneve, 35, Fasc. 2, 137-142.

Al-Shaibani, S., Carter, D.J. & Zaninetti, L. 1983. Geological and Micropaleontological investigations in the Upper Triassic (Asinepe Limestone) of Seram, Outer Banda Arc, Indonesia. Arch. Sc. Geneve, Vol. 36, Fasc. 2, pp. 297-313.

Al-Shaibani, S., Carter, D.J. and Zaninetti, L. 1984. Microfaunes associees aux Involutinidae et aux Milioliporidae dans le Trias superieur (Rhetien) de Seram, Indonesie; Precisions stratigraphiques et Paleoecologie. Arch. Sc. Geneve, Vol. 37, Fasc. 3, pp. 301-316.

Altıner, D. et Zaninetti, L. 1980. Le Trias dans la region de Pinarbasi, Taurus oriental, Turquie: unites lithologiques, micropaleontologie, milieux de depot. Riv. Ital. Paleont., v. 86, n. 4, pp. 705-760.

Altıner, D., Yılmaz, I.Ö., Özgül, N., Bayazıtoglu, M. and Gaziulusoy, Z. E. 1999. High resolution sequence stratigraphic correlation in the Upper Jurassic (Kimmeridgian) – Upper Cretaceous (Cenomanian) peritidal carbonate deposits, Western Taurides, Turkey. Geological Journal, 34, 139–150.

Amodio, S. 2006. Foraminifera diversity changes and paleoenvironmental analysis: the Lower Cretaceous shallow-water carbonates of San Lorenzello, Campnian Apennines, southern Italy. Facies, 52, 53-67.

Atakul, A. 2006. Lower-Middle Carboniferous boundary in Central Taurides, Turkey (Hadım area): paleontological and sequence stratigraphic approach. M. S. Thesis, Middle East Technical University, Ankara, Turkey, 201 p. (unpublished).

Balog, A., Haas, J., Read, J.F., Coruh, C. 1997. Shallow marine record of orbitally forced cyclicity in a Late Triassic carbonate platform, Hungary. J Sediment Research**,** 67 (4)**,** 661-675.

Bassant, P., Van Buchem, F.S.P., Strasser, A. and Görür, N. 2005. The stratigraphic architecture and evolution of the Burdigalian carbonate-siliciclastic sedimentary systems of the Mut Basin, Turkey. Sedimentary Geology, 173, 187-232.

Bayazıtoğlu, M. 1998. Short distance sequence stratigraphic correlation in a carbonate succession of Fele area (North of Beyşehir Lake), Western Taurides, Turkey. M. S. Thesis, M.E.T.U., Ankara, Turkey, 125 p.(unpublished).

Beccaletto, L., Bartolini, A.C., Martini, R., Hochuli, P.A. and Kozur, H. 2005. Biostratigraphic data from the Çetmi Melange, nothwest Turkey: Paleogeographic and tectonic implications. Palaeo. vol. 221, pp. 215-244.

Bernal, J.P., Eggins, S.M., Mc Culloch, M.T. 2006. Dating of chemical weathering processes by in situ measurement of U-series disequilibria in supergene Fe-oxy/hydroxides using LA-MC-ICPMS. Chemical Geology, Vol. 235, Issue 1-2, 76-94

Bernouilli, D., Graciansky, P.C. and Monod, O., 1974. The extension of the Lycian nappes SW Turkey into the Southeastern Aegean Islands. Eclogea Geol. Helv., V. 61 (1), 39-90.

Bilgin, R., Metin, Y., Çörekçioğlu, E., Bilgiç, T. and Şan Ö. 1997. Bozburun-Marmaris-Köyceğiz-Dalaman (Muğla) Dolayının Jeolojisi. MTA Rapor no: 502.

Blumenthal, M. M. 1944. Bozkır güneyinde Toros sıradağlarının serisi ve yapısı. İstanbul Üniversitesi Fen Fakültesi Mec., seri B, 9, 95-125.

Blumenthal, M. M. 1947. Beyşehir-Seydişehir hinterlandındaki Toros daglarının jeolojisi. Maden Tetkik Arama Enst. Ankara, seri D, 2, 242 p.

Blumenthal, M. M. 1951. Batı Toroslarda Antalya ardı ülkesinde jeolojik araştırmalar. Maden Tetkik Arama Enst. Ankara, seri D, 5, 194 p.

Blumenthal, M. M. 1952. Toroslarda yüksek Aladağ silsilesinin coğrafyası, stratigrafisi ve tektoniği hakkında yeni etütler, Maden Tetkik Arama Enst. Ankara, seri D, 6.

Blumenthal, M. M. 1956. Yüksek Bolkardağın Kuzey Kenar Bölgelerinin ve Batı Uzantılarının Jeolojisi. Maden Tetkik Arama Enst. Ankara, seri D, 7, 151 p.

Bosellini, A. 1967. La tematica Depozionale Della Dolomia Principale. Boll. Soc.Geol., 86, 133-169.

Bosellini, A. and Hardie, L.A., 1988. Facies e cicli della Dolomia Principale delle Alpi Venete. Mem. Soc. Geol. 30, 245-266.

Brinkmann, R., 1975. Geology of Turkey. Amsterdam, Elsevier, 158p.

Brönnimann, P., Poisson, A. et Zaninetti, L. 1970. L'unite du Domuz Dag (Taurus lycien-Turquie) Microfacies et Foraminiferes du Trias et du Lias. Riv. Ital. Paleont., 76, n. 1, pp. 1-36.

Brönnimann, P., Zaninetti, L., Moshtaghian, A. and Huber, H. 1974. Foraminifera and microfacies of the Triassic Espahk formation, Tabas area, east central Iran. Rivista Italiana di Paleontologia e Stratigrafia, v. 80, n. 1, pp. 1-48.

Brunn, J.H., Dumont, J.F., Graciansky, P Ch. De, Gutnic, M., Juteau, Th., Marcoux, J., Monod, O. and Poisson, A., 1971. Outline of the Geology of the Western Taurides. In: Geology and History of Turkey, Campbell (A.S.ed.), Petrol. Explor. Soc. Of Libya, Tripoli, 225-255.

Buffen, A., Leventer, A., Rubin, A. 2007. Diatom assemblages in surface sediments of the northwestern Weddell Sea, Antarctic Peninsula Marine Micropaleontology, Vol. 62, Issue 1, 7-30.

Burchell, M. T., Stefani, M. and Masetti, D., 1990, Cyclic Sedimentation in the Southern Alpine Rhaetic: The Importance of Climate and Eustasy in Controlling Platform-Basin Interactions, Sedimentology, 37: 795-815.

Ciarapica, G. et Zaninetti, L. 1984. Foraminiferes et biostratigraphie dans le Trias superieur de la serie de la spezia (Dolomies de Coregna et formation de la Spezia, Nouvelles formations), Apennin Septentrional. Revue de Paleobiologie. 3/1, 117-134.

Ciarapica, G. et Zainetti, L. 1985. Le cas de "*Glomospirella friedli-Angulodiscus* ? *gaschei*" (=*Aulotortus friedli*, Aulotortinae, Involutinidae, Foraminifere Trias): analyse structurale et revision taxonomique. Arch. Sc. Geneve, vol. **38**, fasc. 1, pp. 71-86.

Ciarapica, G., Cirilli, S., Passeri, E. et Zaninetti, L. 1987. "Andriti di Burano" et "Formation du Monte Cetona" (Nouvelle Formation), biostratigraphie de deux series-types du Trias superieur dans l'Apennin Septentrional. Revue de Paleobiologie. 6/2, 341-409.

Covelli, S., Fontolan, G., Faganeli, J. 2006. markers in the Holocene stratigraphic sequence of the Gulf of Trieste (northern Adriatic Sea). Marine Geology, Vol. 230, Issue 1-2, 29-51.

Cozzi, A., Hinnov L.A. and Hardie, L.. 2003. Facies and cyclostratigraphy of Dachstein Limestone in the Julian Alps (NE Italy): a new insights on the Lofer cyclothem controversy. In: Abstracts of the field symposium on Triassic geochronology and cyclostratigraphy. September 2003 St. Christina, Italy, p. 33.

Çiner, A. 1996. Distribution of small-scale sedimentary cycles throughout several selected basins. Turkish J. of Earth Sciences, Tübitak, Doğa, 5, 25-37.

Çiner, A., Deynoux, M., Ricou, S. and Koşun, E. 1996a. Cyclicity in the middle Eocene Cayraz carbonate formation, Haymana Basin, Central Anatolia, Turkey. Paleogeography, Paleoclimatology, Paleoecology, 121, 3-4, 313-329.

Çiner, A., Deynoux, M. and Koşun, E. 1996b. Cyclicity in the Yamak turbidite complex of the Haymana Basin, Central Anatolia, Turkey. Geologische Rundschau, 85, 4, 669-682.

Çiner, A., Koşun, E. and Deynoux, M. 2002. Fluvial, evaporitic and shallow marine facies architecture, depositional evolution and cyclicity in the Sivas Basin (Lower to Middle Miocene), Central Turkey. Journal of Asian Earth Sciences, 21, 2, 147-165.

Dager, Z. 1975. Study on Involutina species occured in Taurus Mountains. Bull. Geol. Soc. Turkey, 18, pp. 151-156.

Davies, N.S., Sansom, I.J., Turner, P. 2006. Trace fossils and paleoenvironments of a Late Silurian marginal-marine/alluvial system: The Ringerike Group (Lower Old Red Sandstone), Oslo region, Norway. Palaios, Vol. 21, Issue 1, 46-62.

Demirtaşlı, E., 1987. Batı Toroslar'da Akseki-Manavgat-Köprülü arasında kalan alanın jeoloji incelemesi. MTA Rapor 8779, Ankara.

Dimitrijevic, M.N. and Dimitrijevic, M.D. 1991. Triassic carbonate platform of the Drina-Ivanica element (Dinarides). Acta Geol. Hung., 34 (1-2), 15-44.

Donato, B. and Alberto, B. 1998. Late Triassic (Carnian) foraminifers of northeastern Cortina d'Ampezzo (Tamarin, San Cassano Fm., Dolomites, Italy). Ann. Mus. Civ. Rovereto, 12, 117-146.

Dumont, J.F., Gutnic, M., Marcoux, J., Monod, O. and Poisson, A. 1972. Les Trias des Taurides Occidentales (Turquie) Definition du Bassin Pamphylien: Un Nouveau Domaine a Ophiolites a la marge externe de la chaine Taurique. IV Colloque sur la Géologie des Régions Egéennes, 1-16.

Dumont, J.F. and Kerey, E. 1975. Eğridir gölü güneyinin temel jeolojik etüdü. Türkiye Jeoloji Kurultayı Bülteni, 18/2, 169-174.

Dumont, J.F. and Monod, O. 1976. Dipoyraz Dağ masifinin Triyasik karbonatlı serisi (Batı Toroslar, Türkiye). MTA Dergisi, 87, 26-39.

Dumont, J.F. and Zaninetti, L. 1985. Decouverte de Triasina hantkeni MAJZON (Foraminifere) dans un faisceau calcaire a Polypiers (Rhabdophyllia) de la formation rhetico-hettangienne prepiemontaise (Nappe de Rochebrune SE de Briançon, Alpes occidentales). Arc. Sc. Geneve, Vol. 38/1, 63-70.

Einsele, G., Ricken W. and Seilacher, A. 1991. Cycles and Events in Stratigraphy - basic concepts and terms. In: W. R. G. Einsele, W. Ricken & A. Seilacher (eds.), Cycles and Events in Stratigraphy, Berlin, Heidelberg, New York, Springer Verlag, 1-19.

Ekmekçi, E., Özkan-Altıner, S., Altıner, D., Yılmaz, Ö., Erdoğan, K., Şener S., Coşkun, B. Şenel, M. and Işıntek, İ. 2006. Torosların Geç Triyas-Liyas yaşlı istiflerinin foraminifer Biyostratigrafisi ve Mikrofasiyes özellikleri. MTA Rapor No. 10889, p. 73.

Enos, P. and Samankassou, E. 1998. Lofer cycles revisited (Late Triassic, Northern Alps, Austria). Facies, 38, 207-228.

Enos, P. and Samankassou, E. 2002. Lateral variations in Dachstein Limestone (Triassic, Austria). In: Abstracts of the 16th Int. Sedimetological Congress. Johannesburg, p. 88.

Fermani, P., Mataloni, G., Van de Vijver, B. 2007. Soil microalgal communities on an antarctic active volcano (Deception Island, South Shetlands). Polar Biology. Vol. 30, 1381-1393.

Fischer, A.G. 1964. The Lofer Cyclothems of the Alpine Triassic. Kansas Geological Survey Bulletin, 169, 107-149.

Fischer, A.G. 1975. Tidal deposits, Dachstein Limestone of the North-Alpine Triassic. In: Ginsburg RN (ed) Tidal deposits: a casebook of recent examples and fossil counterparts. Springer, Berlin Heidelberg New York, pp 234-242.

Fischer, A.G. 1991. Orbital cyclicity in Mesozoic strata. In: Einsele, G., Ricken, W. and Seilacher, A. (eds.): Cycles and events in stratigraphy. 49-92.

Flügel, E. 2004. Microfacies of carbonate rocks: Analysis, Interpretation and Application. Springer Berlin Heidelberg New York, 976p.

Fontaine, H., Beauvais, L., Poumint, C, and Vachard, D., 1979. Données nouvelles sur le Mésozoque de 1'Ouest des Philippines. Découverte de Rhétien marin. Bull. Soc. Geol. Fr., Suppl., 3, 117-121.

Frechengues, M., Peybernes, B., Martini, R. et Zaninetti, L. 1993. Ladinian-Carnian Benthonic Foraminifera from the “Muschelkalk” of the French and Spanish Pyrenees to the east of the Garonne. Revue de Micropaleontologie, 36/2, 111-120.

Fruth, I. and Scherreiks R. 1975. Facies and Geochemical correlations in the Upper Hauptdolomit (Norian) of the Eastern Lechtaler Alps. Sedimentary Geology, 13, 27-45.

Fruth, I. and Scherreiks R. 1982. Hauptdolomit (Norian)- Stratigraphy, Paleogeography and Diagenesis. Sedimentary Geology, 32, 195-231.

Fruth I. and Scherreiks R., 1984, Hauptdolomit – Sedimentary and Paleogeographic Models (Norian, Northern Calcareous Alps), Geologische Rundschau, 73: 305-319.

Gawlick H.and Böhm F., 1999, Sequence Stratigraphy of Late Triassic Distal Periplatform Limestones from the Northern Calcareous Alps – an example from the Kalberstein Quarry (Berchtesgaden Hallstatt Zone), Tubinger Geowissenschaftliche Arbeiten, Series A, Vol.52, pp.146-147.

Gaziulusoy, Z. E. 1999. A sequence stratigraphical approach from microfacies analysis to the Aptian-Albian peritidal carbonates of Polat Limestone (Seydişehir), Western Taurides, Turkey. M. S. Thesis, M.E.T.U., Ankara, Turkey, 97 p. (unpublished).

Gianolla, P., De Zanche V. and Roghi, G., 2003, An Upper Tuvalian (Triassic) Platform-Basin System in the Julian Alps: the Start-up of the Dolomia Principale (Southern Alps, Italy), Facies, 49, 135-150.

Ginsburg, R.N. 1971. Landward movement of carbonate mud: a new model for regressive cycles in carbonates (abs). Bull. Am. Assoc. Petrol. Geol. 55, 340-341.

Ginsburg, R.N., Hardie, L.A., Bricker, O.P., Garrett, P. and Wanless, H.R., 1977. Exposure index: a quantitative approach to defining position within the tidal zone. In: Hardie, L.A. (Ed.), Sedimentation on the Modern Carbonate Tidal Flats of Northwestern Andros Island, Bahamas. Johns Hopkins University, Baltimore, Studies in Geology, 22, 7-11.

Goldhammer, R. K., Dunn, P. A. and Hardie, L. A. 1987. High frequency glacio-eustatic sea-level oscillations with Milankovitch characteristics recorded in Middle Triassic platform carbonates in northern Italy. Am. J. Sci., 287, 853-892.

Goldhammer R. K., Dunn, P.A. and Hardie, L.A. 1990, Depositional Cycles, Composite Sea Level Changes, Cycle Stacking Patterns, and the Hierarchy of Stratigraphic Forcing: Examples from Alpine Triassic Platform Carbonates. Geological Society of America Bulletin, 102, 553-562.

Gomez, J.J. and Goy, A. 2005. Late Triassic and Early Jurassic paleogeographic evolution and depositional cycles of the Western Tethys Iberian platform system (Eastern Spain). Paleogeography, Paleoclimatology, Paleoecology, 222, p. 77-94.

Graciansky, P., Ch. 1968. Teke yarımadası (Likya) Torosları'nın üstüste gelmiş ünitelerinin stratigrafisi ve Dinaro-Toroslar'daki yeri. MTA Dergisi, 71, 73-91.

Graciansky, P., Ch., de. 1972. Recherches geologiques dans le Taurus Lycien occidental: These Univ. Paris-Sud centre d'Orsay, Ser. A, No. 896, 571p.

Grover, G. and Read, J.F. 1978. Fenestral and associated vadose diagenetic fabrics of tidal flat carbonates, Middle Ordovician New Market Limestone, southwestern Virginia. J. Sed. Petrol., 48/2, 453-473.

Gutnic, M., Monod, O., Poisson, A. and Dumont, J.F. 1979. Geologie des Taurides Occidentales (Turquie), Mem. Soci, geol. France, 55, 109 p.

Haas, J. 1982. Facies analysis of the cyclic Dachstein Limestone formation (Upper Triassic) in the Bakony Mountains, Hungary. Facies, 6, 75-84.

Haas, J. 1991. A basic model for Lofer cycles. In: Einsele G., Ricken W., Seilacher A. Cycles and events in stratigarphy. Springer, Berlin Heidelberg New York, pp. 722-732.

Haas, J. 2004. Characteristics of peritidal facies and evidences for subaerial exposures in Dachstein-type cyclic platform carbonates in the Transdunabian Range, Hungary. Facies, 50, 263-286.

Haas, J. and Budai, T. 1995. Upper Permian-Triassic facies zones in the Transdunabian Range. Rivista Italiana di Paleontologia e Stratigrafia, vol. 101, no. 3., pp. 249-266.

Haas J. and Demeny A., 2002. Early Dolomitisation of Late Triassic Platform Carbonates in the Transdanubian Range (Hungary), Sedimentary Geology, 151: 225-242.

Haas J. and Tardy-Filacz T., 2004. Facies Changes in the Triassic-Jurassic Boundary Interval in an Intraplatform Basin Succession at Csovar, Sedimentary Geology, 168, 19-48.

Haas, J., Lobitzer, H. and Monostori, M. 2007. Characteristics of the Lofer cyclicity in the type locality of the Dachstein Limestone (Dachstein Plateau, Austria). Facies, 53, 113-126.

Haq., B.U., Hardenbol, J. and Vail, P. 1988. Mesozoic and Cenozoic chronostratigraphy and cycles of sea level change; In Sea Level Changes: An integrated approach, S.E.P.M. Special publication, N.42, p. 71-108.

Haude, H. 1972. Stratigraphie und Tektonik des südliche Sultan Dağ (SW Anatolian) zeit, Deutsch. Geol. Ges. Bd., 123, 411-421.

Hofrichter, J. and Winkler, G. 2006. Statistical analysis for the hydrogeological evaluation of the fracture networks in hard rocks. Environmental Geology, Vol. 49, Issue 6, 821-827.

Hussain, M. 2007. Elemental chemistry as a tool of stratigraphic correlation: A case study involving lower Paleozoic Wajid, Saq, and Qasim formations in Saudi Arabia. Marine and Petroleum Geology, Vol. 24, Issue 2, 91-108.

Ilgar, A. and Nemec, W. 2005. Early Miocene lacustrine deposits and sequence stratigraphy of the Ermenek Basin, Central Taurides, Turkey. Sediment. Geol., 173: 233-275.

Işıntek, İ. 2002. Foraminiferal and algal biostratigraphy and petrology of the Triassic to Early Cretaceous carbonate assemblages in the Karaburun Peninsula (Western Turkey). Phd Thesis. p. 263 (unpublished).

Işıntek, İ., Kayseri, M.S., Akgün, F. and Yağmurlu, F. 2005. Foraminiferal, algal and palynological data from the coal bearing Triassic Rhaetian-Liassic boundary in the Üzümdere Formations of the Anamas-Akseki Autocthon north of Yakaköy, Aksu-Isparta, Southern Turkey. Abstract Book of the Interbational Earth Sciences Colloquıum on the Aegean Regions, p. 53.

Jadoul, F., Garzanti, E. and Fois, E. 1990. Upper Triassic-Lower Jurassic stratigraphy and paleogeographic evolution of the Zanskar Tethys Himalaya (Zangla unit). Riv. Ital. Paleont., 95, n. 4, 38-40.

Jadoul, F., Galli, M.T., Calabrese, L. and Gnaccolini, M. 2005. Stratigraphy of Rhaetian to Lower Sinemurian carbonate platforms in western Lombardy (southern Alps, Italy): Paleogeographic implications. Rivista Italiana di Paleontologia e Stratigrafia, vol. 111, no. 2., pp. 285-303.

Kamoun, F., Martini R., Peybernes, B. and Zaninetti, L. 1994. Caracterisation micropaleontologique du “Rhetien” dans l’axe nord-sud (Tunisie Centrale); comparison avec le Rhetien de la dorsale et de plate-forme Saharienne. Riv. It. Paleont. Strat. 100/3, 365-382.

Kamoun, F., Peybernes, B., Martini, R., Zaninetti, L., Vila, J.M., Trigui, A. and Rigane, A., 1997. Associations de foraminiferes benthiques dans les sequences de depot du Trias moyen ?-superieur de l’Atlas Tunisien central et meridional. Geobios, 31, 6, 703-714.

Karakitsios, V., Tsaila-Monopolis, S. and Pakos, T. 1990. Donnees nouvelles les niveaux inferieurs (Trias superieur) de la serie calcaire ionienne en epire (Grece continentale). Consequences stratigraphiques. Revue de Paleobiologie. 9/1, 139-147.

Kobayashi, F., Martini, R., Rettori, R., Zaninetti, L., Ratanasthien, B., Saegusa, H. and Nakaya, H. 2006. Triassic foraminifers of the Lampang Group (Northern Thailand). Journal of Asian Earth Sciences, 27, 312-325.

Koehn-Zaninetti, L. 1968. Les Foraminiferes du Trias de la region de l'Almtal (Haute-Autriche). Texte condense de la these, No. 1467, 14p..

Koehn-Zaninetti, L. et Brönnimann, P. 1968. Angulodiscus? gaschei, n. sp., un Foraminifere de la Dolomie principale des Alpes Calcaires septentrionales (Autriche). C.R. des Seances, Vol. 2, Fasc. 1, pp. 74-80.

Kristan, E. 1957. Ophthalmidiidae und Tetrataxinae (Foraminifera) aus dem Rhät der Hohen Wand in Niederösterreich-Wien. Jahrb. Geol. B.-A., 100.

Kristan-Tollmann, E. 1964. Die Foraminiferen aus der rhatischen Zlambachmergeln der Fischerwiese bei Aussee im Salzkammergut. Jb. Geol. Bundesant., 10, 1-189.

Kristan-Tollmann, E. and Tollmann, A. 1962. Das mittelostalpine Rhät-Standardprofil aus dem Stangalm-Mesozoikum (Kärnten). Mitt. Geol. Ges. Wien, 56, n. 2, 539-589.

Lefevre, R. 1967. Nouvel element dans la geologie du Taurus Lycien: les Nappes d'Antalya (Turquie). C. R. De l'Academie des Sciences, 7 (serie D265), 1365-1368.

Loeblich, A.R. and Tappan, H. 1988. Foraminiferal Genera and Their Classification. Van Nostrand Reinhold, Newyork, 869p.

Majzon, L. 1954. Contributions to the stratigarphy of the Daschstein Limestone. Acta Geol. Acad. Sci. Hung., 243-249.

Mancinelli, A., Chiocchini, M., Chiocchini R.A. and Romano, A. 2005. Biostratigraphy of Upper Triassic-Lower Jurassic carbonate platform sediments of the central-southern Apennines (Italy). Rivista Italiana di Paleontologia e Stratigrafia, vol. 111, no. 2., pp. 271-283.

Marcoux, J. 1979. Antalya naplarının genel yapısı ve Tetis güney kenarı paleocoğrafyasındaki yeri. T.J.K Bülteni, 22/1, 1-6.

Martini, R., Gandin, A. and Zaninetti, L. 1989. Sedimentology, stratigraphy and micropaleontology of the Triassic evaporitic sequence in the subsurface of Boccheggiano and in some outcrops of southern Tuscany (Italy). Riv. Ital. Paleont., v. 95, n. 1, pp. 3-28.

Martini, R., Zaninetti, L., Cornee J.J., Villeneuve, M., Tran, N. and Ta, T.T. 1997. Occurence of the Triassic foraminifers in carbonate deposits from the Ninh Binh Area (North Vietnam). C.R. Acad. Sci. Paris, Sciences de la terre et des planetes, 326, 113-119.

Martini, R., Zaninetti, L., Lathuilliere, B., Cirili, S., Cornee, J. and Villeneuve, M. 2004. Upper Triassic carbonate deposits of Seram (Indonesia): paleogeographic and geodynamic implications. Paleogeography, Paleoclimatology, Paleoecology, 206, 75-102.

Metz, K. 1939. Beitrage zu Geologie des Kilikischen Taurus im gebiete des Aladağ. Sitz Ber. Ak. Wien, Abt., 1, 148, 7-10.

Metz, K. 1956. Ein Beitragzur Kenntnis des gebirgsbaues von Aladağ und Karanfildağ und ihres Westrandes (Kilikischer Taurus). Maden Tetkik Arama Enst. Dergisi, 48, 68-78.

Michalik, J. 1980. A Paleoenvironmental and Paleoecological analysis of the west Carpathian part of the northern Tethyan nearshore region in the Latest Triassic Time. Riv. Ital. Paleont., v. 85, n. 3-4, 1047-1064.

Michalik, J. 1993. Mesozoic tensional basins in the Alpine-Carpathian shelf. Acta Geologica Hungarica. 36, 395-403.

Michalik, J., Lintnerová O., Gazdzicki, A. and Soták, J. 2007. Record of environmental changes in the Triassic-Jurassic boundary interval in the Zliechov Basin, Western Carpathians. Paleogeography, Paleoclimatology, Paleoecology, 244, 71-88.

Mithchum, R. M., Vail, P. R. and Thomson, S. 1977. Seismic stratigraphy and global changes of sea level, part 2: The depositional sequences as a basic unit of for stratigraphic analysis. Applications to Hydrocarbon Exploration: Association of Petroleum Geologist Memoir, 26, 53-62.

Mithchum, R. M., Jr. and Van Wagoner, J. 1991. High-frequency sequences and their stacking patterns: sequence-stratigraphic evidence of high-frequency eustatic cycles. Sedimentary geology, 70, 131-160.

Monod, O. 1977. Recherches geologiques le Taurus occidental au sud de Beyşehir (Turquie); These, Universite Paris XI Orsay. p. 422.

Novak, M. 2003. Upper Triassic and Loer Jurassic beds in the Podutik area near Ljubljana (Slovenia). Geologija, 46/1, 65-74.

Oberhauser, R. 1964. Zur Kenntnis der Foraminiferengattungen Permodiscus, Trocholina und Triasina in der alpinen Trias und ihre Einordnung zu den Archaedisciden. Verh. Geol. Bundesant. 2, 196-210.

Ogorelec, B. and Buser, S. 1996. Dachstein Limestone from Krn in Julian Alps (Slovenia). Geologija, 39, 133-155.

Okay, A.İ. and Altıner, D. 2007. A Condensed Mesozoic succession north of İzmir: a fragment of the Anatolide-Tauride platform in the Bornova Flysch Zone. Turkish Journal of Earth Sciences, 16, 1-23.

Özgül, N. 1976. Some geological aspects of the Taurus orogenic belt-Turkey. Society of Turkey Bulletin, 19, 65-78 (in Turkish with English abstract).

Özgül, N. 1984. Stratigraphy and tectonic evolution of the Central Taurides. In.Tekeli O. and Göncüoglu M. C. (eds), Geology of the Taurus Belt. Mineral Research and Exploration Institute of Tukey Publication, 77-90.

Özgül, N. 1997. Stratigraphy of the tectono-stratigraphic units in the region Bozkýr-Hadim-Taşkent (northern Central Taurides). Mineral Research and Exploration Institute of Turkey (MTA) Bulletin, 119, 113-174 (in Turkish with English abstract).

Özgül, N and Turşucu, A. 1984. Stratigraphy of the Mesozoic carbonate sequence of the Munzur Mountains (Eastern Taurides). In.Tekeli O. and Göncüoglu M. C. (eds), Geology of the Taurus Belt. Mineral Research and Exploration Institute of Tukey Publication, 173-180.

Özgül, N and Kozlu, H. 2002. Data on the stratigarphy and tectonics of the Kozan-Feke region (Eastern Taurides). TAPG Bulletin, 14/1, 1-36.

Perinçek, D. and Kozlu, H. 1984. Stratigraphy and structural relations of the units in the Afşin-Elbistan-Doğanşehir region (Eastern Taurus). In.Tekeli O. and Göncüoglu M. C. (eds), Geology of the Taurus Belt. Mineral Research and Exploration Institute of Tukey Publication, 181-198.

Perri, E., Mastandrea, A., Neri, C. and Russo, F., 2003. A Micrite-Dominated Norian Carbonate Platform from Northern Calabria (Southern Italy), Facies, 49, 101-118.

Peybernes, B., Martini, R., Taugourdeau-Lantz, J. and Zaninetti, L. 1988. Micropaleontological characterization of the Rhethian stage between Garonne and the Mediteranean (French Pyrenees). Revue de Paleobiologie. **7**/1, 137-161.

Peynircioğlu, A.A. 2005. Micropaleontological analysıs and facies evolution across the Tournaisian – Visean boundary in Aladağ unit (Central Taurides, Turkey) M. S. Thesis, Middle East Technical University, Ankara, Turkey, 76 p. (unpublished).

Philipson, A., 1915. Reisen und Forschungen im westlichen Klienasien: Pet. Mitt. H. 167p.

Poisson, A. 1977. Recherches geologiques dans les Taurides occidentales (Turquie). These, Univ. Paris-sud, 795p.

Posamentier, H.W., Jervey, M.T. and Vail, P.R. 1988. Eustatic Controls on Clastic Deposition I-Conceptual Framework. Sea Level Changes-An Integrated Approach, SEPM Special Publication No.42, 109-124.

Preto, N. and Hinnov, L.A. 2003. Unravelling of the Origin of Carbonate Platform Cyclothems in the Upper Triassic Dürrenstein Formation (Dolomites, Italy). Journal of Sedimentary Research, Vol. 73, No. 5, p. 774-789.

Pütürgeli, E. 2002. Meter-scale shallowing upward cycles in the Midian (Upper Permian) strata (Central Taurides, Turkey). M. S. Thesis, Middle East Technical University, Ankara, Turkey, 103 p. (unpublished).

Read, J.F. 1985. Carbonate platform facies models. The American Association of Petroleum Geologists Bulletin, V. 69, No.1, p. 1-21.

Read, J.F. and Goldhammer, R.K. 1988. Use of Fischer plots to define third-order sea-level curves in Ordovician peritidal cyclic carbonates, Appalachians. Geology, 16, 895-899.

Salaj, J., 1969. Essai de Zonation dans le Trias des Carpates Occidentales d'apres les Foraminiferes. Geol. Prace, Spravy, vol. 48, 123-128.

Salaj, J., Biely, A. and Bistricky, J. 1967. Trias-Foraminiferen in den Westkarpeten. Geol. Prace, 42, 119-136.

Sander, B. 1936. Beitrage zur Kenntnis der Anlagerungsgefüge. Miner Petr Mitt, 48**,** 27-139.

Sarg, J.F. 1988. Carbonate sequence stratigarhy. In Sea level changes: An integrated approach, S.E.P.M. Special Publication, 42, 155-181.

Sarkar, B.C., Mahanta, B.N., Saikia, K. 2007. Geo-environmental quality assessment in Jharia coalfield, India, using multivariate statistics and geographic information system Environmental Geology, Vol. 51, Issue **7**, 1177-1196.

Satterley, A.K. 1996. The Interpretation of Cyclic Sucessions of the Middle and Upper Triassic of the Northern and Southern Alps. Earth-Science Reviews, 181-207.

Satterley, A.K. and Brandber, R. 1995. The genesis of Lofer cycles of the Dachstein Limestone, Northern Calcareous Alps, Austria. Geol. Rundsch, 84, 287-292.

Sattler, U. and Schlaf, J., 1999. Sedimentology and microfacies of the bedded Dachstein limestone of the Julian Alps in Slovenia (Late Triassic). Mit. Ges. Geol. Bergboustud. Österr, 42, 1-224.

Schwarzacher, W. 1948. Über die sedimantare Rhythmik des Dachsteinkalkes von Lofer. Geol Bundesanstalt, 10-12, 175-188.

Schwarzacher, W. 1954. Die Grossrhythmik des Dachsteinkalkes von Lofer. Tschermaks Mineral Petrogr. Mitt., 4, 44-54.

Schwarzacher, W. 2005. The stratification and cyclicity of the Dachstein Limestone in Lofer, Leogang and Steinernes Meer (Northern Calcareous Alps, Austria). Sedimentary Geology, 181, 93-106.

Schwarzacher, W. and Haas, J. 1986. Comparative statistical analysis of some Hungarian and Austrian Upper Triassic peritidal carbonate sequences. Acta Geol. Hung, 29, 173-210.

Segura, F.S., Pardo-Pascual, J.E., Rossello, V.M. 2007. Morphometric indices as indicators of tectonic, fluvial and karst processes in calcareous drainage basins, South Menorca Island, Spain. Earth Surface Processes and Landforms, Vol.32,1928-1946.

Sheps, K. 2004. Quantitative paleoenvironmental analysis of carbonate platform sediments on the Marion Plateau (NE Australia, ODP Leg 194). Ph.D. Thesis, University of South Florida, 97 p. (unpublished).

Shinn, E. A. 1983a. Birdseyes, fenestrae, shrinkage pores and loferites: A reevaluation. Journal of Sedimentary Petrology, 53, 619-628.

Shinn, E. A. 1983b. Tidal flat environment. In Scholle, P.A., Bebout, D.G. & Moore, C.H. (Eds.) Carbonate depositional environments. Tulsa, A.A.P.G. Memoir 33, 173-210.

Shinn, E.A. and Lidz, B.H. 1988. Blackened limestone pebbles: fire at subaerial unconformities. In: James, N.P. and Choquette, P.W. (eds.): Paleokarst. 117-131.

Sloss, L.L. 1963. Sequences in the cratonic interior of North America. Geol. Soc. America Bull, 74, 93-113.

Strasser, A. 1988. Shallowing-upward sequence in Purbeckian peritidal carbonates (Lowermost Createaceous, Swiss and French Jura mountains). Sedimentology, 35, 369-383.

Strasser, A., 1994. Milankovitch cyclicity and high-resolution sequence stratigraphy in lagoonal-peritidal carbonates (Upper TithonianeLower Berriasian, French Jura mountains). In: De Boer, P.L., Smith, D.G. (Eds.), Orbital Forcing and Cyclic Sequences. Special Publication of Internal Association of Sedimentologists, 19, 285-301.

Strasser, A. and Davaud, E. 1983. Black pebbles of the Purbeckian (Swiss and French Jura): lithology, geochemistry and origin. Eclogae Geol. Helvetiae, 76, 551-580.

Şafak, Ü., Kelling, G., Gökçen, N.S. and Gürbüz, K. 2005. The mid-Cenozoic succession and evolution of the Mut basin, southern Turkey, and its regional significance. Sedimentary Geology. 173, 121-150.

Şen, A., 2002, Meter-scale subtidal cycles in the Middle Carboniferous of Central Taurides, Southern Turkey and response of fusulinacean foraminifers to sedimentary cyclicity, M. Sc. Thesis, Middle East Technical University, Ankara, Turkey, 121 p.

Şenel, M. 1997. 1:100 000 ölçekli Türkiye Jeoloji Haritaları Isparta-J12 Paftası. Jeoloji Etütleri Dairesi, MTA Genel Müdürlüğü, Ankara (unpublished).

Şenel, M., 1984, Discussion on the Antalya Nappes. In; Tekeli, O. and Göncüoğlu, M.C. (eds). Geology of the Taurus Belt Int. Symp. Proc. MTA , Ankara, 41-51.

Şenel, M., Selçuk, H., Bilgin, Z.R., Şen, A.M., Karaman, T., Dinçer, M.A., Durukan, E., Arbas, A., Örçen, S. and Bilgin, R. 1989. Çameli (Denizli)-Yeşilova (Burdur)-Elmalı (Antalya) dolayının jeolojisi: MTA Rap. 9761, Ankara (unpublished).

Şenel, M., Dalkılıç, H., Gedik, İ., Serdaroğlu, M., Bölükbaşı, S., Metin, S., Esentürk, K., Bilgin, A.Z., Uğuz M.F., Korucu, M. and Özgül, N., 1992. Eğirdir-Yenisarbademli-Gebiz ve Geriş-Köprülü (Isparta-Antalya) arasında kalan alanların jeolojisi. General Directorate of Mineral Research and Exploration, Report No: 9390, 1-559 (unpublished).

Şenel, M., Akdeniz, N., Öztürk, E.M., Özdemir, T., Kadınkız, G., Metin, Y., Öcal, H., Serdaroğlu, M. and Örçen, S. 1994. Fethiye (Muğla)-Kalkan (Antalya) ve kuzeyinin jeolojisi: MTA Rap. 9429, Ankara (unpublished).

Şenel, M., Gedik, İ., Dalkılıç, H., Serdaroğlu, M., Bilgin, A.Z., Uğuz M.F., Bölükbaşı, A.S., Korucu, M. and Özgül, N., 1996. Isparta büklümü doğusunda, otokton ve allokton birimlerin stratigrafisi (Batı Toroslar). MTA Dergisi, 118, 111-160.

Şenel, M. and Bilgin, Z.R. 1997. 1:100 000 ölçekli Türkiye Jeoloji Haritaları Marmaris-L6 Paftası. Jeoloji Etütleri Dairesi, MTA Genel Müdürlüğü, Ankara (unpublished).

Şenel, M., Dalkılıç, H., Gedik, İ., Serdaroğlu, M., Metin, S., Esentürk, K., Bölükbaşı, A.S. and Özgül, N., 1998. Orta Toroslar'da Güzelsu Koridoru ve Kuzeyinin Jeolojisi. MTA Dergisi, 120, 171-197.

Şengör, A. M. C., and Yılmaz, Y., 1981, Tethyan evolution of Turkey: A plate Tectonic Approach, Tectonophysics, 75: 181-241.

Tekeli, O., Aksay, A., Ürgün, B.M. and Işık, A. 1983. Geology of the Aladağ Mountains. International Symposium on the geology of the Taurus belt, 143-159.

Tomasovych A., 2004, Microfacies and Depositional Environment of an Upper Triassic Intra-Platform Carbonate Basin: The Fatric Unit of the West Carpathians (Slovakia), Facies, 50, 77-105.

Tryon, R.C. 1939. Cluster Analysis. Ann Arbor, MI: Edwards Brothers.

Turati, D.D. and Radrizzani, C.P. 1982. Segnalazione di un livello fossilifero del Trias superiore in localita Pra Brusche (Bellagio, F.32 I NW). Riv. Ital. Paleont., v. 87, n. 4, 46-50.

Tuzcu, N., Wernli, R. et Zaninetti, L. 1982. L'age de la "Serie Calcaire" dans la region de Karaman, Taurus Occidental, Turquie. Etude des Foraminiferes du Trias superieur, Paleoenvironnement de depot. Arch. Sc. Geneve, Vol. 35, Fasc. 2, pp. 127-135.

Ünal, E., Altıner, D., Yılmaz, I. Ö. and Özkan-Altıner, S. 2003. Cyclic sedimentation across the Permian-Triassic boundary (Central Taurides, Turkey). Rivista Italiana di Paleontologia e Stratigrafia, 109, N. 2, 359-376.

Vail P.R., Mitchum, R.M. and Thompson, S. 1977a. Seismic Stratigraphy and global changes of sae level, Part 3; Relative changes of sea level from coastal onlap. In Seismic Strratigraphy-Application to hydrocarbon exploration, A.A.P.G. Memoir 26, p. 63-81.

Vail P.R., Mitchum, R.M. and Thompson, S. 1977b. Seismic Stratigraphy and global changes of sae level, Part 4; Global cycles of relative changes of sea level. In Seismic Strratigraphy-Application to hydrocarbon exploration, A.A.P.G., Memoir 26, p. 83-97.

Van Wagoner, J.C. 1985. Reservoir facies distribution as controlled by sea-level change: Abstracts with Programs. Society of Economic Paleontologists and Mineralogists Midyear Meeting, Golden, Colorado, p. 91-92.

Van Wagoner, J.C., Posamentier, H.W., Mitchum, R.M., Vail, P.R., Sarg, J.F., Loutit, T.S. and Hardenbol, J. 1988, An Overview of the Fundamentals of Sequence Stratigraphy and Key Definitions, Sea-Level Changes-An Integrated Approach. SEPM Special Publication, No. 42, 39-44.

Varol, B., Kazancı, N. and Altıner, D. 1986. Presence of the Middle-Upper Triassic in the autochthonous Geyik Dağı Unit of the eastern Taurus (Sarız-

Tufanbeyli region, Kayseri). Bulletin of Mineral Research and Exploration, 108, 111-113.

Varol, B., Özgüner, A.M., Koşun, E., İmamoğlu, Ş., Daniş, M. and Karakullukçu, T. 2000. Batı Karadeniz Bölgesi Glokonilerinin Depolanma Ortamları ve Sekans Stratigrafisi. MTA Dergisi, 122, 1-23.

Vegh-Neubrandt, E., Dumont ,J.F., Gutnic M., Marcoux, J., Monod, O. et Poisson, A. 1976. Megalodontidae du Trias superieur dans la chaine taurique (Turquie meridionale). Geobios, t. 9 (2), 199-222.

Weber, M.E., Fenner, J., Thies, A. and Cepek, P. 2001. Biological response to Milankovitch forcing during the Late Albian (Kirchrode I borehole, northwest Germany). Paleogeography, Paleoclimatology, Palaeoecology, 174, 269-286.

Weynschenk, R. 1956. *Aulotortus*, a new genus of Foraminifera from the Jurassic of Tyrol, Austria. Contr. Cush. Found. Foram. Res., **7**, pt. 1, 26-28.

Wilson, J.L. 1975. Carbonate facies in geologic history. New York, Springer-Verlag, 469p.

Woodcock, N. H. and Robertson, A. H. F. 1977. Origin of some ophiolite-related metamorphic rocks in the 'Tethyan' belt. Geology, 5, 373–376.

Wright, V.P. 1984. Peritidal carbonate facies models: A review. Geological Journal, **19**, 309-325.

Xu, J., Wang, P., Huang, B., Li, Q. and Jian, Z. 2005. Response of planktonic foraminifera to glacial cycles: Mid-Pleistocene change in the southern South China Sea. Marine Micropaleontology, 54, 89-105.

Yan, H. 1980. Sketch of the Triassic foraminiferal biostratigarphy of northwestern Sichuan (Szechuan), China. Riv. Ital. Paleont., v. 85, n. 3-4, 1167-1174.

Yılmaz, I. Ö. 1997. Sequence stratigraphy and dasyclad algal taxonomy in the Upper Jurrasic (Kimmeridgian) – Upper Cretaceous (Cenomanian) peritidal carbonates of the Fele area, Western Taurides, Turkey. M. S. Thesis, M.E.T.U., Ankara, Turkey, 223 p. (unpublished).

Yılmaz, I. Ö. and Altıner, D. 2001. Use of sedimentary structures in the recognition of sequence boundaries in the Upper Jurassic (Kimmeridgian)–Upper Cretaceous (Cenomanian) peritidal carbonates of the Fele (Yassýbel) area (Western Taurides, Turkey). International Geology Review (Published in association with the International Division of the Geological Society of America and Economic Geology, ISSN 0020-6814), 43 (8), 736-754.

Yılmaz, İ. Ö., and Altıner, D. 2006a. Cyclic palaeokarst surfaces in Aptian peritidal carbonate successions (Taurides, southwest Turkey): internal structure and response to mid-Aptian sea-level fall. Cretaceous Research, 27, 814 – 827.

Yılmaz, I. Ö. and Altıner, D. 2006b. Cyclostratigraphy and sequence boundaries of inner platform mixed carbonate-siliciclastic successions (Barremian-Aptian) (Zonguldak, NW Turkey). Journal of Asian Earth Sciences. In Press, Corrected Proof, Available online 29 November 2006.

Yılmaz, İ. Ö., and Altıner, D. 2007. Cyclostratigraphy and sequence boundaries of inner platform mixed carbonate–siliciclastic successions (Barremian–Aptian) (Zonguldak, NW Turkey). Journal of Asian Earth Sciences 30, 253-270.

Yılmaz, İ. Ö. 2008. Cretaceous pelagic red beds and black shales (Aptian−Santonian), NW Turkey: Global Oceanic Anoxic and Oxic Events. Turkish Journal of Earth Sciences (In Press).

Zaninetti, L. 1976. Les Foraminiferes du Trias. Riv. Ital. Paleont., 82, n. 1, pp. 1-258.

Zaninetti, L. 1984. Les Involutinidae (Foraminiferes). Proposition pour une subdivision. Revue de Paleobiologie. 3/2, 205-207.

Zaninetti, L. and Brönnimann, P. 1971. Les effets de recristallisation sur la paroi des Involutinidae (Foraminiferes) triasiques. Paläont. Z., 45, ½, 69-74.

Zaninetti, L., Brönnimann, P., Bozorgnia, F. et Huber, H. 1972. Etude lithologique et micropaleontologique de la formation d'Elika dans la coupe d'Aruh, Alborz central, Iran septentrional. Arch. Sc. Geneve. Vol. 25, fasc. 2, pp. 215-249.

Zaninetti, L. and Brönnimann, P. 1974. Etude micropaleontologique comparee des Involutinidae (Foraminiferes) triasiques d'Elika, d'Espahk et de Nayband, Iran. Ecl. Geol. Helv., v. 67, n. 2, pp. 403-418.

Zaninetti, L. and Brönnimann, P. 1975. Triassic foraminifera from Pakistan. Riv. It. Paleont. Strat., 81/3, 257-280.

Zaninetti, L. et Thiebault, F. 1975. Les Foraminiferes du Trias superieur du massif du Taygete (Peloponnese meridional, Grece). Arch. Sc. Geneve, Vol. 28, Fasc. 2, pp. 229-236.

Zaninetti, L., Brönnimann, P., Huber, H. et Moshtaghian, A. 1978. Microfacies et microfaunes du Permien au Jurassique au Kuh-e Gahkum, Sud-Zagros, Iran. Rivista Italiana di Paleontologia e Stratigrafia, v. 84, n. 4, pp. 865-896.

Zaninetti, L., Ciarapica, G. et Martini, R. 1986. Presence de *Palaelituonella meridionalis* (Luperto, 1965) (synonyme *Palaelituonella majzoni* Berczi-Mack, 1981) (Foraminiferes) dans des calcaires recifaux du Trias ("Calcaire d'Abriola" P.P) Apennin Meridional. Revue de Paleobiologie. 5/1, 33-35.

Zankl H., 1967, Die Karbonatsedimente der Obertrias in den Nördlichen Kalkalpen, Geologische Rundschau, 56, 128-139.

Zhang, S.X., Barnes, C.R., Jowett, D.M.S. 2006. The paradox of the global standard Late Ordovician-Early Silurian sea level curve: Evidence from conodont community analysis from both Canadian Arctic and Appalachian margins. Palaeogeography Palaeoclimatology Palaeoecology, Vol. 236, Issue 3-4, 246-271.

Ziegler, J.G.K. 1938. Garbi Toros mınıkasında yapılmış olan maden ve jeoloji tetkikatı. MTA Rap. No: 768, p. 953 (unpublished).

APPENDIX A

EXPLANATION OF PLATES

PLATE 1

1. *Triasina hantkeni* MAJZON, Leylek-2 Section, Sample No. C-41
2. *Triasina hantkeni* MAJZON, Leylek-2 Section, Sample No. C-45
3. *Triasina hantkeni* MAJZON, Kuzca-2 Section, Sample No. K-30
4. *Triasina hantkeni* MAJZON, Kuzca-2 Section, Sample No. K-26
5. *Triasina hantkeni* MAJZON, Kuzca-3 Section, Sample No. K-35
6. *Triasina hantkeni* MAJZON, Kuzca-4 Section, Sample No. K-51
7. *Triasina hantkeni* MAJZON, Kuzca-2 Section, Sample No. K-31
8. *Aulotortus communis* (KRISTAN), Leylek-1 Section, Sample No. B-40
9. *Aulotortus communis* (KRISTAN), Leylek-1 Section, Sample No. B-40
10. *Aulotortus communis* (KRISTAN), Kuzca-2 Section, Sample No. K-30
11. *Aulotortus communis* (KRISTAN), *8*th parasequence of Leylek-2 Section, Sample No. C-33M
12. *Aulotortus* sp., 5th parasequence of Leylek-2 Section, Sample No. C-25-O

PLATE 1

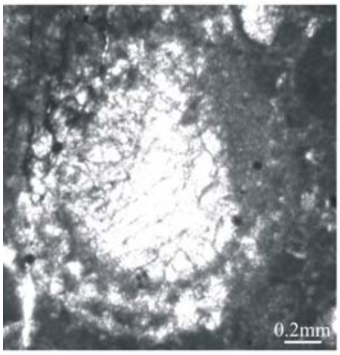

1

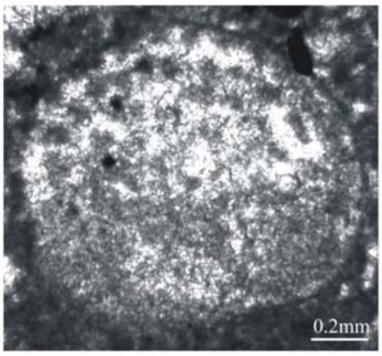

2

3

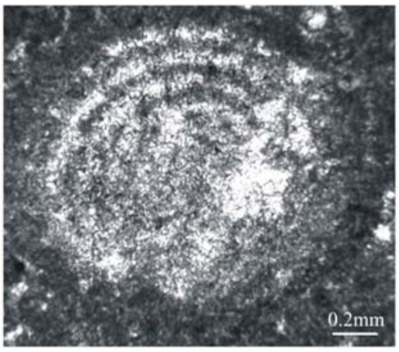

4

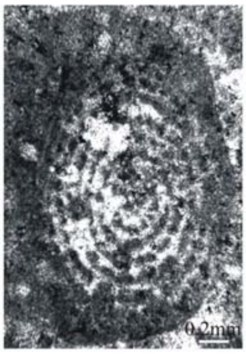

5

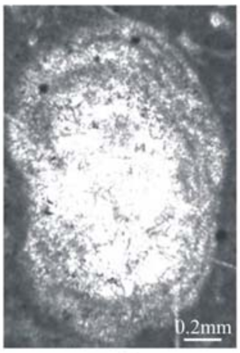

6

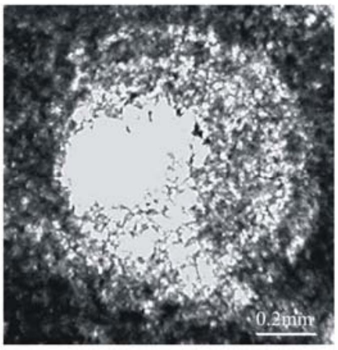

7

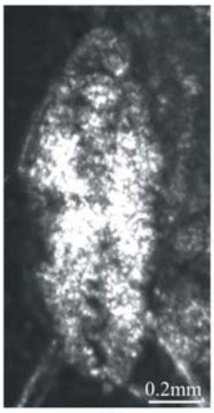

8

9

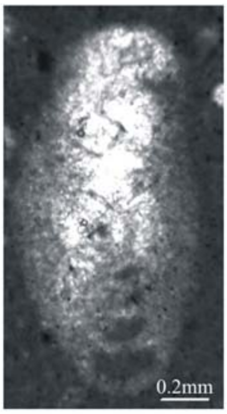

10

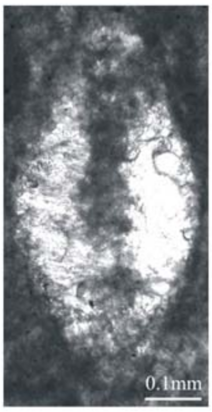

11

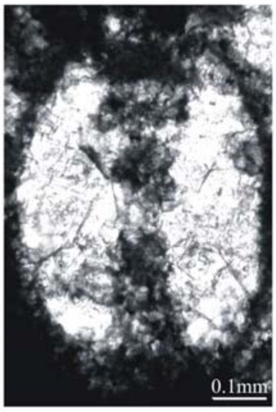

12

PLATE 2

1. *Aulotortus tumidus* (KRISTAN-TOLLMANN), Kuzca-2 Section, Sample No. K-26
2. *Aulotortus tumidus* (KRISTAN-TOLLMANN), Kuzca-2 Section, Sample No. K-29
3. *Aulotortus tumidus* (KRISTAN-TOLLMANN), Marmaris-2 Section, Sample No. M-105
4. *Aulotortus tumidus* (KRISTAN-TOLLMANN), 18th parasequence of Leylek-1 Section, Sample No. B-47F
5. *Aulotortus* sp., Leylek-1 Section, Sample No. B-40
6. *Aulotortus gaschei* (KOEHN-ZANINETTI et BRONNIMANN), 4th parasequence of Leylek-2 Section, Sample No. C-25A
7. *Aulotortus gaschei* (KOEHN-ZANINETTI et BRONNIMANN), 4th parasequence of Leylek-2 Section, Sample No. C-25A
8. *Aulotortus impressus* (KRISTAN-TOLLMANN), Leylek-2 Section, Sample No. C-48
9. *Aulotortus impressus* (KRISTAN-TOLLMANN), 7th parasequence of Leylek-1 Section, Sample No. B-20A
10. *Aulotortus impressus* (KRISTAN-TOLLMANN), 4th parasequence of Leylek-2 Section, Sample No. C-25A
11. *Aulotortus* sp., Marmaris-1 Section, Sample No. M-88

PLATE 2

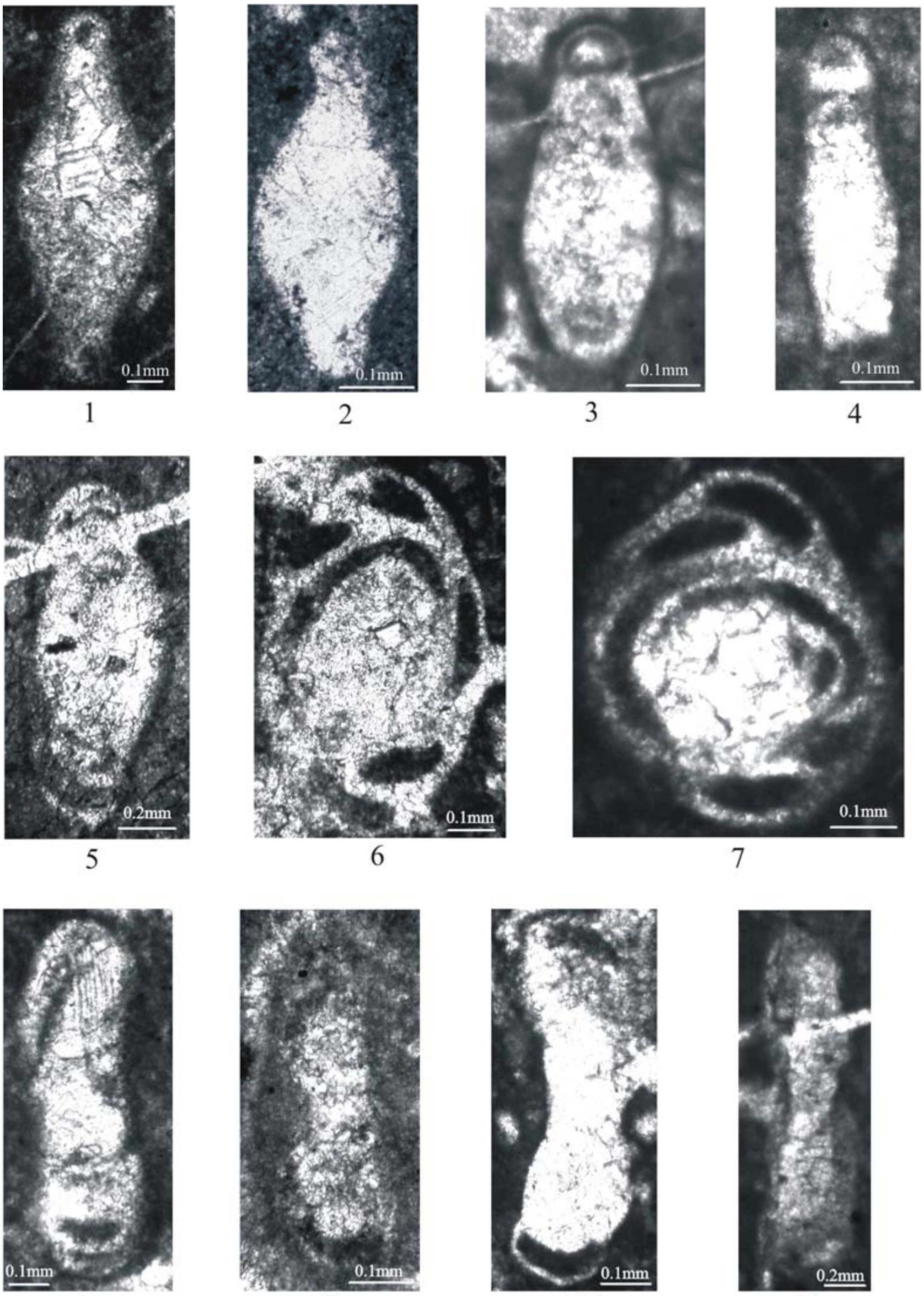

0.1mm
0.1mm
0.1mm
0.1mm
1
2
3
4
0.2mm
0.1mm
0.1mm
5
6
7
0.1mm
0.1mm
0.1mm
0.2mm
8
9
10
11

PLATE 3

1. *Aulotortus* gr. *sinuosus* WEYNSCHENK, Leylek-1 Section, Sample No. B-40
2. *Aulotortus* gr. *sinuosus* WEYNSCHENK, Leylek-1 Section, Sample No. B-40
3. *Aulotortus* gr. *sinuosus* WEYNSCHENK, Marmaris-2 Section, Sample No. M-105
4. *Aulotortus* gr. *sinuosus* WEYNSCHENK, Marmaris-2 Section, Sample No. M-105
5. *Aulotortus* gr. *sinuosus* WEYNSCHENK, Marmaris-1 Section, Sample No. M-72
6. *Aulotortus* gr. *sinuosus* WEYNSCHENK, Marmaris-1 Section, Sample No. M-66
7. *Aulotortus* gr. *sinuosus* WEYNSCHENK, Marmaris-2 Section, Sample No. M-105
8. *Aulotortus* gr. *sinuosus* WEYNSCHENK, Marmaris-2 Section, Sample No. M-105
9. *Aulotortus* gr. *sinuosus* WEYNSCHENK, 4th parasequence of Leylek-2 Section, Sample No. C-25A

PLATE 3

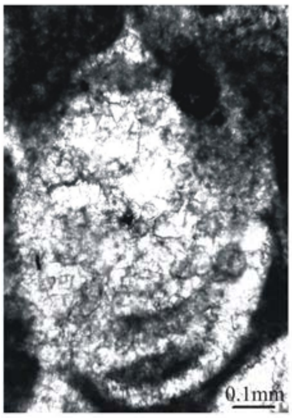

1

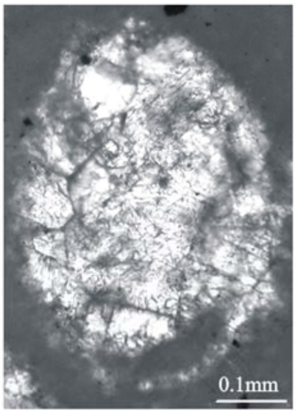

2

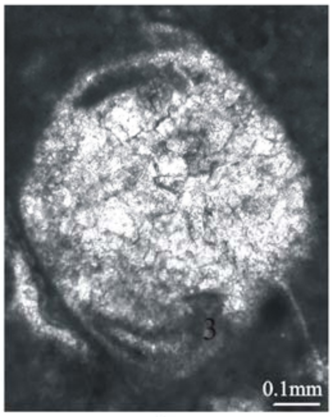

3

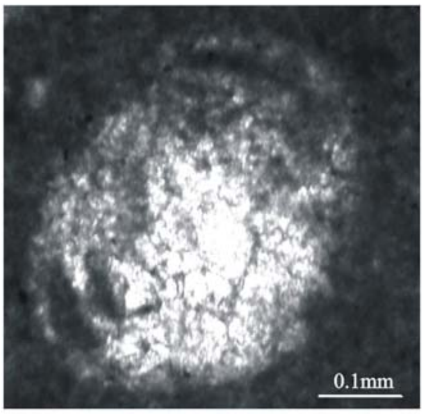

4

5

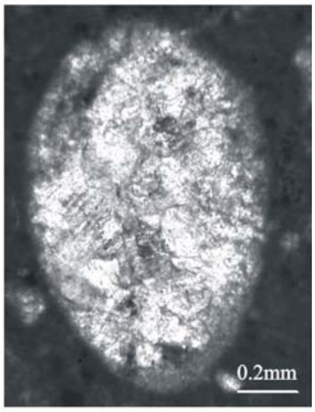

6

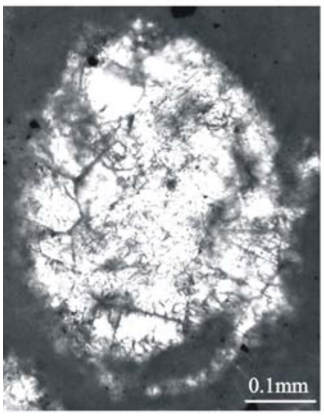

7

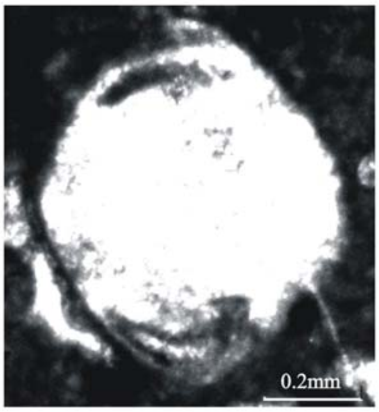

8

9

PLATE 4

1. *Aulotortus tenuis* (KRISTAN), Marmaris-1 Section, Sample No. M-88
2. *Aulotortus tenuis* (KRISTAN), Marmaris-2 Section, Sample No. M-106
3. *Aulotortus tenuis* (KRISTAN), 4th parasequence of Leylek-2 Section, Sample No. C-25A
4. *Aulotortus tenuis* ? (KRISTAN), 7th parasequence of Leylek-2 Section, Sample No. C-33G
5. *Aulotortus tenuis* ? (KRISTAN), 7th parasequence of Leylek-2 Section, Sample No. C-33G
6. *Aulotortus praegaschei* (KOEHN-ZANINETTI), Leylek-2 Section, Sample No. C-45
7. *Aulotortus friedi* (KRISTAN-TOLLMANN), Marmaris-1 Section, Sample No. M-85
8. *Aulotortus friedi* (KRISTAN-TOLLMANN), Marmaris-2 Section, Sample No. M-100
9. *Aulotortus sinuosus oberhauseri* (SALAJ), Marmaris-2 Section, Sample No. M-105
10. *Aulotortus sinuosus pragsoides* (OBERHAUSER), Marmaris-2 Section, Sample No. M-105
11. *Aulotortus sinuosus pragsoides* (OBERHAUSER), 4th parasequence of Leylek-2 Section, Sample No. C-25B

PLATE 4

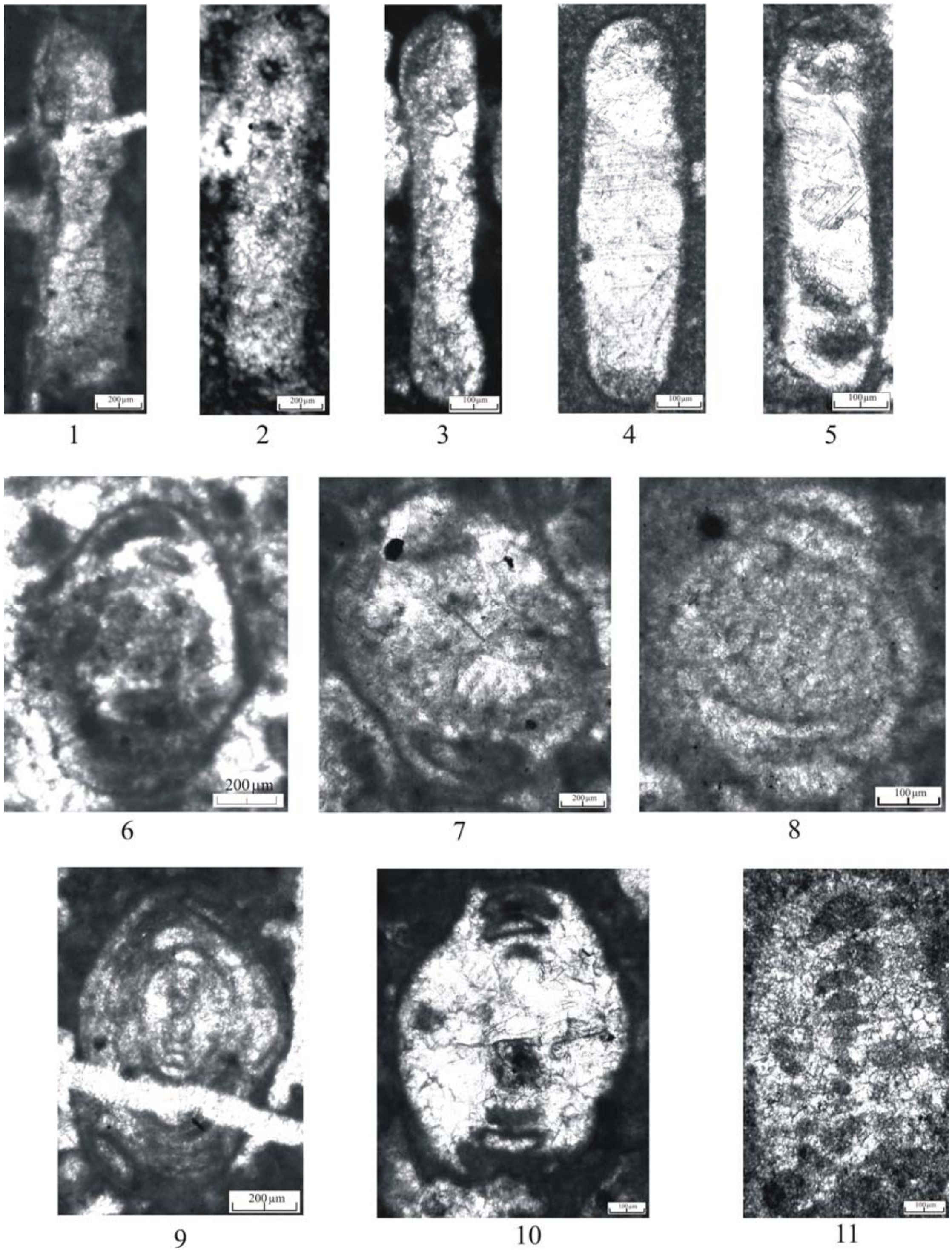

PLATE 5

1-2 *Auloconus permodiscoides* (OBERHAUSER), Kuzca-2 Section, Sample No. K-24

3. *Auloconus permodiscoides* (OBERHAUSER), 18th parasequence of Leylek-1 Section, Sample No. B-47F

4. *Auloconus permodiscoides* (OBERHAUSER), 18th parasequence of Leylek-1 Section, Sample No. B-47F

5. *Auloconus* sp., Kuzca-4 Section, Sample No. K-45

6. *Auloconus* sp., Marmaris-2 Section, Sample No. M-112

7. *Auloconus* sp., Marmaris-2 Section, Sample No. M-112

8. *Glomospira* sp., Leylek-2 Section, Sample No. C-22

9. *Glomospira* sp., Leylek-2 Section, Sample No. C-22

PLATE 5

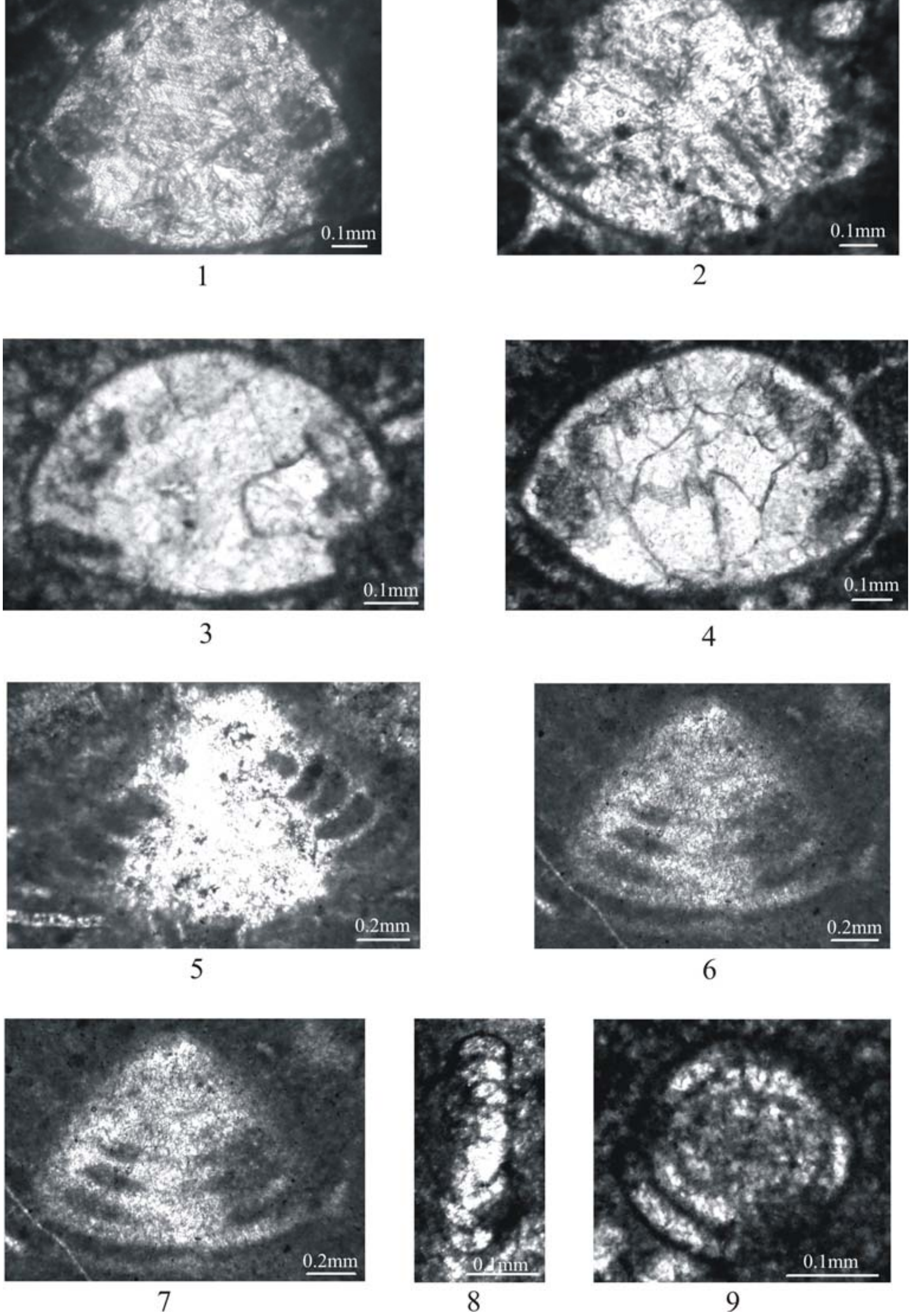

PLATE 6

1. *Auloconus* sp., Kuzca-4 Section, Sample No. K-45
2. *Auloconus* sp., Leylek-1 Section, Sample No. B-51
3. *Auloconus* sp., Kuzca-3 Section, Sample No. K-41
4. *Auloconus* sp., Kuzca-2 Section, Sample No. K-24
5. *Auloconus* sp., Marmaris-2 Section, Sample No. M-143
6. *Auloconus* sp., Leylek-2 Section, Sample No. C-48
7. *Auloconus* sp., 18th parasequence of Leylek-1 Section, Sample No. B-47F
8. *Auloconus* sp., 11th parasequence of Leylek-2 Section, Sample No. C-47C

PLATE 6

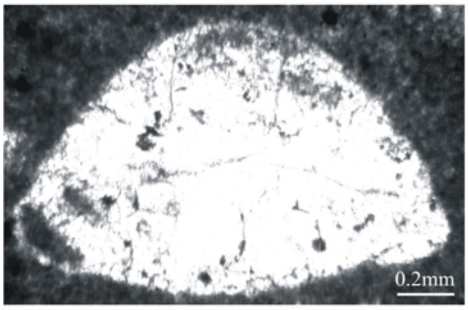

1

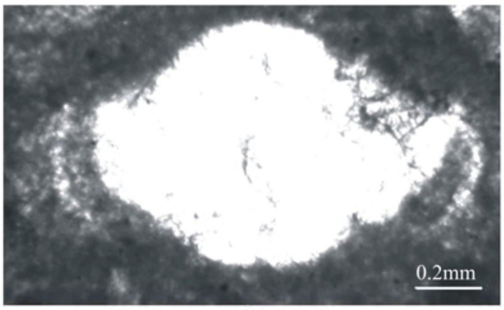

2

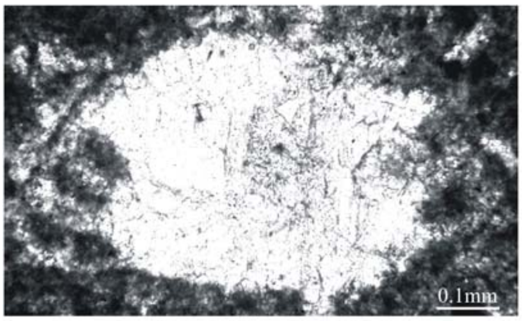

3

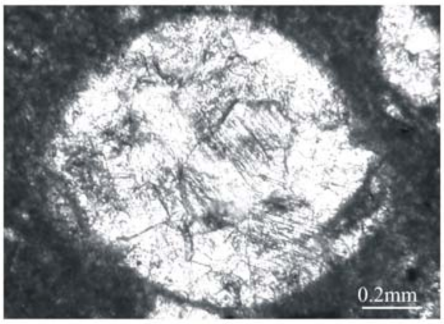

4

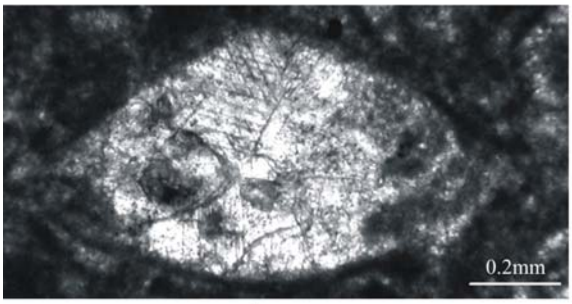

5

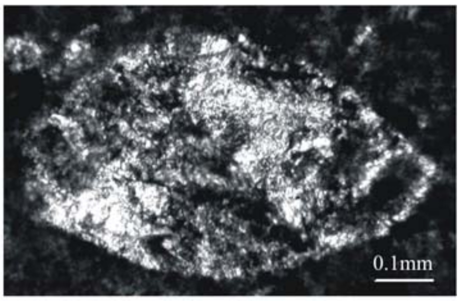

6

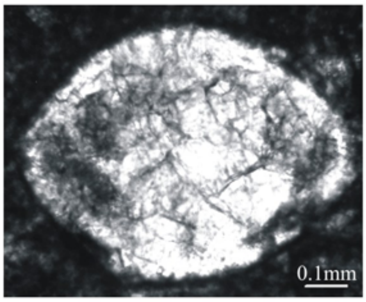

7

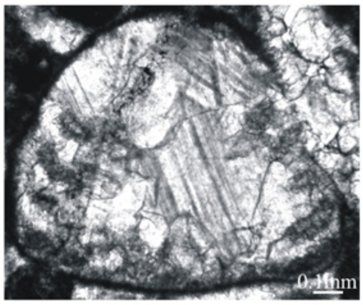

8

PLATE 7

1. *Auloconus* sp., 11th parasequence of Leylek-2 Section, Sample No. C-47C
2. *Auloconus* sp., 11th parasequence of Leylek-2 Section, Sample No. C-47C
3. *Auloconus* sp., 11th parasequence of Leylek-2 Section, Sample No. C-47C
4. *Auloconus* sp., 11th parasequence of Leylek-2 Section, Sample No. C-47C
5. *Glomospirella* sp., Marmaris-2 Section, Sample No. M-105
6. *Glomospirella* sp., Marmaris-2 Section, Sample No. M-105
7. *Glomospirella* sp., Marmaris-2 Section, Sample No. M-105
8. *Glomospirella* sp., Marmaris-2 Section, Sample No. M-143
9. Nodosarid foraminifer A, Leylek-2 Section, Sample No. C-44
10. Nodosarid foraminifer A, Kuzca-2 Section, Sample No. K-23

PLATE 7

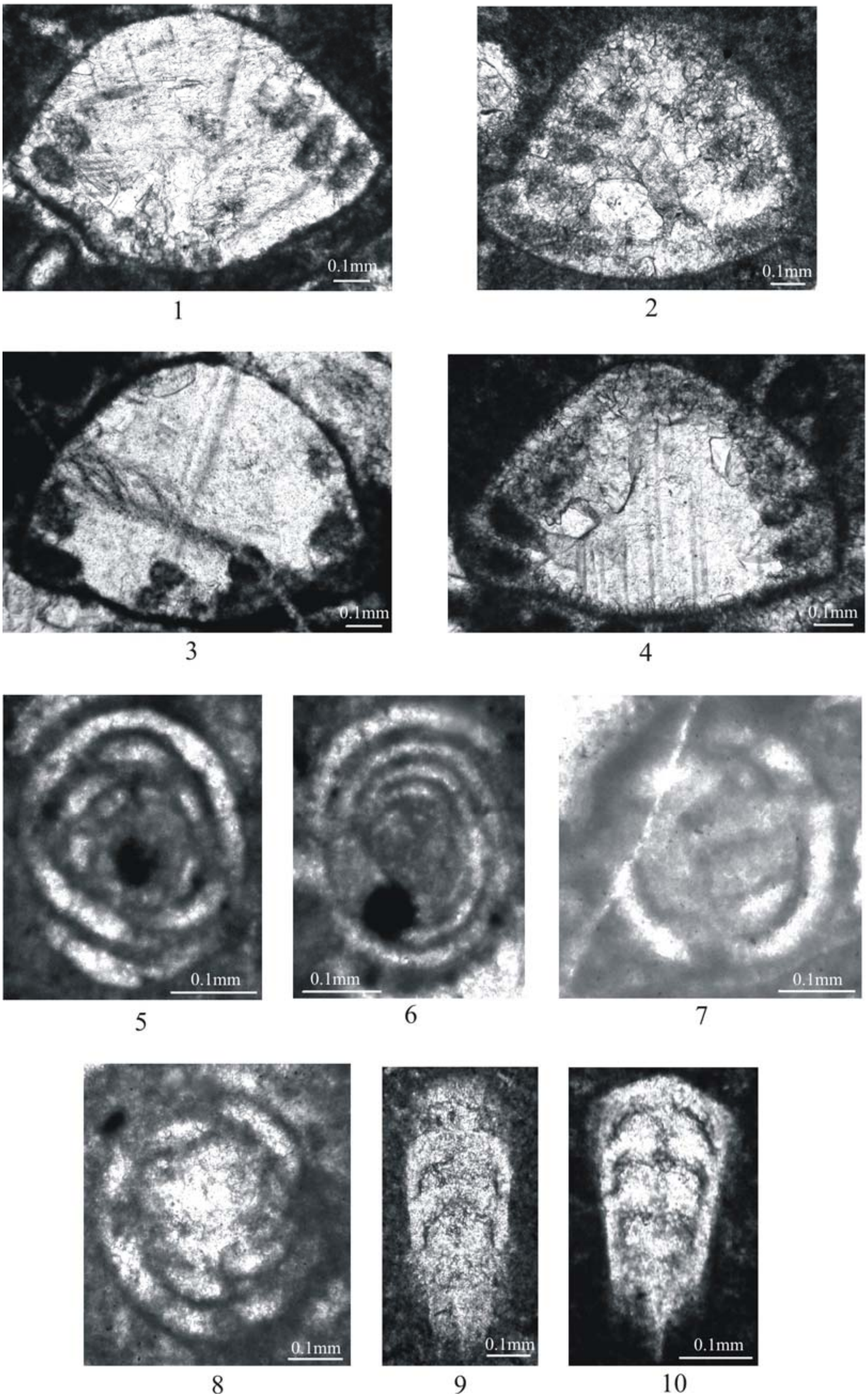
0.1mm
1
0.1mm
2
0.1mm
3
0.1mm
4
0.1mm
5
0.1mm
6
0.1mm
7
0.1mm
8
0.1mm
9
0.1mm
10

PLATE 8

1. Nodosarid foraminifer B, Leylek-2 Section, Sample No. C-22
2. Nodosarid foraminifer B, 18th parasequence of Leylek-1 Section, Sample No. B-47F
3. Nodosarid foraminifer B, 18th parasequence of Leylek-1 Section, Sample No. B-47L
4. Nodosarid foraminifer C, Marmaris -2 Section, Sample No. M-143
5. Unknown foraminifera, Kuzca-3 Section, Sample No. K-40
6. Trochamminid foraminifer A, Leylek-2 Section, Sample No. C-21
7. Trochamminid foraminifer B, Kuzca-3 Section, Sample No. K-37
8. Trochamminid foraminifer B, 9th parasequence of Leylek-2 Section, Sample No. C-33P
9. Trochamminid foraminifer C, Marmaris-2 Section, Sample No. M-100
10. Trochamminid foraminifer C, 13th parasequence of Leylek-1 Section, Sample No. B-33D
11. Algae, Marmaris-2 Section, Sample No. M-100
12. *Thaumatoporella parvovesiculifera* RAINERI, 13th parasequence of Leylek-1 Section, Sample No. B-33E
13. *Parafavrenia* sp., Leylek-1 Section, Sample No. B-20

PLATE 8

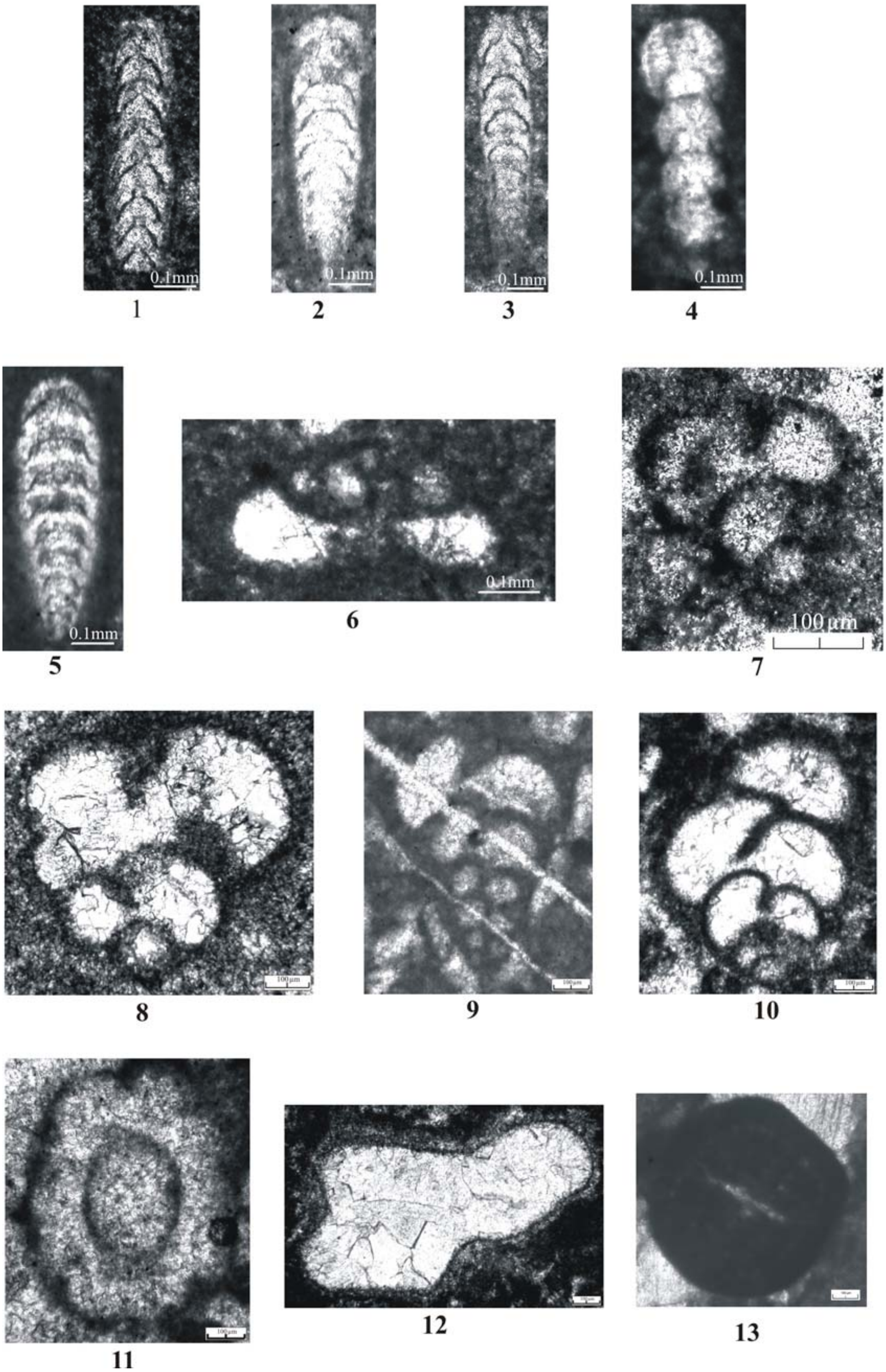

APPENDIX B: Countings of the microfossils and the percentages of pelloids in some of the samples

Sample No.	*Aulotortus*	*Auloconus*	Nodosariidae	Trochamminidae	Pelloid
B-20-A	9	0	0	0	80%
B-20-B	40	0	0	0	75%
B-20-C	40	0	0	0	80%
B-20-D	71	1	1	0	85%
B-20-E	189	4	0	2	70%
B-20-F	22	1	0	0	0%
B-20-G	39	1	0	1	75%
B-20-H	6	0	0	0	0%
B-20-I	0	0	0	0	0%
B-20-J	1	0	0	0	0%
B-20-K	0	0	0	0	0%
B-20-L	0	0	0	0	0%
B-33-A	10	0	0	0	10%
B-33-B	33	0	0	0	15%
B-33-C	29	0	0	0	5%
B-33-D	67	0	0	2	10%
B-33-E	35	0	0	0	0%
B-33-F	0	0	0	0	0%
B-33-G	20	0	0	0	0%
B-33-H	9	0	0	0	0%
B-33-I	0	0	0	0	0%
B-33-J	0	0	0	0	0%
B-33-K	0	0	0	0	0%
B-33-L	0	0	0	0	0%
B-33-M	6	1	1	0	80%
B-33-N	1	0	0	1	0%
C-25-A	63	0	0	1	
C-25-B	8	0	0	0	
C-25-C	4	2	0	0	
C-25-D	12	1	1	0	
C-25-E	0	0	0	0	
C-25-F	0	0	0	0	
C-25-G	0	0	0	0	
C-25-H	2	0	0	0	
C-25-I	0	0	0	0	
C-25-J	0	0	0	0	
C-25-K	0	0	0	0	
C-25-L	0	0	0	0	
C-25-M	0	0	0	0	
C-25-N	213	0	0	2	
C-25-O	279	4	0	1	
C-25-P	0	0	0	0	
C-25-R	7	0	0	0	
C-25-S	0	0	0	0	
C-25-T	0	0	0	0	

Sample No.	Aulotortus	Auloconus	Nodosariidae	Trochamminidae	T. hantkeni
C-25-U	28	0	1	0	
C-25-V	1	0	0	0	
C-25-Y	0	0	0	0	
C-25-Z	0	0	0	0	
C-25-Z1	4	0	0	0	
C-25-Z2	0	0	0	0	
C-25-Z3	0	0	0	0	
C-25-Z4	1	0	0	0	
C-33-C	7	0	0		
C-33-D	1	0	0		
C-33-E	0	0	0		
C-33-F	15	0	0		
C-33-G	4	2	0		
C-33-H	3	0	0		
C-33-I	0	0	0		
C-33-J	158	8	0		7
C-33-K	69	5	0		3
C-33-L	36	6	0		0
C-33-M	39	4	0		0
C-33-N	0	0	0		0
C-33-O	29	3	1	0	
C-33-P	0	0	0	1	
C-33-R	66	4	1	1	
C-33-S	40	4	0	0	
C-33-T	0	0	0	0	
C-33-U	13	0	0	0	
C-33-V	101	6	0	0	
C-33-Y	1	0	0	0	
C-33-Z	2	0	0	0	
C-33-Z1	27	2	0	0	
C-33-Z2	0	0	0	0	
C-33-Z3	84	2	0	0	
C-33-Z4	0	0	0	0	

CURRICULUM VITAE

PERSONAL INFORMATION

Surname, Name: Coşkun Tunaboylu, Burcu

Nationality: Turkish (TC)

Date and Place of Birth: 8 November 1976, Ankara

Marital Status: Married

Phone: +90 312 2873430/1597

Email: bcoskunb@gmail.com

EDUCATION

Degree	Institution	Year of Graduation
MS	Hacettepe Unv. Geological Engineering	2000
BS	Hacettepe Unv. Geological Engineering	1997
High School	Yükseliş College, Ankara	1993

WORK EXPERIENCE

Year	Place	Enrollment
2000-Present	General Directorate of Mineral Research and Exploration	Geology Engineer
1997-2000	Hacettepe University Department of Geological Engineering	Research Assistant